UNIVERSITAT POLITÈCNICA DE VALÈNCIA

UNIVERSITÉ DE REIMS CHAMPAGNE-ARDENNE

Doctoral Program in Agricultural Resources and Technologies

DOCTORAL THESIS

Sustainable management of grapevine trunk diseases in vineyard: Deliver biocontrol agents and associated molecules

Catarina da Cunha Maia Leal

Supervisors:

Dr. Florence Fontaine

Dr. Josep Armengol Fortí

Dr. Patricia Trotel-Aziz

Dr. David Gramaje Pérez

Valencia, September 2022

"*If we knew what it was we were doing,*

it would not be called research, would it?"

Albert Einstein

"*Success is 1% inspiration, 98% perspiration,*

and 2% attention to detail."

Phill Dunphy

Acknowledgments

To my supervisors Prof. Dr. Josep Armengol, Dr. Florence Fontaine, Dr. Patricia Trotel-Aziz and Dr. David Gramaje, for their continuous support of my Ph.D. work, for their patience, motivation, and immense knowledge. Thank you for allowing me to integrate your teams, in which I learned and grew so much academically and personally.

To Prof. Dr. Cecília Rego and Prof. Dr. François Halleen, for agreeing to take time out of their busy schedules to be part of my thesis committee, guiding me on the right path.

To Dr. Cédric Jacquard for hosting me in the RIBP lab during these three years.

To Belchim Crop Protection® for partially financing this work, and for providing all the needed support during this project.

To the nursery that allowed us to do our experiments, and provided all the support needed, as well as their workers that took time to accommodate and help us with our works.

To my friends, for supporting me through the good and the bad moments of this last few years. Thank you for listening and taking care of me when I needed the most. For all the good times, good talks and good food we shared I will always be thankful.

A very special thanks to my family for the support without which this goal would have been impossible. For believing in me, even when I didn´t believed in myself. To my mother and father for unwittingly becoming my example to follow in life, supporting me and motivating me to always do what makes me happy. For giving up their time and dreams so I can always reach mine, I will be eternally grateful to you. And to my brother for his unconditional love and support.

Index

Abbreviation list

ABA: abscisic acid
BCAs: biocontrol agents
BF: black foot
***Bs* PTA-271:** *Bacillus subtilis PTA-271*
BOT: Botryosphaeria dieback
CWDEs: Cell wall degrading enzymes
DAMPs: damage-associated molecular patterns
DNA: Deoxiribonucleic acid
dpi: days post-inoculation
EPS: exopolysaccharides
ET: ethylene
GTDs: grapevine trunk diseases
hpi: hours post inoculation
IAA: Indole-3-acetic acid
ISR: induced systemic resistance
JA: jasmonic acid
LPS: lipopolysaccharides
MAMPs: microbial associated molecular patterns
NO: nitric oxide
***Np*-Bt67:** *Neofusicoccum parvum* BT67
NRP: non-ribosomally synthesized peptides
PA: polyamines
PK: polyketides
RNA: Ribosomal ribonucleic acid
RNA-seq: RNA sequencing
RP: ribosomally synthesized antimicrobial peptides
RiPP: post-translationally modified RP
ROS: reactive oxygen species
SA: salicylic acid
***Ta* SC1:** *Trichoderma atroviride* SC1
ViC: inorganic volatile compound
VOC: organic volatile compound

Abstract

Grapevine (*Vitis vinifera* L.) plants are exposed to a wide variety of pathogens, such as bacteria, viruses, phytoplasmas, fungi and nematodes. Since nursery stages, grapevine material can be infected with innumerous pathogens, that can cause unsuspected significant diseases. Nowadays, grapevine fungal trunk diseases (GTDs) are amongst the main constraints for the productivity of this crop. Once infected, plant productivity is decreased, leading to a plant slow or apoplectic death that causes important economic losses and limits vineyard sustainability. With recent environmental conscious practices, chemical treatments for GTDs have been hardly reduced, leaving viticulturists with few effective treatments. Investigation of biocontrol agents (BCAs) capable to forestall or at least to minimize the impact of GTDs, while being a sustainable treatment, is viewed as a research priority. One potential BCA was deeply characterized, and together with a biological commercial product, both BCAs were tested against several GTD pathogens, in greenhouse under controlled conditions, and during the grapevine propagation process. Results from the full genomic analysis of *Bacillus subtilis* PTA-271 (as BCA with a potential) show a functional swarming motility system, strong survival capacities and a set of genes encoding for bioactive substances known to stimulate plant growth or defenses, influence beneficial microbiota, and counteract pathogen aggressiveness. When tested against *Neofusicoccum parvum* Bt67 (thereafter *Np*-Bt67) in greenhouse cuttings, *B. subtilis* PTA-271 (*Bs* PTA-271) and *T. atroviride* SC1 (*Ta* SC1) proved that the cultivar contributes to their beneficial effects against *Np*-Bt67. The simultaneous application of both BCAs was further proved to be even more effective to protect Tempranillo cuttings. Moreover, the transcriptomic analysis from the same samples showed extensively the plant physiology changes induced by the pathogen but also by each BCA, *Bs* PTA-271 on Chardonnay and *Ta* SC1 on Tempranillo, to protect grapevine from *Np*-Bt67 infection. Thus, Chardonnay cuttings infected with *Np*-Bt67 showed overexpressed genes implicated on abscisic acid (ABA) biosynthesis and signaling pathways. In Tempranillo, the infection with *Np*-Bt67 leads to more substantial changes in gene expression, related mostly with amino acid import, chloroplast and photosystem related processes, plant responses to biotic stimulus, and biosynthesis of secondary metabolites. Protection induced by *Bs* PTA-271 in Chardonnay targets genes related to ABA biosynthesis, phenylpropanoid pathways and secondary metabolites, and cell wall

structure/organization in relationship with carbohydrate metabolism that requires much more consideration. Protection with *Ta* SC1 in Tempranilllo requires a larger number of changes related to transporters, cell wall integrity and extension, cell division and pathogen induced cell death, multidirectional active proteins, and microbiome interactions.

During the grapevine nursery process, the results demonstrated a significant reduction on the percentage of infected plants with Botryosphaeria dieback and Black-foot pathogens in the material treated with *Ta* SC1 and *Bs* PTA-271 respectively. The simultaneous treatments with both BCAs presented a reduction on infected plants with both Botryosphaeria dieback and Black foot pathogens. When testing the effect of *Bs* PTA-271 and *Ta* SC1 in grapevine rhizosphere microbiome of two different soil infected with Black foot pathogens, results show that the inoculation of BCAs seems to improve the rhizosphere microbiome networks and sanitation status, however, the beneficial effect of BCAs can be soil-dependent. Moreover, as observed in the other experiments, the combination of both BCAs improves their beneficial effect in the rhizosphere microbiome.

Overall, this study brought new insights on the use of one or more BCAs against several GTD pathogens, from nursery to adult grapevines. Moreover, highlighted both BCAs mode of action in grapevine protection. Thus, these findings provide, not only a better understanding of BCAs, grapevine, and pathogens interactions, but are also a strong contribution for the future development of sustainable GTDs management strategies.

Keywords: *Bacillus subtilis* PTA-271, Biocontrol agents, Defense mechanisms, Grapevine trunk diseases, Microbiome, Nursery process, Plant protection, Sustainable disease management, *Trichoderma atroviride* SC1, *Vitis vinifera* L.

Resumen

Las plantas de vid (*Vitis vinifera* L.) están expuestas a una gran variedad de patógenos, como bacterias, virus, fitoplasmas, hongos y nematodos. Desde las etapas de vivero, las plantas de vid pueden estar infectadas con innumerables patógenos, que pueden causar enfermedades importantes. En la actualidad, las enfermedades fúngicas de la madera de la vid (GTDs) se encuentran entre los principales factores que limitan la productividad de este cultivo. Una vez las vides están infectadas, la productividad de la planta disminuye, provocando una muerte lenta o apoplética, que causa importantes pérdidas económicas y limita la sostenibilidad del viñedo. Con la creciente concienciación ambiental, los fungicidas de síntesis química para el control de las GTDs se han reducido, dejando a los viticultores con pocos tratamientos efectivos disponibles. La investigación de agentes de control biológico (BCAs) capaces de prevenir, o al menos minimizar, el impacto de las GTDs, se considera una prioridad de investigación. En esta Tesis Doctoral se caracterizó en profundidad un agente de biocontrol potencial y, junto con un producto comercial biológico ya registrado, ambos BCAs fueron probados contra varios patógenos agentes causales de GTDs, en invernadero bajo condiciones controladas, y también durante el proceso de propagación de la vid en vivero.

Los resultados del análisis genómico completo de *Bacillus subtilis* PTA-271 muestran un sistema funcional de motilidad de enjambre, una fuerte capacidad de supervivencia y un conjunto de genes que codifican sustancias bioactivas conocidas por estimular el crecimiento o las defensas de las plantas, influir en la microbiota beneficiosa y contrarrestar la agresividad de los patógenos. Cuando *B. subtilis* PTA-271 se probó contra *Neofusicoccum parvum* BT67 en plantas injertadas de invernadero, *B. subtilis* PTA-271 y *Trichoderma atroviride* SC1 demostraron que el cultivar contribuye a los efectos beneficiosos de *Bs* PTA-271 y *Ta* SC1 contra *Np*-Bt67. La aplicación simultánea de ambos BCAs demostró ser beneficiosa contra este patógeno en vides del cultivar Tempranillo. El análisis transcriptómico de las mismas muestras mostró ampliamente los cambios en la fisiología de la planta inducidos tanto por *Bs* PTA-271 como por *Ta* SC1 para proteger la vid ante la infección por *Np*-Bt67. En Chardonnay, las plantas infectadas con *Np*-Bt67 presentan genes sobreexpresados que están implicados en las vías de señalización del acido absicico (ABA). En Tempranillo, la infección con *Np*-Bt67 provoca cambios de expresión en más de 200 genes, relacionados sobre todo con la

importación de aminoácidos, procesos relacionados con el cloroplasto y el fotosistema, respuestas de la planta a estímulos bióticos y biosíntesis de metabolitos secundarios. La protección de *Bs* PTA-271 en Chardonnay implica a genes relacionados con la biosíntesis de ABA, las vías de los fenilpropanoides, los metabolitos secundarios, y la estructura y organización de la pared celular. La protección de *Ta* SC1 en las plantas de Tempranilllo implica un mayor número de cambios, que abarcan tanto el metabolismo primario como el secundario, relacionados con cambios en las señales hormonales, como con el aicdo absicico (ABA). Durante el proceso de producción de la vid en vivero, los resultados demostraron una reducción significativa del porcentaje de plantas infectadas con los patógenos asociados a las enfermedades de decaimiento por Botryosphaeria y Pie negro en el material de vivero tratado con *Ta* SC1 y *Bs* PTA-271 respectivamente. Los tratamientos simultáneos con ambos BCAs presentaron una reducción en el porcentaje de plantas infectadas con ambos tipos de patógenos. Al probar el efecto de *Bs* PTA-271 y *Ta* SC1 en el microbioma de la rizosfera de la vid de dos suelos diferentes infectados con patógenos del pie negro, los resultados muestran que la inoculación de los BCAs parece mejorar las redes del microbioma de la rizosfera y el estado de saneamiento, sin embargo, el efecto beneficioso de los BCAs puede ser dependiente del suelo. Además, como se observó en otros experimentos, la combinación de ambos BCAs mejora su efecto beneficioso en el microbioma de la rizosfera.

En general, este estudio aportó nuevos conocimientos sobre el uso de uno o más BCAs contra varios patógenos asociados a las GTDs, tanto en el vivero como en vides adultas (viñedo). Además, se destacó el modo de acción de ambos BCAs en la protección de la vid. Por lo tanto, estos hallazgos proporcionan, no sólo una mejor comprensión de las interacciones entre los BCAs, la vid y los patógenos, sino que también son una fuerte contribución a una estrategia de gestión sostenible de las GTDs.

Palabras clave: Agentes de biocontrol, *Bacillus subtilis*, Enfermedades de la madera de la vid, Gestión sostenible de enfermedades, Mecanismos de defensa de la planta, Microbioma de la vid, Proceso de vivero de la vid, Protección contra patógenos, *Trichoderma, Vitis vinífera* L.

Resum

Les plantes de vinya (*Vitis vinifera* L.) estan exposades a una gran varietat de patògens, com a bacteris, virus, fitoplasmes, fongs i nematodes. Des de les etapes de viver, les plantes de vinya poden estar infectades amb innombrables patògens, que poden causar malalties importants. En l'actualitat, les malalties fúngiques de la fusta de la vinya (GTDs) es troben entre els principals factors que limiten la productivitat d'aquest cultiu. Una vegada les vinyes estan infectades, la productivitat de la planta disminueix, provocant una mort lenta o apoplética, que causa importants pèrdues econòmiques i limita la sostenibilitat de la vinya. Amb la creixent conscienciació ambiental, els fungicides de síntesi química per al control de les GTDs s'han reduït, deixant als viticultors amb pocs tractaments efectius disponibles. La investigació d'agents de control biològic (BCAs) capaços de previndre, o almenys minimitzar, l'impacte de les GTDs, es considera una prioritat d'investigació. En aquesta Tesi Doctoral es va caracteritzar en profunditat un agent de biocontrol potencial i, juntament amb un producte comercial biològic ja registrat, tots dos BCAs van ser provats contra diversos patògens agents causals de GTDs, en hivernacle sota condicions controlades, i també durant el procés de propagació de la vinya en viver.

Els resultats de l'anàlisi genòmica completa de *Bacillus subtilis* PTA-271 mostren un sistema funcional de motilitat d'eixam, una forta capacitat de supervivència i un conjunt de gens que codifiquen substàncies bioactivas conegudes per estimular el creixement o les defenses de les plantes, influir en la microbiota beneficiosa i contrarestar l'agressivitat dels patògens. Quan *B. subtilis* PTA-271 es va provar contra *Neofusicoccum parvum* BT67 en plantes empeltades d'hivernacle, *B. subtilis* PTA-271 i *Trichoderma atroviride* SC1 van demostrar que la cultivar contribueix als efectes beneficiosos de *B*s PTA-271 i *Ta* SC1 contra *Np*-Bt67. L'aplicació simultània de tots dos BCAs va demostrar ser beneficiosa contra aquest patogen en vinyes del cultivar Ull de llebre. L'anàlisi transcriptómico de les mateixes mostres va mostrar àmpliament els canvis en la fisiologia de la planta induïts tant per *Bs* PTA-271 com per *Ta* SC1 per a protegir la vinya davant la infecció per *Np*-Bt67. En Chardonnay, les plantes infectades amb *Np*-Bt67 presenten gens sobreexpresados que estan implicats en les vies de senyalització de l'acidifique absicico (ABA). En Ull de llebre, la infecció amb *Np*-Bt67 provoca canvis d'expressió en més de 200 gens, relacionats sobretot amb la importació d'aminoàcids, processos

relacionats amb el cloroplast i el fotosistema, respostes de la planta a estímuls biòtics i biosíntesis de metabòlits secundaris. La protecció de *Bs* PTA-271 en Chardonnay implica gens relacionats amb la biosíntesi d'ABA, les vies dels fenilpropanoides, els metabòlits secundaris, i l'estructura i organització de la paret cellular. La protecció de *Ta* SC1 en les plantes de Tempranilllo implica un major nombre de canvis, que abasten tant el metabolisme primari com el secundari, relacionats amb canvis en els senyals hormonals, com amb l'acid abcísic (ABA). Durant el procés de producció de la vinya en viver, els resultats van demostrar una reducció significativa del percentatge de plantes infectades amb els patògens associats a les malalties de decaïment per Botryosphaeria i Peu negre en el material de viver tractat amb *Ta* SC1 i *Bs* PTA-271 respectivament. Els tractaments simultanis amb tots dos BCAs van presentar una reducció en el percentatge de plantes infectades amb tots dos tipus de patògens. En provar l'efecte de *Bs* PTA-271 i *Ta* SC1 en el microbioma de la rizosfera de la vinya de dos sòls diferents infectats amb patògens del Peu negre, els resultats mostren que la inoculació dels BCAs sembla millorar les xarxes del microbioma de la rizosfera i l'estat de sanejament, no obstant això, l'efecte beneficiós dels BCAs pot ser dependent del sòl. A més, com es va observar en altres experiments, la combinació de tots dos BCAs millora el seu efecte beneficiós en el microbioma de la rizosfera.

En general, aquest estudi va aportar nous coneixements sobre l'ús d'un o més BCAs contra diversos patògens associats a les GTDs, tant en el viver com en vinyes adultes (vinya). A més, es va destacar la manera d'acció de tots dos BCAs en la protecció de la vinya. Per tant, aquestes troballes proporcionen, no sols una millor comprensió de les interaccions entre els BCAs, la vinya i els patògens, sinó que també són una forta contribució a una estratègia de gestió sostenible de les GTDs.

Paraules clau: Agents de biocontrol, *Bacillus subtilis*, Malalties de la fusta de la vinya, Gestió sostenible de malalties, Mecanismes de defensa de la planta, Microbioma de la vinya, Procés de viver de la vinya, Protecció contra patògens, *Trichoderma*, *Vitis vinífera* L.

Chapter I

Introduction

1.1. *Vitis vinifera* – One of the oldest and most important crops worldwide

The European grapevine *Vitis vinifera L.*, belonging to the Vitaceae family genus *Vitis*, is the wild ancestor of most cultivated vines diversified into countless varieties of significant economic interest. It is from this vine that almost all the wines in the world are produced. Around 6,000 cultivated varieties exist throughout the world, with just over 200 in France. Subspecies are also described for *Vitis vinifera*, among which *V. vinifera subsp. sylvestris* (more simply referred to as *V. sylvestris*) which includes populations returned to the wild, and *V. vinifera subsp. vinifera* (more simply referred to as *V. vinifera*) which includes cultivated varieties resulting from the domestication of wild species (Levadoux et al. 1956). To differentiate *V. sylvestris* from *V. vinifera* subspecies, phenotypic attributes are considered, such as: flower sex (dioecious male or female for wild populations, versus hermaphroditic for cultivated grapevines) and seed morphology (spherical with a small beak for sylvestris, and pyriform with a well-developed beak for domesticated cultivars) (Zohary et al. 1995; Terral et al. 2010; Lacou et al. 2011; Imazio et al. 2013; De Andrés et al. 2012).

Domestication of *V. vinifera subsp. vinifera* selected morphological characteristics that favors the plant cultivaton and exploitation. Propagation of *vinifera* varieties gave preferences to the largest, juiciest, and tastiest berries, to gradually select identical grape varieties. In Western Europe, grape varieties can also result from selections and crosses between local wild plants and plants already selected. Therefore, from *V. vinifera* subsp. *vinifera*, the various grape varieties make up the vast range of vine varieties cultivated worldwide, with more than 6,000 "cultivars" or “cépages” (a botanical term for varieties of plant species obtained by crossing and cultivated). Genetic diversity is thus generally preserved within a cultivar genome of *V. vinifera*, except when mutations may accumulate over time to generate distinguishable clones and significantly increase the genomic variability (Riaz et al. 2002; Zhou et al. 2019, Franks et al. 2002). The most concentrated areas with the presence of *V. vinifera* are Central and Southern Europe, Western and Middle East of Asia, China, Mediterranean coast of Africa, South Africa, North America, South America, Australia, and New Zealand, however, nowadays, *V. vinifera* is also present in America, Africa, Asia, and Oceania.

Considering the genotype impact of the variety, the cultivar or even the clone, it is important to consider genomic traits when choosing for the plant characteristics.

Additionally, cultivated grapevines are mainly grafted propagated (> 80%), so their genetic diversity could be further increased both by the scion (aerial part of the grafted plant, variety, or cultivar) and the rootstock (underground part of the grafted plant). For instance, some rootstocks are described to promote the plant protection against pathogens and abiotic stress (drought, waterlogging, adaptation to different soils, nutrients intake, etc.), and to influence the scion vigor and grape composition (Gindro et al. 2003; Marchi 2001; Monteiro et al. 2013; Larignon et Dubos, 1997; Chacón-Vozmediano et al. 2021; Yıldırım et al. 2018), but there is no specific cultivar or clone resistant to grapevine trunk diseases (GTDs) (Bertsch et al. 2013).

The use of specific training systems or management techniques is also described to influence plant features (Reynolds et al. 2009; Leao et al. 2019; Zahavi et al. 2001). Depending on the training system, it is possible to facilitate mechanical maintenance (e.g. cut to reduce the density of perennial woods), avoid competition between grapevines, control the light exposure, floor and canopy management, etc., to ultimately result in healthier plants, with better quality bunches and higher yields (Reynolds et al. 2009).

1.2. Focus on Biotic factors inducing plant diseases, as a Challenge to productivity

Diseases are one of the most important factors decreasing plant health, and consequently, the quantity and quality of plant resources/productivity (Lucas 2009; Flood 2010). Plant diseases are caused by microorganisms (viruses, bacteria, fungi, mycoplasmas, viroids), that can be carried by other biotic factors such as animals (birds, insects, mammals, nematodes, parasitic competitor plants), and can be facilitated by abiotic factors (i.e., climate changes and soil physico-chemical parameters) or pollutants (Abdulkhair and Alghuthaymi 2016).

Several biotrophic pathogens (pathogens that establish a long-term feeding relationship with the living cells of their hosts, rather than killing the host cells as part of the infection process) threaten grapevine every year. The main phytosanitary threat in all regions remains the mildews (Bois et al. 2017). Powdery mildew is caused by *Erysiphe necator*, seen as ash-grey to white powdery growth on green tissue of the vine (Gadoury et al. 2012), and downy mildew caused by *Plasmopara viticola*, can be seen as yellow leaf lesions that look oily, with a cottony growth (mycelium), on the lower leaf surface (Gessler et al. 2011).

Full necrotrophic pathogens (pathogens that kill host plant cells and use the contents to support their own growth.) are also threatening for vineyard productivity. Indeed, the grey mold caused by *Botrytis cinerea* is another important grapevine disease leading to heavy yield losses, and for which pathogen pressure can changes yearly. This disease occurs when the grapes turn soft and brown, showing a fluffy grey mold on the grapes (Emanuel et al. 2000). Black rot caused by *Guignardia bidwellii*, also concerns the viticulture community, showing brown spots on the leaves and shoots, that dry and die (Pezet and Jermini 1989).

Finally, focus is made on some important pathogens described as hemibiotroph (initially invade live cells prior to transitioning to a necrotrophic lifestyle to obtain nutrients from killing the host cells) that increasingly threaten grapevine and other woody plants productivity. Indeed, more and more species of woody plants exhibit an inevitably decline called dieback (degeneration of plant tissues following a succession of multiple negative events), which leads to the death of the plant in the long term (low dieback phenotype) or in the short term (apoplectic dieback phenotype) (Anderson et al. 2004; Manion 1999; Ciesla et al. 1994). Due to undetermined period of latency between the asymptomatic to symptomatic states, early detection and management remain of these diseases, presents a challenge in nurseries, mother fields and vineyards, and only few preventives, but no effective and sustainable curative methods, are available (Mondello et al. 2018a,b). This situation worries the fruit and vine growers all around the world, triggering numerous investigations to better understand their causes, the ways to avoid and to treat them. Although per year, 0.5 to 1.5% of the woody plants die due to different factors such as fungi, fire, grazing and climate change, the main mortality factor remains undetermined (Boyd et al. 2013; Bettenfeld et al. 2020). Among them, grapevine trunk diseases (GTDs) are one of the most important groups of plant diseases for grape growers in all wine regions worldwide. These diseases are caused by several fungi that colonize and live in the plant perennial woods for undetermined period of latency (asymptomatic state) before triggering symptoms (symptomatic state) causing necrotic wood lesions that lead to the occurrence of typical leaf symptoms with discolorations and finally to a completely dead branch (Mondello et al. 2018; Bertsch et al. 2013). GTDs for which new pathogens and vectors are described and discovered yearly, and for which there is uncertainty about the role of the annual pathogen load on both the disease symptom expression and the speed of its expression. Focus will also be made on the grapevine plant and immune defenses.

1.3. Plant defenses to Biotic stresses

Main plant defenses are already described (Figure 1.) when the plant metabolism reacts against the pathogen and related associated motifs (MAMPs and PAMPs recognized by the plant receptors PRRs), damages (DAMPs recognized by the plant receptors PRRs), or against the effectors (such as phytotoxins) secreted by the pathogen inside the plant cell. Early (minutes to hours) to late defenses (days or longer) are described but are not necessarily specific from the virulence to the activation of local and distal defense signalling (Li et al. 2020). **Plant pattern recognition receptors (PRRs)** perceive a wide range of elicitors, including pathogen-derived cell wall/membrane components (**the SYSTEMIC dimension of plant defenses**, e.g., peptidoglycan, chitin), pathogen associated proteins (**PAMPs** Pathogen-Associated Molecular Patterns, e.g., flagellin, effectors), and host-derived danger associated molecular patterns (**DAMPs** Damage Associated Molecular Patterns, e.g., cuticle) (Ziv et al. 2018). In few minutes (3 min) **reactive oxygen species** (ROS, such as H_2O_2) are generated in the apoplast as secondary signalling messenger that activates **ions fluxes** such as Ca^{2+} influx (Li et al 2020 for review). Some minutes later (5 min) a complex series of **phosphorylation-dependent signalling cascade** is activated, including mitogen-activated protein kinases (MAPK) and calcium-dependent protein kinase (CPDK) as synergistic, pro-immune activators (Li et al. 2020). MAPK and CDPK acts as defenses executor proteins that lead to nuclear-based **transcriptional reprograming** (changes in microfilament remodelling are detected within 5–15 min), before activating by phosphorylation (in 0-12 hours post infection, hpi) the stress-responsive **transcription factors** (TF, eg. AP2/ERF, bHLH, bZIP, MYB, NAC, WRKY, etc.). These **TFs then transcriptionally activate** (6-24 hpi) **sustained and robust defense processes on a large-scale and in the long-term**: (**a**) induction of defense hormone accumulation and signaling, (**b**) cytoskeleton/organelle remodeling, (**c**) regulation of the secretome and cell wall/apoplast composition, and (**d**) cellular motion (e.g., stomatal closure) as described by Li et al. (2020). When pathogens possess multiple elicitors (e.g., PAMPs, effectors), various synergistic signaling cascades are stimulated. In such conditions, it is difficult to reason by measuring each early (ca. minutes to hours) events, but rather by evaluating changes over the duration of the interaction, which can last days or longer. Thus, the activation of immunity is not a sequential series of events, but rather, represents a complex network of processes, each

of which can be activated or attenuated multiple times during the host-pathogen interaction.

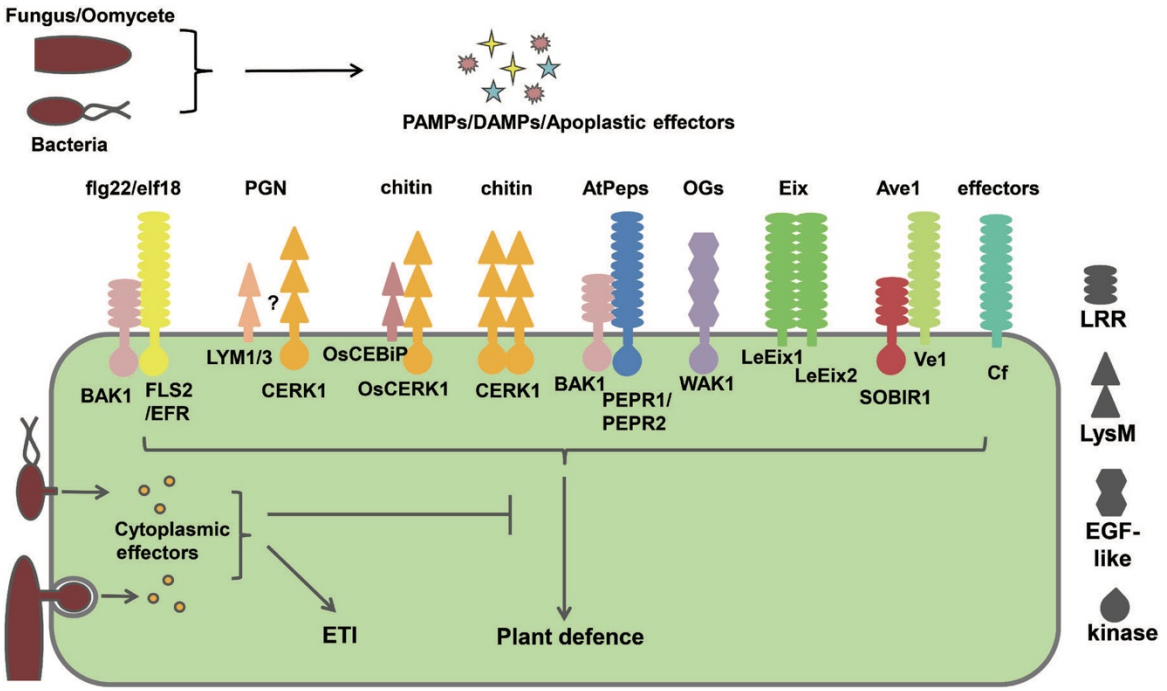

Figure 1. Representative PRRs and their ligands. During bacterial, fungal and oomycete pathogen infection, many danger signals such as pathogen-derived PAMPs and effectors, and plant- derived DAMPs are recognized by plasma membrane-localized RLK and RLP complexes. Pathogens can secrete effectors to suppress plant defense response. However, many of the effectors are recognized by NLRs to activate effector-triggered immunity (ETI). The LRR-RLKs FLS2 and EFR recognize bacterial flg22 and elf18, respectively. BAK1 is a co-receptor and forms a hetero-dimer with FLS2 or EFR upon ligand stimulation. Bacterial peptidoglycan (PGN) is recognized by LysM RLPs LYM1 and LYM3. LysM RLK CERK1 is also required in PGN recognition and probably forms a complex with LYM1 and LYM3 although the direct interaction has not been demonstrated. Rice and Arabidopsis have homologous yet distinct chitin receptors. The Arabidopsis CERK1 directly binds chitin and forms a homo-dimer. In rice, LysM RLP OsCEBiP is the chitin receptor and interacts with OsCERK1 for full signaling. The fungal ethylene-inducing xylanase (Eix) is recognized by tomato LRR-RLPs LeEix1 and LeEix2 complex. Tomato Ve1 recognizes the apoplastic effector Ave1 and interacts with homologs of Arabidopsis SOBIR1 which is a positive cell death regulator. In addition, several pathogen-derived effectors, e.g., Avr2, Avr4, Avr9 and Avr4E, are recognized by LRR RLPs Cf-2, Cf-4, Cf-9 and Cf-4E. Oligogalacturonides (OGs) are a classical DAMP

and recognized by WAK1. Besides, LRR-RLKs PEPR1 and PEPR2 are receptors for another group of DAMPs, AtPeps, and are shown to interact with BAK1. **Note 1:** PRRs = RLKs (= receptor-like kinases) + RLPs (= receptor-like proteins). **Note 2:** PRRs share certain features: they are single-transmembrane receptor-like kinases or receptor-like proteins, containing a leucine-rich repeat (LRR), LysM, EGF-like, or lectin domain for ligand binding within the apoplast (Boutrot and Zipfel 2017) (Adapted from Wu and Zhou 2013).

In parallel to the activation of **local immune signaling**, plants also employ long-distance signaling as a mechanism to prime defense activation in advance of pathogen proliferation. This strategy enables to halt pathogen spread via the mobilization of a core, evolutionarily conserved, class of highly specific signaling molecules. Once mobilized, these signals activate defense responses in distal uninfected cells and tissues, which reduces secondary pathogen invasion, proliferation, and disease. Consequently, noninfected cells are primed to enter a pro-immune status. This process, referred to as systemic acquired resistance (SAR) (Durrant and Dong 2004; Shine et al. 2019), provides protection against a broad range of pathogens, including bacteria, fungi, and viruses.

Following pathogen perception, a broad spectrum of **distal immune signaling** is activated (the **systemic dimension** of plant defenses). The first, the electrical wave due to ions fluxes stimulates membrane potential without transporting molecules to distal cells. Based on the robustness and speed of the Ca2+ signal, it is reasonable to hypothesize that the **Ca2+ wave** represents the first phase of long-distance signaling in response to biotic stress perception. The second class of immune signal that has been described is broadly classified as **messenger/signal molecules**, including **hormones** (e.g., SA, JA/ET), **RNA, proteins, and peptides**. These signal molecules, which transmits by themselves, are long-distance messengers transmitting signals with high specificity, robustness, and durability, at the expense of speed. Moreover, each of these characteristics determines their biological function to induce and maintain the second phase of distal immunity, when massive pathogen inhibitory molecules are synthesized (Li et al. 2020). To facilitate the activation and **propagation of distal signals**, plants use not only symplastic and apoplastic pathways, but also vascular systems (e.g., phloem). **Phytohormones are long-range mobile signalling molecules**, which play an essential role in stress signalling. Salicylic acid (SA, phenylpropanoid path) is useful to protect the

plant against biotrophic pathogens, while Jasmonic acid (JA, lipoxygenase path) / ethylene (ET) are described as useful against necrotrophic pathogens and pests. Due to crosstalk between induced TF, other phytohormones (e.g., abscisic acid, ABA, etc.) can also interfere with plant defenses against pathogens. Once mobilized, **signal molecules activate defense responses in distal uninfected cells and tissues**, to reduce secondary pathogen invasion, proliferation, and disease. Consequently, noninfected cells also show a pro-immune status called **systemic acquired resistance (SAR)** (Durrant and Dong 2004; Shine et al. 2019) (Figure 2.).

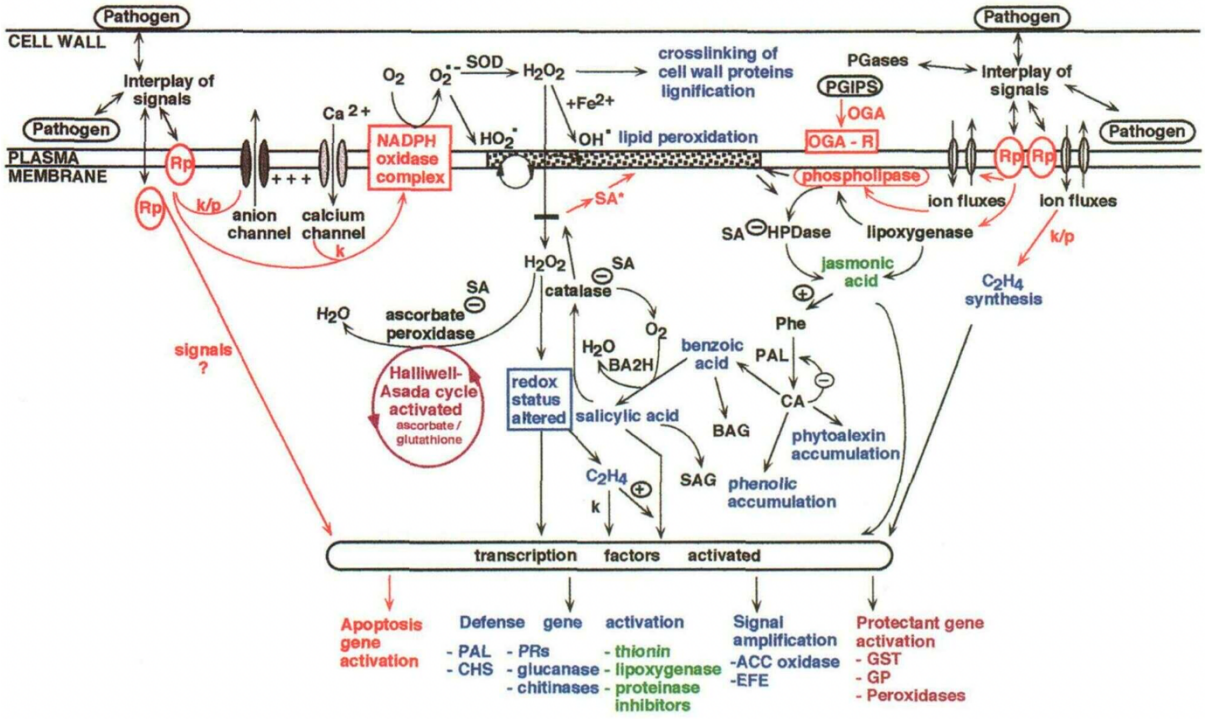

Figure 2. Complexity of Signaling Events Controlling Activation of Defense Responses. Plant receptor proteins (Rp) intercept pathogen-derived or interaction-dependent signals. These signals include the direct or indirect products of Avr genes, physical contact, and general components of each organism, such as chitin, enzymes, and plant cell wall fragments. Plant receptor proteins may or may not be the products of R genes. The immediate downstream signaling events are not known but involve kinases, phospha- tases, G proteins, and ion fluxes. Several distinct and rapidly activated outcomes are recognized, including the production of ROS, direct induction of defense gene transcription, or possibly apoptosis genes, JA biosynthesis, and/or ethylene biosynthesis. Amplification of the initial defense response occurs through the generation of additional

signal molecules, other ROS, lipid peroxides and BASA. This, in turns, induce other defense-related genes and modify defense proteins and enzymes. Concomitant alterationsto cellular redox status and/or cellular damage will activate preformed cell protection mechanisms and induce genes encoding various cell protectants. Defense-related stress may also induce cell death. Cross-talk between the various induced pathways will coor- dinatethe responses. (+) indicates positive and (-) indicates negative interactions. Components and arrows indicated in red are only postulated to be present in plant cells, whereas those in blue indicate known plant defense responses; green indicates plant defense responses also activated by JA, and purple indicates plant protection mechanisms. ACC oxidase, 1-aminocyclopropane-1-carboxylate oxidase; BAG, benzole acid gluco-side;BA2H,benzoleacid 2hydroxylase;CA,cinnamicacid;CHS,chalconesynthase;EFE,ethylene-formingenzyme;HO2 ,hydroperoxylradical; HPDase, hydroxyperoxidedehydrase; GP, glutathione peroxidase; GST, glutathione S-transferase; k, kinase; O2~, superoxide anion; OH , hydroxyl radical; OGA and OGA-R, oligalacturonide fragments and receptor; p, phosphatase; PAL, phenylalanine ammonia-lyase; PGases, polygalac- turonases; PGIPS, plant polygalacturonic acid inhibitor proteins; Phe, phenylalanine; PR, pathogenesis related; Rp, plant receptor protein; SA and SAG, salicylic acid and salicylic acid glucoside; SA*, SA radical; and SOD, superoxide dismutase (Adapted from Hammond-Kosack and Jones 1996).

To date, plants are described to activate different defense mechanisms depending on pathogen lifestyle (Garcia-Brugger et al. 2006). Jasmonic acid- (JA) and ethylene- (ET) dependent defense responses of plants appear to be useful to combat necrotrophic pathogens, whereas the salicylic acid (SA) dependent defense responses are useful against

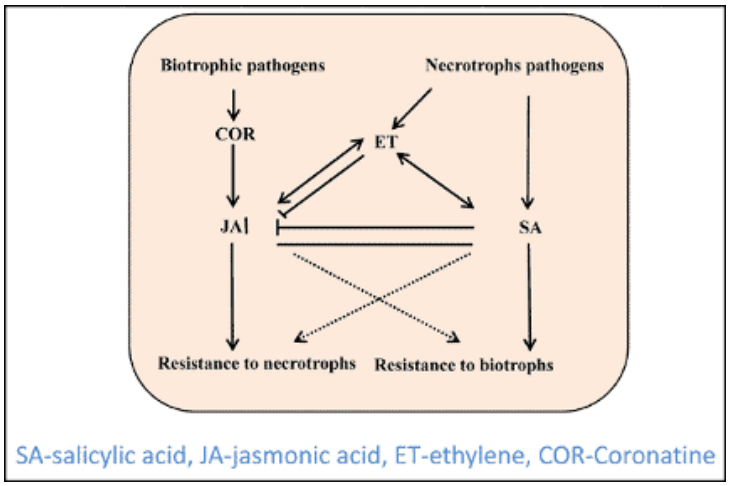

biotrophic pathogens. But what do we know about GTD such as Botryosphaeriaceae described as hemibiotrophic?

Figure 3. Type of defense pathways induced by biotrophic and necrotrophic pathogens. Adapted from Yang et al. 2015.

During their coevolution with pathogens, plants have developed a **set of defense reactions** based on **two levels of immunity according to the zig-zag model** theorized by Jones and Dangl (2006): PTI (PAMP-Triggered Immunity) and ETI (Effector-Triggered Immunity) (Figure 4.).

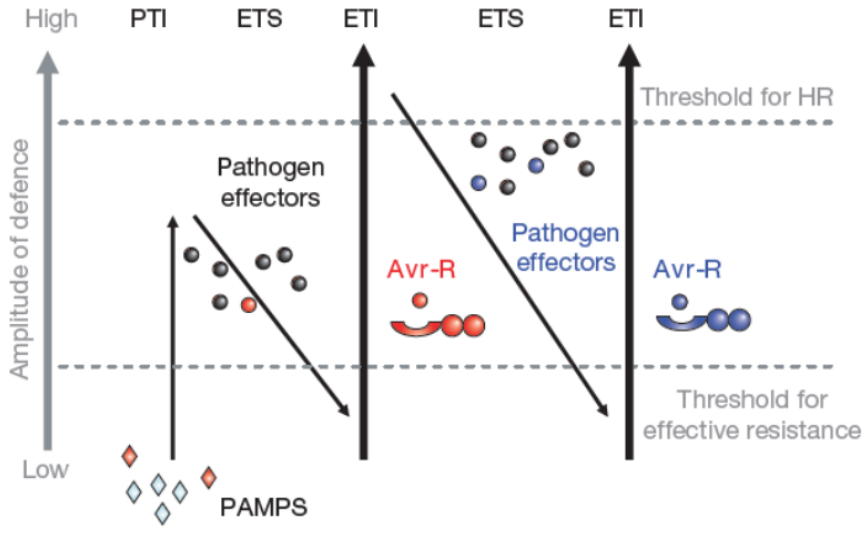

Figure 4. This model of plant immunity consists of four phases. The first phase consists of the recognition by the plant of highly conserved molecules of the pathogens called Pathogen-Associated Molecular Patters (PAMPs). This phase is referred to as PTIPAMP. Some adaptive pathogens are able to bypass the PIl by solving a class of molecules used as drivers, this model is called ETS (Eftector-Triggered Susceptibility). Resistant plants possess resistance The resistant plants have resistance proteins (R) that recognize a given detector and trigger EII (Elector Triggered Immunity). The pathogen can suppress the ETI by various means. The coevolution between health and its pathogenic agent leads to an "arms". The coevolution between health and its pathogenic component leads to an "arms race" that can last for several cycles of bites on the evolutionary scale. The amplitude of the defense reactions associated to the phases of PTI and ETT differ.

indicated on the graph with two thresholds for the development of a resistance and elective against a pathogen. Adapted from Jones and Dangl (2006).

The establishment of a PTI-type immune response requires the recognition of the pathogen molecules (PAMPs or DAMPs) by the plant receptors (PRR). **PAMPs/MAMPs** (e.g., flagellin, lipopolysaccharides LPS, elongation factor EF-Tu, chitin, glucans, etc.) **and endogenous DAMPs** (eg. galacturonic acid, oligogalacturonides) **elicits PTI** (first level of plant immunity) as indicated above: (1) PAMPs/MAMPs are recognized by the host PRR receptors belonging to the class of Receptor-Like Proteins (RLPs) or Receptor-Like Kinases (RLKs) (Naito et al. 2008; Zipfel and Robatzek 2010; Monaghan and Zipfel 2012), as well as endogenous DAMPS, once the plant cells wall are attacked by the pathogen CWDEs (Seong and Matzinger, 2004). It seems that the specificity of PAMP/ PRR recognition is a result of the coevolution of the plant and its pathogen. (2) signaling pathways activating PTI (ROS, ion fluxes and Ca signaling, MAPK/CDPK, activating TF and TF-dependent expression of defense genes. (3) hormonal signaling. (4) activation of TF responsive to hormone and expression of the related TF-dependent defense genes. (5) **PTI leads to the secretion of several types of molecules designed to limit or stop the development of the pathogen** (Wise et al. 2007). The class of molecules most produced under infection conditions is the **Pathogenesis-Related (PR) proteins** (van Loon et al. 2006). This class includes 17 families based on sequence homologies and antimicrobial properties. Among the PR proteins are chitinases that degrade the fungal wall, protease inhibitors that inhibit the activity of fungal CWDEs, etc. Some of them are specific to a pathogen, while others have a broader spectrum of action. PR1 of infected tobacco has strong antimicrobial activity (Van Loon and Van Kammen 1970) and is commonly used as a marker gene for PTI reactions. PR1 antimicrobial properties are related to its ability to physically interact with ergosterols in the plasma membrane of the pathogen's plasma membrane and cause damage (Gamir et al. 2017). **Secondary metabolites** are also involved in defense reactions: phytoalexins (the most abundant antimicrobial compound), terpenes (Avenacin A-1 from oats), alkaloids (tomatine from tomatoes, camalexin from *A. thaliana*) or phenols (pisatine from peas) (Bednarek 2012). **The final means of combating the invasion of a pathogen is the focused secretion of callose**, a glucan polymer secreted by the plant at infection sites to form a physical barrier (Luna et al. 2010). Callose deposits

are also frequently used as a marker for the induction of PTI or its suppression by suitable pathogens.

ETS or effector-mediated repression of defense responses is the second phase of the zigzag model, in response to apoplastic or cytoplasmic effectors. Effectors are known to manipulate the structure or functions of the host cell, and **some of them are recognized by the plant.** Resistant plants were able to resist infection by an adapted pathogen through a highly specific gene-for-gene interaction (Flor 1971, Thakur and sohal 2013, Xu et al. 2020). According to this model, **effectors of the pathogen are recognized by resistance proteins (R) of the resistant plant.** The recognition of this effector leads to a second level of immunity called effector-triggered Immunity (ETI). **The recognized effector is then qualified as an avirulence protein**, and its **recognition leads to a whole set of defense reactions**, including most often a **localized cell death called hypersensitive response (HR)** and the **stopping of the colonization of the plant by the pathogen**. Unlike PTI, which is common to several plants in the same phylogenetic group, **ETI is genotype specific.** Effector recognition is most often mediated by two types of resistance proteins: membrane receptors of the RLP or RLK type, and cytoplasmic proteins Nucleotide-binding/Leucine Rich repeat (NLR). This leads to signaling pathways and the activation of ETI-specific defense reactions (activation of resistance proteins and signaling pathways leading to ETI). In contrast, when either the Avr gene in the pathogen or the R gene in the host is absent or mutated, recognition does not occur and the plant is said to be susceptible, resulting in disease (Flor 1071; De Witt 1995).

In natura, generally, the first infecting pathogen immunizes the plant against further infection by homologous pathogens, even though the plant may not carry a gene that determines crop-specific resistance. If the plant's promptness to resist subsequent attacks by pathogens spreads to the entire plant, the response is called systemic acquired resistance (SAR) to distinguish from the local one (LAR, with strong HR). The development of SAR is often associated with various cellular defense responses as described in Figure 3 (Ryals et al. 1996).

1.4. Fungal trunk diseases: a challenge for grapevine productivity

During their entire lifespan, grapevine (*Vitis vinifera* L.) plants are exposed to a wide variety of pathogens, such as bacteria, viruses, phytoplasmas, fungi and nematodes

(Armijo et al. 2016). Nowadays, grapevine fungal trunk diseases (GTDs) are amongst the main constraints for the productivity of this crop. GTD pathogens can infect and severely damage grapevines from nurseries to mature plants in vineyards (Fig. 5). Once infected, plant productivity is decreased, leading to a plant slow or apoplectic death that causes important economic losses and limits vineyard sustainability (Bertsch et al. 2013; Fontaine et al. 2016; Mondello et al. 2018).

In nurseries, it has been proven that the plant material can be infected with several GTD pathogens from the scion or rootstock mother blocks (Berbegal et al. 2020; Berlanas et al. 2020; Gramaje and Armengol 2011; Gramaje and Di Marco 2015), which can act as a primary source of infection (Edwards and Pascoe 2004; Edwards et al. 2001; Gramaje and Di Marco 2015; Pascoe and Cottral 2000; Waite et al. 2018). Additionally, most nursery fields allow mother vines to sprawl on the ground, which in combination with flood irrigation, can favor new fungal infections (Halleen and Fourie 2016; Hunter et al. 2004; Stamp 2003). In many cases, the presence of GTDs in the scion and rootstock mother plants is not directly related to visible external symptoms, emphasizing the high potential risk of mother vines as an inoculum source for GTD pathogens all along the vegetative propagation process (Aroca et al. 2010; Fourie and Halleen 2004; Hrycan et al. 2020).

GTD pathogens can be detected at various stages of the nursery propagation process. One of the earliest is during the hydration (soaking in water) mainly prior to cold storage, either by the water itself or by field-acquired microorganisms dispersing into the soaking water from one single contaminated plant (Gramaje and Armengol 2011; Waite and Morton 2007). Additionally, several wounds are produced in the nursery process, during disbudding, grafting, or upon root transfer in the field. These large numbers of cuts and wounds make the nursery propagation material very susceptible to infections, providing many entry points for GTD pathogens, both during the nursery process and in nursery fields (Berbegal et al. 2020; Lade et al. 2022; Waite et al. 2018).

Surveys conducted in the main grape growing countries worldwide highlighted that nursery propagation material used for new plantations is mainly infected with fungi involved in **Petri disease** (caused by *Phaeomoniella chlamydospora* and several *Cadophora* and *Phaeoacremonium* species) and **Black foot** (caused by species from *Cylindrocarpon*-like asexual morphs belonging to the genera *Campylocarpon*, *Cylindrodendrum*, *Cylindrocladiella*, *Dactylonectria*, *Ilyonectria*, *Neonectria*, *Pleiocarpon* and *Thelonectria*) (Akgül et al. 2022; Berlanas et al. 2020; Edwards et al.

2007; Gramaje and DiMarco 2015; Guerin-Dubrana et al. 2019). Petri disease and black foot are the two most common GTDs observed in young vineyards (<5 years old) (Gramaje and Armengol 2011). Foliar symptoms associated with both diseases (overall stunting, delayed budbreak, shortened internodes, chlorotic foliage with necrotic margins, and wilting of leaves or entire shoots) can not only overlap but resemble symptomatology associated with abiotic disorders making these diseases hard to diagnose (Gramaje and Armengol 2011). However, Petri disease can be recognized by the presence of a dark-colored sap due to the presence of phenolic compounds in the xylem vessels of trunk, while black foot can be recognized by black, sunken, necrotic lesions on roots and reddish-brown discoloration in the base of the trunk of infected vines (Gramaje and Armengol 2011). Based on these phenotypes, many authors have attributed a drastic increase in grapevine mortality to Petri disease and black foot in new plantings over the last few years (Agustí-Brisach and Armengol 2013; Agustí-Brisach et al. 2016; Aroca et al. 2010; Carlucci et al. 2017). The annual financial cost of the replacement of dead cv Tempranillo plants due to both diseases is estimated to be 7.16 million €/year in La Rioja (northern Spain) (Martínez-Diz et al. 2019).

Indeed, in the nursery fields, many GTDs-infected plants from the propagation process can develop internal symptoms, invisible externally, but allowing pathogens to spread to other plants. New infections can also occur in these nursery fields, as well as in vineyards, yet adding load and pressure from the fungal pathogens by their air-dispersed spores still present in the environment (Fig. 5), such as the ascospores or conidia of many GTD pathogens, which are released from perithecia or pycnidia embedded in the bark and/or on the surface of dead grapevine wood (Eskalen and Gubler 2001; Gramaje et al. 2018; Rooney-Latham et al. 2005; Trese et al. 1980; Úrbez-Torres et al. 2010). Additionally, as non-host specific, many of these pathogens can be found in a wide range of woody perennial crops as new sources of inoculum when they are close to vineyards (Carter 1991; Gramaje et al. 2016; Hrycan et al. 2020; Petzoldt et al. 1983). Favourable environmental conditions for the release of ascospores and conidia are rainy events or high relative humidity, with temperatures above freezing that favour spore germination (Úrbez-Torres et al. 2010; Van Niekerk et al. 2010). Consecutive dissemination of spores is ensured by rain droplets, wind, and arthropods until they reach the cuts or pruning wounds, their major entry points, to germinate and start colonizing new xylem vessels and pith parenchyma cells (Gramaje et al. 2018; Mostert et al. 2006; Moyo et al. 2014) (Fig.5). Depending on the pathogen, wounds can remain susceptible to infection for up to

2 to 4 months (Rolshausen et al. 2010; Van Niekerk et al. 2010). As the wood of diseased vines can be simultaneously infected by various fungal pathogens typically associated with different GTDs, internal and external symptoms can overlap, making them hard to identify. Additionally, GTD pathogens possess an undetermined latency period (asymptomatic status) that can last up to 10 years, leading to a late diagnosis when only considering the visual external plant phenotype, and subsequently making them hard to treat.

In vineyards, the most relevant GTDs affecting young and mature vines are the following:

Eutypa dieback is caused by fungi belonging to the Diatrypaceae family, the most virulent and common of which is *Eutypa lata* (Kuntzmann et al. 2010). Foliar symptoms of Eutypa dieback include stunted shoots with chlorotic leaves that are often cupped and with necrotic margins. The foliar symptomatology is reproduced with purified toxic metabolites secreted by *E. lata* in woody plants (Mahoney et al. 2005; Molyneux et al. 2002; Tey-Rulh et al. 1991). Foliar symptoms can appear 3 to 8 years after infection (Tey-Rulh et al. 1991) and can vary from year to year (Sosnowski et al. 2007). Bunches on stunted shoots ripen unevenly, are small, and in severe cases, the berries shrivel and die. Woody symptoms of Eutypa dieback include cordon dieback, with loss of spurs and internal, necrotic, wedge-shaped staining in the cross-section of cordons and trunks. External cankers appear as the dieback progresses, characterized by flattened areas of the wood with no bark, leading to eventual vine death (Gramaje et al. 2018).

Botryosphaeria dieback (BOT) is caused by Botryosphaeriaceae fungi from the genera *Botryosphaeria, Diplodia, Dothiorella, Lasiodiplodia, Neofusicoccum, Neoscytalidium, Phaeobotryosphaeria* and *Spencermartinsia* (Mondello et al. 2018). BOT often presents as lack of spring growth from affected spurs with shoot dieback, bud, and xylem necrosis (Úrbez-Torres 2011). Pycnidia develop from dead or cankered wood. The main wood symptom of BOT is wedge-shaped perennial cankers, or circular to non-uniform central staining of the wood observed in cross-sections of affected wood (Mondello et al. 2018; Úrbez-Torres 2011). Visible external symptoms can appear in the field only 1 or 2 years after infection (Urbez-Torres et al. 2006) and are mainly observed in mature vineyards (over 8-year-old).

Esca and Grapevine Leaf Stripe Diseases (GLSD) are due to a broad range of taxonomically unrelated fungal trunk pathogens associated with esca diseased vines (Mondello et al. 2018). However, the function of these fungi and how they interact with the primary fungi responsible for disease symptoms is still unclear. The main hypothesis

is that young vines infected with pioneer fungi such as *P. chlamydospora*, *Cadophora* spp. or *Phaeoacremonium spp.* can later develop esca symptoms following a further colonization by several basidiomycetous species from the genera *Inocutis*, *Inonotus*, *Fomitiporella*, *Fomitiporia*, *Phellinus* or *Stereum* (Cloete et al. 2015). Two forms are also known to affect grapevines: chronic (mild) and acute (apoplectic). In the chronic or mild form, called GLSD, the most characteristic foliar symptom is the 'tiger-stripe' pattern, in which leaves display multiple banding discolorations surrounding dry, light, or red-brown necrotic tissue on the leaf blade, often bordered by narrow red or yellow blotches (Surico 2009). The acute or apoplectic form, called "esca proper", is characterized by a sudden wilting of the entire plant or of one arm or several shoots. Leaf symptoms include scorching, dropping, and shriveling. The drying of grape clusters is also frequently observed (Mugnai et al. 1999). Foliar symptoms of both forms of esca appear in late spring or summer and can vary from year to year. Cross-sections of esca affected trunks reveal a variety of internal woody symptoms, such as black spots in the xylem, eventually surrounded by pink to brown discoloration of the wood, brown to black vascular streaking, or dry wood with a silver appearance. In oldest vines, the wood may develop a white to soft yellow rot (Fischer 2002).

Phomopsis dieback (PD) can be caused by species of the genera *Diaporthe* (Baumgartner et al. 2013; Dissanayake et al. 2015; Úrbez-Torres et al. 2013). Among them, the most frequent species isolated of this genus in Europe are *D. eres* and *D. ampelina* (syn. *Phomopsis viticola*) (Guarnaccia et al. 2018). Both species are shown to be pathogenic on grapevine (Guarnaccia et al. 2018). The most characteristic symptoms attributed to PD include perennial cankers in the framework of the vine and lack of budbreak from infected spurs (Úrbez-Torres et al. 2013).

Cytospora canker is caused by *Cytospora* species, known to be destructive to over 85 woody plants (Adams et al. 2005, 2006; Sinclair et al. 1987). They colonize the periderm and underlying sapwood of Angiosperms, causing brown/black discolouration of the wood and loss of hydraulic conductivity within the xylem. However, it was not long ago that this genus has been associated with diseased grapevines. Fotouhifar et al. (2010) reported two *Cytospora* species, isolated from diseased or dead grapevine wood in Iran, although the pathogenicity of these two species was not tested. Species like *Cytospora chrysosperma* (Adams et al. 2006) were isolated from symptomless grapevine wood and was thus classified as endophytes by Gonzalez and Tello (2011). Therefore, over a long time, *Cytospora* species were not considered as grapevine pathogens, and were not

associated with GTDs. However, recent studies have characterized pathogenic *Cytospora* isolates such as *C. chrysosperma* from wood cankers of declining grapevines as pathogens that cause symptoms like those of other GTDs (Arzanlou and Narmani, 2015). New *Cytospora* species were further characterized as pathogenic to grapevine in America (*C. viticola* and *C. vinacea*) and Turkey (*C. viticola*) as indicated by Lawrence et al. (2017) and Oksal et al. (2020). More studies are now required to better understand the interactions between Cytospora canker and that of other GTD pathogens. The epidemiology of Cytospora canker has been deeply studied in other woody plants, and this information might help to guide future research on the spread of this disease in vineyards. As *Cytospora* species are primarily wound pathogens in tree crops (Biggs, 1989), they may infect vines through the pruning wounds generated on grapevines every season.

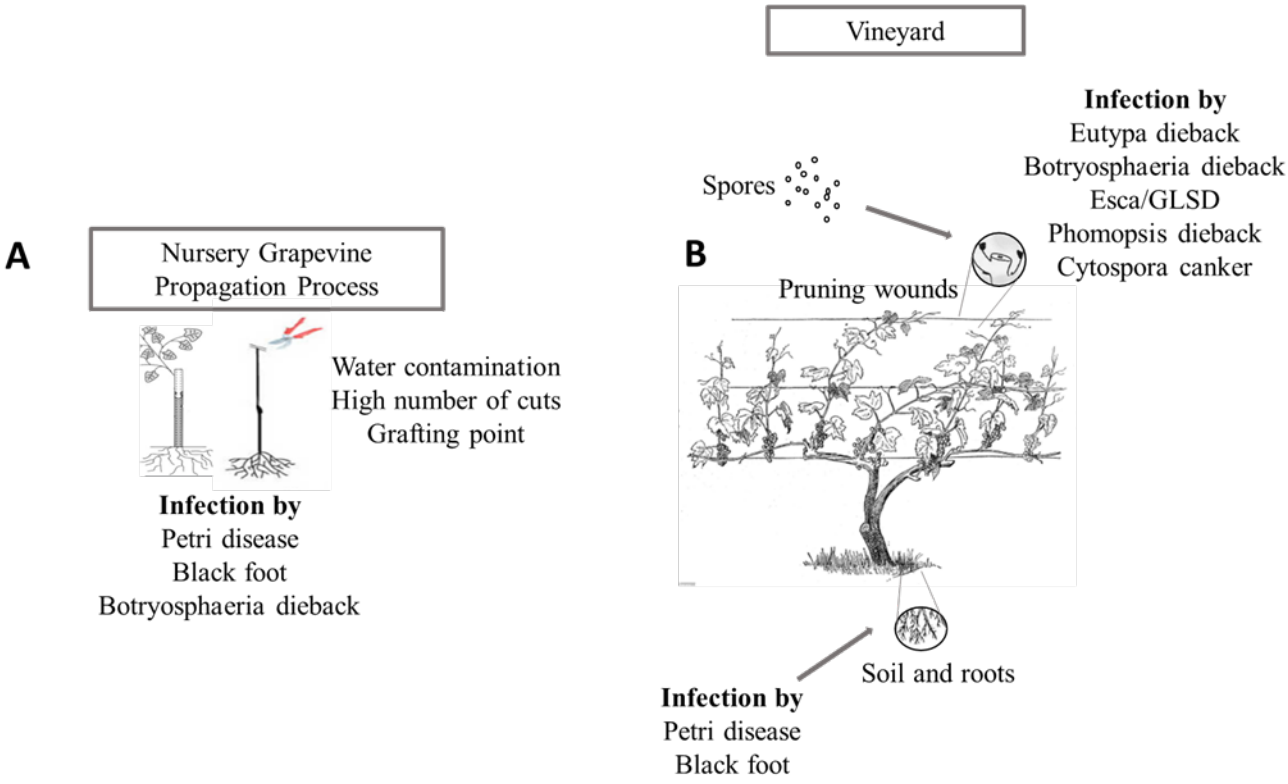

Figure 5. GTD infections during grapevine life cycle from (A) Nursery grapevine propagation process to (B) Nursery fields and mature grapevines in vineyards.

1.5. Are there any cultivar traits of tolerance or susceptibility of *Vitis vinifera* against GTDs?

V. vinifera* subsp. *vinifera (more simply referred to as *V. vinifera*) results from a human domestication to select morphological characteristics that favor grapevine cultivation and exploitation. Propagation of *V. vinifera* varieties gave preferences to the largest, juiciest, and tastiest berries, to gradually select identical grape varieties (a population for a variety). Grape varieties can also result from selections and crosses between local wild plants and plants already selected. Therefore, from *V. vinifera* subsp. *vinifera*, the various grape varieties make up the vast range of vine varieties cultivated worldwide, with more than 6,000 "cultivars" or “cépages” (a botanical term for varieties of plant species obtained by crossing and cultivated). Genetic diversity is thus generally preserved within a cultivar genome of *V. vinifera*, except when mutations may accumulate over time to generate distinguishable clones and significantly increase the genomic variability (Franks et al. 2002; Riaz et al. 2002; Zhou et al. 2019).

Nowadays, *V. vinifera* is present worldwide, the most concentrated areas being: Central and Southern Europe, Western and Middle East of Asia, China, Mediterranean coast of Africa, South Africa, North America, South America, Australia, and New Zealand (Figure 6A). Current patterns of genetic variation in *V. vinifera* grapes are associated with geographic and climatic variation (Magris et al. 2021). Distribution of GTDs around the world (Figure 6B) also depends on geographic and climatic variations (Kenfaoui et al. 2022; Songy et al. 2019).

A **B**

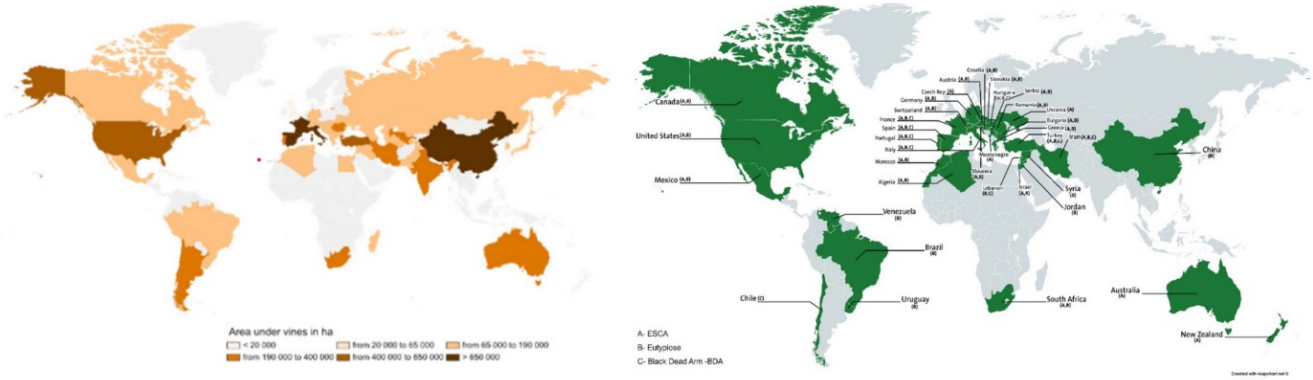

Figure 6. A. Area under vines in 2018 (OIV), B: Global distribution of grapevine fungal trunk diseases (Kenfaoui et al. 2022).

Considering that both (i) genotype diversity within grapevine varieties, cultivars or even clones, and (ii) GTD distribution and pressure, depend on the geographical area, it could be important to deeply consider the *V. vinifera* genomic traits to better combat GTD pathogens worldwide, for instance by investigating a genomic comparison of vines from distinct geographical/climatic areas. Additionally, as cultivated grapevines are mainly grafted propagated (> 80%), their genetic diversity could be further increased, by both the scion (aerial part of the grafted plant, variety) and the rootstock (underground part of the grafted plant) (Ollat et al. 2014; Songy et al. 2019).

The susceptibility of cultivars to GTDs has been studied (Bertsch et al. 2013; Borgo et al. 2016; Fussler et al. 2008; Martínez-Diz et al. 2019; Murolo and Romanazzi 2014; Songy et al. 2019; Sosnowski et al. 2007; Travadon et al. 2013). Some cultivars could be considered susceptible to some GTDs such as Chardonnay and Merlot due to the higher proportion of symptomatic vines observed under specific climatic conditions (Andreini et al. 2009; Bruez et al. 2013; Christen et al. 2007; Murolo and Romanazzi, 2014). Grapevines with small xylem vessels appear less prone to express leaf symptoms due to limited xylem cavitation (induced by drought), and thus tend to be more resistant to some GTDs, such as Petri disease and Eutypa dieback (Pouzoulet et al. 2014; Ramsing et al. 2021). Rootstocks play an important role in grapevine production for their capacity to promote plant protection against pathogens and abiotic stress (drought, waterlogging, adaptation to different soils, nutrients intake, etc.), and to influence the scion vigor and grape composition (Chacón-Vozmediano et al. 2021; Gindro et al. 2003; Larignon and Dubos, 1997; Marchi 2001; Marín et al. 2021; Monteiro et al. 2013; Songy et al. 2019; Yıldırım et al. 2018). In a study of wood necrosis in rootstock mother vines, Liminana et al. (2009) determined that rootstock 1103 Paulsen was the least susceptible to GTDs (33% mean percent necrotic area) and 101-14 MGT was the most susceptible (71% mean percent necrotic area). Murolo and Romanazzi (2014) also noted that vines grafted to the drought tolerant 1103 Paulsen rootstock had lower incidence of esca symptoms than those grafted to SO4.

V. vinifera* subsp. *sylvestris (more simply referred to as *V. sylvestris*) is another subspecies of *V. vinifera* that includes populations returned to the wild. A great genetic

diversity was also observed within *V. sylvestris* varieties, depending on the soil, the environment, and the local climate (Regner et al. 1998). For GTDs, Guan et al. (2016) reported that populations of *V. sylvestris* provide interesting genetic resources for breeding new strategies with enhanced resistance to BOD. Comparing *V. vinifera* and *V. sylvestris* susceptibility responses to Botryosphaeriacaea infection, revealing a concept in which the phenylpropanoid metabolism of resistant genotypes is rapidly and specifically channeled to bioactive stilbenes (Khattab et al. 2021). Resistant lines would thus accumulate specific bioactive stilbenes such as viniferine trimers, to contrast with susceptible genotypes accumulating significant higher proportion of glycosylated stilbenes (Khattab et al. 2021).

1.6. Events that occur between the time spores of GTD pathogens encounter the plant and the appearance of symptoms: focus on Botryosphaeriaceae and their virulence factors.

In the Botryosphaeriaceae, asexual reproduction is the most common mode of reproduction (Baskarathevan et al. 2012a; Phillips et al. 2002; Van Niekerk et al. 2006). As indicated in the part 1 and in Figure 7, ascospores of GTD pathogens infect grapevines through pruning wounds, grafting wounds or natural wounds, and colonise the woody tissues. These wounds are entry points over a long period of time and natural inoculation depends on environmental conditions (time of year, climatic conditions).

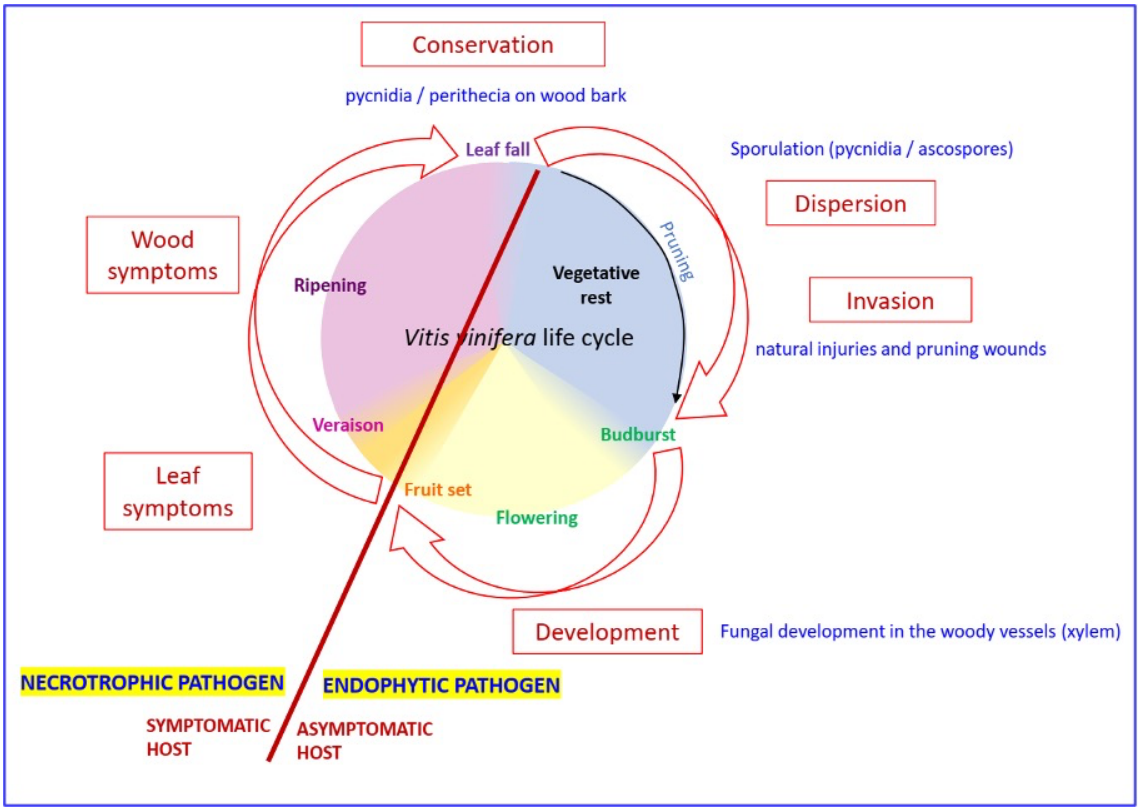

Figure 7. Life cycle of *Botryosphaeriaceae* in relation to the development cycle of the vine. Adapted from Larignon et al. (2001).

Botryosphaeriaceae can remain latent as endophytes until the host plant is exposed to stress (Dakin et al. 2010; Hrycan et al. 2020; Slippers and Wingfield 2007). As heterotrophs, they use cell wall degrading enzymes (CWDEs) to take nutrients from the host showing no signs of disease (Giovannoni et al. 2020). Among CWDEs classified as carbohydrate active enzymes (CAZy) are those attacking lignin (ligninases such as laccases, polyphenol-oxidases, manganese peroxidases), cellulose (such as glucanases, cellobiohydrolases, glucosidases), hemicellulose (hemicellulases such as xylanases, xylosidases, arabinofuranosidases), and pectin (pectinases such as polygalacturonases, pectate lyases).

Several endophytic fungi are ubiquitous and can therefore colonise different hosts according to two modes of transmission: (1) vertical transmission (hypha penetration into a seed, pollen grain or propagule of the host plant) characterised by the colonization of a new progeny host of the primary host. The endophytic fungus remains genetically identical (propagation by asexual reproduction). (2) Horizontal transmission is characterised by the colonization of a new host that is usually unrelated to the primary

host. It proceeds from the dissemination of spores by a dispersal vector. After germination, the hypha penetrates the new host either through the stomata or by direct penetration through the epidermis (Rodriguez et al. 2009). Most species with endophytic stage, such as *Botryosphaeriaceae*, present a horizontal mode of transmission (Rodriguez et al. 2009; Slippers and Wingfield 2007).

Fungal endophytes are described to interfere with plant ecology, fitness, and evolution (Rodriguez et al. 2009; Slippers and Wingfield 2007). Depending on the environmental conditions and the physiological state of the host, the lifestyle of the fungus can change from endophyte to necrophyte parasite. This type of pathogenic fungus is called hemibiotroph (Rajarammohan 2021). It is pathogenic in its necrotrophic state in the case of the hemibiotrophic *Botryosphaeriaceae,* with an intracellular growth that distinguish them from the true necrotrophic pathogens, considered as "extracellular hemibiotrophs" (Rajarammohan 2021). During its endophytic lifestyle, the hemibiotroph can positively impact its host (Kogel et al. 2006). During its necrotrophic phase, the hemibiotroph has a negative impact on its host in the short or long term through an excess of deleterious nutrients on the host (such as phytotoxins and other virulence and pathogenicity factors). Depending on the biotope and environmental conditions, fungal species could adopt several modes of life during its existence (Kogel et al. 2006). This is particularly the case of endophytic *Botryosphaeriaceae* species, such as *Neofusicoccum parvum* which is considered as pathogenic once turning necrotroph (Figure 8).

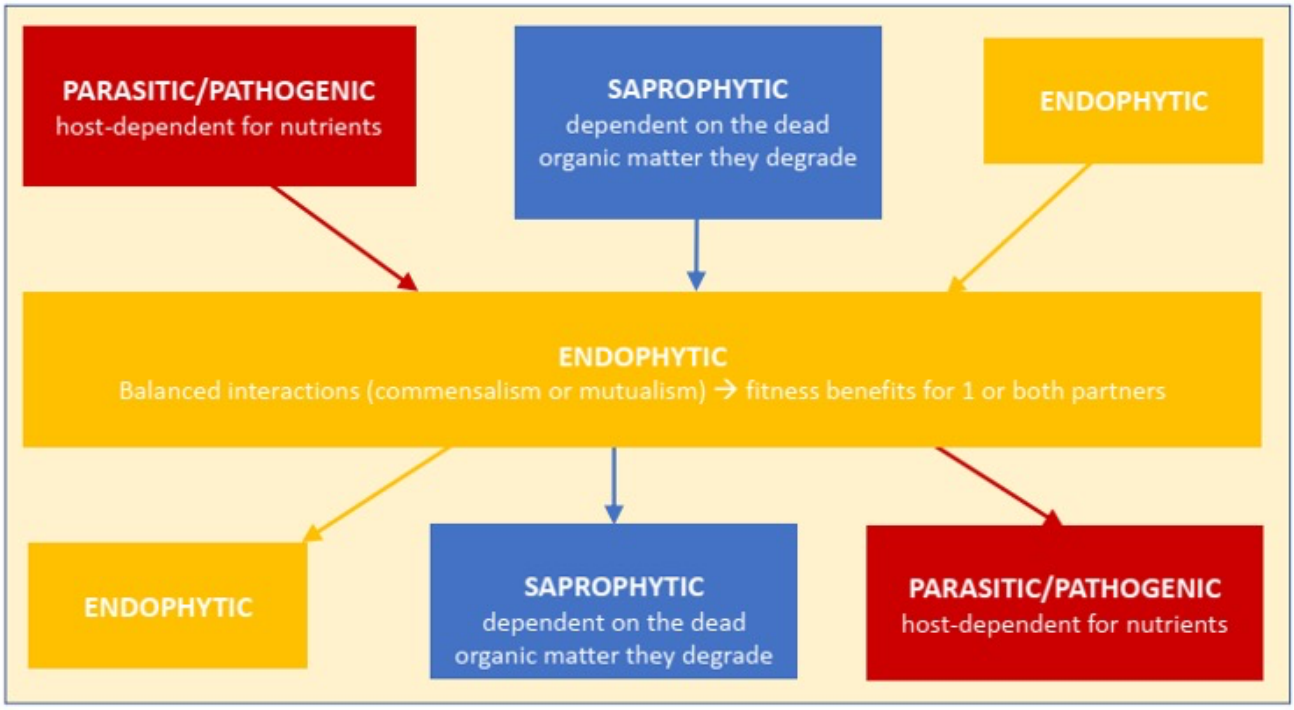

Figure 8. Life cycle of *Botryosphaeriaceae* in relation to the development cycle of the vine. Adapted from Larignon et al. (2001).

Switching its lifestyle ("bang-mixed" to "bang-bang" strategies) would allow the pathogen to increase its aggressiveness to complete its life cycle and thus ensure its population survival when it senses a decrease in the size of the plant resource pool depending on biotic and abiotic pressures (Andanson et al. 2010). The "bang-mixed" strategy operates when the host resources are considered inexhaustible, and only limited by the maximum number of energy channels (suction ways) that the pathogen can develop. In this case, the infection strategy is first characterised by a latent phase entirely dedicated to intra-host growth, followed by an infectious period, where part of the energy is allocated to spore production and the other part to the maintenance of intra-host multiplication structures, whose density remains constant. For the "bang-bang" strategy (aggressive infection), the pathogen senses a finite resource pool, thus a fixed size since the beginning of the infection. In this case, the infection strategy is first characterised by a latent phase dedicated to intra-host growth, followed by an infectious period switching energy exclusively towards the production of spores (avoidance of any extinction risk), thus leading to a decrease in the intra-host multiplication structures.

Plant genotype can impact the size of the resource pool depending on the metabolic changes induced upon environmental changes (Cordovez et al. 2019). Pathogen aggressiveness can thus adapt to the plant susceptibility/responses to its environment. Severity of disease symptoms were reported to vary with grapevine cultivars, inoculated tissues, and abiotic conditions (Chacon et al. 2020; Leal et al. 2021b; Ramirez-Suero et al. 2014; Spagnolo et al. 2014; Songy et al. 2019; Urbez-Torres 2011).

Pathogen genotype can parallely acquire new traits to ensure its survival and fitness (lifespan, way of reproduction, dispersal, spore germination, etc.) upon abiotic and biotic changes. We can thus speculate that hemibiotroph could constitute a transition towards necrotrophy, which would represent their evolutionary achievement (Horbach et al. 2011). In a changing environment with selection pressures, only one part of the fungal population succeeds to reproduce, thanks to acquired traits (e.g., tolerance to temperature changes, resistance to xenobiotic, etc.). Research is still in progress to better understand pathogen adaptation and aggressiveness to environmental factors both *in planta* and *in vitro*, focusing on fungal morphology, physiology and behaviour leading to survival and adaptability. Analyses need to be strengthened to better understand the weight of genetic polymorphism in the adaptation and aggressiveness of pathogens in a changing environment, to ensure its survival (Trotel-Aziz et al. 2022).

Among pathogenic factors are CWDEs, phenolic phytotoxins (toxins), growth regulators (hormones), effector proteins, and fungal viruses (Peng et al. 2021). Incompatible interactions would thus enable the plant metabolism to react against the pathogen and related associated motifs (PAMPs, Pathogen-Associated Molecular Patterns, e.g., effector proteins) thanks to external plant receptors PRRs (Plant pattern Recognition Receptors) that should be able to elicit a first level of plant immunity (PTI, PAMP triggered immunity). Research on these extracellular aspects remains to be deeply explored for GTD pathogens. To date BOT symptoms are described to result mainly from the synergistic actions of CWDEs and phytotoxic metabolites produced and secreted by these fungi inside the plant cells (Abou-Mansour et al. 2015; Masi et al. 2018; Salvatore et al. 2021; Stempien et al. 2017; Trotel-Aziz et al. 2019, 2022). BOT fungi are indeed only detected in wood (entry through CWDEs), but never in symptomatic leaves (Larignon et al. 1997), whereas phytotoxins are suspected to be involved in the production of foliar symptoms once transported from the infection site to the leaves via the xylem (Mugnai et al. 1999).

In general, effectors secreted by pathogens (eg. secondary metabolites (SM) such as phytotoxins) can suppress plant triggered immunity (such as PTI) responses and facilitate plant colonization, by targeting plant susceptibility (S) proteins, resulting in an effector-triggered susceptibility (ETS) (Li et al. 2020a; Peng et al. 2021; Van Schie and Takken 2014). Literature also describes a second layer of defenses, involving plant resistance (R) proteins (eg. nucleotide-binding leucine-rich repeat proteins, NLRs) able to recognize and detoxify the pathogen-produced effectors, resulting in effector-triggered immunity (ETI) (Jones and Dangl 2006; Kourelis and Van der Hoorn 2018; Peng et al. 2021). But to evade such effector recognition, pathogens can undergo loss or mutation of the corresponding effector genes (Jones and Dangl 2006). Pathogens and plants are thus evolving in a perpetual arm race due to relatively fast evolution of effectors, as well as of the R and S proteins (Jones and Dangl 2006; Peng et al. 2021; Rouxel and Balesdent 2017; Rouxel et al. 2011). Effectors increasing virulence are called virulence factors, while effectors recognized by R proteins are called avirulence factors (Avr proteins) (Peng et al. 2021; Stotz et al. 2014).

Focusing now on Botryosphaeriaceae species, several phytotoxic SM are produced and have already been identified (Table 1), but their specific roles in the infection process remain to be clarified (Abou-Mansour et al. 2015; Andolfi et al. 2012; Djoukeng et al. 2009; Evidente et al. 2010; Larignon et al. 1997; Masi et al. 2018; Reveglia et al. 2019, 2020; Salvatore et al 2021; Trotel-Aziz et al. 2019, 2022). In general, phytopathogenic toxins are mostly low-molecular-weight SM that can produce specific symptoms such as wilting, growth inhibition, chlorosis, necrosis, and leaf spotting (Yin et al. 2016). At very low concentrations, phytopathogenic toxins are described to act on cell membrane, mitochondria, chloroplasts, and to inhibit the synthesis of proteins and nucleic acids in the host plant, resulting in physiological disorders, cell death, and even death of the plant itself (Peng et al. 2021; Shang et al. 2016; Soyer et al. 2015; Zeilinger et al. 2016).

Table 1. Biosynthetic Gene Clusters (BGCs) involved in Secondary Metabolism (SM) of the *Neofusicoccum parvum* isolate Np-UCR-NP2-v3 showing significant similarities (>30%, protein level) with SM gene clusters from other fungi. The genome sequence of the reference isolate Np-UCR-NP2-v3 was analyzed with AntiSMASH fungal version, with defaults parameters (Blin et al. 2019). **Adapted from Trotel-Aziz et al. (2022).**

Gene Type	Most similar known cluster	Similarity with known BGCs
NRPS	dimethylcoprogen hexadehydroastechrome / terezine-D / astechrome	100% 37%
NRPS,T1PKS	pyranonigrin E ilicicolin H	100% 50%
T1PKS	azanigerone A terremutin/terreic acid melanin (-)-mellein alternapyrone patulin	33% 44% 100% 100% 60% 33%
terpene	dimethylcoprogen	100%

According to Li et al. (2020), it is reasonable to assume that hemibiotrophic pathogens such as *Botryosphaeriaceae* have already acquired the potential to inhibit the plant's defense responses during their endophytic phase, thus before confronting any plant immune system. To do that, appressorium are useful structures enabling pathogen temporal advance (effector accumulation) to bypass plant defenses, by secreting these effectors simultaneously with the plant's perception of the pathogen. Especially since no R proteins were yet identified in grapevine to stop BOT. Maybe it can be explained by the high level of polymorphism in genes involved in phytotoxin synthesis, such as (-)-terremutin and (*R*)-mellein biosynthesis among *N. parvum* isolates (Trotel-Aziz et al. 2022). This high level of genetic variations within a species, could be a consequence of the evolution and adaptation of *N. parvum* to its biotic environment (Garcia et al. 2021). It is important to remind that *N. parvum* is described as a highly aggressive plant pathogenic fungus of the *Botryosphaeriaceae* family (Larignon et al. 2015; Urbez-Torres 2011). Additionally, Trotel-Aziz et al. (2019, 2022) highlighted that, once inside the plants, phytotoxins succeed to weaken grapevine immunity to promote BOT symptoms. Altogether, these recent results strongly suggest that (1) the *N. parvum* phytotoxins are effectors that trigger ETS in grapevine, and that (2) grapevine alone would not succeed to combat BOT, pointing that beneficial microorganisms could be helpful to compensate such grapevine weakness.

Genetic differences also exist among the isolates of *N. parvum* that are described as a highly aggressive plant pathogenic fungus of the *Botryosphaeriaceae* family (Larignon

et al. 2015; Úrbez-Torres 2011), especially regarding genes involved in phytotoxin biosynthesis (Trotel-Aziz et al. 2022).

1.7. Grapevine protection and defenses when facing pathogens leading to GTDs: focus on *N. parvum.*

When exposed to GTDs, grapevine symptoms (as indicated in part 1; i.e., delayed budburst, stunted development, leaf chlorosis, stem necrosis, canker, dead branch to full plant death) can vary depending on the pathogen genotype.

Focusing on three *N. parvum* isolates (*Np*-Bt67*, Np*B *and NpB*-UV9) differing in their aggressiveness and SM profiles, *Np*-Bt67 was characterized by its ability to produce large amount of (-)-terremutin without (*R*)-mellein and is the most pathogenic on Chardonnay grapevine (Trotel-Aziz et al. 2022). It causes strong BOT symptoms (dead branch) within 10 days on grapevine cuttings (Leal et al. 2021b; Trotel-Aziz et al. 2019). *Np*B produced mid-amounts of both (*R*)-mellein and (-)-terremutin, while *Np*B-UV9 produced large amount of (*R*)-mellein without (-)-terremutin, and both were less pathogenic isolates on grapevine (stem necrosis without dead branch) than *Np*-Bt67 (Trotel-Aziz et al. 2022). Comparing the effects of fungal isolates and purified (-)-terremutin on cuttings, authors suggested that (-)-terremutin and (*R*)-mellein would act more as a virulence factors (i.e. increasing quantitatively the disease) than as pathogenicity factors (i.e. required to trigger the disease) upon infection (Chooi et al. 2015; Reveglia et al. 2020; Trotel-Aziz et al. 2022).

Despite they differed in their aggressiveness, the wild-type isolates *Np*-Bt67 and *Np*B displayed similar trends in plant defenses induction: an up-regulation of salicylic acid (SA) responsive genes (*PR2*, *PR5* and *PR10*), while the expression of jasmonic acid and ethylene (JA/ET) responsive genes was either unaffected or moderately up-regulated (Trotel-Aziz et al. 2022). Yang et al. (2015) reported that the plant SA-dependent defenses are not helpful to combat necrotrophic fungi and that SA-signalling could antagonize the expression of the useful JA-responsive defenses, resulting in facilitation of disease development. Among upregulated genes during cuttings infection with pathogens, are also those encoding for enzymes involved in the biosynthesis of antimicrobial phytoalexins (*PAL*, *STS*) and in detoxification process (*GST1*) (Trotel-Aziz et al. 2022). *GST1* is also strongly upregulated in plantlets treated with (-)-terremutin, therefore suspected to ensure detoxification of this phytotoxin (Trotel-Aziz et al. 2022).

In contrast, phytotoxins supply to plantlets repressed the expression of *CHI* (chalcone isomerase involved in flavonoid synthesis), while they did not impact the expression of *PAL* and *STS* known to produce phytoalexins potentially metabolizable by Botryosphaeriaceae (Stempien et al. 2017). Trotel-Aziz et al. (2022) further suggested that (-)-terremutin could inhibit the expression of flavonoid pathway to favour the stilbene production (since they share a common precursor), resulting in enhancing pathogen fitness. Additionnally, these auhors demonstrated that (-)-terremutin weakened the expression of the useful host JA-dependent-defenses, confirming therefore that (-)-terremutin production by *N. parvum* would support the pathogen own development in infected grapevine tissues by interfering with host defenses. Finally, these authors suggested that *GST1, PR2*, *PR3*, *PR4*, *PR5* and *PR10* are useful defenses against *N. parvum*, being the most up-regulated in response to the most aggressive *Np-Bt67* isolate, while not at all upregulated in plantlets treated with (-)-terremutin (except *GST1* as explained above). They also hypothesized that the repression of *PR1* could be beneficial for plant protection against *N. parvum*, since *PR1* was only down-regulated in response to the less aggressive isolate *NpB*, while it was up-regulated by both phytotoxins. Regarding the responsiveness of these genes to hormones, *PR1*, *PR5* and *PR10* are described to be regulated by SA (Caarls et al. 2015; Dufour et al. 2013; Naznin et al. 2014), *PR3* and *PR4* by JA/ET, and *PR2* by various phytohormones such as SA, JA/ET, and abscisic acid (ABA) (Liu et al. 2011).

Comparing cultivars with distinct susceptibility to GTDs (Chacon et al. 2020; Fontaine et al. 2016b; Reveglia et al. 2021; Travadon et al. 2013), an early detection of defense compounds (such as the PR2 and PR5 proteins) was observed in tolerant genotypes (Claverie et al. 2020; Spagnolo et al. 2014). A greater susceptibility to BOT has also been reported for Tempranillo compared to Chardonnay (Cobos al. 2019; Leal et al. 2021b; Luque et al. 2009). Leal et al. (2021b) indicated a greater constitutive expression of some targeted defense genes in Tempranillo compared to Chardonnay (eg. SA-responsive genes), even upon challenge with *Np-Bt67*, possibly explaining Tempranillo's highest susceptibility to BOT. Authors conclude that grapevine susceptibility to BOT is cultivar-dependent and suggest that a possible high basal content of SA in Tempranillo could explain its highest susceptibility to *N. parvum*. Indeed, JA is described as useful to combat necrotrophs, but many studies have reported that endogenously accumulated SA antagonises JA-dependent defences, thus prioritising SA-dependent resistance over JA-dependent defence (Pieterse et al. 2012; Van der Does et al. 2013). Supporting this

hypothesis, Leal et al. (2021b) highlighted a common feature for both cultivars: SA-dependent defences were strongly decreased in plants protected by an additional supply of beneficial microorganisms acting as biocontrol agents (BCA; see Part 6 for more details about BCA), to contrast with symptomatic plants. Lacking self-defence means, the plant can ultimately opt for an avoidance strategy, by inducing a dead branch to confine the BOT fungi. But this strategy may emerge late once the plant is infected by a cryptic pathogen that can modulate its host cellular environment, for instance by producing oxalic acid that may suppress the initiation of the host cell death in the early stages of infection (Rajarammohan 2021; Williams et al. 2011). Fortunately, following pathogen infection and CWDE activities, plants can recognize neoproduced DAMPs (Damage Associated Molecular Patterns) as signalling molecules able to activate death signaling and turn resilient (Hou et al. 2019). As for a systemic acquired resistance (SAR) triggered by a tolerant/resistant plant upon a pathogen attack (Durrant and Dong 2004; Shine et al. 2019), DAMPs can mediate an immune priming in the distal cells and tissues, to prevent pathogen progression. DAMPs are perceived by plasma membrane localized receptors, whose activation leads to the initiation of signaling cascades (e.g., MAPK, Ca^{2+}) and transcriptional reprograming (Hou et al. 2019). DAMPs can be peptides, ATP, proteins released from damaged cells, and degraded cell wall polysaccharides that function as PTI amplifiers (Hou et al. 2019). Among peptide signaling molecules are systemin and pep1 able to trigger JA biosynthesis, and related systemic defenses against a fungal pathogen. Among ATP is the extracellular adenosine 5-triphosphate (eATP) that can also modulate the expression of genes involved in SA and JA signalling once eATP was perceived by the lectin receptor kinase DORN1 (DOes not Respond to Nucleotides) that induces the PTI-like signalling processes. The co-factor NAD^+ is also a host-derived-elicitor of immune signalling able to activate PTI-like responses, especially those specific to SA. Among proteins from damaged plant cell is HMGB3. Among degraded polysaccharides from damaged plant cell are oligogalacturonides (OGs), cellooligomers, xyloglucan and oligosaccharides, methanol. Functioning as PTI amplifier, DAMPs signaling is essential to compensate MAMP (Microbial-Associated Molecular Patterns) signaling when MAMP-triggered defenses are compromised by a malfunctioning/disappearance of natural endophytic beneficial microorganisms (see Part 6 for more details about BCA and related MAMPs).

Altogether, little information exists to establish a list of potential markers of grapevine cultivar resistance or tolerance to GTD pathogens, especially considering that the pathogen bypasses the plant's useful defences, leaving it defenseless since the plant alone seems to have no useful means of self-defence (Figure 9). Currently, Leal et al. (2021b) clearly established that SA-dependent defenses are strongly decreased in plants protected by BCAs and stated that complementary approaches are in progress to highlight any useful changes induced by BCAs in cultivars to protect them against GTDs, considering both repressed and induced responses.

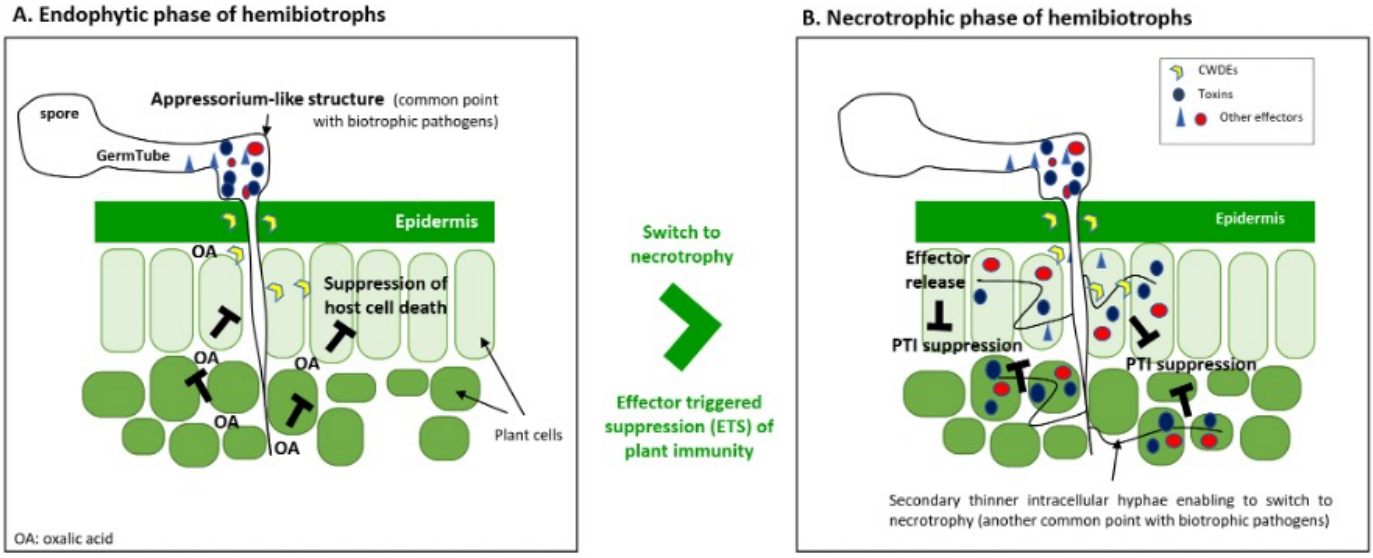

Figure 9. Suspected mode of colonization of hemibiotrophic fungal pathogens such as *Neofusicoccum parvum* in grapevine. **(A)** Endophytic phase of hemibiotrophic fungus forms an appressorium that develops hyphae (haustorium) enabling to store phytotoxins, but also to deliver cell wall degrading enzymes (CWDEs, to obtain nutrients from the living tissue) and OA (oxalic acid, or equivalent molecule, to prevent host cell death). **(B)** Necrotrophic phase of hemibiotrophic fungus starts with the formation of secondary thinner intracellular hyphae able to deliver effectors such as phytotoxins into the host, to prevent the PTI (PAMPs Triggered Immunity) by suppressing the useful host defenses, resulting in the host death rapidly. Hyphal penetration is facilitated by the dissolution of the host cell wall by an increased secretion of CWDEs. Efforts to identify and characterize determinant early-stage effectors, or to confirm the determinant value of those previously cited, still need to be deeply investigated to search for effectors potentially recognized by the host surveillance system (R-genes), and thus pave the way for gene-for-gene

resistance and self-combat against hemibiotrophic pathogens. Adapted from Pradhan et al. (2021).

1.8. Does GTD pathology may ultimately depend on a fine tune regulation of grapevine microbiome?

Considering that grapevine alone has no useful means of self-defense, whereas it can be strongly protected when treated with beneficial microorganisms, we can wonder about the importance of its microbiome and microbiota in their protective effects against GTDs. Indeed, besides fungi, the endophytic bacterial and viral microbiome of grapevine and their roles in GTDs are largely unexplored (Bettenfeld et al. 2021; Nerva et al. 2022).
Few studies have compared the composition of the microorganism community in asymptomatic and symptomatic vines. Fotios et al. (2021) provided evidence that GTD symptomatic plants support a specific wood microbiome, showing cultivar and biogeography-dependent patterns, possibly useful to discriminate healthy from diseased vines. They also pointed out the strong interactions between the bacterial and fungal wood microbiome in asymptomatic vines, which still need to be investigated deeply to find out new bacterial BCAs. Nerva et al. (2019) characterised the microbiome from grapevines showing or not esca symptoms and found more than 100 distinct fungal isolates from 20 different families, in symptomatic plants compared to asymptomatic plants. They also reported 38 new mycoviruses, some capable of infecting grapevine trunk pathogens. Del Frari et al. (2019) also investigated the mycobiome of grapevines wood in a vineyard with history of esca. They identified 289 taxa, including five genera reported for the first time in association with grapevine wood symptoms of esca (*Debaryomyces, Trematosphaeria, Biatriospora, Lopadostoma,* and *Malassezia*). Interestingly, the mycobiome qualitative and quantitative composition of the woody tissue in proximity to symptomatic leaves, as well as in symptomatic canes, was highly similar to that in the woods of plants not exhibiting yet leaf symptomatology. This observation supports the current understanding that leaf symptoms are not directly linked with the sole presence of pathogenic fungal communities in the woods. In good accordance, *Botryosphaeriaceae* are described as non-pathogenic endophytes before switching pathogenic (once necrotroph). Altogether, these recent results strongly suggest that endophytic microorganisms (beneficial bacteria

and beneficial fungi) and/or virus are key partners to consider conditioning the grapevine health status once infected by a fungal pathogen responsible of GTDs.

Focusing on the bacterial genera from asymptomatic and symptomatic Greek grapevines, Fotios et al. (2021) identified a strong enrichment of *Bacillus* (and widely of members of the family Bacillaceae) and *Streptomyces* in the former asymptomatic. This enrichment was particularly prominent in the cv Xinomavro and Agiorgitiko, while in Vidiano both *Bacillus* and *Corynebacterium* were ubiquitous. Bruez et al. (2015, 2020) also identified *Bacillus* spp. as major components of the wood bacterial community in vines, but they did not observe any significant differentiation in their abundance between symptomatic and asymptomatic plants. The prevalence of *Bacillus* and *Streptomyces* genera in asymptomatic plants (Fotios et al. 2021), coexisting with the GTD pathogens *Phaeoacremonium, Phaeomoniella* and *Seimatosporium*, suggests the capacity of these bacterial genera to act as BCAs in several plants including grapevines (Alfonzo et al. 2009, Viaene et al. 2016). Indeed Rezgui et al. (2016) and Haidar et al. (2016) reported a high suppressive activity of native endophytic *Bacillus* strains isolated from vines against several GTD-related pathogens, like *P. chlamydospora, Lasidiodiplodia pseudotheobromae, N. parvum* and *Schizophyllum commune*. Endophytic *Streptomyces* were also isolated from asymptomatic grapevines, then shown to prevent the development of *P. chlamydospora* and *P. minimum in planta* and *in vitro* (Alvarez-Perez et al. 2017). Similarly, Trotel Aziz et al. (2019) and Leal et al. (2021b) showed that a native *B. subtilis* strain PTA-271, isolated from grapevine rhizosphere, was able to attenuate BOT through the different direct and indirect key levers indicated in part 6, and the origin of these mechanisms being also deeply investigated by a genomic analysis of this BCA (Leal et al. 2021a).

Focusing on the fungal genera from asymptomatic compared to symptomatic plants, the wood mycobiome of healthy vineyards is dominated by endophytes, some of which hold potential for biological control of wood pathogens amongst the genera *Trichoderma, Aureobasidium, Acremonium, Cladosporium, Alternaria* and *Epicoccum* (Dissanayake et al. 2018; González and Tello 2011; Pancher et al. 2012). Mycoviruses from grapevine microbiome, like the ones from the genus betapartitivirus or betachrysovirus detected by Nerva et al. (2019), are also suspected to influence the effect of beneficial microorganisms like *Trichoderma*. Indeed, Chun et al. (2018) reported that *T. harzianum* isolates infected with betapartitivirus displayed an increased antagonistic activity compared to the virus-free isolates. Ongoing high-throughput isolation efforts continue to explore in depth the

rich beneficial endophytic bacterial/fungal/viral community of asymptomatic plants (healthy or resilient ones) versus symptomatic ones, considering that: (i) grapevine may support diverse communities from roots to berries (Bokulich et al. 2014; Deyett et al. 2020; Fotios et al 2021; Zarraonaindia 2016) and (ii) grapevine genotype may also influence its microbiome composition (Berlanas et al. 2019; Bettenfeld et al. 2021; Marasco et al. 2018).

To date, the broadly knowledges accumulated when considering a "one pathogen – one disease" hypothesis has allowed us to identify new plant diseases and disease-causing organisms, as well as to develop effective control strategies. However, this hypothesis is not sufficient to explain the disease process, as emerging evidence have indicated that complex pathogenic communities (or pathobiome) contribute to disease development (Mannaa and seo 2021). Living in close association with diverse communities of microbes and virus, the plant should be considered as a 'holobiont' viewed as a complex system in continuous interaction with its resident microbes and surrounding environment (Gordon et al. 2013). Microorganisms with their functional genes represent the plant microbiome (or phytobiome) whose qualitative and quantitative composition may differ among each plant, as well as over the different stages of growth or depending on the organs and tissues of a same plant. To date, BCAs such as *Trichoderma* and *Bacillus* are described to (1) assist plants in nutrient uptake, (2) support plant growth at different stages starting from seed germination, and (3) promote plant resistance to biotic and abiotic stress. Pathogenic microbes are also part of the phytobiome (Baltrus 2017), and obviously some microbial genera are beneficial members at certain stages of a plant species (supporting growth) and turn pathogenic at another stage or in other plant species (i.e., some *Rhizoctonia* members are beneficial to some plants, while others are devastating pathogens). Therefore, the plant holobiont can be summed up as a continuous fight/equilibrium between the allies of pathogenic microbes (or pathobiome) (Bass et al. 2019; Mannaa and Seo 2021) and the allies of beneficial microbes (or symbiome). Healthy plants are closely associated with a stable and diverse community of beneficial microorganisms (symbiome) that serve the important functions of the host. Recent advancements in multi-omics (metagenomics, meta-transcriptomics, meta-proteomics and metabolomic) have especially pointed out the occurrence of diseases with multi-species of causal agents and mixed infections, referred as "disease complex" (i.e. esca complex). Therefore, the "one pathogen - one disease" hypothesis based on the fundamental Koch's postulates is not sufficient to describe the disease process in a

realistic way, particularly when complex communities of organisms are involved (Broberg et al. 2018). Thus, even when considering a single pathogen, other plant endophytic microorganisms are likely to modulate the pathogenic effects and should thus be considered as part of the disease process (Bettenfeld et al. 2020; Brader et al. 2017; Stopnisek et al. 2016).

1.9. Microorganisms with biocontrol potential against GTDs: Focus on *Bacillus* spp. and *Trichoderma spp.*

Biocontrol microorganisms commonly found in nature include bacteria, fungi, virus, yeasts, and protozoans, controlling plant diseases either directly or indirectly (Köhl et al. 2019). Focus is now made on Bacillus *spp.* and *Trichoderma* spp. as the two main microorganisms-based BCAs used in viticulture (Harman 2006; Mondello et al. 2018; Muckherjee et al. 2012; Waghunde et al. 2017), and the most widely investigated against GTDs (Berbegal et al. 2020; Di Marco et al. 2002, 2004; Halleen et al. 2010; John et al. 2008; Leal et al. 2021b; Martínez-Diz et al. 2021a,b; Schmidt et al. 2012; Trotel-Aziz et al. 2019).

***Bacillus subtilis* assets**

A broad range of beneficial molecules are produced or encoded by the genome of *Bacillus* spp. (Table 3), both to induce or elicit plant defenses (with MAMPs, such as phytohormones precursors, lipopolysaccharides, siderophores, etc.) and to directly compete, antagonize, or alter plant pathogens or their aggressiveness (Kloepper et al. 2004; Leal et al. 2021a; Ongena and Jacques 2008). Among *Bacillus* spp., *B. subtilis* is one of the most frequently tested against GTDs (Mondello et al. 2018), and *B. subtilis* PTA-271 has shown promising results in reducing infections caused by the aggressive strain *N. parvum* Bt67 (Trotel-Aziz et al. 2019). *Bacillus* spp. are also known for the stable biofilm they can form, and for their attachment and persistence on the plant roots; being considered as highly protective against any stress (Chen et al. 2013).

Assets of *Bacillus* species (summarised in Figure 10) and especially those of *B. subtilis* PTA-271 for sustainable biocontrol strategy against GTDs were deeply described by Leal et al. (2021a). This starts with the *B. subtilis* motility and adhesion capacities, allowing it

to colonize plant roots. Motility is due to the flagellum, enabling to move towards a vital nutrient source by chemotaxis thanks to genes involved in both the flagella maintenance (*flh* genes) and chemotaxis (*che* genes) (Henrischen 1972; Leal et al. 2021a).

The direct pathogen attack by *Bacillus spp* can then be achieved by several types of molecules also encoded by the *B. subtilis* genome (Leal et al. 2021a). *B. subtilis* can control fungal phytopathogens through the production of the exoenzymes CAZymes (carbohydrate activity enzymes) such as CWDEs, able to degrade the fungal cell wall with proteases and chitinases (Liu et al. 2011). Additionally, volatile organic compounds (VOCs) like 3-hydroxy 2-butatone and acetoin, and volatile inorganic compounds (VICs) like nitric oxide (NO), can inhibit fungal spore germination and hyphal growth (Chen et al. 2008). Other antimicrobial molecules, such as bacillaene, subtilosin and bacilysin can contribute to *Bacillus* direct confrontation with fungal pathogens. The lytic enzymes chitosanases and proteases are also pointed to produce the lipopeptides (LP) surfactin and fengycin described as powerful fungicides against pathogen survival. Finally, bacterial siderophores, like bacillibactin, can also directly alter pathogen fitness and aggressiveness, by depriving pathogen growth of iron while providing it for plant growth. *Bacillus spp*. can also stimulate the plant defenses and induce the plant Systemic Resistance (ISR) (Devendra et al. 2007; Leal et al. 2021b; Magnin-Robert et al. 2007; Pieterse et al. 2002; Trotel-Aziz et al. 2008, 2009; Van Loon 2000) by the mean of several types of eliciting molecules (MAMPs) encoded by the *B. subtilis* genome (Leal et al. 2021a). Cell surface components of *Bacillus*, such as lipopolysaccharides (LPS) and Flagella, can trigger the plant defense-associated responses leading to ISR (Choudhary et al. 2007; Erbs and Newmann 2003; Gómez-Gómez 2004; Meziane et al. 2005). Hormonal changes can also be induced by *B. subtilis* that can synthetize precursors of SA, ABA, and GA, involved in stress regulation (Blake et al. 2021; Leal et al. 2021a; Pacifico et al. 2019; Zhang et al. 2010;). Microorganisms also produce several transcription factors (TF) able to regulate plant defenses pathways (Liu et al. 2011), but also polyamines described as plant cell protectors upon water deficit (Ebeed et al. 2017; Leal et al. 2021a), temperature changes (Tian et al. 2012) and salinity (Leal et al. 2021a). The Lipopeptides (LP) surfactin and fengycin encoded by the genome of *Bacillus* spp. (*sfr* and *fen* genes) are also described as ISR elicitors (Heloir et al. 2019; Leal et al. 2021a; Ongena and Jacques 2008), as well as the DAMPs monomers formed by *Bacillus* CWDEs from pathogen Exopolysaccharides and LPS (i.e., chitosan, glucans, etc.) (Heloir et al. 2019; Leal et al. 2021a; Pieterse et al. 2014).

Bacillus spp. can also increase the plant root growth, and consequently plant productivity (Hashem et al. 2019). Indeed, according to Leal et al. (2021a), *B. subtilis* can improve nutrient availability, modulate the homeostasis of plant growth hormones, and improve plant tolerance to abiotic stresses. Regarding nutrient availability, *B. subtilis* can improve the intake of several nutrients promoting the plant growth, such as nitrogen, phosphorus, and iron (Hayat et al. 2010; Leal et al. 2021a). Plants are unable to directly use atmospheric nitrogen but rely on the help of microbial symbionts. *B. subtilis* is known to fix atmospheric nitrogen as well as to promote nodulation by other bacteria (Blake et al. 2021; Elkoca et al. 2007). Microorganisms can also induce the uptake of urea, a very good nitrogen source (Glick 2012; Zaidi et al. 2010) and release organic acids such as gluconic acid able to increase the phosphate bioavailability for plants (Glick 2012; Van Schie et al. 1987). The siderophores produced by *B. subtilis*, like bacillibactin, have an affinity for iron, transporting it near the plant roots, and increasing its intake (Powel et al. 1982). Regarding hormones, *B. subtilis* strains can produce tryptophan, the main precursor of auxin (IAA), described to promote the plant lateral root development, resulting in increased intake of nutrients by the root system (Glick 2012). The production of polyamines precursors by *Bacillus* can improve the plant growth too, since these molecules are described to induce cell division, to promote the regeneration of plant tissues and cell cultures (Chen et al. 2019), and to delay senescence. *B. subtilis* can also produce hydroxy-2-butanone (acetoin), 2,3-butanediol and cytokinin (Arkhipova et al. 2005), but also abscisic acid (ABA) described as one of the major plant hormones involved in abiotic stress regulation (Blake et al. 2021). Woo et al. (2020) recently showed that inoculation with *B. subtilis* GOT9 increases the tolerance of *Arabidopsis thaliana* and *Brassica campestris* to drought

***Trichoderma* spp. assets**

As summarised in Figure 10, *Trichoderma spp.* have been described to directly antagonize GTD pathogens by competition for nutrients or space, by parasitism using CWDEs to enter its host, and by antibiosis (Sood et al. 2020). Effects of *Trichoderma* spp. on plants have been described, such as the biostimulation of the plant growth, but also the induction of local and systemic defense responses (Sood et al. 2020). Finally, genes encoded by the genome of *Trichoderma* spp. have also highlighted self-protection systems and mechanisms involved in microbiome protection against biotic and abiotic stress.

The direct pathogen attack by *Trichoderma spp.* can be ensured by several kind of molecules, and especially CWDEs. Once a phytopathogenic fungus is detected, *Trichoderma* first moves towards the other fungus to parasite it (Chet et al. 1981). Transporters take first an active part to this mycoparasitism, such as the tripeptide transporter ThPTR2 and the ABC transporter Taabc2 dependent on ATP, but also genes encoding for *Trichoderma* adherence such as *Qid74* (Srivastava et al. 2014). *Trichoderma* then produces several CWDEs to degrade the cell walls of these other fungi. CWDE activities release oligomers from pathogen cell wall (as DAMPs), such as the oligalacturonides (OGs) considered as elicitors able to induce the production of endochitinases by *Trichoderma*, enzymes continuing to attack the pathogen cell wall (Srivastava et al. 2014). Among CWDEs are N-acetyl-β-D-glucosaminidase (exc1, exc2), endochitinase (ech42), chitinase (chit42, chit33), protease (Prb1), adenalyte-cyclase (tac1), xylanase (xyl) and cellulase, serine protease (tvsp1), β-glucanase (bgn 13.1) such as the β-1,3- and β-1,6-glucanase (tvbgn2, tvbgn3), β-1,3-glucosidase (tag83), and endo-poly-galacturonase (ThPG1) (For review check Sharma et al. 2011). The chitinases and endochitinases encoded by *Tga1*, *ech42*, *Th-Chit* are also described to produce antifungal metabolites, such as antibiotics with activity against phytopathogens (Cardoza et al. 2006; Reithner et al. 2005; Saiprasad et al. 2009; Woo et al. 1999). *Trichoderma* also contains genes encoding for β-Tubulins, described as cell structural components able to interact with benzimidazole fungicides to reinforce *Trichoderma*'s biocontrol process without inducing pathogen resistance (Buensanteai et al. 2010; Li and Yang 2007). Production of VOCs is also ensured by the *trichodiene synthase* (*tri5*) encoding for trichodermin, and by *Thctf1* encoding for 6-pentyl-2H-pyran-2-one (6pp) (Gallo et al. 2004; Lazazzara et al. 2021; Rubio et al. 2009; Sharma et al. 2011; Tijerino et al. 2011). All these antibiotic aggressive molecules can be stored in the appressoria formed by *Trichoderma* when in touch with the target fungus it aims to kill (Schirmböck et al. 1994).

Trichoderma spp. can stimulate plant defenses by the mean of several kind of molecules. Among these *Trichoderma*'s MAMPs recognized as elicitors by the plant to trigger ISR are proteins such as VOCs (Lazazzara et al. 2021), but also: the ET-inducing xylase (xynz/Eix), ThPG1, hydrophobin-like SSCP orthologues and swollenin TasSwo with local and systemic impacts, and cellulases triggering the SA and ET dependent defenses in the host plant (for review, see Hermosa et al. 2012). DAMPs resulting from the degradation of the fungal pathogen's chitin, such as OG, can also trigger the plant ISR, as well as the phytohormone like compounds such as IAA-like compounds produced by

Trichoderma species (Hermosa et al. 2012). Indeed, *Trichoderma* secretion of IAA near the plant roots stimulates ET biosynthesis via the *in-planta* ACC synthase. In turn, ET triggers an increase in ABA biosynthesis; ABA being described as an essential signal for plant resistance to pathogens by modulating JA biosynthesis (Adie et al. 2007). Stepanova et al. (2007) further indicated that ET and IAA in the roots can reciprocally regulate each other's biosynthesis. In contrast, some enzymes of *Trichoderma* can metabolise the plant precursor of ET, namely ACC, thus decreasing its availability for ET biosynthesis *in planta* (Viterbo et al. 2010; Jaroszuk-Ściseł et al. 2019). Consequently, reductions in ET *in planta* may successfully promote plant growth through gibberellin signaling (Jaroszuk-Ściseł et al. 2019; Viterbo et al. 2010). Regarding secondary metabolites, they can act as MAMPs at a low concentration, while at high doses they have an antimicrobial power (Hermosa et al. 2012). Among them are: 6-pentyl-α-pyrone, harzianolide and harzianopyridone, described both to activate plant defenses and to regulate the plant growth, suggesting that the defense mechanisms of plants and their developmental responses to *Trichoderma* share common components. Another secondary metabolite is alamethicin, a peptaibol described to elicit JA and ET dependent defenses (Vinale et al. 2008; Viterbo et al. 2007).

Trichoderma can also increase the plant root growth, and consequently plant productivity (Sood et al. 2020) by impacting the plant hormonal balance (as indicated in the previous paragraph), but also by increasing the plant nutrient uptake and nitrogen use, and helping to solubilize soil nutrients (Pozo et al. 2002). How these processes occur at the molecular level is still unknown, but it is known that there are differences in the responses of plants depending on their species.

Finally, *Trichoderma* protects itself against biotic stresses. Indeed, *Trichoderma* species have genes that encode for molecules responsible for tolerance to biotic stresses, such as putative Kelch-repeat protein (Thkel1) that regulates glucosidase activity and enhance tolerance to salt and osmotic stress (Hermosa et al. 2011). *Hsp70* gene leads to an increase of fungal resistance to heat, salt, osmotic stress, and oxidation (ManteroBarrientos et al. 2008), and *TvGST* gene is related to cadmium tolerance (Dixit et al. 2011; Sharma et al. 2011).

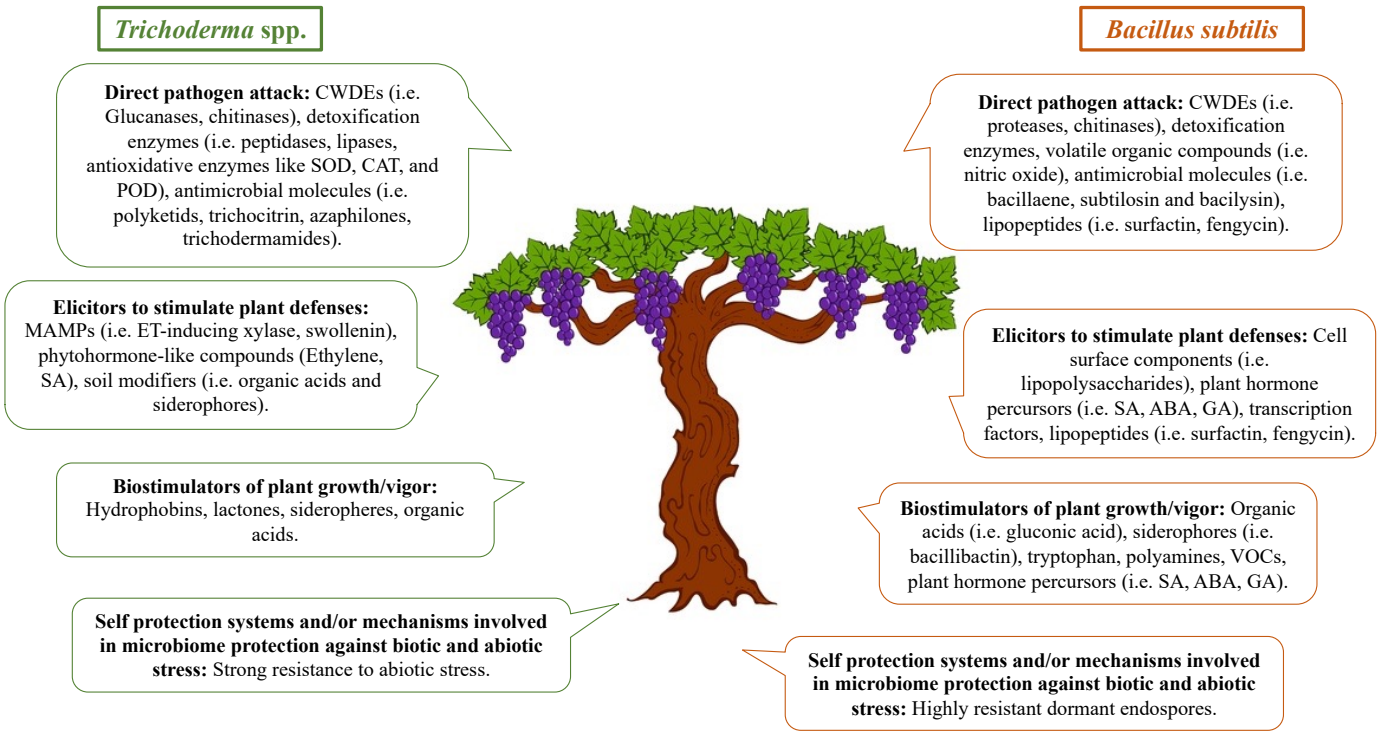

Figure 10. *Trichoderma* spp. and *Bacillus subtilis* biocontrol mechanisms and molecules.

1.10. How to develop a durable sustainable management of GTDs? From nursery to vineyard.

The control of GTDs is a major challenge for vine growers, nurserymen, and scientists, mostly because of their complexity compared to other grapevine diseases (Gramaje and Armengol 2011). One of the most problematic aspects of GTD pathogens is their indeterminate latency (endophytic asymptomatic status) and subsequent internal lesions development leading to silent extensive damages of wood before the first external

symptoms appear (Calzarano and Di Marco 2007; Mondello et al. 2018). This leaves winegrowers with few options to reduce the impact of GTDs in vineyards when the symptoms turn visibles. In nurseries too, infected asymptomatic cuttings can be very dangerous when used to establish new plantations. Thus, a lack of GTD control would lead to an unsuspected spread of infected plants, first in the nursery and then in the vineyard (Aroca et al. 2010; Gramaje and Armengol 2011; Gramaje and Di Marco 2015). Therefore, securing the future of management against GTDs in both nursery and vineyard using biocontrol, but also disease-resistant varieties and cultural practices is a prerequisite (Barzman et al. 2015; Collinge et al. 2019; Raymaekers et al. 2020). The Europe definition of biocontrol involves 4 categories that can be used for preventive or curative practices, among which microorganisms BCAs, semiochemicals (bio-based active molecules with a signal value between living organisms), natural substances (chemical coumpound from animal, plant or mineral origin, found in nature) and invertebrate BCAs (IBMA website). Currently, few curative methods exist, among which are curettage (Cholet et al. 2021; Mondello et al. 2018; Pacetti et al. 2021) and low copper-based fungicides (Battiston et al. 2021; Mondello et al. 2022; Reis et al. 2021). Hot-water treatments are also used successfully in nurseries to disinfest plant material since the 19th century (Baker 1962; Birchfield and Van Pelt 1958).

Cultural practices, as well as the use of microorganisms BCAs are among the best candidates for the sustainable preventive control of GTDs, while the use of disease-resistant varieties still requires further study to discriminate the grapevine R-genes that target key early-stage effectors (Elena and Luque 2016; Úrbez-Torres et al. 2010).

Some products of biological control have already been registered against GTD pathogens (Mondello et al. 2018), and increasing research is currently devoted to the effect of BCAs in nursery, with *Trichoderma species*. Among them, *T. atroviride* SC1 was shown to strongly reduce the infections caused by some GTD pathogens in several cultivars, among which Tempranillo, both in nurseries and established vineyards at the registered dose rate of 2 g/L, equivalent to the density of 2×10^{10} conidia/L recommended by the commercial product (Berbegal et al. 2020; Leal et al. *submitted*; Martínez-Diz et al. 2021a; Pertot et al. 2017;). Other BCAs (e.g., *B. subtilis*, *Fusarium lateritium, Erwinia herbicola, Cladosporium herbarum, Aureobasidium pullulans, Pythium oligandrum* and *Rhodotorula rubra*) and natural molecules (e.g., chitosan and cysteine) have also been reported to be effective against GTDs pathogens *in vitro* or in nurseries, alone or in combination with fungicides (Bertsch et al. 2013; Leal et al. 2021b; Trotel-Aziz et al.

2019). In vineyards, *Trichoderma*-based registered products against GTDs are applied in pruning wounds (Berbegal et al. 2020; Blundell et al. 2022; Martinez-Diz et al. 2021; Mounier et al. 2016; Úrbez-Torrez et al. 2020). Pruning wounds application aims to prevent infections caused by the annual contamination with spores of fungal pathogens (Di Marco et al. 2002, 2004; Halleen et al. 2010; John et al. 2005; Kotze et al. 2011; Mutawila et al. 2011, 2015; Sosnowski et al. 2004; Pitt et al. 2012). *Trichoderma*-based commercialized products are called Vintec® which contains *Ta* SC1, or Remedier® that contains *Trichoderma asperellum* and *Trichoderma gamsii* (Di Marco et al. 2022). Among the commercialized BCA strains are Serenade® which contains *B. subtilis*. Research is also in progress considering the use of combined BCAs in nursery (Leal et al. *submitted*).

Before being considered for formulation then commercialisation, numerous beneficial microorganisms are assayed for their protective effect *in planta* under controlled conditions (Di Marco et al. 2002, 2004; John et al. 2005; Haidar et al. 2016; Leal et al. 2021b; Trotel-Aziz et al. 2019; Yacoub et al. 2016). Such plant model in controlled conditions enable to better understand the origin of a BCA efficiency against GTDs, by deciphering grapevine-BCA-pathogen interactions (Reis et al. 2019). The BCAs modes of actions can include (1) a direct antagonism against the pathogen or its virulence/pathogenicity factors, and/or (2) the triggering of grapevine ISR by the mean of MAMPs. For instance, *Bs* PTA-271 has been shown to induce ISR by priming the expression of the plant JA/ET-dependent defenses in Chardonnay rootlings infected with *N. parvum* (Trotel-Aziz et al. 2019) as it did with a true necrotroph such as *Botrytis cinerea* (Trotel-Aziz et al. 2008). Against *N. parvum*, *Bs* PTA-271 was also shown to be antagonistic by delaying the pathogen mycelial growth, and finally was shown to detoxify the virulence factors (*R*)-mellein and (-)-terremutin produced by *N. parvum* (Trotel-Aziz et al. 2019). *Bs* PTA-271 fungistatic effect might be explained by the release of various antifungal compounds, including surfactins or other lipopeptides which production was shown to depend on temperature (Leal et al. 2021a; Ongena and Jacques 2008; Pinto et al. 2018; Trotel-Aziz et al. 2019). Such a fungistatic effect gives the plant more time to defend itself and reduces the biosynthesis and secretion of the pathogen's virulence factors. Indeed, once inside the plant phytotoxins were shown to strongly lower the expression of most of the plant induced defenses (Trotel-Aziz et al. 2019), and (-)-terremutin was especially shown to repress the host useful JA/ET-dependent defenses against *Np-Bt67* (Trotel-Aziz et al. 2022). Fortunately, *Bs* PTA-271 can detoxify both (-

)-terremutin and (*R*)-mellein (Trotel-Aziz et al. 2019). Authors suggested that this detoxifying capacity of PTA-271 was another asset to counter pathogen aggressiveness, preventing the phytotoxin level from reaching a too high level that will contribute to reprogram the useful immunity of the grapevine, thus favoring the bypassing of the host defenses by the pathogen and thus promoting the disease.

However, cultivars were also shown to condition BCAs efficiency towards BOT in controlled conditions. When comparing cultivars with distinct susceptibility to GTDs (Cobos al. 2019; Leal et al. 2021b; Luque et al. 2009), Leal et al. (2021b) suggested that the high basal expression of SA-dependent defenses in Tempranillo may both explain this cultivar highest susceptibility to *Np-Bt67* and the ineffectiveness of *Bs* PTA-271 alone to protect Tempranillo against *Np-Bt67*. Indeed, it has already been reported that early activation of SA signaling could antagonize the expression of the JA/ET-dependent defenses (Pieterse et al. 2012; Van der Does et al. 2013), although the latter are known to be useful for the plant (as basal or as induced) to fight a pathogen once entered in its necrotrophic phase (Yang et al. 2015). Combining BCAs with complementary ways of protection would thus enable to develop strongest biocontrol strategies and covering a wider range of pathogens and cultivars, especially susceptible ones. To improve the efficiency of single BCA, combinations with other BCAs or with naturel products are currently underway.

Indeed, literature reports that the combination of two or more BCAs can improve the management of plant diseases (El-Tarabily 2006; Guetsky et al. 2001; Leal et al. 2021b; Magnin-Robert et al. 2013; Weller 1988; Yobo et al. 2011), probably due to additive or synergistic effects of combined mechanisms in a complex changing environment (Meyer and Roberts 2002). Since the BCA *T. atroviride* is one of the most widely used commercialized biopesticides to control GTDs (Gramaje et al. 2018; Mondello et al. 2018), assays combining *T. atroviride* with *B. subtilis* PTA-271 were carried out by Leal et al. (2021b) in greenhouse conditions. These authors reported for the first time the biocontrol potential of the combination of Bs PTA-271 and Ta SC1 against *Np-Bt67* in Tempranillo (91% protection), greater than Ta SC1 alone (80% protection), despite Bs PTA-271 and Ta SC1 can antagonize each other. This beneficial BCAs collaboration against *Np-Bt67* confirms the interest of using both BCAs in combination to optimize both the plant ISR and the BCA direct antagonism against *Np-Bt67* in some cultivars such as Tempranillo. It is also believed that the combination of

several BCAs would ensure a more successful transfer of biocontrol efficacy from the greenhouse to the vineyard conditions.

Combining BCAs with natural products are currently underway, such as Bs PTA -271 and/or Ta SC1 with the molecules listed in Figure 10 (namely: elicitors of grapevine ISR against GTDs and/or direct effectors of the GTD pathogens). As mentioned earlier, such practices will (1) enable to seriously reduce the amount of chemicals used in the field, (2) restore the beneficial biodiversity damaged by years of unreasonable chemical control, (3) make the BCA products more effective in vineyards, and (4) improve the quality of the transfer of BCA results from the greenhouse to the vineyards, with the strongest guarantee of their reproducibility *in-situ*.

1.11. Objectives

The biggest concerns to GTDs integrated management approaches, are the improvement of the phytosanitary quality of the nursery produced grapevines, and the prevention of infections through pruning wounds in the vineyard from the moment of planting. Biocontrol agents (BCAs) *Bacillus subtilis* and *Trichoderma* spp. have been shown to be promising strategies to be applied in vineyard as well as in nurseries, against GTDs. A better knowledge of the BCAs mode of action, as well as GTD pathogens aggressive molecules, and grapevine's own defensive capacity against GTD pathogens, is a key component to better understand the antagonistic effects or immunostimulatory effects of BCAs or their natural molecules. This project proposes to integrate 2 BCAs in nursery treatments to optimize the integrated control of GTDs. The efficiency of *T. atroviride* SC1 and *B. subtilis* PTA-271 was also be investigated in greenhouse, as well as their effect in grapevine rhizosphere microbiome.

We aim to (Figure 11):

1) Characterize in detail the genome of *B. subtilis* PTA-271 in order to explore its biotechnological potential for biocontrol of GTD pathogens (Chapter II). This study will also allow to identify potential beneficial molecules encoded by the genome of *T. atroviride* SC1 and *B. subtilis* PTA-271 (Chapter II).

2) Explore the protective potential (in terms of efficacy and modes of action) of the two BCAs, alone or in combination, against a very aggressive pathogen involved in GTDs and artificially inoculated to two grapevines with different sensitivities to this pathogen, under controlled conditions (Chapter III).

3) Screening for plant defense markers against GTD-causing pathogens (Chapter IV).

4) Understand the colonization and biocontrol potential of the 2 BCAs, *T. atroviride* SC1 and *B. subtilis* PTA-271, against different pathogens responsible for GTDs in nurseries (under natural conditions) (Chapter V).

5) Explore the potential of the 2 BCAs to modulate the microbiome of grapevine plants in contact with GTD pathogens in two different soil types. (Chapter VI).

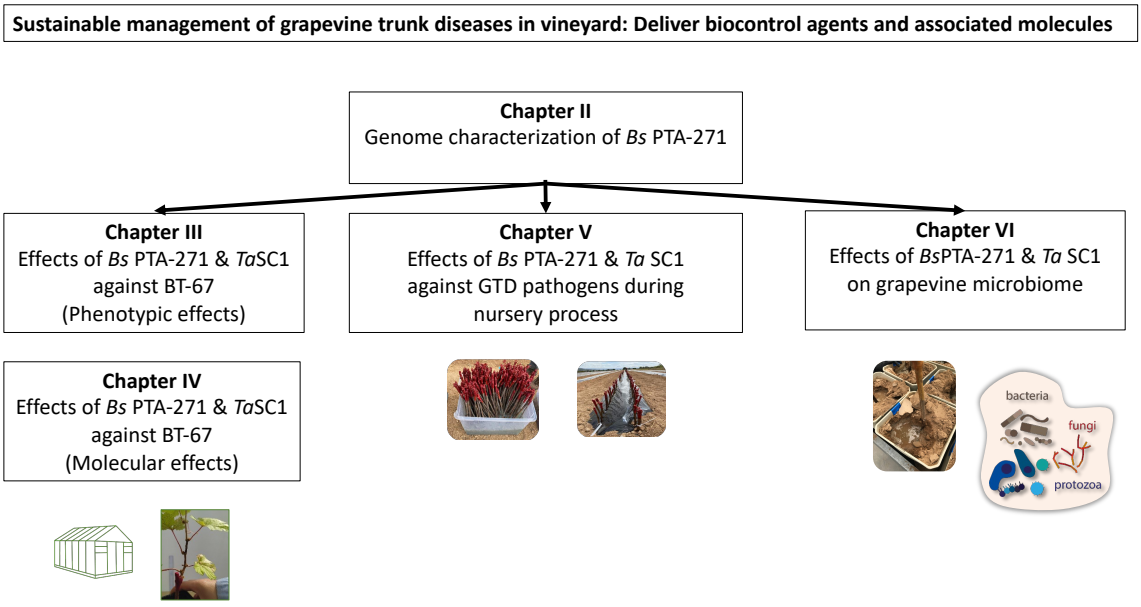

Figure 11. Aims of each chapter of the thesis entitled "Sustainable management of grapevine trunk diseases in vineyard: Deliver biocontrol agents and associated molecules".

Chapter II

Genome sequence analysis of the beneficial *Bacillus subtilis* PTA-271 isolated from a *Vitis vinifera* (cv. Chardonnay) rhizospheric soil: assets for sustainable biocontrol

2.1. Introduction

Bacillus subtilis is a Gram-positive endospore-forming bacterium from *Bacillus* genera considered as a promising plant beneficial organism that can survive in the soil for extended time periods under harsh environmental conditions (Nicholson et al. 2000). Benefits of species from the *Bacillus* group are well described in many sectors of industry, agriculture, and viticulture (Borriss 2011). Focusing on the *B. subtilis* species, it has been described to provide plants with a broad range of benefits that include induced systemic resistance (ISR) upon pathogen attacks, growth promotion, or the direct control of plant pathogens (Magnin-Robert et al. 2007; Trotel-Aziz et al. 2019; Trotel-Aziz et al. 2008; Wang et al. 2018).

Primed defenses during ISR are regulated either by jasmonic acid (JA) and ethylene (ET) signaling or by salicylic acid (SA) signaling (Pacifico et al. 2019; Pieterse et al. 2009; Pieterse et al. 2014; Van Loon et al. 1998). Beneficial microorganisms may modulate the plant hormonal balance by either altering hormone synthesis or by producing similar hormones or their precursors (ET, SA, auxins, gibberellins, cytokinins, polyamines…) (Pacifico et al. 2019). Numerous bacterial elicitors of ISR are also reported in several plant species, such as exopolysaccharides (EPS), lipopolysaccharides (LPS), siderophores such as the iron-regulated pyoverdin, iron, flagella, biosurfactants, N-acyl-L-homoserine lactone, N-alkylated benzylamine and volatile compounds (Kloepper et al. 2004; Pacifico et al. 2019; Van Loon et al. 1998; Zamioudis et al. 2015). Some of these have already been identified in species of *B. subtilis* or *Bacillus* genera (Akram et al. 2015; Audrain et al. 2015; Kloepper et al. 2004; Pacifico et al. 2019). Changes in the phytohormonal-balance also impact plant growth and development, since the reduction of ET may promote plant growth (Glick 2014; Pacifico et al. 2019; Xie et al. 2014). Microbiota support plant growth and development by modulating nutrient availability through mineralization and chelation, as well as through the production of volatile compounds that support biocontrol (Sharifi and Ryu 2018; Tyagi et al. 2018). Efficient beneficial effects of *Bacillus* spp. also assume direct and indirect bacterium and microbiota preservation, upon abiotic and biotic stressful conditions (Huang et al. 2014; Pacifico et al. 2019). When biocontrol agents protect themselves through extrusion transporters, detoxifying enzymes, quenching enzymes and pathogen homologous

enzymes, they also contribute indirectly to plant protection (Pacifico et al. 2019). Finally, *B. subtilis* produces an extensive range of antimicrobial molecules, chelators and lytic enzymes that limit pathogen fitness and aggressiveness (Caulier et al. 2019). According to literature, these beneficial molecules include ribosomally synthesized antimicrobial peptides (RP, including the post-translationally modified peptides RiPP), non-ribosomally synthesized peptides (NRP), polyketides (PK), as well as other uncommon antimicrobial volatile compounds (the inorganic and organic ViCs and VOCs, respectively) and terpenoid secondary metabolites as listed in Table 1. Individual strain specificities may thus impact both biochemical conditions and species ratios, and in turn interactions among complex microbial communities and their hosts.

Table 1. *Bacillus subtilis* known antimicrobial molecules, chelators and lytic enzymes (Caulier et al. 2019; Lopes et al. 2018; Wang et al. 2018).

RP	**Bacteriocins**	such as the lantibiotics: lanthionine, nysin and subtilin, the pediocin-like peptides, the thuricin-like peptides and other linear peptides
	Quorum quenching enzymes	such as lactonase, decarboxylase, acylase and deaminase),
	Cell wall degrading enzymes (CWDE)	such as cellulases, proteases, chitinases, glucanases, etc…
	Detoxifying-enzymes	such as transferases and oxygenases
NRP	**Thiotemplate NRPs-lipopeptides**	such as fengycin, surfactin, iturin, bacillomycin
	Thiotemplate NRPS-siderophores to compete pathogen nutrition	such as the catecholic siderophores: itoic acid and bacillibactin
	Non-thiotemplate NRPs	such as the di- and tri- peptides rhizocticins, bacylisin, chlorotetain and the cyclic polypeptides bacitracin and mycobacillin
PK	**Acetogenins, ansamycins, enedyines, macrolides, polyenes, polyethers and tetracyclines** (such as bacillaene, difficidin and macrolactin that selectively inhibit protein synthesis)	
VICs	**Carbonated, hydrogenated, sulfur or nitrogen-containing compounds** (such as H_2, HCN, H_2S, NH_3).	
VOCs	**Fatty acids derivatives** (70% of the VOC)	such as the benzenoids 1,3-butadiene or 2,3-butanediol
	Sulfur-containing VOCs (VSCs)	such as dimethyl disulfide DMDS, dimethyl trisulfide DMTS, S-methyl thioacetate or S-methyl butanethioate
	Nitrogen-containing VOCs	such as azoles, pyrazines, pyridines, pyridazines, and pyrimidines
Other II^{ary} metabolites	**Terpenoids**	such as isoprene and monoterpene a-terpineol

Focusing on *B. subtilis* PTA-271, its protective effect has been published in grapevine against *Neofusicoccum parvum* and *Botrytis cinerea* (Magnin-Robert et al. 2007; Trotel-Aziz et al. 2008; Trotel-Aziz et al. 2019), the causal agents of Botryosphaeria dieback and grey mold respectively. The ability of *B. subtilis* species to sporulate in order to resist climate changes and common disinfectants (Nicholson et al. 2000), combined with the fact that *B. subtilis* PTA-271 is a non-pathogenic species, make this microorganism suitable to control a wide spectrum of pathogens among which the most economically significant grapevine trunk disease (GTD) pathogens currently lack of efficient control strategies (Mondello et al. 2018; Trotel-Aziz et al. 2019). In this study, we report the draft genome sequence of the *B. subtilis* strain PTA-271, analyze and compare with other known *Bacillus* strains sequences, to expand our knowledge of *B. subtilis* PTA-271 benefits, as well as design efficient and sustainable biocontrol strategies for viticulture.

2.2. Material and methods

B. Subtilis PTA-271 general information and features

B. subtilis PTA-271 was isolated in 2001 (Table 2) from the rhizospheric soil of healthy Chardonnay grapevines (*V. vinifera* L., cv Chardonnay) from a vineyard located in Champagne (Marne, France). Rhizospheric samples were directly suspended in a sterile 0.85% NaCl solution (1 g of soil: 10 ml of NaCl) and bacterial isolates were obtained by serial dilutions of the soil samples (10^7, 10^3, 10^2 cfu/g soil) in triplicate onto LB-agar (Luria–Bertani-agar), King's B-agar and glycerol–arginine-agar plates by incubating at 30 °C for 24–72 h. All different colonies were then re-isolated on LB-agar, cultured in LB at 30 °C for 24 h and screened for their protective role against *Botrytis cinerea* by using grapevine plantlet leaf assays pretreated with bacterium (Trotel-Aziz et al. 2008). Selected biocontrol microorganisms were then identified, calculated to establish the density formula, and stored in a sterile 25% glycerol solution at − 80 °C for complementary purposes. The classification and general features of *B. subtilis* PTA-271 are in Table 2. The taxonomic information for this strain was already described by Trotel-Aziz et al. (2008) and remains unaltered to this date.

Table 2. Classification and features of *Bacillus subtilis* PTA-271 according to MIGS recommendations (Field et al. 2008).

MIGS ID	Property	Term	Evidence code
	Classification	Domain *Bacteria*	TAS
		Phylum *Firmicutes*	TAS
		Class *Bacilli*	TAS
		Order *Bacillate*	TAS
		Family *Bacilaceae*	TAS
		Genus *Bacillus*	TAS
		Sepecies *Bacillus subtilis*	TAS
		Strain: PTA-271	
	Gram strain	Gram-positive	IDA
	Cell shape	Rod-shaped	IDA
	Motility	Motile	NAS
	Sporulation	spore-forming	NAS
	Temperature range	Unreported	
	Optimum temperature	37°C	NAS
	pH range, optimum	4-9.5, 8	NAS
	Carbon source	Organic carbon compounds	NAS
MIGS-6	Habitat	Soil, grapevine	IDA
MIGS-6.3	Salinity	0-50 g/l; salt tolerant	NAS
MIGS-22	Oxygen requirement	Aerobic	NAS
MIGS-15	Biotic relationship	Free-living	IDA
MIGS-14	Pathogenicity	Non-pathogenic	NAS
MIGS-4	Geographic location	Champagne region, Marne, France	IDA
MIGS-5	Sample collection	2001	IDA
MIGS-4.1	Latitude	49° 15’ 15’’ N	
MIGS-4.2	Longitude	4° 09’ 28’’ E	
MIGS-44	Altitude	105-206 m	

B. subtilis PTA-271 genomic sequencing information

Genome project history

B. subtilis PTA-271 was selected for sequencing due to its efficient capacity to protect grapevine against several pathogens with distinct lifestyles such as Botrytis cinerea and *Neofusicoccum parvum* (Magnin-Robert et al. 2007; Trotel-Aziz et al. 2008; Trotel-Aziz et al. 2019) This beneficial microorganism can not only modulate grapevine defenses, but also antagonize the growth of pathogens and detoxify aggressive molecules. These beneficial bacteria provide protection against a broad spectrum of pathogens, due to its genetic traits of physical and chemical tolerance (endospore forming, withstand large pH and salinity range, Table 2). Altogether, there are advantages to sequence the *B. subtilis* PTA-271 genome to better understand its key beneficial levers and develop better sustainable biocontrol strategies regardless of field conditions or soil parameters (pH, salinity, etc.).

The whole genome shotgun project has been deposited at DDBJ/ENA/GenBank under the accession JACERQ000000000. The version described in this paper is version JACERQ000000000 and all related information is represented in Table 3.

Table 3. *Bacillus subtilis* PTA-271 genomic sequencing information.

MIGS ID	Property	Term
MIGS 31	Finishing quality	High-quality draft
MIGS28	Libraries used	Illumina paired-end library (2×300 bp insert size)
MIGS29	Sequencing platforms	Illumina MiSeq
MIGS31.2	Fold coverage	300 X
MIGS30	Assemblers	SPAdes
MIGS32	Gene calling method	Prodigal v.2.6
	Locus tag prefix	H0Z15
	WGS accession : SUBID BioProjet BioSample	 SUB7775359 PRJNA646528 SAMN15546529
	DDBJ/ENA/GenBank accession	JACERQ000000000
MIGS13	Source Material Identifier	*Bacillus subtilis* PTA-271
	Project relevance	Biocontrol, Grapevine, GTD

Genomic DNA preparation

Genomic DNA of *B. subtilis* PTA-271 was extracted using the Wizard® Genomic DNA Purification kit (Promega), from the pellet of a 1 mL-overnight culture incubated at 28 °C in LB medium. DNA integrity was confirmed on a 0.65% agarose gel electrophoresis in TAE buffer. DNA concentration and quality were read from 1 µL of DNA with the NanoDrop-ONE spectrophotometer (Ozyme).

Library preparation and genome sequencing

DNA library for bacterial genome sequencing was prepared from 0.5 nanograms of high-quality genomic DNA using the Nextera XT DNA Sample Preparation Kit (Illumina, San Diego, USA) and sequenced using paired-end (PE) 2 × 300 bp on the MiSeq® Illumina® platform at Genoinseq (Cantanhede, Portugal). All the procedures were performed according to standard manufacturer protocols.

Genome assembly and annotation

Sequenced reads were demultiplexed automatically by the Illumina® Miseq® sequencer using the CASAVA package (Illumina, San Diego, USA) and quality filtered with Trimmomatic version 0.30 (Bolger et al. 2014). High-quality adapter-free reads were assembled with SPAdes version 3.9.0 (Bankevich et al. 2012) and contigs with size < 500 bp or coverage lower 10x were removed from the assembly. Assembly metrics were calculated with Quast version 4.6.1 (Gurevish et al. 2013). Contigs were checked for contamination and completeness using CheckM 1.0.9 (Parks et al. 2015). Coding gene predictions were made with Prodigal version 2.6 (Hyatt et al. 2010), rRNA and tRNA genes were detected using Barrnap version 0.8 and CRISPR regions were detected by Minced version 0.2.0. Coding gene annotation was performed with Prokka version 1.12 (Seemann 2014) using the following repositories: SwissProt (The UniProt Consortium, 2017), HAMAP (Pedruzzi et al. 2015), TIGRFAMs (Haft et al. 2003) and Pfam (Finn et al. 2016). Coding genes were also annotated for Pathway using KEGG (Kanehisa et al. 2019), for peptidases using MEROPS (Rawlings et al. 2016) and for carbohydrate-active enzymes with dbCaN (Yin et al. 2012).

2.3. Results and discussion

B. subtilis PTA-271 genome properties and comparison with other bacillus strains

The general features of *B. subtilis* PTA-271 are in Table 4 and Fig. 1, performed using Artemis version 16.0.0. The draft genome sequence of *B. subtilis* PTA-271 presented an estimated genome size of 4,001,755 bp divided in 20 contigs. The G + C content of this sequence was 1,751,999 bp, representing about 43.78% of the whole genome. Genome analysis showed that *B. subtilis* PTA-271 contained 4038 genes, among which 3945 (97.69%) were protein coding genes. This genome draft predicts 92 RNA genes among which 11 rRNA genes were identified and no CRISPR repeats. From 4,001,755 bp of the genome size, 3,550,299 bp correspond to coding genes representing 88.73% of the whole genome. From this, 3440 genes had function prediction, 3183 were assigned to the COG categories described in Table 5, and 3517 genes had Pfam domain descriptions.

Table 4. Genome statistics.

Attribute	Value	% of Total[a]
Genome size (bp)	4,001,755	100
DNA coding (bp)	3,550,899	88.73
DNA G + C (bp)	1,751,999	43.78
DNA scaffolds	20	-
Total genes	4,038	100
Protein coding genes	3,945	97.69
RNA genes	92	2.27
Genes with function prediction	3,440	85.19
Genes assigned to COGs	3,183	78.82
Genes with Pfam domains	3,517	87.10
CRISPR repeats	0	0

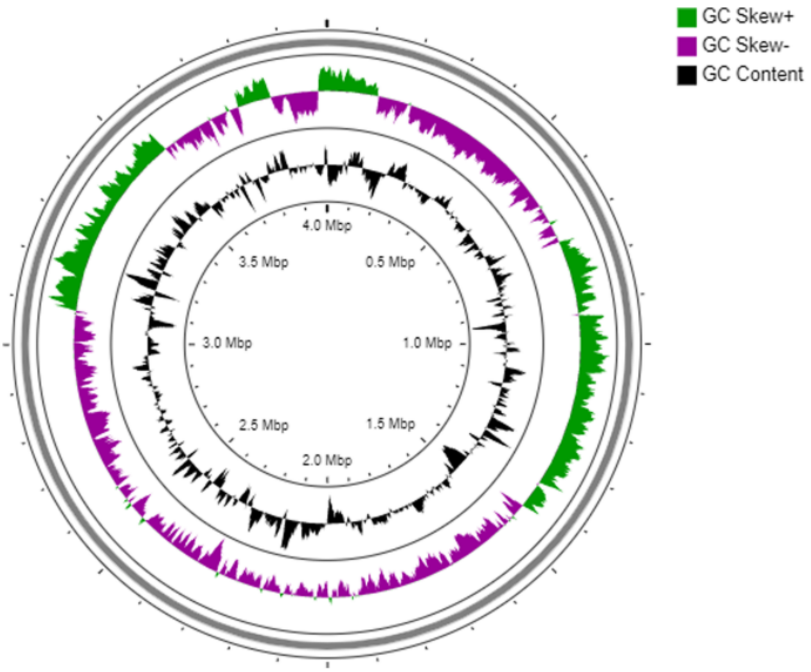

Figure 1. Circular map of the *Bacillus subtilis* PTA-271 genome. Map generated with CGView server (Stothard and Wishart 2005).

Table 5. Number of genes associated with general COG functional categories

Code	Value	%age[a]	Description
J	173	4.38	Translation, ribosomal structure and biogenesis
A	0	0	RNA processing and modification
K	313	7.93	Transcription
L	118	2.99	Replication, recombination and repair
B	1	0.02	Chromatin structure and dynamics
D	39	0.98	Cell cycle control, cell division, chromosome partitioning
V	59	1.49	Defense mechanisms
T	171	4.33	Signal transduction mechanisms
M	210	5.32	Cell wall/membrane/envelope biogenesis
N	62	1.57	Cell motility
U	49	1.24	Intracellular trafficking, secretion, and vesicular transport
O	109	2.76	Posttranslational modification, protein turnover, chaperones
C	183	4.63	Energy production and conversion
G	313	7.93	Carbohydrate transport and metabolism
E	328	8.31	Amino acid transport and metabolism
F	86	2.17	Nucleotide transport and metabolism
H	134	3.39	Coenzyme transport and metabolism
I	118	2.99	Lipid transport and metabolism
P	184	4.66	Inorganic ion transport and metabolism
Q	91	2.30	Secondary metabolites biosynthesis, transport and catabolism
R	443	11.22	General function prediction only
S	360	9.12	Function unknown
W	0	0	Extracellular structures
Y	0	0	Nuclear structure
Z	1	0.02	Cytoskeleton
-	762	19.31	Not in COGs

B. Subtilis PTA-271 assets for plant sustainable biocontrol

Bacillus species offer a broad range of benefits to plants: (1) plant growth promotion, (2) induced systemic plant defenses and protection against pathogens, and (3) prevention of pathogen fitness or aggressiveness, by producing many compounds able to interact with the host plants, the pathogens or their tripartite intricate communication. Considering this, the genome analysis of *B. subtilis* PTA-271 tried to highlight some useful characteristics

directly or indirectly beneficial for a sustainable plant protection against a broad spectrum of pathogens.

Motility and adhesion: assets for plant root colonization

Motility of a bacterium is due to the flagellum, enabling it to move towards a vital nutrient source (chemotaxis). In this sense, *B. subtilis* PTA-271 contains genes (Supplementary Table S1) putatively encoding for flagella maintenance (flh genes) and chemotaxis (che genes). Once reaching a comfortable area, adhesion is due to bacterium pili, allowing the initiation of biofilm formation where both chemotaxis and gene exchanges among microorganisms of microbiota can be amplified.

B. subtilis spp. are also described for their strong swarming motility (Henrichsen 1972). The gene swrC putatively encoding for swarming motility protein is predicted in the genome of B. subtilis PTA-271 (Supplementary Table S1). Swarming motility requires the production of functional flagella, pili and surfactant to reduce surface tension.

Motilities and adhesion are considered advantageous characters for a successful host colonization and *B. subtilis* spp. are already described to grow in biofilm mode involved in root colonization (Davey and O'toole 2000). To this end, the transcription factors (TF) Spo0A and AbrB were described as positive and negative regulators of biofilm formation, respectively (Hamon and Lazazzera 2001). Genes putatively encoding for these 2 TFs are also predicted in the genome of *B. subtilis* PTA-271 as Spo0A and AbrB (Supplementary Tables S1 and S2).

Beneficial microorganisms that successfully colonize the plant, particularly by the root system, would be advantageous, both for plant growth promotion and for plant biocontrol (Lugtenberg and Kamilova 2009; Santoyo et al. 2016).

Biofertilizing and morphogenic effects: assets for plant vigor

Plant nutrition depends on soil retention capacity of minerals and nutrient availabilities, thus both on chelating process, mineralization by decomposers and minerals bioavailability towards the plant consumer. Upon nitrogen starvation, some bacteria are

described to upregulate the ure gene cluster, since urea is an easy nitrogen source. Such ure genes are predicted in *B. subtilis* PTA-271 genome (ureA, ureB, ureC). This cluster of genes is known to be controlled by the global nitrogen-regulatory protein TnrA, also predicted in *B. subtilis* PTA-271 genome (Supplementary Table S2). Regarding other nutrient access due to phosphate-solubilizing bacteria (PSB) (Glick 2012; Wang et al. 2018; Zaidi et al. 2010), genes encoding for proteins involved in the production of gluconic acid and precursor of citric acid are also predicted in the genome of *B. subtilis* PTA-271 (S19-40_03830, S19-40_03828). Organic acids may lower the soil pH to solubilize phosphate and thus increase its availability to the plant (Glick 2012). Bacterial secondary metabolites (PyrroloQuinoline Quinone, PQQ) are also known to control gluconic acid production (Van Schie et al. 1987), and *B. subtilis* PTA-271 has 3 genes predicted to be related to PQQ production pqqL, pqqF and pqqC (Toyama et al. 1997). Additionally, *B. subtilis* PTA-271 contains the phytase gene phy, described in the other *Bacillus* spp. to encode for phosphatases able to hydrolyze organic complex in order to liberate phosphate and make it available for plants (Konietzny and Greiner 2004). Iron is another very important nutrient for plant growth and development. *B. subtilis* PTA-271 possesses the fur gene (Supplementary Table S2) described in the literature to encode for a regulatory protein coordinating the homeostasis of iron uptake depending on its availability in the soil (Andrews et al. 2003). Regarding soils containing abundant ferric form (Fe3+) which is poorly available to plants, the literature described bacteria producing siderophores with high specificity and affinity for iron, capable of binding, extracting and transporting iron near the plant roots (Powell et al. 1982). *B. subtilis* PTA-271 genome also predicted the production of such siderophores, namely the catecholic siderophore 2,3-dihydroxybenzoate-glycine-threonine trimeric ester bacillibactin encoded by 5 genes (dhbA to dhbF). Surfactants produced by beneficial bacteria also contribute to increase the availability of hydrophobic nutrients. In this sense, *B. subtilis* PTA-271 is suspected to produce surfactin (with srfAA to srfAD), a powerful biosurfactant due to its amphiphilic nature that strongly anchor with lipid layers, interfering with the structure of biological membranes (Ongena and Jacques 2008).

Plant root morphology is also described to impact nutrient uptake and thus plant growth due to the stimulation of lateral root formation and root hair formation (Bohn-Courseau 2010; Bottini et al. 2004). Plant hormones are key elements for root morphology changes. Some beneficial bacteria are also described to produce them (Bottini et al. 2004).

Regarding *B. subtilis* PTA-271 genome, it predicts the trp group, described in literature to produce tryptophan as the main precursor of the auxin IAA (indole-3-acetic acid) (Glick 2012). The genome of *B. subtilis* PTA-271 also predicts genes such as yvdD (Supplementary Table S2), linked in the literature to cytokinin synthesis which is known as a plant growth regulator (cell division, organogenesis) in combination with IAA. Gibberellins (GA) produced by some bacteria also affect the plant growth and survival (Bottini et al. 2004). Regarding the *B. subtilis* PTA-271 genome, it predicts ispD and GerC3_HepT, described in the literature to be respectively linked to 2-C-methyl-D-erythritol 4-phosphate (MEP) and geranylgeranyl diphosphate (GGPP) production, two successive precursors of GA and abscisic acid (ABA) synthesis in plants (Rodríguez-Gacio et al. 2009).

Genes described to encode for other plant growth regulators, namely polyamines (PAs), are also predicted in the genome of *B. subtilis* PTA-271. Among them: speA, speB, speG and speE are respectively described in literature to encode for putative ADC (arginine decarboxylase), agmatinase (leading to putrescine), then spermidine- and spermine-synthases. Additionally, genes encoding for putative S-adenosyl-methionine (SAM) decarboxylase (speH) and SAM-methyltransferase (S19-40_00450) are predicted in *B. subtilis* PTA-271 genome, and these proteins are mentioned to complete PA synthesis from putrescine (Aziz et al. 1997). PAs are known to promote flowering and to play important roles in inducing cell division, promoting regeneration of plant tissues and cell cultures (Chen et al. 2019), as delaying senescence (Pandey et al. 2000).

Volatile compounds (VOCs) produced by some beneficial rhizospheric bacteria have also been identified as elicitors promoting plant growth. Regarding *B. subtilis* PTA-271, its predicted genes encode putatively for (1) acetoin (acuA, acuC…) and (2) 2,3-butanediol (butA and butC) (Bitas et al. 2013; Caulier et al. 2019). VOCs are especially reported to interact with plant hormones (Ortíz-Castro et al. 2009; Xie et al. 2009; Zhang et al. 2007).

Host induced defenses and microbiota preservation: assets for plant protection

Plant induced defenses upon biotic stress

Host primed defenses during ISR are regulated by hormones, depending on either JA and ET signaling or SA signaling (Pacifico et al. 2019; Pieterse et al. 2009; Pieterse et al.

2014; Villena et al. 2018). Beneficial microorganisms may modulate the plant hormonal balance or directly elicit the plant defenses. Regarding the genome of *B. subtilis* PTA-271, the metK gene is predicted to encode for SAM synthase that would appear ISR-useful for plants which possess the complementary ET metabolic machinery (Aziz et al. 1997; Pandey et al. 2000). SA is another hormone for which several genes encoding its metabolic pathways (from synthesis to hydrolysis) are predicted in B. subtilis PTA-271 genome, among which pchA putatively encoding for the salicylate biosynthesis isochorismate synthase.

Many elicitors also induce host immunity, coming from microorganisms (MAMPs, microbial associated molecular patterns) but also from the plant host (DAMPs, damage-associated molecular patterns). MAMPs can act from the external surface of a beneficial microorganism (flagellin) or result from a secretion outside or inside the host (surfactin, fengycin, VOCs, etc.) (Felix et al. 1999; Heloir et al. 2019; Ongena et al. 2007; Ortíz-Castro et al. 2009). Flagellin proteins are putatively encoded by the hag gene predicted in *B. subtilis* PTA-271 (Supplementary Table S1). The lipopeptides surfactin and fengycin are other elicitors of plant ISR putatively encoded by some genes predicted in the genome of *B. subtilis* PTA-271 (srf and fen genes, respectively). VOCs produced by rhizospheric bacteria, as the 3-hydroxy 2-butanone and acetoin which are putatively encoded by *B. subtilis* PTA-271 genome, are also well known to induce ISR (Ortíz-Castro et al. 2009). Among VICs, the ubiquitous nitric oxide (NO) is another signal molecule (Sánchez-Vicente et al. 2019). Different genes related to NO metabolic pathways are predicted in *B. subtilis* PTA-271 genome, among which the gene nos putatively encoding for a NO synthase oxygenase. Exopolysaccharides (EPS) and lipopolysaccharides (LPS) are other elicitors reported in several *Bacillus* genera (Akram et al. 2015; Audrain et al. 2015; Kloepper et al. 2004; Pieterse et al. 2014; Van Loon et al. 1998; Villena et al. 2018; Zamioudis et al. 2015). Regarding the genome of B. subtilis PTA-271, it predicts several genes putatively encoding for EPS (S19-40_00800, S19-40_00870, S19-40_00999, S19-40_01009, S19-40_01427) and LPS (lptB, lapA, lapB), additionally to the other elicitors predicted to be encoded by *B. subtilis* PTA-271 genome (siderophores, flagella, N-acyl-L-homoserine lactone, etc.).

DAMPs are alternative elicitors produced by lytic enzymes (chitosan, glucans, etc.) of microorganisms (either beneficial or pathogenic) or plants (Heloir et al. 2019). Genes

encoding for lytic enzymes are predicted in *B. subtilis* PTA-271 genome, such as those encoding for putative chitosanase and ß-glucanase (Supplementary Table S3). Many other genes are also predicted to encode for lytic enzymes in the *B. subtilis* PTA-271 spore cortex (Supplementary Table S4) for which the roles remain unclear.

Plant induced defenses upon abiotic stress

Some previously cited hormones are also useful for plant defense against abiotic stress, such as ABA and GA (Pacifico et al. 2019), of which precursors are predicted to be encoded by genes identified in the genome of *B. subtilis* PTA-271 (GerC3_HepT, ispD). From GGPP, the kaurene pathway may lead to GA, while the phytoene path may lead to ABA (Rodríguez-Gacio et al. 2009), and in the genome of *B. subtilis* PTA-271, yisP (a crtb KEGG gene) encodes for a putative 15-cis-phytoene/all-trans-phytoene synthase. ET is another useful hormone for plant defense against abiotic stress (Pacifico et al. 2019), and *B. subtilis* PTA-271 genome has genes identified to putatively produce SAM (metK). Altogether these data predict that *B. subtilis* PTA-271 genome may putatively encode for key precursors of phytohormones that may influence actively ABA and ET contents in plants. In plants, ABA, GA and ET signaling pathways interfere altogether through different transcription factors (TF) or small proteins (GiD, DELLA, EIN, etc.) that physically interact (Liu and Hou 2018; Zentella et al. 2007). In the genome of *B. subtilis* PTA-271, many genes are predicted to encode for sigma factors and many TF (Supplementary Table S2). It is noteworthy to understand that useful TF upon abiotic stress could also be useful upon biotic stress. The set of genes under common regulatory controls (operons) are also listed in the Supplementary Table S2.

PAs such as those predicted to be encoded by the genome of *B. subtilis* PTA-271 are also described to protect plant cells upon water deficit (Ebeed et al. 2017), temperature changes (Tian et al. 2012) and salinity (Saha et al. 2015).

Microbiota quality and preservation

As energy and carbon sources, plant root exudates (sugars, organic acids, amino acids, lipophilic compounds, etc.) would enable the selective recruitment of biosurfactant producers (Koo et al. 2005; Siciliano and Germida 1998). In return, these beneficial bacteria can facilitate the bioavailability of root exudates and biofilm formation, thus the colonization of host-plants by beneficial bacteria (Koo et al. 2005; Newton and Fray

2004; Ongena and Jacques 2008), maybe such as *B. subtilis* PTA-271 which is suspected to produce surfactin. SA was also shown to mediate changes in the composition of root exudates, then in the qualitative microorganism recruitment by plants (Huang et al. 2014). Regarding the *B. subtilis* PTA-271 genome, some genes are also predicted to produce SA (pchA), highlighting another key lever that putatively influence the composition of plant microbiome.

Beneficial microbial interactions can additionally depend on bacterial auto-inducers (AI) that are low-molecular weight signal molecules activating the interactive competences of a bacterium in a quorum-sensing (QS) dependent manner (Newton and Fray 2004). Among AI, the furanosyl-borate-diester (AI-2) is described as universal for interspecies communication both in Gram-positive and Gram-negative bacteria (Duanis-Assaf et al. 2016). Regarding *B. subtilis* PTA-271 genome, the predicted luxS gene putatively encodes for AI-2 production, while the predicted EntF and AM373 putatively encode oligopeptides or auto-inducing peptide (AIP) precursors. AIP is another class of AI consisting of 5–34 amino acids residues and produced by Gram-positive bacteria for their intercellular communication (Verbeke et al. 2017).

When interacting with the environment, a microorganism must also remain metabolically active to exert beneficial effects. Upon biotic interactions, *Bacillus* species are exposed to host defenses that include reactive oxygen species (ROS) (Sukchawalit et al. 2001). Regarding the system of sensing, protection and regulation of ROS in the genome of *B. subtilis* PTA-271, genes are predicted to putatively encode for resistance to hydroperoxide (ohrA, ohrB, ohrR). Upon abiotic stress, beneficial bacteria must survive dehydration, wounding, cold, heat or salinity that in turn lead to regulation of the water status. For this end, bacterial species can control their intracellular solute pools (Booth and Louis 1999; Levina et al. 1999). Regarding the genome of *B. subtilis* PTA-271, genes predicted to encode for potassium uptake proteins (KtrA, KtrB) putatively enable survival in high salinity environments. Interestingly, the genome of *B. subtilis* PTA-271 also predicts genes to detoxify or resist compounds accumulating in the environment (Sato and Kobayashi 1998; Vaillancourt et al. 2006), such as arsenite (arsR), organic pesticides or nitroaromatic compounds (sugE, qacC, mhqR, mhqA) among others (Supplementary Tables S2 and S5).

Upon extreme environmental conditions, some beneficial bacteria can sporulate, turning on endospore form (Errington 1993; Nicholson et al. 2006). Regarding the genome of *B. subtilis* PTA-271, several genes are predicted to be involved in the sporulation process (Supplementary Table S4): spo (sporulation control), ger (germination control), cot (endospore external layer) and cw (spore cortex lytic enzymes), putatively enabling it to survive long lasting periods while preserving all beneficial strengths for plant profits.

Direct confrontation with pathogens or aggressive molecules

Upon direct confrontation, *Bacillus* species also need to protect themselves against pathogen defenses. In addition to ROS protection, diverse transporters mediate antibiotic extrusion, whether specific to a substance or a group of substances. Regarding the genome of *B. subtilis* PTA-271, the specific transporters predicted would putatively confer it resistance towards: tetracyclin (tetA, tetR, tetD), fosfomycin (fosB), erythromycin (msrA, msrB), bacillibactin (ymfD), bacitracin (BceA, BceB, BcrC), bleomycin (ble) and riboflavin (ribZ, rfnT) for example. Among the non-specific transporters (or multidrug transporters) predicted in the genome of *B. subtilis* PTA-271 are: mepA, ebrA and ebrB; ykkD and ykkC; bmrA and bmr3; emrY, among others.

Bacillus species can additionally directly detoxify some pathogen aggressive molecules targeting plants, such as phytotoxins, by the mean of antitoxins or detoxifying enzymes such as transferases and CYP450s (Lyagin and Efremenko 2019; Karlovsky 1999). In the genome of *B. subtilis* PTA-271, the main transferases predicted are glutathione-S-transferases GST, malonyl-transferases MT, glucosyl-transferases GT and many others, while the main CYP450s predicted are mono-oxygenases and dioxygenases (Supplementary Table S5). Quenching enzymes constitute another lever for beneficial bacteria to directly target pathogen aggressive molecules, by preventing their QS-dependent production (Chen et al. 2013; Pacifico et al. 2019). Indeed, *Bacillus* species share aiiA gene encoding for N-acetyl homoserine lactonase able to hydrolyze the lactone ring of the AHLs (Acyl-homoserine lactones) involved in the QS production of some pathogen virulent factors. The genome analysis of *B. subtilis* PTA-271 predicts such genes putatively encoding for quenching enzymes such as lactonases, β-lactamases, deaminases, deacetylases and other (de)acylases (Supplementary Table S6).

Polyketide synthases (PKS) are another type of transferases, namely acetyltransferases, described to produce plant beneficial molecules as microbicide for phytopathogens: the polyketides (PK) (Cane et al. 1998; Olishevska et al. 2019). Regarding the genome of *B. subtilis* PTA-271, 15 genes are predicted to encode for putative PKS, many others for acetyltransferases or for enzymes sharing similar part of the PKS functions (Supplementary Table S7). According to antiSMASH 5.1.0, *B. subtilis* PTA-271 genome predicts 11 secondary metabolites gene clusters, among which: 1 PKS cluster and 1 hybrid PKS-NRPS cluster (Supplementary Table S8).

An extensive range of pathogen direct effectors are additionally produced by *Bacillus* spp., such as the RP (ribosomally synthesized peptides) and NRP (non-ribosomally synthesized peptides) antimicrobial molecules (Caulier et al. 2019; Yu et al. 2011). Some of them are predicted as encoded by the genome of *B. subtilis* PTA-271, such as: Baillaene (pksD), subtilosin (sboA, albG, albE, alBOT, albB, albA) and bacilysin (bacE, bacF, bacG) (Supplementary Table S3). Lipopeptides are other NRP antimicrobial molecules (Finking and Marahiel 2004; Ongena and Jacques 2008), which encoding genes are predicted in the genome of *B. subtilis* PTA-271 to putatively produce the powerful antifungal substances fengycin and surfactin (Supplementary Table S3). Besides antibiotics and surfactants, bacterial siderophores can also directly alter pathogen fitness and aggressiveness, by depriving pathogen growth of iron while providing it for plant growth (Dutta et al. 2006). Regarding the genome of *B. subtilis* PTA-271, predicted genes putatively encode for the siderophore Bacillibactin (Supplementary Table S3). Lytic enzymes (CWDE) are other important feature of *Bacillus* spp. that can both alter pathogen survival and produce MAMPs (Jadhav et al. 2017). Regarding the genome of *B. subtilis* PTA-271, several genes are predicted to encode for putative CWDE: 1 chitosanase (csn), 1 β-glucanase (bglS), 1 β-glucanase / cellulase (eglS) and about 80 proteases (Supplementary Table S3).

Besides these NRP and RP antimicrobial molecules, the genome of *B. subtilis* PTA-271 also predicts the genes hcnC, acu and but, putatively encoding for the volatile antimicrobial compounds: VIC (hydrogen cyanide, HCN) and VOC (acetoin and 2,3-butanediol), respectively (Bitas et al. 2013; Caulier et al. 2019; Pacifico et al. 2019).

According to COG categories, 2.30% of *B. subtilis* PTA-271 genome is predicted to be devoted to the production of secondary metabolites, considered as one of the most important features in biocontrol activities. AntiSMASH 5.1.0 predicts 11 secondary metabolites gene clusters in *B. subtilis* PTA-271 genome, among which 3 NRPS clusters and 2 RiPPs clusters (Supplementary Table S8).

B. subtilis PTA-271 genome comparison with other genomes

To understand the magnitude of the differences between *B. subtilis* PTA-271 and other *Bacillus* strains, the PTA-271 genome has been compared to the complete genomes of 5 type-strains (*B. subtilis* NCIB 3610, *B. subtilis* 168, *B. subtilis* 9407, *B. amyloliquefaciens* subsp. plantarum strain FZB42, and *B. velezensis* KTCT 13012) (Parker et al. 2019) and 32 non-type strains, represented in Table 6. Among non-type strains showing ≥99% of the 16S ribosomal gene similarity with PTA-271 are 31 distinct strains of *B. subtilis* and 1 *Bacillus velezensis*. For this genomic comparison, was used the GGDC 2.1 web server (Meier-Kolthoff et al. 2014), the DSMZ phylogenomics pipeline to estimate DNA-DNA hybridization (DDH) (Meier-Kolthoff et al. 2014), and the JSpecies WS web server to estimate the Average Nucleotide Identity (ANI) through pairwise comparisons (Richter and Rosselló-Móra 2009). The DDH value was estimated using the recommended formula (formula two) for draft genomes, at the GGDC website (Abuzinadah et al. 1986). The ANI values were calculated using Ezbiocloud (Yoon et al. 2017). The whole data analysis enabled to obtain the intergenomic distances between genomes and their probability of belonging to the same species or subspecies. The general comparison of genomes is reported in Table 6, while the intergenomic distances (DDH estimate and ANI) are shown in Table 7.

Table 6. Comparative NCBI genome analysis of *Bacillus subtilis* PTA-271 with strains showing ≥99% of 16 s similarity.

	Strain	Gb accession number	Isolation source	Country	Genome size (bp)	G+C content (%)	Protein-coding sequences	tRNA coding genes	rRNA
	Bacillus subtilis subsp. subtilis strain PTA-271	-	rhizosphere, roots, leaves and stems (Grapevine)	France	4.002	43.8	3945	81	11
Type-strains	*Bacillus subtilis* 9407	PISO01000016	apple tree	China	4.19	43.4	4012	79	9
	Bacillus subtilis subsp. subtilis NCIB 3610	CP034484	not available/ unknown	not available/ unknown	4.3	43.34	4390	86	30
	Bacillus subtilis subsp. subtilis 168	CP019662	soil	Germany	4.22	43.5	4284	86	30
	Bacillus amyloliquefaciens subsp. plantarum FZB42	CP000560	soil (sugar beet)	Germany	3.92	46.5	3687	89	31
	Bacillus velezensis KCTC 13012	LHCC01000001	river velez	spain	4.04	46.3	3806	80	9
Non type-strains	*Bacillus subtilis* subsp. subtilis QB5413	CP017313	not available/ unknown	France	4.22	42.7	5099	84	30
	Bacillus subtilis SRCM104005	CP035164	food	South Korea	4.14	43.8	4106	86	30
	Bacillus subtilis QB61	CP029461	soil	China	4.12	43.7	4086	85	28
	Bacillus subtilis subsp. subtilis QB5412	CP017312	not available/ unknown	France	4.22	43.5	4252	86	30
	Bacillus subtilis SR1	CP021985	soil	India	4.09	44.2	3911	83	30
	Bacillus subtilis SG6	CP009796	luffa	China	4.08	43.8	4030	84	21
	Bacillus subtilis SRCM103773	CP035397	food	South Korea	4.05	43.6	4113	86	30
	Bacillus subtilis PR10	CP040528	Tobacco rhizosphere soil	China	4.07	43.8	3978	86	30
	Bacillus subtilis GQJK2	CP020367	rhizosphere	China	4.07	43.8	3976	86	30
	Bacillus subtilis subsp. subtilis BS155	CP029052	marine sediment	China	4.33	43.5	2718	86	30
	Bacillus subtilis SRCM103835	CP035400	food	South Korea	4.14	43.8	4108	86	30
	Bacillus subtilis SRCM103837	CP035401	food	South Korea	4.14	43.8	4113	86	30
	Bacillus subtilis SRCM103641	CP035390	food	South Korea	4.11	43.7	4136	86	30
	Bacillus subtilis H19	CP039935	seawater	China	4.06	43.9	4001	86	30
	Bacillus subtilis BS38	CP017314	soybean paste	South Korea	4.01	43.6	3876	86	30
	Bacillus subtilis subsp. spizizenii SW83	CP030925	Turbinaria ornata	India	3.98	43.8	3936	83	8
	Bacillus subtilis subsp. subtilisGFR-12	CP032852	Fermented soybean paste	South Korea	4.2	43.3	4117	87	30
	Bacillus subtilis subsp. subtilis 2KL1	CP032872	Fermented soybean paste	South Korea	4.2	43.3	4110	93	33
	Bacillus subtilis SRCM103886	CP035162	food	South Korea	4.21	43.3	4121	87	30
	Bacillus subtilis subsp. subtilis 2RL2-3	CP032857	Fermented soybean paste	South Korea	4.19	43.4	4083	87	33
	Bacillus subtilis SRCM103576	CP035402	food	South Korea	4.01	43.5	3986	86	30
	Bacillus subtilis subsp. subtilis N4-2	CP032867	Natto	Japan	4.12	43.5	4154	87	30
	Bacillus sp. M4U3P1	CP041372	Suaeda salsa	China	4.12	43.5	4068	87	30
	Bacillus subtilis subsp. subtilis N3-1	CP032865	Natto	Japan	4.12	43.5	4069	87	30

Table 7. Comparative genome distances analysis with other strains, using DNA-DNA hybridization and average nucleotide identities.

	Strains	Gb accession number	DNA-DNA hybridization (DDH method)					Average nucleotide identities (ANIm)	
			Distance	DDH estimate	Probability that DDH >70% (same species)	Probability that DDH >79% (same subspecies)	Difference in % G+C	ANIm (%)	Aligned (bp)
Type-strains	*Bacillus subtilis* 9407	PISO01000016	0.0104	91.60%	96.29%	67.69%	0.56	99.02	1,456,961
	Bacillus subtilis subsp. subtilis NCIB 3610	CP034484	0.0121	90.00%	95.80%	65.28%	0.27	98.88	2,509,972
	Bacillus subtilis subsp. subtilis 168	CP019662	0.0122	90.00%	95.78%	65.19%	0.27	98.87	2,962,217
	Bacillus amyloliquefaciens subsp. plantarum FZB42	CP000560	0.2144	20.50%	0.00%	0.00%	2.69	77.1	1,854,058
	Bacillus velezensis KCTC 13012	LHCC01000001	0.2268	19.40%	0.00%	0.00%	2.84	77.02	437,224
Non type-strains	*Bacillus subtilis* subsp. Subtilis QB5413	CP017313	0.0112	90.90%	96.08%	66.63%	1.05	98.76	2,529,290
	Bacillus subtilis SRCM104005	CP035164	0.0119	90.20%	95.87%	65.63%	0.00	98.84	2,941,570
	Bacillus subtilis QB61	CP029461	0.0119	90.20%	95.85%	65.52%	0.04	98.82	3,023,981
	Bacillus subtilis subsp. subtilis QB5412	CP017312	0.0122	89.90%	95.78%	65.17%	0.27	98.85	2,985,990
	Bacillus subtilis SR1	CP021985	0.0124	89.70%	95.70%	64.82%	0.24	98.86	2,881,899
	Bacillus subtilis SG6	CP009796	0.0124	89.70%	95.70%	64.83%	0.05	98.81	2,968,883
	Bacillus subtilis SRCM103773	CP035397	0.0126	89.50%	95.63%	64.50%	0.16	98.81	2,633,309
	Bacillus subtilis PR10	CP040528	0.0129	89.30%	95.56%	64.15%	0.01	98.77	2,648,038
	Bacillus subtilis GQJK2	CP020367	0.0129	89.30%	95.55%	64.14%	0.01	98.79	2,856,573
	Bacillus subtilis subsp. subtilis BS155	CP029052	0.0131	89.10%	95.49%	63.83%	0.29	98.69	2,805,710
	Bacillus subtilis SRCM103835	CP035400	0.0132	89.00%	95.44%	63.61%	0.02	98.75	2,640,533
	Bacillus subtilis SRCM103837	CP035401	0.0132	89.00%	95.44%	63.61%	0.02	98.76	2,637,514
	Bacillus subtilis SRCM103641	CP035390	0.0137	88.60%	95.29%	62.96%	0.07	98.67	2,561,457
	Bacillus subtilis H19	CP039935	0.0144	88.00%	95.05%	61.95%	0.11	98.62	2,750,901
	Bacillus subtilis BS38	CP017314	0.0149	87.40%	94.84%	61.09%	0.19	98.52	2,702,006
	Bacillus subtilis subsp. spizizenii SW83	CP030925	0.0152	87.20%	94.73%	60.64%	0.02	98.56	2,801,320
	Bacillus subtilis subsp. subtilisGFR-12	CP032852	0.0153	87.10%	94.69%	60.50%	0.47	98.49	2,649,573
	Bacillus subtilis subsp. subtilis 2KL1	CP032872	0.0153	87.10%	94.69%	60.47%	0.43	98.48	2,636,663
	Bacillus subtilis SRCM103886	CP035162	0.0153	87.10%	94.68%	60.45%	0.48	98.49	2,651,166
	Bacillus subtilis subsp. subtilis 2RL2-3	CP032857	0.0153	87.10%	94.68%	60.44%	0.43	98.50	2,597,779
	Bacillus subtilis SRCM103576	CP035402	0.0155	87.00%	94.64%	60.28%	0.29	98.51	2,578,601
	Bacillus subtilis subsp. subtilis N4-2	CP032867	0.0155	86.90%	94.62%	60.21%	0.31	98.52	2,684,907
	Bacillus sp. M4U3P1	CP041372	0.0155	86.90%	94.62%	60.21%	0.32	98.51	2,595,536
	Bacillus subtilis subsp. subtilis N3-1	CP032865	0.0155	86.90%	94.62%	60.20%	0.31	98.54	2,616,955
	Bacillus subtilis subsp. subtilis N2-2	CP032863	0.0155	86.90%	94.62%	60.20%	0.31	98.48	2,667,845
	Bacillus subtilis subsp. subtilis N1-1	CP032861	0.0155	86.90%	94.62%	60.19%	0.29	98.56	2,473,375
	Bacillus subtilis ATCC 21228	CP020023	0.0156	86.90%	94.60%	60.12%	0.33	98.53	2,668,973
	Bacillus subtilis subsp. subtilis MH-1	CP032853	0.0158	86.60%	98.80%	77.62%	0.51	98.44	2,611,384
	Bacillus subtilis SX01705	CP022287	0.0175	85.10%	93.79%	57.14%	0.08	98.31	2,686,386
	Bacillus subtilis subsp. subtilis RO-NN-1	CP002906	0.0203	82.60%	92.41%	52.68%	0.09	98.04	2,857,714
	Bacillus velezensis strain ATR2	NZ_CP018133	0.2144	20.50%	0%	0%	2.69	77.1	1,854,058

Among the type strain genomes, the closest strain to *B. subtilis* PTA-271 was *B. subtilis* 9407, with a 0.0104 distance, a DDH estimate of 91.60%, and an ANIm of 99.02%. As expected, the most distant strain was *B. velezensis* KTCT 13012, with a 0.2268 distance, a DDH estimate of 19.40% and a 0% probability of being the same species, corroborated with an ANIm percentage of 77.02%. Concerning the non-type strain genomes, the closer strains to PTA-271 were *B. subtilis* QB5413, *B. subtilis* SRCM 104005, and *B. subtilis* QB61 with distances of 0.0112, 0.0119 and 0.0119 respectively, and DDH estimates of 90.90, 90.20 and 90.20% respectively. The most distant strain was *B. velezensis* strain ATR2, with a distance of 0.2144 and a DDH estimate of 20.50% corroborated with an ANIm percentage of 77.1%. The most distant *B. subtilis* strain to PTA-271 was *B. subtilis* subsp. subtilis RO-NN-1 with a distance of 0.203 and a DDH of 82.60%.

2.4. Conclusion

With a genome size of 4,001,755 bp containing 97.69% of protein encoding genes, the draft genome of *B. subtilis* PTA-271 highlights all the qualities of a promising plant beneficial microorganism. The most relevant predicted genes encode for: (1) a functional swarming motility system highlighting advantageous colonizing capacity of host and a strong interacting capacity within plant microbiota; (2) a strong survival capacity, due to sporulation but also to complex detoxifying systems, auto-inducing metabolic paths and recruiting capacities for adding microbiota values; and (3) the delivery of many bioactive substances (hormones, elicitors, effectors and quenchers, siderophores and lytic enzymes, etc.), facilitating the stimulation of plant growth or defenses, or else, disturbing pathogen fitness or aggressiveness. Interestingly, the putative capacity of *B. subtilis* PTA-271 to produce a wide range of phytohormone analogous (SA, ET precursor, ABA etc.), as well as diverse direct effectors and lytic enzymes against plant pathogens, highlight a significant potential for biocontrol strategies. Altogether, the plurality of the biomolecules putatively encoded by the genome of *B. subtilis* PTA-271 are putative strengths to impact both biochemical conditions, species ratios and their interactions, predicting an ability to combat a broad spectrum of plant pathogens such as grapevine trunk disease (Trotel-Aziz et al. 2019).

Chapter III

Cultivar Contributes to the Beneficial Effects of *Bacillus subtilis* PTA-271 and *Trichoderma atroviride* SC1 to Protect Grapevine Against *Neofusicoccum parvum*

3.1. Introduction

Global environmental changes promote the incidence of plant diseases by increasing the pathogen pressure or make the plants more susceptible to them (O'Brien 2017; Velásquez et al. 2018). Grapevine trunk diseases (GTDs) are among the most important groups of grapevine diseases all over the world, creating a big concern in all wine-producing countries (Mondello et al. 2018). Attacking the plant perennial part and leading inevitably to the short- or long-term death of vines, the pathogens responsible of GTDs are described as very injurious for the sustainability of the winemaking industry (Hofstetter et al. 2012). As main restrictors for viticulture, GTDs can lead to high economic losses, less table grape for consumers, and social and environmental disturbances (O'Brien, 2017). Both young and mature vines are affected by GTDs, even as nursery staged plants, reducing both productivity and longevity of the vineyard, thereby causing massive economic losses (Gramaje and Armengol 2011).

Botryosphaeria dieback (BOT) is one of the most significant GTDs, triggerable by more than 25 distinct species of Botryosphaeriaceae including the aggressive *Neofusicoccum parvum* (Billones-Baaijens and Savocchia 2019; Larach et al. 2020; Reis et al. 2019; Úrbez-Torres 2011) Symptomatic plants develop a low or apoplectic dieback phenotype, including a low budburst rate, a poor vegetative development, external canker, and internal longitudinal necrotic lesions that can lead to a full dead branch (Billones-Baaijens and Savocchia 2019; Larach et al. 2020; Larignon et al. 2001, 2009; Larignon 2004). Susceptibility to BOT pathogens also differs between cultivars (Chacon et al. 2020; Claverie et al. 2020; Fontaine et al. 2016a; Travadon et al. 2013).

Due to the undetermined period of latency within the vines (asymptomatic state), early detection and management of GTDs remain presently a challenge in both nursery and vineyard, and only few preventives, but no curative methods, are available. Indeed, few chemicals are applied on pruning wounds in vineyards to prevent dissemination of the conidia of fungal pathogens (Sosnowski et al. 2004), preferring cultural practices in vineyard (Mondello et al. 2018) and sanitation methods (Gramaje and Armengol 2011; Gramaje et al. 2018). However, these kinds of treatments cannot eradicate the pathogens once established in a vineyard (Calzarano et al. 2004; Gramaje and Armengol 2011). An

interesting alternative and complement to the previously cited GTDs control methods in vineyard is the use of biological control agents (BCAs) as reported by Mondello et al. (2018). For instance, several microorganisms have already been evaluated, both *in vitro* and *in planta* against BOT pathogens (Compant and Mathieu 2017; Compant et al. 2013; Di Marco et al. 2004; Hunt et al. 2001; John et al. 2004; Trotel-Aziz et al. 2019). Among them there are bacterial BCAs such as *Pseudomonas*, *Bacillus*, and *Enterobacter* species, and fungal BCAs such as several *Fusarium* and *Trichoderma* species (Mondello et al. 2018). Some of them, such as *Trichoderma atroviride*, *Trichoderma harzianum*, *Bacillus subtilis*, and *Bacillus amyloliquefaciens*, are already commercialized against some GTDs pathogens, or against other hemibiotrophic and necrotrophic pathogens including *Botrytis cinerea*, *Fusarium oxysporum*, or many others (Alfiky and Weisskopf 2021; Elad 2000; Kuzmanovska et al. 2018; Schmidt and Panstruga 2011; Thambugala et al. 2020;).

To date, *Trichoderma* species are the most used fungal-based BCA in viticulture (Harman 2006; Muckherjee et al. 2012; Waghunde et al. 2016) and have been also widely investigated as BCA against GTDs (Berbegal et al. 2020; Di Marco et al. 2002, 2004; Halleen et al. 2010: John et al. 2008; Martínez-Diz et al. 2021a,b). *Trichoderma* spp. are described to directly antagonize GTD pathogen aggressiveness by competition for nutrients and space, mycoparasitism, cell-wall degrading enzymes, and antibiosis (Harman 2006; Pieterse et al. 2014; Van Wees et al. 2008; Vinale et al. 2008; Waghunde et al. 2016). *Trichoderma* spp. have also been described as plant growth and defense stimulators (Harman 2006; Pieterse et al. 2014; Van Wees et al. 2008; Vinale et al. 2008; Waghunde et al. 2016). Among *Trichoderma* spp., *Ta* SC1 was shown to strongly reduce the infections caused by some GTD pathogens in nurseries and established vineyards at the registered dose rate of 2 g/L, equivalent to the density of 2×10^{10} conidia/L recommended by the commercial product (Berbegal et al. 2020; Martínez-Diz et al. 2021a; Pertot et al. 2016). *Bacillus* strains are another group of microorganisms extensively studied as BCA and reported to directly and indirectly protect plants against pathogens with different lifestyles (Magnin-Robert et al. 2007; Nguyen et al. 2020; Trotel-Aziz et al. 2008), including the GTD hemibiotrophic pathogens (Halleen et al. 2010; Kotze et al. 2019; Rezgui et al. 2016; Schmidt et al. 2001; Trotel-Aziz et al. 2019). A broad range of beneficial molecules are produced or encoded by the genome of *Bacillus* spp., both to induce or elicit plant defenses (as with phytohormones

precursors, lipopolysaccharides, siderophores, etc.) and to directly compete, antagonize, or alter plant pathogens or their aggressiveness (Kloepper et al. 2004; Leal et al. 2021; Ongena and Jacques 2008). Among *Bacillus* spp., *B. subtilis* is one of the most frequently tested against GTDs (Mondello et al. 2018), and *B. subtilis* PTA-271 has shown promising results in reducing infections caused by the aggressive strain *N. parvum* Bt67 (Trotel-Aziz et al. 2019). Literature also reports that the combination of two or more BCAs can improve the management of plant diseases (El-Tarabily 2006; Guetsky et al. 2002; Magnin-Robert et al. 2013; Weller 1988; Yobo et al. 2011), probably due to additive or synergistic effects of combined mechanisms in a complex changing environment (Meyer and Roberts 2002).

Beneficial microbial interactions conferred by BCA lead to induced systemic resistance (ISR) in the plant, giving it greater protection to pathogens in spatially separated parts of the plant (Alström 1991; De Vleesschauwer and Höfte 2009; Van Peer et al. 1991; Wei et al. 1991). ISR is associated with an early, strong, and rapid activation of plant defenses upon pathogen infection, a phenomenon known as the priming state (Conrath et al. 2001, 2015; Pieterse et al. 2014). Among the BCA-induced defense responses, the most relevant are jasmonate (JA)- and ethylene (ET)-dependent ones, described as useful defenses against necrotrophs (Nie et al. 2017; Niu et al. 2011; Pieterse et al. 2001, 2014; Verhagen et al. 2004; Van der Ent et al. 2009). However, Niu et al. (2011) also reported that some BCAs may mediate ISR in a salicylic acid (SA)-dependent manner. In brief, the diversity of BCA ways of protection may depend on both the BCA and the pathogen, but also on the plant and even the cultivar (Mutawila et al. 2011; Nguyen et al. 2020; Pacifico et al. 2019; Stempien et al. 2020).

In this study, we evaluated the effect of combining a potential BCA, *Bs* PTA-271, and a BCA-commercial product containing *Ta* SC1, on the protection of two distinct grapevine cultivars, Chardonnay, and Tempranillo, potentially showing distinct susceptibilities to GTDs. The pathogen selected was *Np*-Bt67, described as a very aggressive pathogen associated to BOT. As each BCA has already been recognized as beneficial to at least one cultivar. (Berbegal et al. 2020; Martínez-Diz et al. 2021a; Trotel-Aziz et al. 2019), their beneficial effect was additionally investigated on the other cultivar, as single BCA and in dual combination of two BCAs. To compare the two BCAs, densities were aligned to the density optimized for *Bs* PTA-271 with Chardonnay rootlings. After looking for the protective capacity of BCAs *in planta*, their ways of action leading to protection were

further explored. Thus, the indirect and direct benefits offered by each BCA and their combination were investigated, focusing on both grapevine immunity and the direct beneficial or detrimental physical interplays among the microorganisms *in vitro* (*Bs* PTA-271, *Ta* SC1, and *Np*-Bt67).

3.2. Material and methods

Plant Material and Growth Conditions

Three-node-long cuttings of grapevine *Vitis vinifera* L. cv. Tempranillo (clone RJ-26) and cv Chardonnay (clone 7535) were provided by Viveros Villanueva nursery (Navarra, Spain) and Pommery's vineyards in Reims (France), respectively. Tempranillo cuttings were surface-sterilized for 6 h in a 0.05% cryptonol (8-hydroxyquinoline sulfate) solution, waxed and stored at 4°C in a cold chamber for 3 weeks, and then rehydrated with 0.05% cryptonol solution overnight. Chardonnay cuttings were directly surface-sterilized with 0.05% cryptonol solution overnight. Cuttings of both cv were then rooted as described by Lebon et al. (2005), using an indole-3-butyric acid (1 g/L) solution before being placed by 15 in 350-ml pots containing the soil Sorexto (horticultural soil M4600, Grenoble, France) in a culture chamber (24/20°C Day/night, 55–65% relative humidity day/night, and 16-h photoperiod at 400 μmol/m^2/s). They were watered three times a week. Only rootlings that have developed roots (30% rooting rate in 15 weeks) were kept for further experiments and transferred to individual 200-ml pots with the same culture conditions.

Biocontrol Agent's Growth and Plant Treatments

Bacillus subtilis PTA-271

Bacillus subtilis PTA-271 (GenBank Nucleotide EMBL Accession No. AM293677 for 16S rRNA and DDBJ/ENA/GenBank Accession No. JACERQ000000000 for the whole genome) was isolated in 2001 from the rhizosphere of healthy Chardonnay grapevines (*V. vinifera* L. cv. Chardonnay) from a vineyard located in Champagne (Marne, France) (Leal et al. 2021; Trotel-Aziz et al. 2008). Bacterial growth started by adding 100 µl of glycerol stock suspension to sterile Luria Bertani (LB) medium and incubating at 28°C with agitation (100 rpm). Experiments were performed when the bacterial culture is at the exponential growth phase. After centrifugation (5,000 *g*, 10 min), the pellet was washed once with a sterile 10 mM $MgSO_4$ medium and resuspended in a same $MgSO_4$ medium. Bacterial density was measured by spectrophotometry at 450 and 650 nm, and the mean density was adjusted with a sterile $MgSO_4$ medium before treatment according to Trotel-Aziz et al. (2019). The bacterial suspension was applied twice by drenching the soil at the root level of rootlings at a final density of 10^8 CFU/g soil. Inoculations were carried out when rootlings were 16 weeks old (considered as day 0) and 2 weeks later (day 15) as indicated in Figure 1. Control rootlings were similarly drenched twice with $MgSO_4$solution (Figure 1).

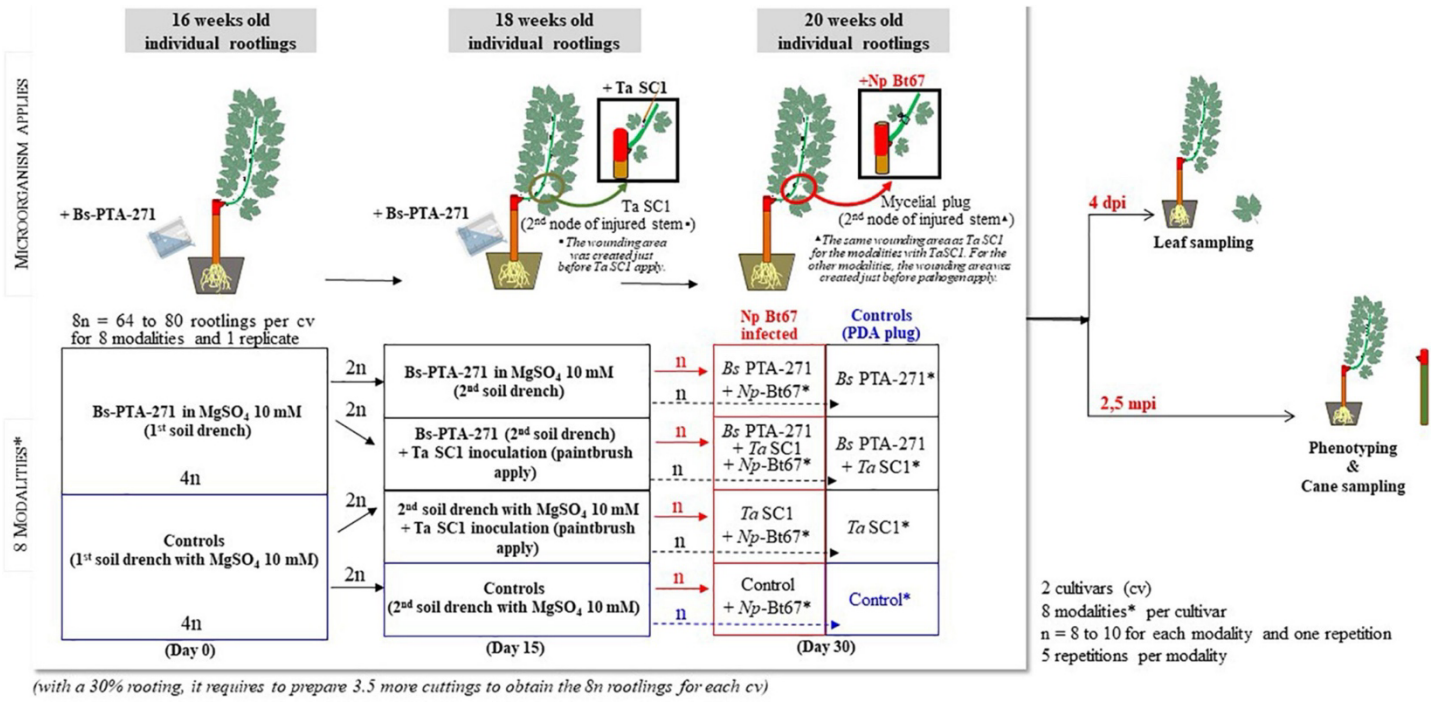

Figure 1. Diagram showing the *Bacillus subtilis* PTA-271 and *Trichoderma atroviride* SC1 inoculations, *Neofusicoccum parvum* strain *Np*-Bt67 infection, and sample collection process. *Modalities: Control, Bs PTA-271, Ta SC1, Bs PTA-271 + Ta

SC1, Control + *Np*-Bt67, Bs PTA-271 + *Np*-Bt67, Ta SC1 + *Np*-Bt67, Bs PTA-271 + Ta SC1 + *Np*-Bt67.

Trichoderma atroviride SC1

Trichoderma atroviride SC1 (Vintec®, Belchim Crop Protection, Bi-PA; 10^{10} conidia per gram of formulated product) was suspended in water at 10^8 CFU/ml to compare the effect of each BCA at an equal density. In order to also take advantage of an eliciting effect, the *Ta* SC1 fungal suspension was applied once with a paintbrush to the second node of the previously wounded lignifying stem (5 mm diameter and 1 mm deep; made just before *Ta* SC1 apply) of 18-week-old rootlings (Figure 1). The inoculation site was immediately covered with parafilm (day 15).

Pathogen Strain and Growth

Neofusicoccum parvum strain Bt67 isolated from Portuguese vineyards (Estremadura region) is inscribed in the HIA collection (Lisbon University, Portugal). This fungus was maintained on potato dextrose agar (PDA, Sigma, Saint-Quentin-Fallavier, France) plates and stored at 4°C (Trotel-Aziz et al. 2019). The resulting mycelium was plated on PDA medium and incubated in the dark at 22°C for 7 days before inoculation.

Pathogen Inoculation to Plants, Quantification of Disease Symptoms, and Re-isolation of the Pathogen

Half of the 20-week-old rootlings that were treated with *Bs* PTA-271 (day 0 and day 15) and/or *Ta* SC1 (day 15) were further infected with the pathogen at the wounding area with a 3-mm-diameter mycelial plug from a 7-day-old culture of *Np*-Bt67 strain (day 30), thus at distinct time points (days 0–30) as summarized in Figure 1. The inoculation site was then covered with moist hydrophilic cotton before sealing with parafilm. The experiment was composed of five repetitions for each modality (treatment), with 8–10 replicate plants per treatment (Figure 1). To confirm that lesions were due to pathogen infection and not to the injury, the control plants were also injured and inoculated with sterile 3-mm PDA plugs (Figure 1). Rootlings, namely, "control," are those that are neither treated with BCA nor infected with the pathogen. After inoculation, vines were kept in the same culture chamber and BOT symptoms were assessed at 2.5 months post-inoculation (mpi) (Figure

1). Disease symptoms were evaluated as described by Trotel-Aziz et al. (2019) by quantifying the percentage of the full dead shoots from inoculated rootlings (Figure 2A, "Full dieback") and by measuring both the external canker area and the internal necrosis length of the other lignified shoots (Figures 2B,C, respectively). To check the success of the infection and the lack of contaminations, re-isolation of pathogen was performed as described by Pinto et al. (2018), by quickly passing the infected stems onto the flame, then removing the top of the necrotic zone with a scalpel, before plating seven small pieces of tissue per plant onto PDA plates. Plates were then incubated at 28°C for at least 7 days. For every repetition of the experiments, re-isolations were performed with seven of the infected rootlings per infected combination (i.e., Np, Bs + Np, Ta + Np, and Bs + Ta + Np) and each replicate, and one negative control rootling per non-infected combination (i.e., Control, Bs, Ta, and Bs + Ta).

Direct Confrontation Tests with Biocontrol Agents and Pathogen

Antagonism among microorganisms was checked *in vitro*, using *B. subtilis* PTA-271, *T. atroviride* SC1, and *N. parvum Np*-Bt67, in dual or three-way confrontation tests on PDA plates (9 mm diameter). *Bs* PTA-271 grown in LB medium and *Ta* SC1 resuspended in sterilized water were both used at 10^8 CFU/ml (5 µl drop), while a 7-day-old mycelium plug (3 mm) was used for the pathogen. Three types of direct confrontation were performed: (A) the pathogen/BCA combinations were plated at the same time, but at distinct areas (i.e., 5 cm away from each other); (B) one or two isolates (*Bs* PTA-271, *Ta* SC1, or *Np*-Bt67) were plated 48 h before the other(s), and at distinct areas; and (C) isolates were plated simultaneously and at the center of the plate. Controls containing one single isolate (*Bs* PTA-271, *Ta* SC1, or *Np*-Bt67) were also made, either on the side of the plate or at the center. All plates were incubated in the dark at 28°C for at least 11 days and photographed daily. Antagonistic effect was characterized by an inhibition zone around the BCA and/or the pathogen. Since the first kind of confrontation (A) added no more information compared to the others (B and C), it was not shown in this study. The experiment was conducted twice with three replicate plates per treatment, and the area occupied by each microorganism was measured daily using ImageJ software (Rueden et al. 2017), based on a reference distance common to all images.

RNA Extraction and Quantitative Reverse-Transcription Polymerase Chain Reaction Analysis

From the *in-planta* assays with rootlings, leaf samples were collected 4 days post-inoculation of pathogen (dpi), ground in liquid nitrogen, and then stored at −80°C. RNA was extracted from powdered 40 leaves of 8 rootlings per replicate of each modality. Total RNA was extracted from 50 mg of leaf powder with Plant RNA Purification Reagent according to manufacturer instructions (Invitrogen, Pontoise, France), and DNase treated as described by the manufacturer's instructions (RQ1 RNase-Free DNase, Promega). RNA quality was checked by agarose gel electrophoresis, and total RNA concentration was measured at 260 nm for each sample using the NanoDrop One spectrophotometer (Ozyme) and adjusted to 100 ng μl^{-1}. First-strand cDNA was synthesized from 150 ng of total RNA using the Verso cDNA synthesis kit (Thermo Fisher Scientific, Inc., Waltham, MA, United States). Polymerase chain reaction (PCR) conditions were the ones described by Gruau et al. (2015). Quantitative reverse-transcription polymerase chain reaction (qRT-PCR) was performed with Absolute Blue qPCR SYBR Green ROX Mix according to manufacturer instructions (Thermo Fisher Scientific, Inc., Waltham, MA, United States), in a BioRad C1000 thermocycler using the Bio-Rad manager software CFX96 Real-Time PCR (BioRad, Hercules, CA, United States). A set of six defense-related genes, selected for their responsiveness to pathogen or priming state induced by beneficial microorganisms (Trotel-Aziz et al. 2019), was tracked by qRT-PCR using specific primers (Table 1). Quantitative RT-PCR reactions were carried out in duplicate in 96-well plates in a 15-µl final volume containing Absolute Blue SYBR Green ROX mix including Taq polymerase ThermoPrime, dNTPs, buffer, and $MgCl_2$ (Thermo Fisher Scientific, Inc., Waltham, MA, United States), 280 nM forward and reverse primers, and 10-fold diluted cDNA according to the manufacturer's protocol. Cycling parameters were 15 min of Taq polymerase activation at 95°C, followed by 40 two-step cycles composed of 10 s of denaturation at 95°C and 45 s of annealing and elongation at 60°C. Melting curve assays were performed from 65 to 95°C at 0.5°C s^{-1}, and melting peaks were visualized to check amplification specificity. EF1 and 60SRP genes were used as references and experiments were repeated five times. Relative gene expression was determined with the formula fold induction: $2(-11Ct)$, where $11Ct = [Ct\ TG\ (US) - Ct\ RG\ (US)] - [Ct\ TG\ (RS) - Ct\ RG\ (RS)]$, where Ct is cycle threshold, Ct value is based on the threshold crossing point of individual fluorescence traces of each sample, TG is target gene, RG is reference gene, the US is an unknown sample, and RS is reference sample. Integration of the formula was performed by the CFX Manager 3.1 software (Bio-Rad). Although the genes analyzed were considered significantly up- or

downregulated when changes in their expression were >2-fold or <0.5-fold, respectively, we still performed a statistical analysis. Control samples for the rootlings model are cDNA from leaves of rootlings untreated with BCA and inoculated with sterile PDA plugs (1× expression level).

Table 1. Primer sequences used for qRT-PCR analysis of defense-related genes (Trotel-Aziz et al. 2019).

Gene	Name	Accession number[1]	Forward primer (5′-3′)	Reverse primer (5′-3′)	Annealing temperature (°C)	Amplicon size (bp)	Efficiency of primers pairs (%)
60RSP	60S ribosomal protein L18	XM_002270599[1]	ATCTACCTCAAGCTCCTAGTC	CAATCTTGTCCTCCTTTCCT	60	166	100.0
EF1	Elongation factor 1-alpha	XM_002284888[1]	AACCAAAATATCCGGAGTAA AAGA	GAACTGGGTGCTTGATAGGC	60	164	100.0
LOX9	Lipoxygenase	NM_001281249[1]	CCCTTCTTGGCATCTCCCTTA	TGTTGTGTCCAGGGTCCATTC	60	101	90.0
PR1	Pathogenesis-related protein 1	XM_002273752[1]	GGAGTCCATTAGCACTCCTTTG	CATAATTCTGGGCGTAGGCAG	60	168	90.0
PR2	Class I beta-1,3-glucanase	NM_0012809671	TCAATGGCTGCAATGGTGC	CGGTCGATGTTGCGAGATTTA	60	155	97.2
GST1	Glutathione-*S*-transferase	NM_001281248[1]	TGCATGGAGGAGGAGTTCGT	CAAGGCTATATCCCCATTTTCTTC	60	98	90.0
PAL	Phenylalanine ammonia lyase	XM_003635637[1]	TCCTCCCGGAAAACAGCTG	TCCTCCAAATGCCTCAAATCA	60	101	92.9
STS	Stilbene synthase	NM_001281117[1]	AGGAAGCAGCATTGAAGGCTC	TGCACCAGGCATTTCTACACC	60	101	94.3

[1]*NCBI accession number.*

Statistical Analysis

Data of canker area and length of external and internal necrosis of the stems were obtained by the analysis of photos using ImageJ software (Rueden et al. 2017). Statistical analyses were carried out using all the vines of three replicates among five for each modality with RStudio software (Horton and Kleinman 2015). For modality significance, mean values were compared by Tukey's test ($p < 0.05$). Results of confrontation tests are from one representative repetition out of two showing the same trends. Statistical analyses were carried out using the SigmaStat 3.5 software. For treatment effect, mean values were compared by Tukey's test ($p < 0.05$). Results of gene expression by qRT-PCR analysis correspond to means ± SEM deviation from three representative repetitions out of five showing the same trends. Statistical analyses were carried out using the XLSTAT

2021.1.1 5 software (Addinsoft, Paris, France). For treatment effect, mean values were analyzed using one-way analysis of variance (ANOVA). When differences in the means were significant, Fisher's LSD *post hoc* test ($\alpha = 0.1$) was applied to determine which treatments were significantly different from others.

3.3. Results

Effects of *Bacillus subtilis* PTA-271 and *Trichoderma atroviride* SC1 on Two Cultivars Infected with *Neofusicoccum parvum* Bt67

In control Chardonnay infected with the pathogen, the results of infection showed a rate of 28 ± 1.24% for dead shoot (full dieback), of 80.6 ± 7.35 mm^2 for external canker size, and of 55.4 ± 9.44 mm for internal necrosis length (see *Np*-Bt67 in Figures 2D–F), while in Tempranillo, they reached 37.5 ± 4.56%, 65.2 ± 6.23 mm^2, and of 77.8 ± 11.95 mm, respectively (see *Np*-Bt67 in Figures 2G–I).

In BCA-treated Chardonnay rootlings then infected with the pathogen, the results of the biocontrol assays showed that *Bs*-PTA-271-pretreated plants presented a significant lower number of plants with full dieback (by approximately 45%) than the infected control (Figure 2D). Infected plants pretreated with *Ta* SC1 did not reduce the full dieback development compared to infected control plants, while infected plants pretreated with both BCAs showed a great variability in the development of full dieback symptoms. Similarly, the external canker area (Figure 2E) and the internal necrosis length of infected Chardonnay (Figure 2F) were solely slightly reduced in *Bs*-PTA-271-pretreated rootlings (by 16 and 22%, respectively), but insignificantly (Figure 2E). In contrast, necrosis length was increased in *Ta* SC1 and both BCAs pretreated plants compared to infected control, although non-significant (Figure 2F).

In BCA-treated Tempranillo rootlings then infected with the pathogen, the results of the biocontrol assays showed that *Ta*-SC1- and combined-BCA-pretreated plants showed a significant lower number of full dieback (by approximately 80 and 91%, respectively) and length of stem internal necrosis (by approximately 70 and 81%, respectively) than the infected control (Figures 2G,I, respectively). In contrast, infected plants pretreated with *Bs* PTA-271 showed that neither full dieback development nor internal stem necrosis reduced, compared to infected control plants. Looking at the external canker area (Figure 2H), none of the treatments with *Bs*-PTA- 271-, *Ta*- SC1-, and combined-BCA-pretreated

plants, consecutively infected, induced any significant difference with the infected control. Therefore, external canker may not appear as a relevant indicator for Np dieback with this experimental model, for both Tempranillo and Chardonnay.

Re-isolations of the pathogen confirmed that (1) there was no background infection elsewhere than in the artificially infected rootlings, satisfying thus the Koch's postulates, and that (2) the pathogen was still alive in both dead and living stems of plants, as well as in infected plants pretreated or not with BCA. From all infected plants, the pathogen was successfully isolated with a percentage of success >90% that indicated no fungicidal effect from BCA toward *Np*-Bt67.

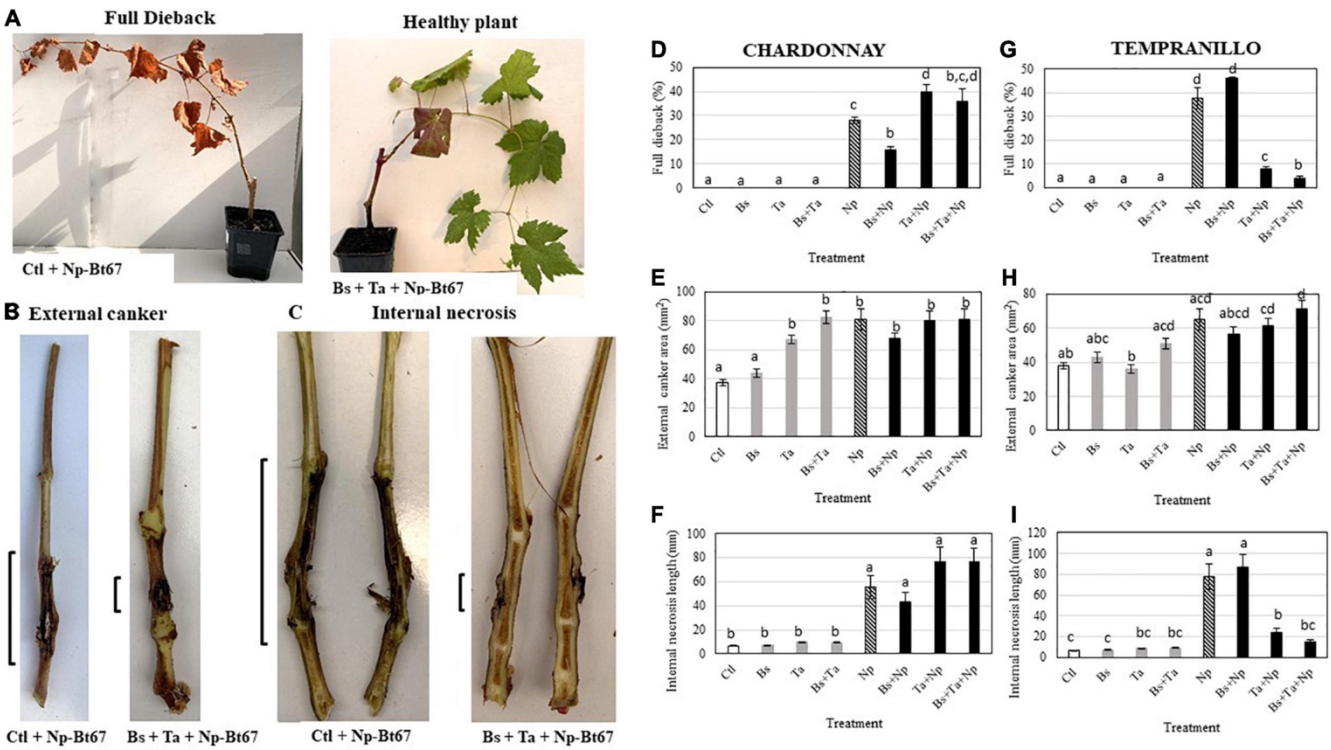

Figure 2. The beneficial combination of *Bacillus subtilis* PTA-271 and *Trichoderma atroviride* SC1 attenuates the Botryosphaeriaceae dieback symptoms induced in Chardonnay (D–F) and Tempranillo (G–I) rootlings by the *Neofusicoccum parvum* strain *Np*-Bt67. One-month pretreated grapevine rootlings with PTA-271, *Ta* SC1, and both BCA (Bs, Ta, and Bs + Ta) and non-treat plants (Ctl) were inoculated with pathogen

mycelium (Np). Non-infected plants were inoculated with sterile medium without pathogen (Control). Compared to healthy asymptomatic rootlings (A, right), the infected symptomatic rootlings showed the typical Botryosphaeria dieback symptoms: full dieback percentage (A left, E), stem external canker (B,E,H) and stem internal necrosis (C,F,I) that were photographed (A–C) and quantified (D–I)at 2.5 months post-inoculation. Data are means ± standard deviation (SD) for at least three independent experiments with 10 biological replicates per treatment. Vertical bars with different letters are significantly different (multiple comparison procedures with Tukey's test, $p < 0.05$).

Effects of Biological Control Agents on the Basal Defense of Chardonnay and Tempranillo

The ability of *Bs* PTA-271 or *Ta* SC1 or both BCAs to enhance grapevine immunity was addressed in leaves of control rootlings. Six selected defense genes were targeted by qRT-PCR: the lipoxygenase *LOX9* involved in oxylipin synthesis and described as dependent to JA/ET (Hamiduzzaman et al. 2005; Naznin et al. 2014); *PR1* described to be regulated by SA (Dufour et al. 2013; Naznin et al. 2014; Caarls et al. 2015); the β-1,3-glucanase *PR2* described to be regulated by various phytohormones such as SA, JA, and ET (Liu et al. 2010); the glutathione-*S*-transferase *GST1* putatively involved in the detoxification process; the phenylalanine ammonia-lyase *PAL* catalyzing the first step in the phenylpropanoid pathway; and the stilbene synthase *STS* involved in the synthesis of phytoalexins. Since BCAs were not detected in leaves (not shown) where defenses were induced, the induction of plant defense by BCAs is systemic.

Data showed some differences in the level of expression of the basal defense genes between the greenhouse cultivars (Figure 3), despite the fact that rootlings all grew in the same chamber of the greenhouse with similar culture conditions. The cultivar Chardonnay exhibited a weak constitutive expression of targeted defense genes (Figure 3A) compared to Tempranillo (Figure 3B). In Chardonnay (Figure 4 and Supplementary Figure 1A), the application of *Bs* PTA-271 at root level induced a 2.8-fold increase of *PR1* and *PR2* expression in leaves, while the application of *Ta* SC1 at stem level did not induce any consistent changes in the expression of these same defense genes in leaves. Interestingly, the application of both BCAs induced the expression of the greatest number of targeted genes in the leaves: a 2.6-fold expression of *LOX9*and a 6.6- or 6.8-fold

expression of *PR2* and *STS*, respectively. *Bs* PTA-271, alone or together with *Ta* SC1, may thus act as a priming stimulus for Chardonnay cultivar.

A

CHARDONNAY								
	Rootlings				Rootlings challenged with pathogen			
4 dpi	Control	Bs	Ta	Bs + Ta	Ctl + Np	Bs + Np	Ta + Np	Bs + Ta + Np
LOX9	1,00 a	0,68 a	1,11 a	2,62 a,b,c	4,34 b,c,d,e	1,18 a,b	1,80 a,b,c,d	7,39 c,d,e,f
PR1	1,00 b	2,85 b	0,51 a,b	2,65 a,b	0,81 a,b	0,13 a	1,20 a,b	3,42 b
PR2	1,00 a	2,86 a,b	1,06 a	6,64 a,b	4,74 a,b,c	3,94 a,b	6,55 b,c,d	13,04 c,d,e
GST1	1,00 a,b	1,55 a	0,24 a	0,69 a	2,98 a,b,c	0,91 a	1,32 a	3,12 a,b,c
PAL	1,00 a,b,c,d	0,95 a	0,90 a,b	1,50 a,b,c	3,70 c,d,e	1,91 a,b,c,d,e	3,35 b,c,d,e	14,30 e,f
STS	1,00 a	1,42 a,b	1,35 a,b	6,89 a,b,c	9,86 d,e,f,g	4,13 a,b,c,d	11,17 d,e,f,g	27,86 e,f,g,h

B

TEMPRANILLO								
	Rootlings				Rootlings challenged with pathogen			
4 dpi	Control	Bs	Ta	Bs + Ta	Ctl + Np	Bs + Np	Ta + Np	Bs + Ta + Np
LOX9	8,20 e,f,g,h	7,34 d,e,f,g,h	19,97 h,i	15,11 g,h,i	43,97 i	13,97 f,g,h,i	13,26 h,i	5,14 c,d,e,f,g
PR1	41,09 c	38,51 c	37,23 c	58,55 c	82,17 c	144,52 c	88,57 c	59,31 c
PR2	5,68 b,c,d	4,99 a,b,c	74,02 e,f	15,57 c,d,e,f	179,29 f	67,72 f	31,78 d,e,f	6,51 b,c,d
GTS1	1,83 a,b,c,d	1,57 a,b,c	22,05 d,e	17,68 c,d,e	33,24 b,c,d,e	11,64 c,d,e	20,56 e	4,70 a,b,c,d
PAL	8,53 e,f,g	10,28 e,f	36,69 f,g	30,69 f,g	112,01 g	58,70 g	32,43 g	5,74 d,e
STS	7,71 c,d,e,f	9,98 b,c,d,e,f	47,94 g,h	40,94 f,g,h	167,18 h	43,24 g,h	102,82 h	7,15 b,c,d,e

Figure 3. *Bacillus subtilis* PTA-271 and *Trichoderma atroviride* SC1 attenuates induced differential expression of defense-related genes in leaves of Chardonnay (A) and Tempranillo (B)rootlings before and after pathogen challenge. Twenty-week-old rootlings untreated or pretreated with PTA-271 or SC1 or both were further infected with sterile PDA plugs (Control, Bs, Ta, and Bs + Ta, respectively) or with mycelium plugs of *Np*-Bt67 (Ctl + Np, Bs + Np, Ta + Np, and Bs + Ta + Np, respectively). Transcript levels of defense-related genes monitored by qRT-PCR in plant leaves after 4 days of inoculation. Uninfected control of Chardonnay was considered as a reference sample (1× expression level) for both cultivars, and heatmaps represent changes in the transcript expression levels as indicated by the color shading. Data are the means from three representative replicates among five showing the same trends. Different letters indicate statistically significant differences between the treatments (ANOVA, Fisher's LSD *post hoc* test, $\alpha = 0.1$). Legends for genes are LOX9, lipoxygenase 9; PR1, pathogenesis-related protein 1; PR2, class I β-1,3-glucanase; GST1, glutathione-*S*-transferase 1; PAL, phenylalanine ammonia lyase; STS, stilbene synthase.

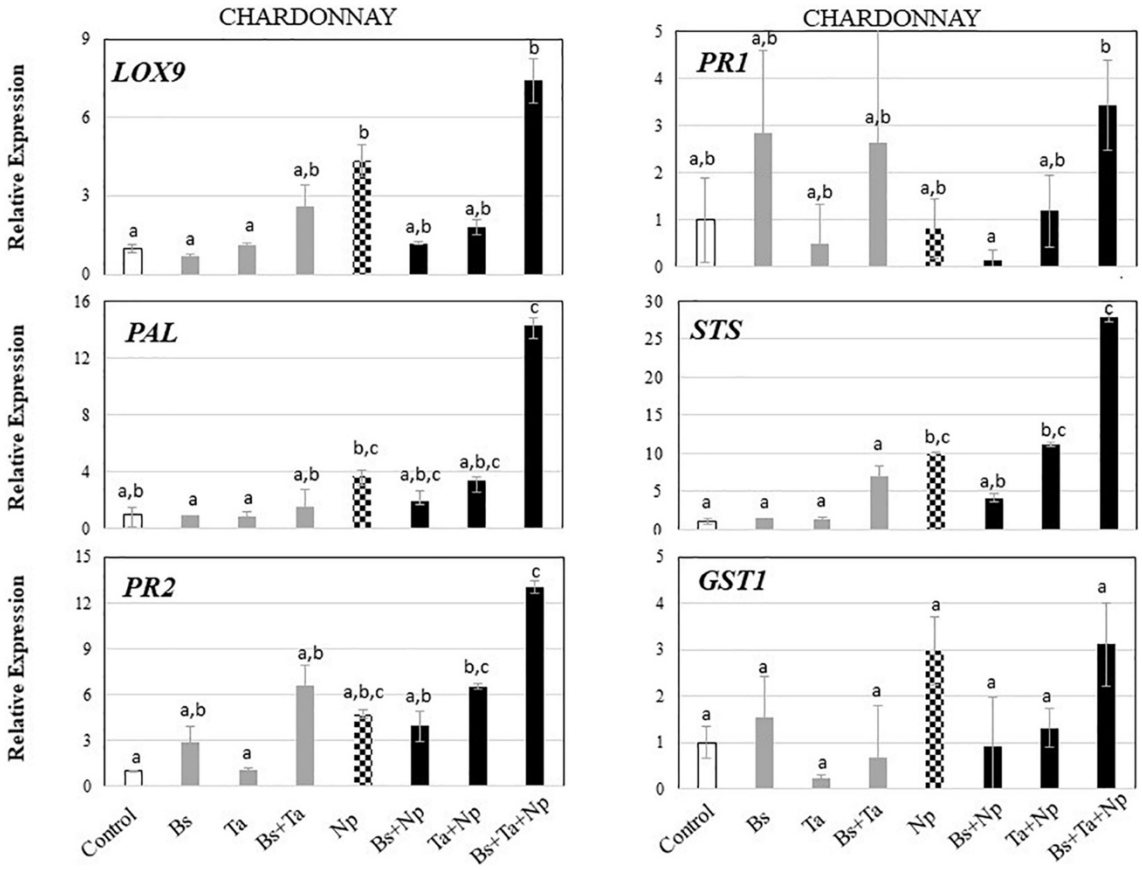

Figure 4. *Bacillus subtilis* PTA-271 and *Trichoderma atroviride* SC1 attenuates induced differential expression of defense-related genes in leaves of Chardonnay rootlings before and after pathogen challenge. Twenty-week-old rootlings untreated or pretreated with PTA-271 or SC1 or both were further infected with sterile PDA plugs (Control, *Bs*, *Ta*, and *Bs* + *Ta*, respectively) or with mycelium plugs of *Np* (Ctl + *Np*, *Bs* + *Np*, *Ta* + *Np*, and *Bs* + *Ta* + *Np*, respectively). Transcript levels of defense-related genes monitored by qRT-PCR in plant leaves after 4 days of inoculation. Uninfected control was considered as the reference sample (1× expression level). Data are the means from three representative replicates among five showing the same trends. Different letters indicate statistically significant differences between the treatments (ANOVA, Fisher's LSD *post hoc* test, $\alpha = 0.1$). Legends for genes are as in Figure 2.

Tempranillo (Figure 3B) showed a high basal expression of the targeted gene responsive to SA (i.e., PR1) compared to Chardonnay (Figure 3A). Interestingly, while the application of *Bs* PTA-271 (Figure 5 and Supplementary Figure 1B) did not induce any consistent changes of defense gene expression, that of *Ta* SC1 induced the expression of the greatest number of studied genes: by a factor of 2.4 for LOX9, 13.0 for PR2, 12.0 for

GST1, 4.3 for PAL, and 6.2 for STS. To contrast with Chardonnay, no relevant number of targeted genes were overexpressed with the application of both BCAs (2.7-fold for PR2, 9.6-fold for GST1, 3.6-fold for PAL, and 5.3-fold for STS) compared to Ta SC1 alone. Ta SC1, alone or together with Bs PTA-271, may thus act as a priming stimulus for Tempranillo.

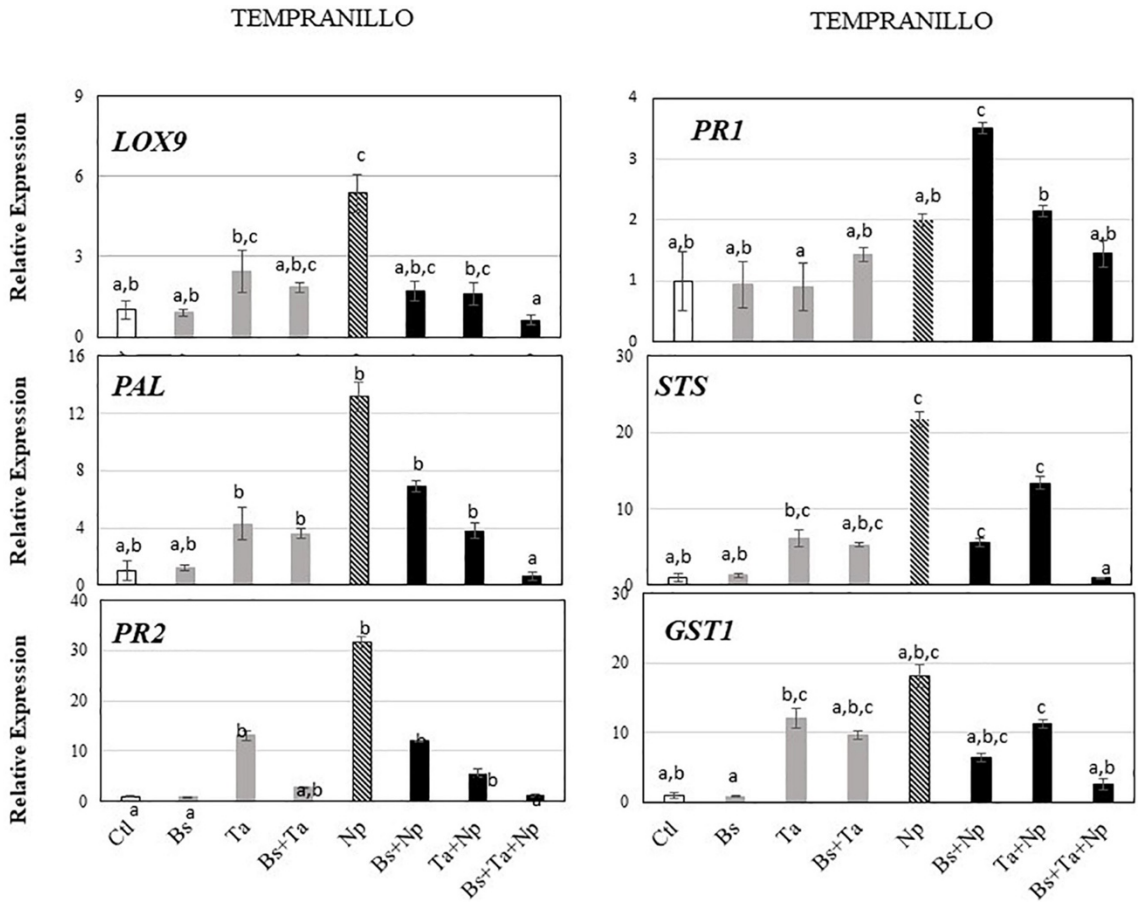

Figure 5. *Bacillus subtilis* PTA-271 and *Trichoderma atroviride* SC1 attenuates induced differential expression of defense-related genes in leaves of Tempranillo rootlings before and after pathogen challenge. Twenty-week-old rootlings untreated or pretreated with PTA-271 or SC1 or both were further infected with sterile PDA plugs (Control, *Bs*, *Ta*, and *Bs* + *Ta*, respectively) or with mycelium plugs of *Np*-Bt67 (Ctl + *Np*, *Bs* + *Np*, *Ta* +

Np, and *Bs* + *Ta* + *Np*, respectively). Transcript levels of defense-related genes monitored by qRT-PCR in plant leaves after 4 days of inoculation. Uninfected control was considered as the reference sample (1× expression level). Data are the means from three representative replicates among five showing the same trends. Different letters indicate statistically significant differences between the treatments (ANOVA, Fisher's LSD *post hoc* test, $\alpha = 0.1$). Legends for genes are as in Figure 2.

Effects of Biological Control Agents on the Induced Defense of Chardonnay and Tempranillo Upon Pathogen Challenge

In leaves of Chardonnay rootlings infected with *Np*-Bt67, data from qRT-PCR showed that except for *PR1* (0.8-fold expression), the expression of all targeted defense genes was consistently upregulated from 2.9- to 9.8-fold (4.3 for *LOX9*, 4.7 for *PR2*, 2.9 for *GST1*, 3.7 for *PAL*, and 9.8 for *STS*) (Figure 4 and Supplementary Figure 1A). As indicated before, in the absence of pathogen infection, *Bs* PTA-271 only induced a weak expression of *PR2* and *PR1* (2.8-fold increase) but was not significant according to ANOVA analysis (Figure 4 and Supplementary Figure 1A), suggesting that *Bs* PTA-271 may act as a priming stimulus in Chardonnay. However, upon pathogen challenge, no post-priming was observed in *Bs*-PTA-271-pretreated plants since it did not induce any stronger activation of the targeted plant immune defenses compared to Chardonnay-infected control at 4 dpi (Figure 3). In contrast, *Ta* SC1 showed no sign of priming stimulus in control Chardonnay, but it induced similar expression of *PR2* (6.5-fold increase) and *STS* (11.1-fold increase) than infected control (4.7 and 9.8, respectively). Interestingly, the application of both BCAs enabled to reach the highest level of Chardonnay defense gene expression upon pathogen challenge (3.1–27.8) compared to infected control (0.8–9.8), a priming effect shown as consistent according to the discriminating capacity of the qRT-PCR technique, but still not yet significant according to the ANOVA analysis. Anyway, such a synergy at 4 dpi can result from a priming stimulus by *Bs* PTA-271, followed by a post-primed phase upon pathogen inoculation with a more rapid and strong activation of immune defenses due to interactions among each actor (*Bs* PTA-271, *Ta*SC1, *Np*-Bt67, and Chardonnay).

In leaves of Tempranillo infected with *Np*-Bt67, the expression of all targeted defense genes was consistently upregulated from 2.0- to 31.5-fold, and significantly for *LOX9*, *PR2*, *PAL*, and *STS* (Figure 5 and Supplementary Figure 1B). Compared to infected Chardonnay (Figure 3A), expression of the basal defense genes was significantly stronger in infected Tempranillo (Figure 3B), highlighting a higher basal defense level in Tempranillo toward *Np*-Bt67 than in Chardonnay at 4 dpi. The ability of each BCA or both to enhance Tempranillo immunity was also addressed (Figure 5and Supplementary Figure 1B). As reported above, in the absence of pathogen infection, *Ta* SC1 alone induced a consistent expression of almost all the targeted defenses (2.44–13.03 for *LOX9*, *PR2*, *GST1*, *PAL*, and *STS*), suggesting that *Ta* SC1 may act as a priming stimulus for Tempranillo cultivar, but in a lesser extent when combined with *Bs* PTA-271 (1.84–9.66). However, upon pathogen challenge, no post-priming was observed in *Ta* SC1-pretreated rootlings since it did not induce any stronger expression of the targeted immune defenses than in the Tempranillo-infected control at 4 dpi, but lower (Figure 5 and Supplementary Figure 1B). Regarding *Bs* PTA-271 effect (i.e., Bs + *Np*), while it showed no sign of priming stimulus in control Tempranillo, it induced the expression of almost all targeted defenses, but similarly to *Ta* SC1, thus in a lower extent than the infected control (thus, no more priming in that condition with *Bs* PTA-271). Additionally, the pretreatment with both BCAs induced a lower expression level of Tempranillo defense genes upon pathogen challenge (0.63–2.57) than in infected control (2.0–31.56). However, such apparent non-expression of Tempranillo defenses at 4 dpi did not presume any useful induced defenses at other key times or among other defenses that were not targeted in this study.

Taking the uninfected control of Chardonnay as the reference sample for both cultivars, we can compare the immunity between Tempranillo and Chardonnay upon pathogen challenge (Figures 3A,B, respectively). As observed in control condition (i.e., high basal expression of *PR1*), infected Tempranillo showed once again a high expression of this targeted gene presumably responsive to SA, compared to Chardonnay. This suggests that Tempranillo would use SA-dependent defense pathways toward *N. parvum*, even when overexpressing *PR2*, *GST1*, *PAL*, and *STS*, unlike Chardonnay. These data thus highlight the possible role of SA signaling in Tempranillo, especially when infected and pretreated with *Bs* PTA-271 (i.e., *PR1*). Curiously, the JA/ET-responsive gene *LOX9* was also highly upregulated in infected Tempranillo, while *LOX9* was severely downregulated in

infected Tempranillo pretreated with single or both BCAs, as well as *PR2*, *PAL*, and *STS*. Opposite trends were observed in Chardonnay: (i) no prominent role of SA signaling in infected Chardonnay, especially when pretreated with *Bs* PTA-271; and (ii) *LOX9* was not so highly upregulated in infected Chardonnay (i.e., Ctl + Np), but *LOX9* was upregulated in infected Chardonnay pretreated with both BCAs, and *PR2*, *PAL*, and *STS* with *Ta*SC1 or both BCAs. These data could suggest the prominent role of JA/ET signaling in Chardonnay, especially when infected and pretreated with BCA. Interestingly, *PR2*, *PAL*, and *STS* are common defenses induced by each BCA against *Np*-Bt67 for the two cultivars, possibly through two distinct signaling pathways.

Direct Beneficial or Detrimental Interplays Between *Bacillus subtilis* PTA-271, *Trichoderma atroviride* SC1, and the Pathogen *Neofusicoccum parvum*-Bt67

Regarding the *in vitro* tests with *Np*-Bt67 (Figure 6), results showed that *Bs* PTA-271 and *Ta* SC1 antagonize *Np*-Bt67 when plated 48 h before the pathogen. As shown in Figures 6A,B, the growth of *Np*-Bt67 was consistently reduced by *Ta* SC1 or *Bs* PTA-271 in dual confrontation compared to the control. However, while the growth of *Np*-Bt67 was completely repressed from day 3 by *Ta* SC1 (Figure 6A), it was half-repressed by *Bs* PTA-271 (Figure 6B), enabling the pathogen to grow consistently less than the control over the same time period. Thus, *Ta* SC1 antagonistic effect was stronger than that of *Bs* PTA-271, although only a fungistatic effect was observed between them (since when transplanted, the pathogen grows back).

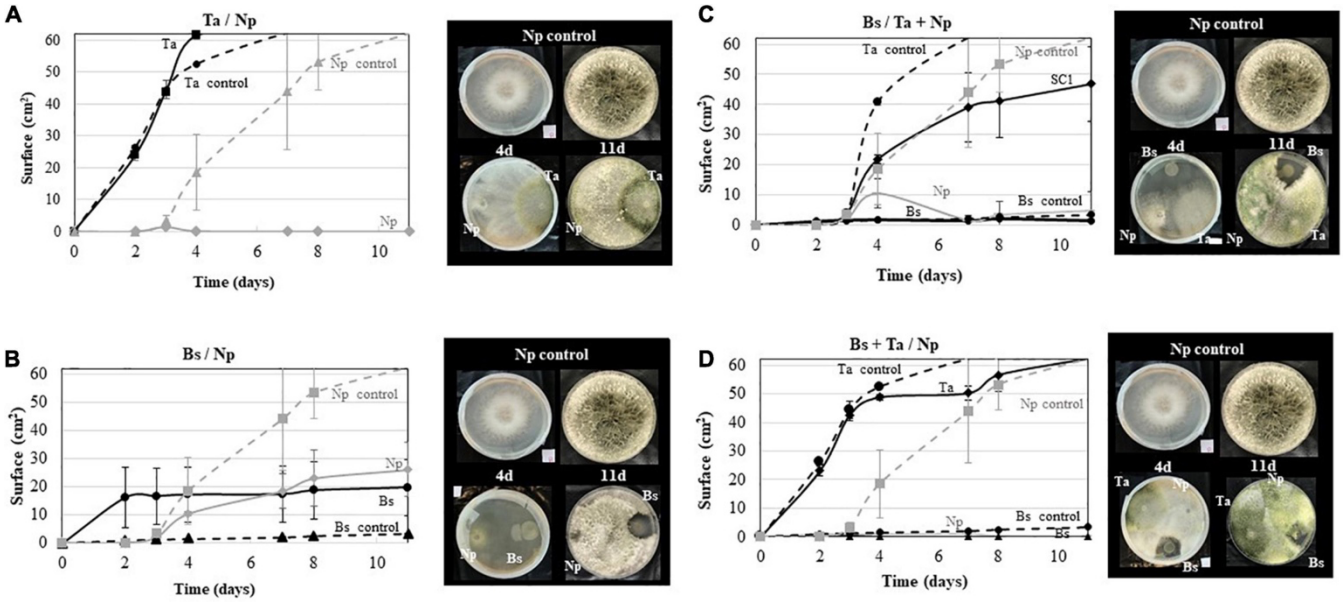

Figure 6. Antagonistic activity of *Bacillus subtilis* PTA-271 and *Trichoderma atroviride* SC1 against the *Neofusicoccum parvum* strain Bt67. (A) *T. atroviride* SC1 (Ta) was applied 48 h before *N. parvum* (Np) in the opposite sides of PDA plates. (B) *B. subtilis* PTA-271 (Bs) was applied 48 h before *N. parvum* (*Np*-Bt67) in the opposite sides of PDA plates. (C) *B. subtilis* PTA-271 (Bs) was applied 48 h before *N. parvum* (Np) and *T. atroviride* (Ta) at distinct areas of the PDA plates. (D) *B. subtilis* PTA-271 (Bs) and *T. atroviride* SC1 (Ta) were applied 48 h before *N. parvum* (*Np*) at distinct areas of the PDA plates. All plates were incubated at 28°C. Pictures of each plate condition were taken from day 1 to day 11 after the first inoculation. Photos on top are the control of *Np*-Bt67 and photos at the bottom indicate the confrontation assay at day 4 (left) and day 11 (right).

In three-way confrontations (Figures 6C,D), the antagonistic effect of *Bs* PTA-271 against *Np*-Bt67 was still reinforced in the presence of *Ta* SC1, even applied 48 h later (Figure 6C). Such benefit was yet reinforced when the two BCAs were both applied 48 h before the pathogen, in which the growth of *Np*-Bt67 was close to 5 mm^2 (Figure 6D). However, it should be noted that *Ta* SC1 did not grow as fast when applied 48 h after *Bs* PTA-271, since *Ta* SC1 slopes are not parallel but weaker in Figure 6C than in Figure 6D.

To check the *Ta* SC1 capacity to keep its antagonistic effect when applied simultaneously with *Bs* PTA-271, dual confrontations were made between the two BCAs applied in the same area, with or without pathogen (Figure 7). As shown in Figure 7A, the growth of *Ta* SC1 was slowed down with *Bs* PTA-271, leading to a smaller *Ta* SC1 area than for the *Ta* SC1 control over the same time period. Interestingly, this detrimental effect of *Bs* PTA-271 on *Ta* SC1 disappeared in the three-way confrontation with the pathogen *Np*-Bt67 (Figure 7B), being all applied simultaneously at the same area. Thus, *Ta* SC1 and/or *Bs* PTA-271 may keep their strong antagonistic activity when facing a common adversary.

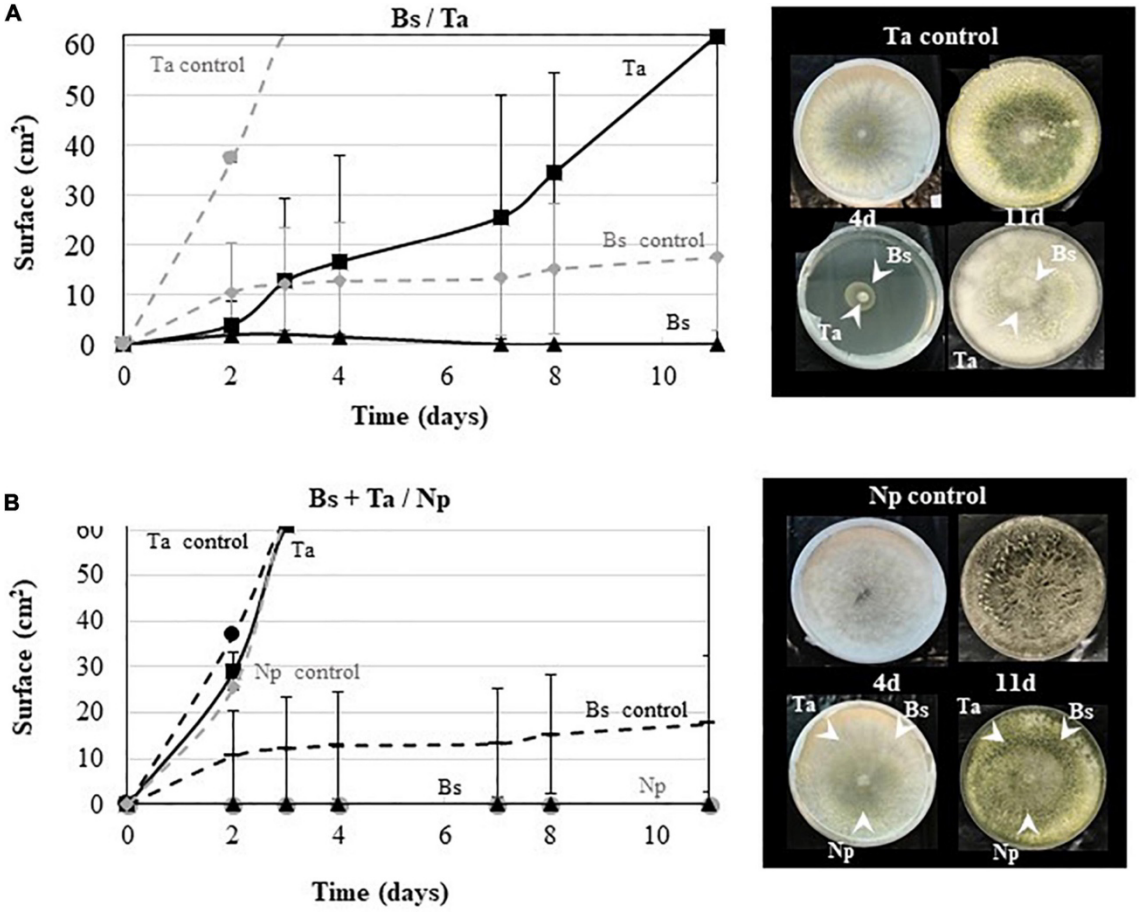

Figure 7. Antagonistic activity of *Bacillus subtilis*PTA-271 and *Trichoderma atroviride* SC1 against *Neofusicoccum parvum* Bt67. (A) *B. subtilis* PTA-271 (Bs) and *T. atroviride* SC1 (Ta) were applied simultaneously in the center of the PDA plates. (B) *B. subtilis* PTA-271 (Bs), *T. atroviride* SC1 (Ta), and *N. parvum* (Np) were applied simultaneously in the center of the PDA plates. All plates were incubated at 28°C.

Pictures of each plate were taken from day 1 to day 11 after the first inoculation. Photos on top are SC1 control (A)and *Np*-Bt67 control (B), and pictures at the bottom indicate the confrontation assay at day 4 (left) and day 11 (right).

3.4. Discussion

In search of an effective protective BCA combination against *N. parvum*, we investigated a potential BCA and a BCA-commercial product, each already described as protectors against GTDs on distinct cultivars: *B. subtilis* PTA-271 with Chardonnay (Trotel-Aziz et al. 2019) and *T. atroviride* SC1 with different cultivars (Berbegal et al. 2020; Martínez-Diz et al. 2021a; Pertot et al. 2016). This study assessed the combined impact of these two BCAs on two cultivars artificially infected or not with one pathogen. *N. parvum* Bt67 was used, as a very aggressive pathogen associated to BOT. Our investigation focused on the capacity of single and combined BCAs to counteract BOT symptoms on both cultivars. To compare the two BCAs, densities were aligned to the density optimized for *Bs* PTA-271. After looking for the protective capacity of BCA *in planta*, their modes of action leading to protection were further explored. Thus, we investigated whether these BCAs could affect pathogen growth *in vitro* and cultivar immunity upon infection *in planta*.

Neofusicoccum parvum Bt67 caused BOT symptoms on the rootlings of the two grapevine cultivars, as shoot full dieback, canker external necrosis, and shoot internal necrosis. Interestingly, the full dieback symptoms were more severe on Tempranillo than on Chardonnay (i.e., 37.5 and 28%, respectively, Figures 2D,G), suggesting a greater susceptibility to BOT for Tempranillo than Chardonnay, as already reported by Luque et al. (2009) and Cobos et al. (2019). Although there is a lack of comparative data between cultivars, the distinct susceptibility of some cultivars to GTDs has already been reported (Chacon et al. 2020; Fontaine et al. 2016b; Reveglia et al. 2021; Travadon et al. 2013), even within a same cultivar from one region to another or depending on the vintage (Mimiague and Le Gall 1994). However, in Chardonnay and Tempranillo rootlings pretreated with one or both BCAs before inoculation of the pathogen, BOT symptoms were significantly reduced with *Bs* PTA-271 or *Ta* SC1, respectively. Grapevine effective protection against *Np*-Bt67 has already been reported with *Bs* PTA-271 on Chardonnay rootlings (Trotel-Aziz et al. 2019), and with *Ta* SC1 on Tempranillo in nursery and vineyards conditions (Berbegal et al. 2020; Blundell et al. 2021).

Additionally, in our experimental conditions, Chardonnay seems to favor the beneficial effect of *Bs* PTA-271, while Tempranillo favors that of *Ta* SC1 beneficial effect, highlighting the relationship between cultivar response and BCA effect. Manter et al. (2010) suggested that the differences between cultivars may result from minor changes in the composition of their endophyte community, with *Trichoderma* species being among the most common endophytic fungal isolates from Tempranillo (González and Tello 2011). Therefore, Tempranillo could be subjected to *Trichoderma*'s influence. Similarly, the efficiency of *Bs* PTA-271 toward Chardonnay may be explained by its origin of sampling from an established Chardonnay vineyard, screened from healthy vines (Trotel-Aziz et al. 2008). In combination and according to our experimental conditions, despite cited as compatible strains (Kumar 2013), *Ta* SC1 + *Bs* PTA-271 are less protective against *Np*-Bt67 in Chardonnay than *Bs* PTA-271 alone. The authors reported that *Trichoderma* spp. can interfere the plant signaling networks and secrete an arsenal of degrading enzymes (i.e., proteases) and secondary metabolites (Alfiky and Weisskopf 2021; Tiwari and Verma 2019), suggesting that *Ta* SC1 may alter both *Bs* PTA-271 integrity and beneficial effects in Chardonnay. However, the application of both BCAs enabled to reach the highest level of Chardonnay defense gene expression upon pathogen challenge (see Figure 3A), and the highest protection in Tempranillo cultivar (see Figure 2G), highlighting that *Ta* SC1 on its own would not interfere with the beneficial effects of *Bs* PTA-271.

Beneficial effects of combined BCAs have yet been reported in different pathosystems (Magnin-Robert et al. 2013; Yobo et al. 2011), and our study reports for the first time the biocontrol potential of the combination of *Bs* PTA-271 and *Ta*SC1 against *Np*-Bt67 in Tempranillo. Our results showed that *Ta* SC1 efficiently protects Tempranillo, and this protection is still observed in rootlings pretreated with both BCAs (see Figure 2G). Thus, a significant benefit is observed when using both BCAs in Tempranillo, despite the fact that they could antagonize each other. In this respect, Leal et al. (2021) reported that the genome of *Bs* PTA-271 encodes for the synthesis of bacillaene, a polyketide already described to antagonize *Trichoderma*spp. (Caulier et al. 2019). Therefore, the positive contribution of *Bs* PTA-271 and *Ta*SC1 to Tempranillo protection against *Np*-Bt67 suggests a fine-tuned orchestrated cooperation of BCAs when facing adversity, as supported by the Figure 7 results and highlighted by Alfiky and Weisskopf (2021). However, the application of BCAs to rootlings was spatially separated.

Empowered with aggressive molecules, *Bacillus* spp. and *Trichoderma* spp. can possibly exert direct beneficial or detrimental interplays within the host's microbiome, and especially on the other BCA and pathogens such as GTDs fungi (Blundell et al. 2021; Di Marco et al. 2002; Haidar et al 2016; Kloepper et al. 2004; Ongena and Jacques 2008; Trotel-Aziz et al. 2019; Úrbez-Torres et al. 2020; Yacoub et al. 2020). *In vitro* dual confrontation tests confirmed the antagonistic activity of *Bs*PTA-271 or *Ta* SC1 toward *Np*-Bt67 since each of them significantly inhibits the mycelium growth of *Np*-Bt67 (see Figures 6A,B). This also prompts us the idea that the not-yet-convincing protection assay of *Bs* PTA-271 and *Ta* SC1 in infected Chardonnay would not result from a detrimental effect of *Ta* SC1 on some putative direct effects of *Bs* PTA-271. Indeed, the strong direct antagonistic activity of *Bs* PTA-271 and *Ta* SC1 toward *Np*-Bt67 also operates when the two BCAs were applied both 48 h before the pathogen (see Figure 6D). This antagonistic benefit is in accordance with the significant synergy of the protection in Tempranillo by both BCAs (see Figure 2G), and it confirms the benefit of using them in combination in Tempranillo to optimize the direct fight against *Np*-Bt67. A similar outcome was reported by Alexander and Phin (2014) using an effective combination of *Bacillus* spp. and *Trichoderma* spp. against *Ganoderma* spp. Such direct effects of BCA against pathogens are important life traits to protect grapevine from BOT, still deprived of effective curative treatments nowadays (Mondello et al. 2018). In nursery too, healthy mother plants require a control of their sanitary status (Pertot et al. 2016), eventually provided by an early inoculation of such beneficial BCA with a strong antagonistic activity toward pathogens.

Direct beneficial or detrimental interplays between BCAs also condition their capacity to live together in symbiosis, even *in planta* as part of the holobiont (Bettenfeld et al. 2020). Dual confrontation was thus also performed between *Bs* PTA-271 and *Ta* SC1. As expected, *Bs* PTA-271 antagonized *Ta* SC1 (see Figure 7A; Caulier et al. 2019; Leal et al. 2021). However, this detrimental effect of *Bs* PTA-271 on *Ta* SC1 disappears in a three-way confrontation with *Np*-Bt67, when they were all applied simultaneously at the same area (see Figure 7B). These data confirm that *Ta* SC1 and *Bs* PTA-271 can positively interact to better confine *Np*-Bt67 and can lead to a direct positive contribution of this combination to the protection of Tempranillo against *Np*-Bt67. However, such a direct positive contribution of combined BCAs did not operate on the infected Chardonnay rootlings. Our experimental conditions could have altered the ability

of *Ta* SC1 to exert its direct fungistatic effect (applied once at 10^8 CFU/ml with a paintbrush over a 5-mm^2 area). This also strongly suggests that Chardonnay itself alters the fine-tuned orchestrated cooperation of BCAs, probably targeting the indirect *Ta* SC1 beneficial effect since BCAs are spatially separated. This prompts us to pursue our investigations further in order to decipher the indirect interactions driving to a beneficial outcome in grapevine control of *Np*-Bt67.

According to our previous works, a focus on grapevine systemic immunity was made by targeting six selected defense genes in leaves: the lipoxygenase *LOX9* involved in oxylipin synthesis and described as dependent to JA/ET; *PR1* described to be regulated by SA; the β-1,3-glucanase *PR2* described to be regulated by various phytohormones such as SA, JA, and ET; the glutathione-*S*-transferase *GST1*putatively involved in the detoxification process; the phenylalanine ammonia-lyase *PAL* catalyzing the first step in the phenylpropanoid pathway; and the stilbene synthase *STS* involved in the synthesis of phytoalexins (Trotel-Aziz et al. 2019). Interestingly, basal immunity results in a weak constitutive expression of the targeted defense genes in Chardonnay compared to Tempranillo (see Figure 3), despite the fact that literature described Chardonnay as less susceptible to BOT than Tempranillo (Luque et al. 2009). Maybe our six targeted genes are not sufficiently exhaustive to presume at this preliminary stage of the susceptible versus tolerant status of both cultivars. However, looking at the specific red and white cultivar responses, the same studied genes are of interest: those specific to white grape cultivars include transcription factors from the ET pathway and lipid metabolism (e.g., lipoxygenase), while those specific to red grape cultivars are linked to the secondary metabolism in connection with the pathway of phenylpropanoids (e.g., PAL and its derivatives) and are expressed more strongly in the red cultivars, to distinguish them from the white ones (Lambert et al. 2012; Massonnet et al. 2017). Upon abiotic or biotic stress, other authors pointed out the highest synthesis of resveratrol in the most tolerant grapevine (Corso et al. 2015, Lakkis et al. 2019), but a gain of protection due to the BCA presence in susceptible cultivar (Lakkis et al. 2019). Considering that susceptible plants rather benefit from the help of BCA to induce their immunity, unlike resistant plants that already have high basal immunity, we examined the immunity induced by both cultivars studied.

In Tempranillo (see Figures 3B, 5 and Supplementary Figure 1B) under our experimental conditions, application of *Bs*-PTA-271 did not induce significant changes in plant defense

responses compared to control, whether infected or not. Since Tempranillo basal immunity strongly upregulates *PR1* as a marker of SA-dependent defenses, we can speculate that high basal SA content might contribute to prevent the beneficial effect of *Bs* PTA-271 on Tempranillo immunity. Our previous study showed that *Bs* PTA-271 primed the expression of the plant JA/ET-dependent defenses in Chardonnay rootlings (Trotel-Aziz et al. 2019), whereas it is reported that early activation of SA signaling could antagonize the expression of these JA/ET-dependent defenses (Pieterse et al. 2012; Van der Does et al. 2013). In this sense, *Bs*PTA-271 did not provide protection in Tempranillo against *Np*-Bt67. These results show therefore that cultivars differing in their basal immunity can condition the success of a BCA protection toward a pathogen. In contrast, *Ta* SC1 alone or together with *Bs* PTA-271 acts as a priming stimulus for Tempranillo, but no post-priming was observed with *Ta* SC1 alone and with *Ta* SC1 + *Bs* PTA-271 upon pathogen challenge. Looking at the defenses induced by these two protective modalities (*Ta* SC1 and *Ta* SC1 + *Bs* PTA-271) against *Np*-Bt67: the SA-dependent defenses (i.e., *PR1*, *PAL*, and *STS*) were rather strongly decreased in protected plants (i.e., asymptomatic despite infected), while they were the highest in symptomatic plants (*Bs* PTA-271). Since Botryosphaeriaceae are known to specifically metabolize grapevine phytoalexins (Stempien et al. 2017), which benefits pathogen fitness, we could suggest that the SA stimulation of the phenylpropanoid pathway and derivatives would wrongly serve the plant. In the case of Tempranillo exposed to Botryosphaeriaceae, the high constitutive expression of SA-dependent defense genes could thus appear as a disadvantage, confirming that Tempranillo would be less tolerant than Chardonnay to BOT, as already reported by Luque et al. (2009) and Cobos et al. (2019). Fortunately, in the Tempranillo pretreated with both BCAs, the expressions of genes *PR1*, *PAL*, and *STS* were repressed, and in the Tempranillo pretreated with *Ta* SC1 alone, the expression of the genes *PAL* and *STS* were repressed. Therefore, the beneficial effect of *Ta* SC1 on Tempranillo to control *Np*-Bt67 could result from a repressive effect on detrimental SA-dependent defenses. Complementary approaches are in progress to screen the induced key levers able to trigger ISR in the whole plant. Additionally, the *Ta* SC1 beneficial effect on Tempranillo could also result from a direct antagonism toward *Np*-Bt67 since it is applied in the same area as *Ta* SC1.

In non-infected Chardonnay rootlings (see Figures 3A, 4 and Supplementary Figure 1A), *Ta* SC1 shoot application did not induce any significant changes of the selected

targeted responses of plant defenses in leaves, while *Bs* PTA-271 root application upregulated the *PR1* and *PR2* gene expression and the combined application induced the expression of almost all targeted genes at a higher level than *Bs* PTA-271 alone. *Bs* PTA-271, alone or together with *Ta* SC1, may thus act as a priming stimulus in Chardonnay. However, upon pathogen challenge (4 dpi, designed as a relevant sampling time point for such experiment), *Bs* PTA-271 did not prime any of the targeted defenses, probably due to low to medium pathogen pressure compared to that reported in Trotel-Aziz et al. (2019). However, *Bs* PTA-271 beneficial effect on Chardonnay is supported by the phenotype of the *Bs*-PTA-271 treated rootlings, showing a significant protection for Chardonnay against *Np*-Bt67 at 2.5 mpi. This contrasts with the detected non-benefit provided by the combined application of both BCAs at 2.5 mpi, despite the fact that defenses were primed at 4 dpi, possibly due to a very high level of reactive oxygen species (ROS) that could amplify the plant defenses. It is interesting to note that *GST1* (involved in the ROS detoxification process) is the only useful targeted gene that was weakly expressed in non-protected Chardonnay pre-treated with both BCAs and further infected with *N. parvum* (see Figure 3A). This may suggest that when a pathway with high induced defenses is not combined with sufficient ROS detoxification, a plant could potentially trigger many symptoms. In our experimental conditions, Chardonnay therefore favors *Bs* PTA-271's beneficial effect, probably thanks to the different key levers including the induced grapevine immunity. Present at the root level, these results and those reported in Trotel-Aziz et al. (2019) suggest that systemic induced immunity conferred by *Bs* PTA-271 drove the plant ISR against *Np*-Bt67. Amazingly, the application of both BCAs enabled to reach the highest level of Chardonnay defense gene expression upon pathogen challenge (see Figure 3A), despite no protection at 2.5 mpi (see Figure 2D). Since *Ta* SC1 contributes to actively reducing the SA-dependent defenses in Tempranillo, one can hypothesize that *Ta* SC1 would also promote the *Bs* PTA-271 way of triggering immunity in Chardonnay. The authors also indicated that *Trichoderma* spp. may produce enzymes (i.e., ACC deaminase) able to shunt ET synthesis (Alfiky and Weisskopf 2021), but in Tempranillo, the application of both BCAs enabled reaching the highest protection (see Figure 2G). Thus, it would be surprising that *Ta* SC1 on its own would succeed to interfere with the beneficial effects of *Bs* PTA-271 in Chardonnay. This opens the discussion of how the cultivar interacts with BCAs and the pathogen to condition the beneficial or detrimental outcome against *Np*-Bt67.

Complementary approaches are already in progress to screen which are the induced key levers useful to control ISR in the whole plant.

3.5. Conclusion

Altogether, our results provide evidence that grapevine susceptibility to BOT is cultivar-dependent, as well as the BCA beneficial effects. *Bs* PTA-271 was confirmed as an effective protector for Chardonnay against *Np*-Bt67, and *Ta* SC1 was shown for the first time as a good protector for Tempranillo. This study also reports for the first time the biocontrol potential of the combination of *Bs* PTA-271 and *Ta* SC1 against *Np*-Bt67 in Tempranillo. This is a promising result for an improved efficiency of sustainable biological control in a proven context of lack of effective chemicals to manage GTDs.

Endowed with aggressive molecules, *Bs* PTA-271 and *Ta* SC1 can antagonize each other, but *Bs* PTA-271 inhibits *Np*-Bt67 development with a greater efficiency in a three-way confrontation. This beneficial BCA collaboration against *Np*-Bt67 still operates in Tempranillo and confirms the interest of using both BCAs in combination to optimize the direct fight against *Np*-Bt67. These results are of great interest for effective curative treatments to obtain healthy mother plants in the nursery and to control BOT in vineyard. However, the direct beneficial effect of combined BCAs did not operate to protect Chardonnay, suggesting that Chardonnay itself probably alters the fine-tuned orchestrated cooperation of BCAs that drives such direct beneficial effect.

Plant systemic immunity was also affected by each BCA. Our findings suggest a common feature for the two cultivars: the defenses that are greatly diminished in BCA-protected plants appear to be those that are responsive to SA, in contrast to symptomatic plants. For Tempranillo, the high basal expression of SA-dependent defenses may thus explain the highest susceptibility to BOT and also the ineffectiveness of *Bs* PTA-271 in our experimental conditions. Complementary approaches are underway to further investigate the responses of each cultivar to both *Bs* PTA-271 and *Ta* SC1 under controlled conditions and upon pathogen challenge.

Chapter IV

Dual RNA sequencing of *Vitis vinifera* Chardonnay and Tempranillo during its beneficial interaction with *Trichoderma atroviride* SC1 and *Bacillus subtilis* PTA-271 against *Neofusicoccum parvum*

4.1. Introduction

Grapevine trunk diseases (GTDs) represent one of the most concerning types of grapevine diseases, worrying viticulturists in all wine-producing countries (Mondello et al. 2018). Indeed, GTDs lead to important economic losses and vineyard sustainability disturbances, restricting both the productivity and the longevity of grapevines (Hofstetter et al. 2012; De la Fuente et al. 2016; O'Brien 2017; Mondello et al. 2018). By affecting the plant perennial part, GTDs lead to an unavoidable short- or long-term death of vines, reminding the very aggressive nature of the pathogens responsible for GTDs and their strong detrimental effect for the sustainability of the winemaking industry (Hofstetter et al. 2012). Both young and mature vines are not spared, as well as nursery staged plants, adding yet to the massive economic losses of the grapevine industry (Gramaje and Armengol 2011). Their undetermined period of latency as endophyte (vines in asymptomatic state) before switching pathogenic (symptomatic plants with chronic and dieback symptoms) makes GTD pathologies difficult to detect (Leal et al. submitted to Phytopathology, 2022). Therefore, an early detection of useful markers and an early management of GTDs remain presently a challenge in both nursery and vineyard (Gramaje and Armengol 2011; Gramaje et al. 2018; Leal et al. 2021b).

Among all, Botryosphaeria dieback (BD) is a common disease of vineyards and nursery plants (Leal et al. submitted to PMS, 2022), and thus represents one of the main GTDs. BD is prompted by several Botryosphaeriaceae species, including the very aggressive *Neofusicoccum parvum* (Úrbez-Torres 2011; Billones-Baaijens and Savocchia 2019; Reis et al. 2019; Larach et al. 2020; Trotel-Aziz et al. 2022). *N. parvum* has a hemibiotrophic lifestyle (Yang et al. 2015; Leal et al. 2022 review submitted to Phytopathology), with an initial heterotrophic endophytic phase allowing fungal hyphae to colonize the plant tissue from any plant wounds (e.g., pruning wounds) (Dakin et al. 2010; Hrycan et al. 2020; Slippers and Wingfield 2007). Botryosphaeriaceae can remain latent as endophytes until the host plant is exposed to stress (Dakin et al. 2010; Hrycan et al. 2020; Slippers and Wingfield 2007). As heterotrophs, they use cell wall degrading enzymes to take nutrients from the host showing no signs of disease (Giovannoni et al. 2020). During this endophytic lifestyle, the hemibiotroph can positively impact its host (Kogel et al. 2006). This stage is followed by a necrotrophic phase during which the hemibiotroph has a negative impact on its host in the short or long term due to an excess of deleterious nutrients secreted inside the host (namely, virulence and pathogenicity

factors). For instance, toxins are secreted by the pathogens inside the host cells that could suppress the plant immune defenses and promote disease symptoms (Leal et al. review submitted to Phytopathology in 2022) possibly actively. Depending on the biotope and environmental conditions, fungal species could reversibly adopt several modes of life during their existence (Kogel et al. 2006; Leal et al. review submitted to Phytopathology, 2022). Once pathogenic, the Botryosphaeriaceae infection causes chronic foliar discoloration and necrosis, but more often triggers a slow or apoplectic dieback that alters the permanent structures of the vines through partial necrosis (localized death of the distal buds, or shoots, or wood canker) or the full trunk necrosis (Larignon et al. 2001; Úrbez-Torres 2011). Such reversible pathogen lifestyle, triggering more or less damaging and/or reversible symptoms for the host makes BD pathology particularly difficult to manage. The development of specific markers for an early detection of this disease, focusing either on pathogen detection or on induced plant defenses, could thus be useful indicators or levers to better manage biocontrol strategies to combat BD.

Since the ban of sodium arsenite in the 2000s, the treatments available for GTDs, both in nursery and vineyard, are mainly preventive and mitigative, with a lack of effective curative treatments that eliminate GTD pathogens from grapevines. Few chemicals are applied on pruning wounds in vineyards to prevent colonization by fungal pathogens (Sosnowski et al. 2004), favoring cultural practices in vineyard (Mondello et al. 2018) and sanitation methods (Gramaje and Armengol 2011; Gramaje et al. 2018). However, these treatments cannot eradicate the pathogens once established in a vineyard (Calzarano et al. 2004; Gramaje and Armengol 2011). To contrast, the biological control based on the use of beneficial microorganisms (BCA) has already shown potential and is still the focus of several studies (Del Frari et al. 2019; Landum et al. 2016; Pertot et al. 2016; Trotel-Aziz et al. 2019; Leal et al. 2021b). Beneficial endophytes are defined as microorganisms that colonize healthy internal plant tissues without causing any apparent disease symptoms, while possibly inducing their host tolerance to environmental stresses and pathogens (Billar de Almeida et al. 2020; Oono et al. 2015). Fungi like those belonging to the *Trichoderma* genus and bacteria including *Bacillus* species, have already demonstrated such efficiency as biological control agents both in grapevine nurseries and vineyards.

Currently, *Trichoderma* species have been extensively investigated for their use against GTDs (Di Marco et al. 2002, 2004; John et al. 2008; Halleen et al. 2010; Berbegal et al. 2020; Martínez-Diz et al. 2021a, b; Leal et al. 2021b) and are the most widely used

fungal-based BCAs commercialized in viticulture (Harman 2006; Muckherjee et al. 2012; Waghunde et al. 2016). It is reported that *Trichoderma* spp. (1) can directly antagonize GTD pathogen aggressiveness through competition for nutrients and space, mycoparasitism, cell-wall degrading enzymes, and antibiosis, and (2) can also act as plant growth and defense stimulators (Harman 2006; Van Wees et al. 2008; Vinale et al. 2008; Pieterse et al 2014; Waghunde et al. 2016; Leal et al. review submitted to Phytopathology, 2022). A second group of beneficial microorganisms, namely *Bacillus* strains, has also been extensively studied as BCAs and reported to protect plants directly and indirectly against pathogens with different lifestyles (Magnin-Robert et al. 2007, 2013; Trotel-Aziz et al. 2008; Nguyen et al. 2020), including the GTD hemibiotrophic pathogens (Schmidt et al. 2001; Halleen et al. 2010; Rezgui et al. 2016; Kotze et al 2019; Trotel-Aziz et al. 2019; Leal et al. 2021b). As for *Trichoderma* species, the genome of *Bacillus* spp. encodes for a broad range of molecules that can both induce or elicit plant defenses (i.e. phytohormones precursors, lipopolysaccharides, siderophores) and compete with, antagonize, or directly modify plant pathogens or their aggressiveness (Kloepper et al. 2004; Ongena and Jacques 2008; Sood et al. 2020; Leal et al. 2021a; Leal et al. review submitted to Phytopathology, 2022).

In a previous study, Leal et al. (2021b) evaluated the effect of *B. subtilis* PTA-271 (*Bs* PTA-271) and *T. atroviride* SC1 (*Ta* SC1), on the protection of the two distinct grapevine cultivars Chardonnay and Tempranillo, against *N. parvum* Bt67 (Np-Bt67). The beneficial effect of each BCA has been proved to be cultivar dependent. *Bs* PTA-271 was confirmed as an effective protector for Chardonnay against Np-Bt67, and *Ta* SC1 was shown effective for Tempranillo plants. Authors further showed that even if the effect of each BCA differed depending on the cultivar, there was a common feature to protected cultivars: the SA-dependent defenses were significantly repressed at a systemic level. Although this study confirmed the beneficial effects of *Bs* PTA-271 and *Ta* SC1 in protecting grapevine against Np-Bt67, and their key action lever, there is still a need to deeply decipher the plant physiological changes induced by each BCA to achieve an effective protection against this pathogen, whatever the cultivar. Indeed, the most precise information will be useful to propose the most effective biocontrol solutions adapted to professional needs.

This recent decade, the RNA sequencing (RNA-seq) method starts such a deciphering of the woody plant responses to phytopathogens and BCAs. The revealing changes in the expression of genes involved in cell wall biosynthesis, but also hormone

signaling and secondary metabolism, could therefore be considered important players in the multi-party plant/pathogen/BCA interactions (Xu et al. 2013, Camps et al. 2010, Yacoub et al. 2020).

In the present study, we intend to extensively decipher the plant physiology changes induced by both *Bs* PTA-271 and *Ta* SC1 to protect grapevine upon Np-Bt67 infection, by using transcriptomic analysis. These transcriptomic analyses are complementary to the work of Leal et al. (2021b) and have been performed with the same pool of leaf samples described as statistically robust. The focus was therefore made on the molecular responses of plant to Np-Bt67 using grapevine cuttings cv Chardonnay and Tempranillo, whether or not they have been previously inoculated with *Bs* PTA-271 and/or *Ta* SC1. To our knowledge, this is the first transcriptomic study on the induced changes by two distinct BCAs to two different grapevine cultivars artificially infected with Np-Bt67.

4.2. Material and methods

Biological material and Experimental design

These transcriptomic analyses are complementary to the work of Leal et al. (2021b) using the same samples as those from the experiments conducted and described in Leal et al. (2021b). Therefore, three-node-long cuttings of grapevine cv. Tempranillo and cv. Chardonnay were rooted in a culture chamber (24/20°C day/night, 55–65% relative humidity day/night, with a 16-h photoperiod at 400 µmol/m2/s) then maintained in individual 200-ml pots under the same conditions. The *B. subtilis* PTA-271 (*Bs* PTA-271) inoculations were carried out on 16 weeks old rootlings (considered as day 0) and 2 weeks later (day 15), by drenching the soil at the root level for a final density of 10^8 CFU/g soil. The inoculation with *T. atroviride* SC1 (*Ta* SC1) was performed once with a paintbrush at the second node of previously wounded lignified stems (5 mm diameter and 1 mm deep) of 18-week-old rootlings, at a final density of 10^8 CFU/ml (day 15) as described by Leal et al. (2021b). Half of the 20-week-old rootlings that were treated with *Bs* PTA-*271* (day 0 and day 15) and/or *Ta* SC1 (day 15) were further infected with Np-Bt67 at the wounding area with a 3-mm-diameter mycelial plug from a 7-day-old culture (day 30) as described by Leal et al. (2021b). The experiment was composed of five repetitions for each treatment, with 8–10 rootlings per repetition for each treatment.

Sample collection

Leaf samples from the rootlings (40 leaves of 8 rootlings per replicate of each treatment) were collected 4 days post-inoculation of pathogen (dpi), ground in liquid nitrogen, and then stored at −80°C for RNA extraction. Three replicates per treatment were then selected for the RNA extraction and RNA-seq analysis.

RNA extraction and DNAse treatment

Total RNA was extracted from 50 mg of leaf powder with Plant RNA Purification Reagent according to manufacturer instructions (Invitrogen, Pontoise, France), and DNase treated as described by the manufacturer's instructions (RQ1 RNase-Free DNase, Promega). RNA quality was assessed with an Experion standard sensitivity RNA chip (Bio-Rad, Hercules, CA), and total RNA concentration was measured at 260 nm for each sample using the NanoDrop One spectrophotometer (Ozyme) and adjusted to 100 ngµl^{-1}.

RNA-seq bioinformatic analysis: sample pairwise comparisons based on *V. vinifera* genes

RNA-seq analysis from the leaf samples were performed by Genewiz® (Azenta Life Sciences, Leipzig, Germany). RNA samples were subjected to poly(A)+ selection, cDNA synthesis, library preparation and deep sequencing using Illumina NovaSeq (2x150 bp reads), leading to 1,328,791,424 reads that were compiled in fastq format.

The estimation of the reads was performed by FastQC (Andrews et al. 2010). Sequence reads were trimmed to remove possible adapter sequences and nucleotides with poor quality using Trimmomatic v.0.36 (Bolger et al. 2014). The trimmed reads were mapped to the Vino_Marie reference genome available on ENSEMBL using the STAR aligner v.2.5.2b. The STAR aligner is a splice aligner that detects splice junctions and incorporates them to help align the entire read sequences.

Unique gene hit counts were calculated using feature Counts from the Subread package v.1.5.2. Only unique reads that fell within exon regions were counted.

Using DESeq2, a comparison of gene expression between the defined groups of samples was performed. The Wald test was used to generate p-values and log2 fold changes. Genes with an adjusted p-value < 0.05 and absolute log2 fold change > 1 were called as differentially expressed genes for each comparison.

Venn diagrams were designed using a webtool from Bioinformatics & Evolutionary Genomics (https://bioinformatics.psb.ugent.be/webtools/Venn/). A Gene Ontology (GO) analysis was performed using the GOslim software. The significant enrichment of GO terms based on hypergeometric distribution followed by FDR <0.05 correction was used for comparison between the experimental set and reference set of grapevine species using ShinyGO v0.61 (http://bioinformatics.sdstate.edu/go/) (Ge et al. 2020).

4.3. Results

Brief reminder of published phenotypic results prior to RNA-seq analysis

Leal et al. (2021b) have shown that grapevine susceptibility to BD is cultivar-dependent, as well as BCA beneficial effects. They confirmed *Bs* PTA-271 as an effective protector for Chardonnay against Np-Bt67, and *Ta* SC1 as a good protector for Tempranillo. Authors additionally highlighted a common feature for both protected cultivars: SA-dependent defenses were strongly decreased by the BCA and suggested that the high basal expression of SA-dependent defenses in Tempranillo explains its highest susceptibility to Np-Bt67. They finally reported the beneficial potential of BCA combination against Np-Bt67 in Tempranillo, but not in Chardonnay, and suggested that Chardonnay itself could interfere the fine-tuned cooperation of BCAs that remains to be further investigated.

RNA-seq analysis on Chardonnay samples

Differentially Expressed Genes (DEGs) in the leaves of plants infected with Np-Bt67

Compared to control plants (Ctl), plants infected with Np-Bt67 (Np) have four genes significantly overexpressed at 4 dpi (**Fig. 1A**), that encode for: a carotenoid cleavage dioxygenase, a GTP-binding protein, a valence synthase, and a putative receptor-like protein kinase. Similar trends are observed when comparing diseased (Np) with protected plants by *Bs* PTA-271 (NpBs) (**Fig. 1Ba**). However, the expression level of Valencene synthase and GTP-binding protein are indifferently overexpressed in the leaves of diseased plants infected with Np-Bt67 (Np) and unprotected with combined BCA (NpBsTa) (**Fig. 1Bb**), suggesting that these two genes would not be useful key markers associated to Chardonnay disease expression. In contrast, the two genes encoding for a carotenoid cleavage dioxygenase and a putative receptor-like protein kinase could be useful markers associated to Chardonnay disease expression of BD. They also could be

consider as key targets to better protect Chardonnay against Np-Bt67 since they are overexpressed in the leaves of diseased plants, but not in the leaves of plants protected by *Bs* PTA-271.

A

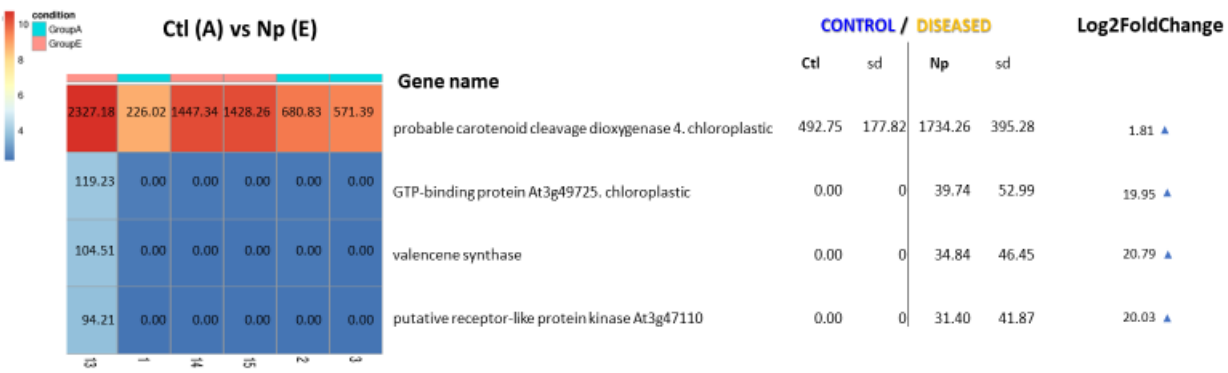

B

a

	DISEASED / Protected	
	Np	NpBs
Valence synthase	38.00	0.00
GTP-binding protein AT3g49725 chloroplastic	43.00	0.00

b

	DISEASED / DISEASED	
	Np	NpBsTa
Valence synthase	34.95	0.00
GTP-binding protein AT3g49725 chloroplastic	39.88	0.00

Figure 1. Differentially expressed genes (DEGs) in Chardonnay leaves at 4 dpi between: **(A)** control plants (Ctl) and diseased plants once infected with *N. parvum* Bt67 (Np); **(Ba)** diseased plants (Np) and plants protected with *Bacillus subtilis* PTA-271 (NpBs); **(Bb)** diseased plants due to unprotective treatment with combined BCA upon pathogen challenge (NpBsTa) and diseased plants due to pathogen infection (Np). sd: standard deviation.

DEGs in leaves of plants protected with *Bs* PTA-271

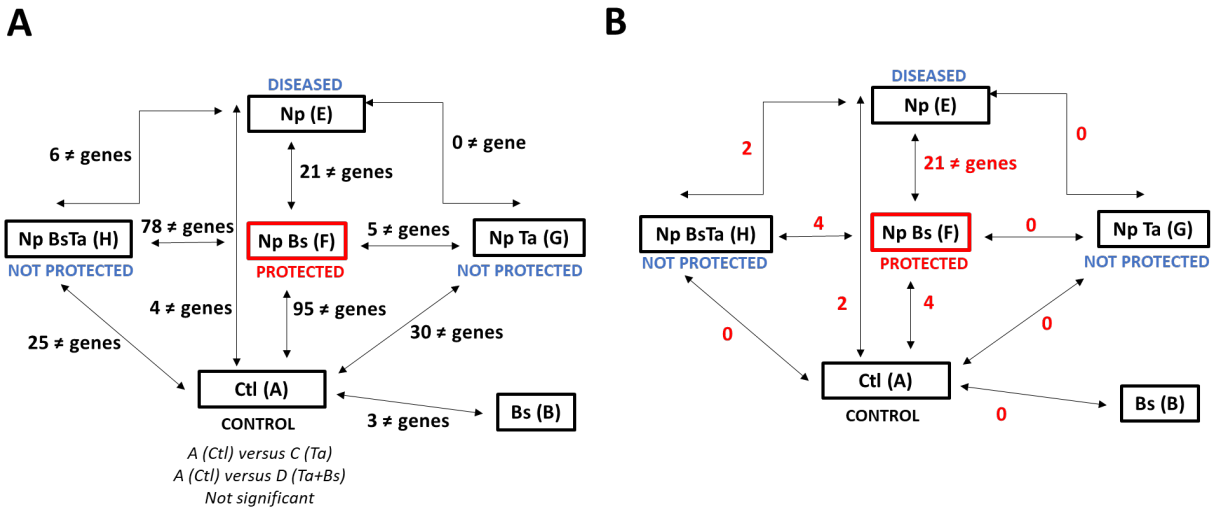

Figure 2. DEGs in Chardonnay leaves at 4 dpi: **(A)** between all treatments, and **(B)** common to the 21 DEGs between Np vs NpBs. Treatments are: twenty-week-old rootlings untreated or pretreated with *Bs* PTA-271 or *Ta* SC1 or both, before being infected for 4 days with sterile PDA plugs (Ctl, Bs, Ta, and Ta+Bs, respectively) or with mycelium plugs of Np-Bt67 (Np, Np Bs, Np Ta, and Np BsTa, respectively).

The comparison between all treatments shows 21 DEGs between diseased infected plants with Np-Bt67 (Np) and infected plants that are protected with *Bs* PTA-271 (Np Bs) (**Fig. 2A**). The expression level of some of these 21 genes is also modulated in the leaves of unprotected plants (**Fig. 2B**, Np BsTa vs Np, and Np BsTa vs Np Bs),

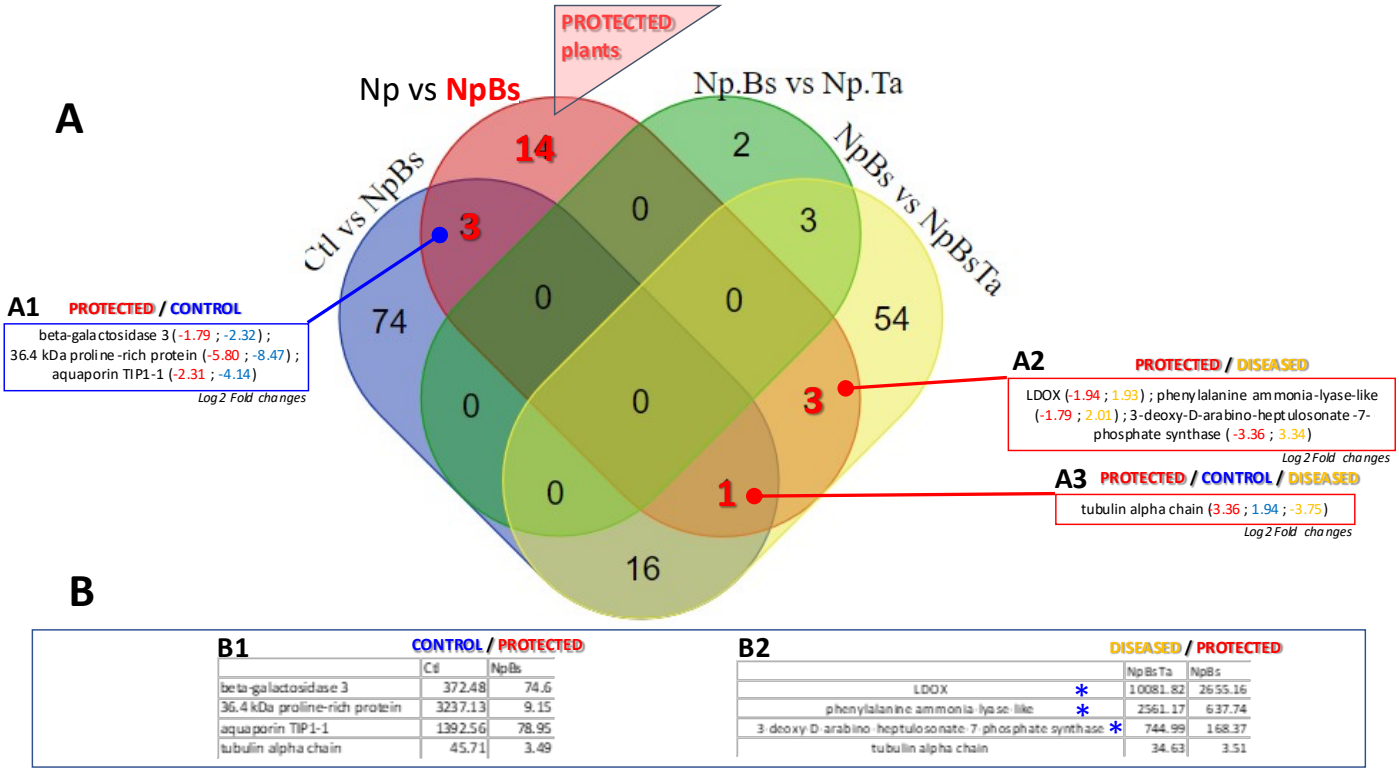

making it necessary to observe in depth their expression level (**Fig. 3**).

Figure 3. Common DEGs in Chardonnay leaves at 4 dpi between: control (Ctl), protected (NpBs) and unprotected treatments (Np, NpTa, NpBsTa) of Chardonnay cultivars. Legend is as in Fig. 2.

As indicated in **Fig. 3**, the 21 DEGs (red) in Chardonnay leaves at 4 dpi between diseased infected plants with Np-Bt67 (Np) and infected plants that are protected with *Bs* PTA-271 (Np Bs): the tubulin alpha chain is overexpressed at similar levels both in the leaves of uninfected Control plants (**Fig. 3BB1**) and in the leaves of diseased plants (**Fig. 3BB2**). This suggests that this gene would not be a useful key marker associated to Chardonnay disease expression. For the genes encoding for the beta-galactosidase 3, the 36.4 kDa proline-rich protein and the aquaporin TIP1-1, similar expression levels are observed in protected plants with *Bs* PTA-271 (NpBs) and in uninfected Control (Ctl)

plants (**Fig. 3BB1**, from 9.15 to 3237.13) as diseased plants (Np, **Fig. 4**, from 288.40 to 569.08). This suggests also that these 3 genes would not be useful key markers associated to Chardonnay disease expression of BD. Genes encoding for LDOX, PAL and a phosphate synthase show opposite trends of expression only in protected plants with *Bs* PTA-271 (NpBs) compared to unprotected diseased plants (**Fig. 3B2, A2 and B2**), suggesting that they could be key targets to consider to better protect Chardonnay against Np-Bt67.

A focus is carried out on the last 14 DEGs of **Fig. 3A**, which are the genes differing in their expression level (**Fig. 4**, highlighted red) between diseased (Np) and protected plants with *Bs* PTA-271 (NpBs). The **Fig. 4** shows all the information for the 21 DEGs observed in Chardonnay leaves at 4 dpi between diseased infected plants with Np-Bt67 (Np) and infected plants that are protected with *Bs* PTA-271 (Np Bs).

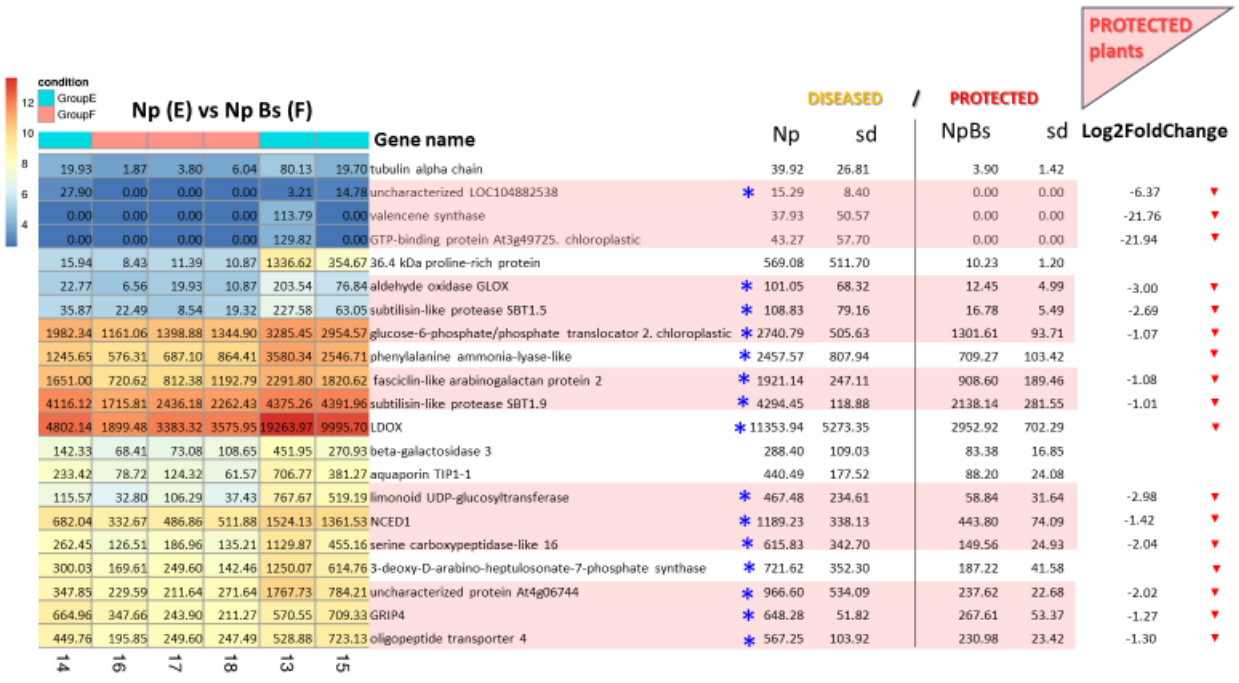

Gene name		DISEASED / Np	sd	PROTECTED / NpBs	sd	Log2FoldChange
tubulin alpha chain		39.92	26.81	3.90	1.42	
uncharacterized LOC104882538	*	15.29	8.40	0.00	0.00	-6.37
valencene synthase		37.93	50.57	0.00	0.00	-21.76
GTP-binding protein At3g49725, chloroplastic		43.27	57.70	0.00	0.00	-21.94
36.4 kDa proline-rich protein		569.08	511.70	10.23	1.20	
aldehyde oxidase GLOX	*	101.05	68.32	12.45	4.99	-3.00
subtilisin-like protease SBT1.5	*	108.83	79.16	16.78	5.49	-2.69
glucose-6-phosphate/phosphate translocator 2, chloroplastic	*	2740.79	505.63	1301.61	93.71	-1.07
phenylalanine ammonia-lyase-like	*	2457.57	807.94	709.27	103.42	
fasciclin-like arabinogalactan protein 2	*	1921.14	247.11	908.60	189.46	-1.08
subtilisin-like protease SBT1.9	*	4294.45	118.88	2138.14	281.55	-1.01
LDOX	*	11353.94	5273.35	2952.92	702.29	
beta-galactosidase 3		288.40	109.03	83.38	16.85	
aquaporin TIP1-1		440.49	177.52	88.20	24.08	
limonoid UDP-glucosyltransferase	*	467.48	234.61	58.84	31.64	-2.98
NCED1	*	1189.23	338.13	443.80	74.09	-1.42
serine carboxypeptidase-like 16	*	615.83	342.70	149.56	24.93	-2.04
3-deoxy-D-arabino-heptulosonate-7-phosphate synthase	*	721.62	352.30	187.22	41.58	
uncharacterized protein At4g06744	*	966.60	534.09	237.62	22.68	-2.02
GRIP4	*	648.28	51.82	267.61	53.37	-1.27
oligopeptide transporter 4	*	567.25	103.92	230.98	23.42	-1.30

Figure 4. Expression levels of the differently expressed genes (DEGs) in Chardonnay leaves at 4 dpi between diseased infected plants with Np-Bt67 (Np) and infected plants that are protected with *Bs* PTA-271 (Np Bs). Highlighted red, are the 14 DEGs not yet analyzed in the Figure 3. Genes marked with an asterisk are suspected to be of interest to understand the mode of action of *Bs* PTA-271 to protect Chardonnay grapevines against Np-Bt67. sd: standard deviation.

Among the 21 DEGs identified in Chardonnay leaves at 4 dpi between diseased infected plants with Np-Bt67 (Np) and infected plants that are protected with *Bs* PTA-271 (Np Bs), 15 genes are related to the mode of action of *Bs* PTA-271 against Np-Bt67 (**Fig. 4**, blue asterisk).

As shown in **Fig. 4**, all the 15 DEGs correlated with *Bs* PTA-271 protective effect on Chardonnay plants infected with Np-Bt67 are repressed in protected plants (NpBs) compared to diseased plants (Np). These genes of interest are: an uncharacterized LOC104882538, an aldehyde oxidase GLOX, a subtilisin-like protease SBT1.5, a glucose-6-phosphate/phosphate translocator 2 chloroplastic, a phenylalanine ammonia-lyase like, a fasciclin-like arabinogalactan protein 2, a subtilisin like protease SBT1.9, a LDOX, a limonoid UDP-glucosyltransferase, NCED1, a serine carboxypeptidase-like 16, a 3-deoxy-D-arabino-heptulosonate-7-phosphate synthase, an uncharacterized protein At4g06744, GRIP4, and an oligopeptide transporter 4.

Predominant Functions (GO) of *V. vinifera* DEGs in leaves of Chardonnay plants infected with Np-Bt67 and protected with *Bs* PTA-271

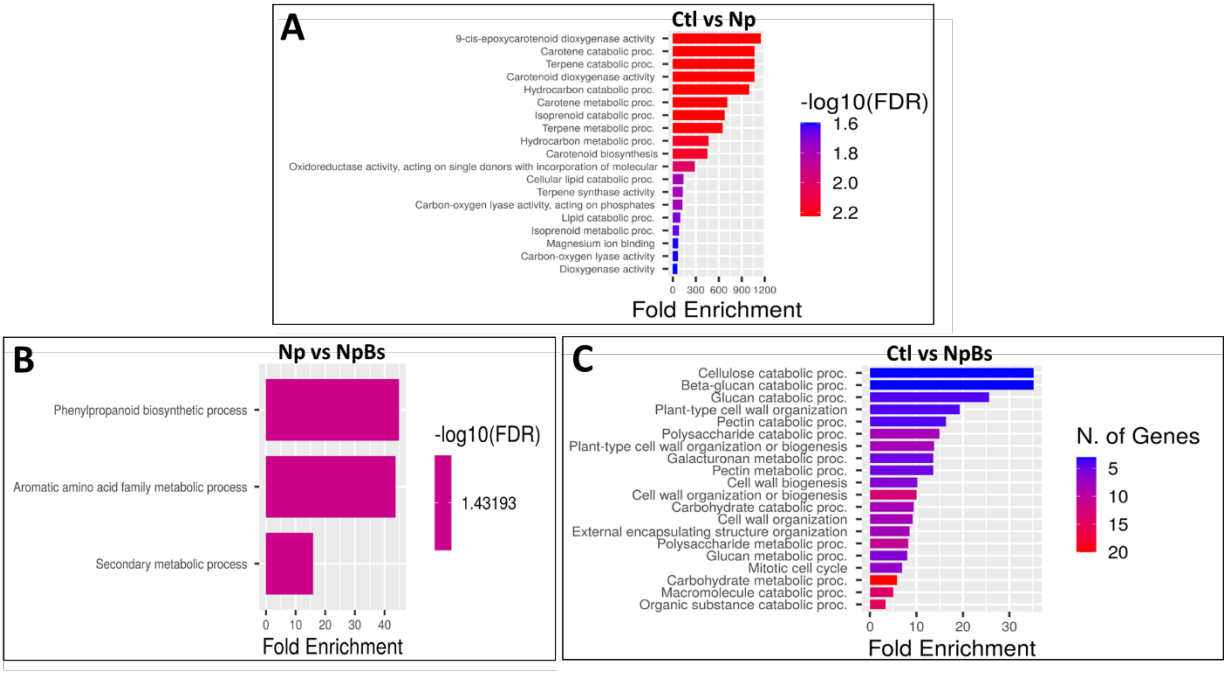

Figure 5. Predominant functions of DEGs in Chardonnay leaves at 4 dpi between: **(A)** control and infected plants (Ctl vs Np), **(B)** infected and protected plants with *Bacillus subtilis* PTA-271 (Np vs NpBs), and **(C)** control and protected plants with *Bacillus subtilis* PTA-271 (Ctl vs NpBs). FDR: False discovery rate.

As shown in **Fig. 5A**, plants infected with Np-Bt67 (Np) have DEGs compared to control plants (Ctl), that may induce changes in dioxygenase activities and oxidoreductase activities, in relationship with pigment production (carotene and carotenoid biosynthesis), hormonal balance (terpene/ isoprenoid pathway and cellular lipidic catabolic processes) and hydrocarbon metabolic processes (among which carbon-oxygen lyase activity, that may act on phosphatases).

In **Fig. 5B**, infected plants protected with *Bs* PTA-271 (NpBs) compared to infected plants (Np) show DEGs associated to changes in the phenylpropanoid biosynthetic process, aromatic amino acid family metabolic process, and secondary metabolic process.

Finally, DEGs in infected plants protected with *Bs* PTA-271 (NpBs) compared to control plants (Ctl), highlight changes in mitotic cell cycle and catabolic processes of organic substances / macromolecules. This impacts thus the cell wall structure organization and biogenesis, through changes in galacturonan, pectin, cellulose, polysaccharide, glucan and carbohydrate metabolic processes **(Fig. 5C)**.

RNA-seq analysis on Tempranillo samples

Major DEGs in the leaves of plants infected with Np-Bt67

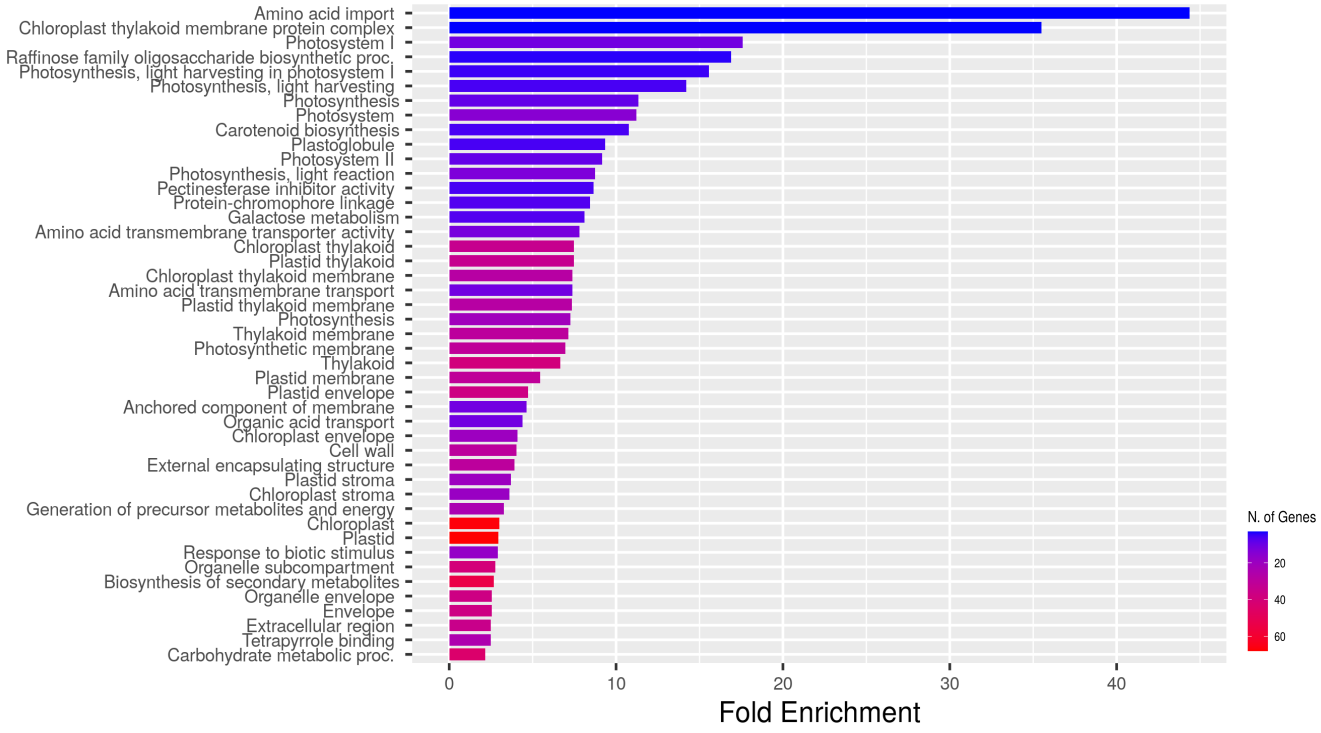

Figure 6. Predominant functions of DEGs in Tempranillo leaves at 4 dpi between control plants and Np-Bt67 infected plants.

Compared to control plants, the leaves of plants infected with Np-Bt67 showed 567 differentially expressed genes (DEGs) at 4 dpi. **Figure 6** only reports the predominant function of these genes which are related to amino acid import, chloroplast, and photosystem related processes, as well as the plant responses to biotic stimulus, and biosynthesis of secondary metabolites.

DEGs in leaves of plants protected with *Ta* SC1

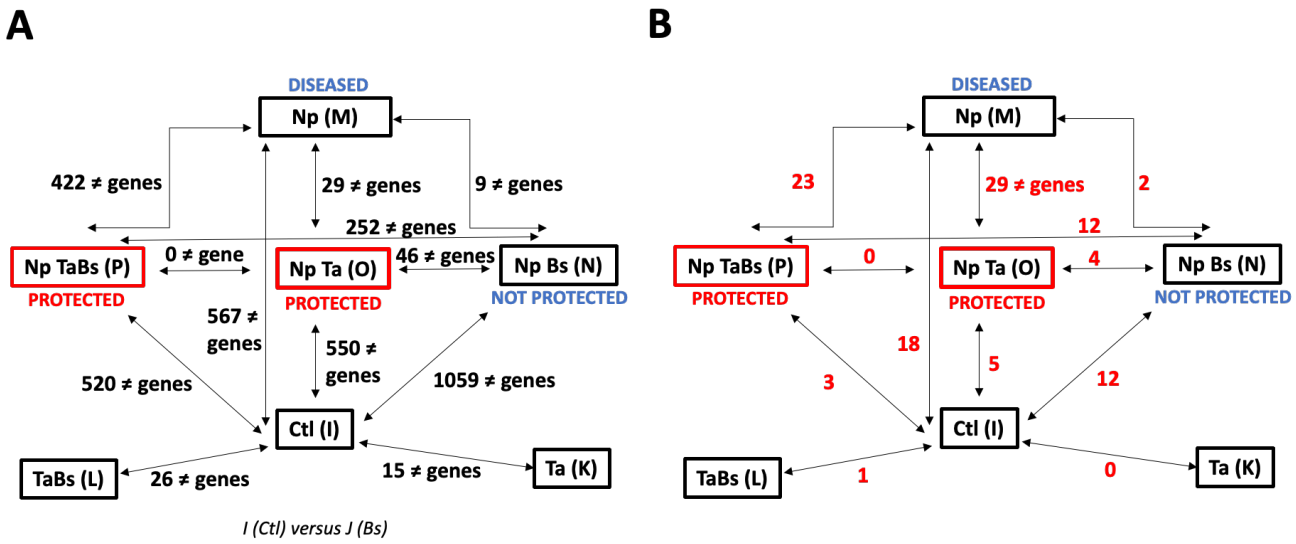

Figure 7. Differently expressed genes (DEGs) in Tempranillo leaves at 4 dpi: **(A)** between all treatments, and **(B) common to the 29** DEGs between Np vs NpTa (B). Treatments are: twenty weeks old rootlings untreated or pretreated with *Bs* PTA-271 or *Ta* SC1 or both, before being infected for 4 days with sterile PDA plugs (Ctl, Bs, Ta, and Ta+Bs, respectively) or with mycelium plugs of Np-Bt67 (Np, Np Bs, Np Ta, and Np BsTa, respectively).

The comparison of all treatments (**Fig. 7A**) shows 29 DEGs between diseased infected plants with Np-Bt67 (Np) and infected plants that are protected with *Ta* SC1 (Np Ta). The expression level of some of these 29 genes is also modulated in the leaves of unprotected plants (**Fig. 7B**, Np TaBs vs Np Bs, and Np Ta vs Np Bs), hence the need for in-depth observation of their expression level (**Fig. 8**).

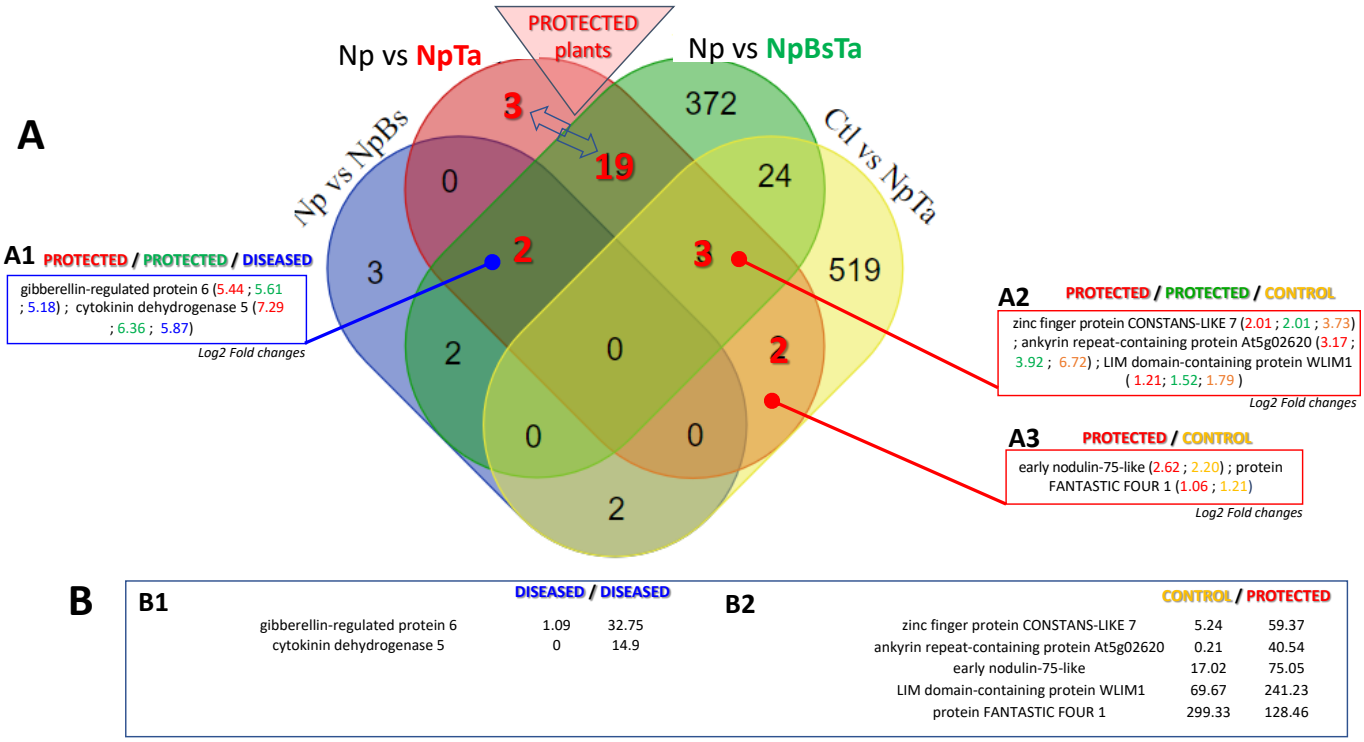

Figure 8. Common DEGs in Tempranillo leaves at 4 dpi between: control (Ctl), protected (NpTa and NpBsTa) and unprotected treatments (Np and NpBs) of Tempranillo cultivars. Legend is as in Fig. 7.

As represented in **Fig. 8**, among the 29 DEGs (red) in Tempranillo leaves at 4 dpi between diseased infected plants with Np-Bt67 (Np) and infected plants protected with *Ta* SC1 (NpTa): cytokinin dehydrogenase 5 and gibberellin-regulated protein 6 are expressed at similar levels (**Fig. 8 AA1**) in protected and unprotected plants. This suggests that these two genes would not be a useful key marker associated to Tempranillo disease expression of BD, nor be key targets to consider to better protect Tempranillo against Np-Bt67. Similarly, patterns are observed for genes encoding zing finger protein CONSTANS-LIKE 7, ankyrin repeat-containing protein At5g02620, LIM domain-containing protein WLIM1 and the protein FANTASTIC FOUR 1 (Fig. 8 **BB2)**. This suggests that these 4 genes would not be useful key markers associated to Tempranillo disease expression of BD. In contrast, gene encoding for the early-nodulin-75-like is less expressed in control (Ctl, 17.02 in **Fig. 8 BB2**) and protected plants with *Ta* SC1 (NpTa, 75.05 in **Fig. 8 BB2**) than in diseased plants (Np, 400.88 in **Fig. 9**).

The last 23 DEGs (**Fig. 8A)** are the genes differing in their expression level between diseased (Np) and protected plants with *Ta* SC1 (NpTa) or with both BCA (NpTaBs) (**Fig. 9**). The **Fig. 9** shows all the information for the 23 DEGs observed in Tempranillo leaves at 4 dpi between diseased infected plants with Np-Bt67 (Np) and infected plants that are protected with *Ta* SC1 (Np Ta).

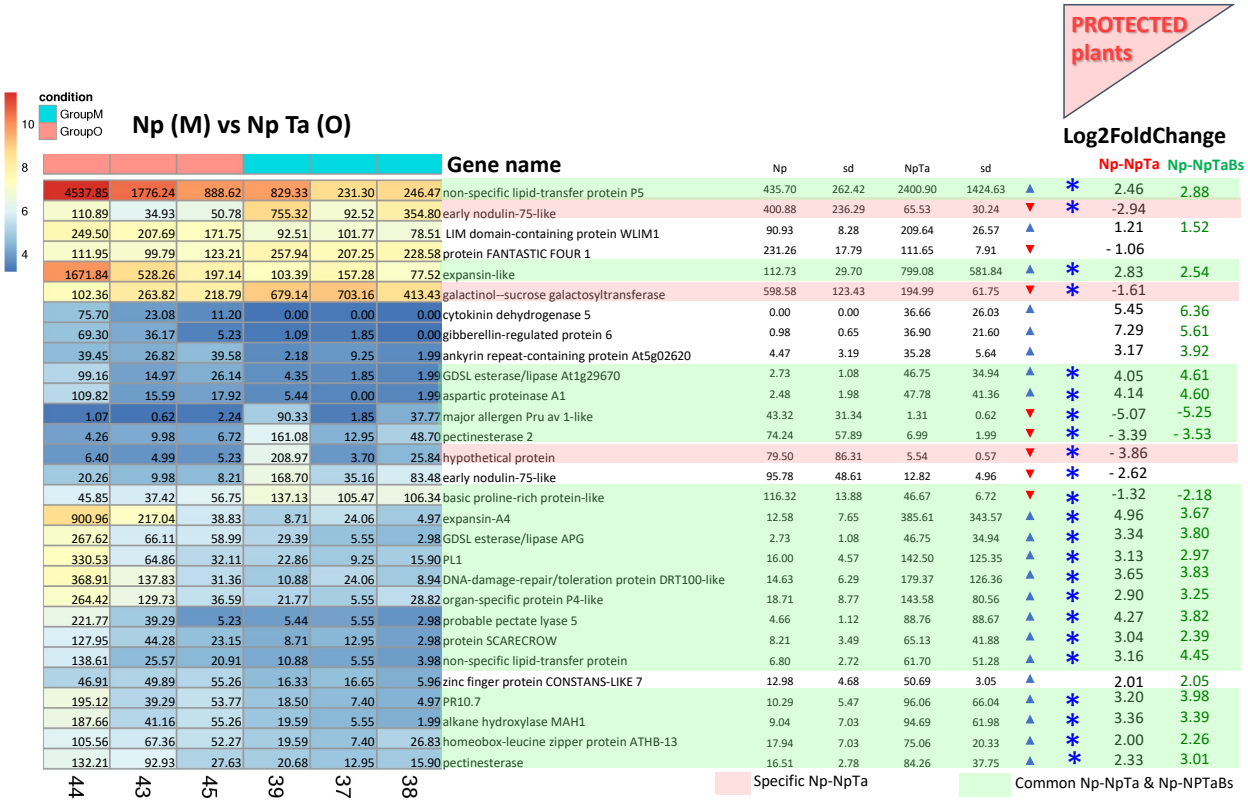

44	43	45	39	37	38	Gene name	Np	sd	NpTa	sd		Np-NpTa	Np-NpTaBs
4537.85	1776.24	888.62	829.33	231.30	246.47	non-specific lipid-transfer protein P5	435.70	262.42	2400.90	1424.63	*	2.46	2.88
110.89	34.93	50.78	755.32	92.52	354.80	early nodulin-75-like	400.88	236.29	65.53	30.24	*	-2.94	
249.50	207.69	171.75	92.51	101.77	78.51	LIM domain-containing protein WLIM1	90.93	8.28	209.64	26.57		1.21	1.52
111.95	99.79	123.21	257.94	207.25	228.58	protein FANTASTIC FOUR 1	231.26	17.79	111.65	7.91		- 1.06	
1671.84	528.26	197.14	103.39	157.28	77.52	expansin-like	112.73	29.70	799.08	581.84	*	2.83	2.54
102.36	263.82	218.79	679.14	703.16	413.43	galactinol--sucrose galactosyltransferase	598.58	123.43	194.99	61.75	*	-1.61	
75.70	23.08	11.20	0.00	0.00	0.00	cytokinin dehydrogenase 5	0.00	0.00	36.66	26.03		5.45	6.36
69.30	36.17	5.23	1.09	1.85	0.00	gibberellin-regulated protein 6	0.98	0.65	36.90	21.60		7.29	5.61
39.45	26.82	39.58	2.18	9.25	1.99	ankyrin repeat-containing protein At5g02620	4.47	3.19	35.28	5.64		3.17	3.92
99.16	14.97	26.14	4.35	1.85	1.99	GDSL esterase/lipase At1g29670	2.73	1.08	46.75	34.94	*	4.05	4.61
109.82	15.59	17.92	5.44	0.00	1.99	aspartic proteinase A1	2.48	1.98	47.78	41.36	*	4.14	4.60
1.07	0.62	2.24	90.33	1.85	37.77	major allergen Pru av 1-like	43.32	31.34	1.31	0.62	*	-5.07	-5.25
4.26	9.98	6.72	161.08	12.95	48.70	pectinesterase 2	74.24	57.89	6.99	1.99	*	- 3.39	- 3.53
6.40	4.99	5.23	208.97	3.70	25.84	hypothetical protein	79.50	86.31	5.54	0.57	*	- 3.86	
20.26	9.98	8.21	168.70	35.16	83.48	early nodulin-75-like	95.78	48.61	12.82	4.96	*	- 2.62	
45.85	37.42	56.75	137.13	105.47	106.34	basic proline-rich protein-like	116.32	13.88	46.67	6.72	*	-1.32	-2.18
900.96	217.04	38.83	8.71	24.06	4.97	expansin-A4	12.58	7.65	385.61	343.57	*	4.96	3.67
267.62	66.11	58.99	29.39	5.55	2.98	GDSL esterase/lipase APG	2.73	1.08	46.75	34.94	*	3.34	3.80
330.53	64.86	32.11	22.86	9.25	15.90	PL1	16.00	4.57	142.50	125.35	*	3.13	2.97
368.91	137.83	31.36	10.88	24.06	8.94	DNA-damage-repair/toleration protein DRT100-like	14.63	6.29	179.37	126.36	*	3.65	3.83
264.42	129.73	36.59	21.77	5.55	28.82	organ-specific protein P4-like	18.71	8.77	143.58	80.56	*	2.90	3.25
221.77	39.29	5.23	5.44	5.55	2.98	probable pectate lyase 5	4.66	1.12	88.76	88.67	*	4.27	3.82
127.95	44.28	23.15	8.71	12.95	2.98	protein SCARECROW	8.21	3.49	65.13	41.88	*	3.04	2.39
138.61	25.57	20.91	10.88	5.55	3.98	non-specific lipid-transfer protein	6.80	2.72	61.70	51.28	*	3.16	4.45
46.91	49.89	55.26	16.33	16.65	5.96	zinc finger protein CONSTANS-LIKE 7	12.98	4.68	50.69	3.05		2.01	2.05
195.12	39.29	53.77	18.50	7.40	4.97	PR10.7	10.29	5.47	96.06	66.04	*	3.20	3.98
187.66	41.16	55.26	19.59	5.55	1.99	alkane hydroxylase MAH1	9.04	7.03	94.69	61.98	*	3.36	3.39
105.56	67.36	52.27	19.59	7.40	26.83	homeobox-leucine zipper protein ATHB-13	17.94	7.03	75.06	20.33	*	2.00	2.26
132.21	92.93	27.63	20.68	12.95	15.90	pectinesterase	16.51	2.78	84.26	37.75	*	2.33	3.01

Figure 9. Expression level of the differently expressed genes (DEGs) in Tempranillo leaves at 4 dpi between diseased infected plants with Np-Bt67 (Np) and infected plants that are protected with *Ta* SC1 (Np Ta). Genes marked with an asterisk are suspected to be of interest to understand the mode of action of *Ta* SC1 to protect Tempranillo grapevines against Np-Bt67. The last column shows the differential expression of the genes of interest in response to the two protective treatments, using either *Ta* SC1 (Np-NpTa) or combined BCA (Np-NpTaBs).

Among the 29 DEGs identified in Tempranillo leaves at 4 dpi between diseased infected plants with Np-Bt67 (Np) and infected plants that are protected with *Ta* SC1 (Np Ta), 23 genes are considered involved in the mode of action of *Ta* SC1 against Np-Bt67 (**Fig. 9**, blue asterisk). Indeed, the analysis performed from **Fig. 7 to Fig. 8** allows to

exclude the 6 irrelevant genes not marked with an asterisk (namely: LIM domain-containing protein WLIM1, the protein FANTASTIC FOUR 1, cytokinin dehydrogenase 5, gibberellin-regulated protein 6, ankyrin repeat-containing protein At5g02620, and zing finger protein CONSTANS-LIKE 7).

As shown in **Fig. 9**, all the 23 DEGs correlated with *Ta* SC1 protective effect on Tempranillo plants infected with Np-Bt67 are either repressed or over-induced in protected plants (NpTa and Np-NpTaBs) compared to diseased plants (Np). There are 7 genes in which the expression is repressed in protected plants: 2 genes encoding for early-nodulin-75-like proteins, a galactinol-sucrose glucosyltransferase, a major allergen Pru av1-like, a pectin esterase 2, a basic proline-rich protein-like, and another gene encoding for a hypothetical protein. There are 16 genes whose expression is over-expressed in protected plants, encoding for: non-specific lipid-transfer protein P5, another non-specific lipid-transfer protein, expansin-like, expansin-A4, GDSL esterase/lipase At1g29670, GDSL esterase / lipase APG, aspartic proteinase A1, PL1, DNA-damage-repair / toleration protein DRT100-like, organ-specific protein P4-like, probable pectate lyase 5, protein SCARECROW, PR10.7, alkane hydroxylase MAH1, homeobox-leucine zipper protein ATHB-13, and pectin esterase.

Predominant Functions (GO) of *V. vinifera* DEGs in leaves of Tempranillo plants infected with *Np-Bt67* and protected with *Ta* SC1

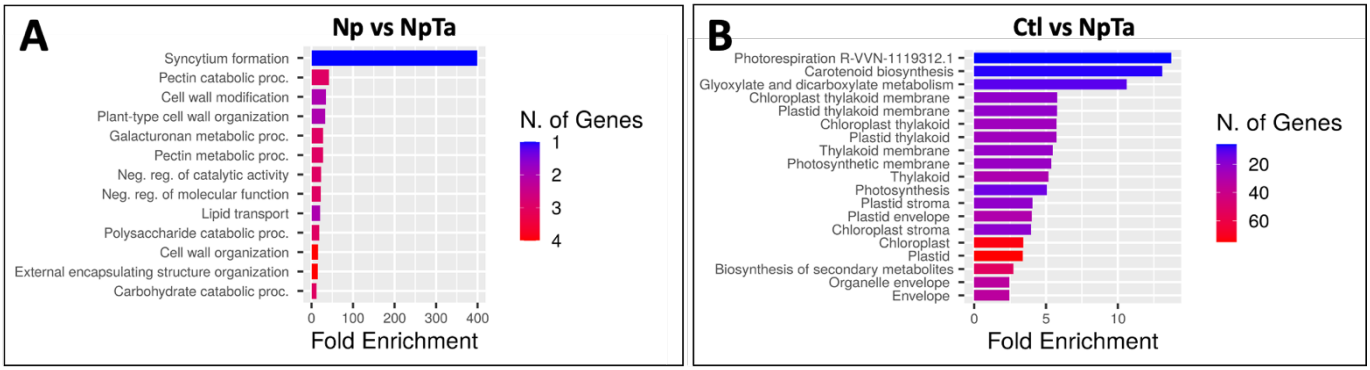

Figure 10. Predominant functions of DEGs in Tempranillo leaves at 4 dpi between: **(A)** infected and protected plants with *Trichoderma atroviride Ta* SC1 (Np vs NpTa), and **(B)** control and protected plants with *Trichoderma atroviride Ta* SC1 (Ctl vs NpTa).

As shown in **Fig. 10A**, the DEGs in infected plants protected with *Ta* SC1 (NpTa) compared to infected plants (Np), are related to cell and cell wall formations (syncytium formation, pectin catabolic process, cell wall modification, plant-type cell wall organization, galacturonan and pectin metabolic process), protein quenching and their expression silencing, but also lipid transport, and carbohydrate/polysaccharide catabolism.

When comparing infected plants protected with *Ta* SC1 (NpTa) to control plants (Ctl), changes concern chloroplast related processes such as photosynthesis and photorespiration, and in biosynthesis of secondary metabolites **(Fig. 10B)**.

4.4. Discussion

In Leal et al. (2021b), we evaluated the effect of *Bs* PTA-271 and *Ta* SC1 on the protection of two distinct grapevine cultivars, Chardonnay and Tempranillo, against Np-Bt67 symptoms. We provided evidence that grapevine susceptibility to BD is cultivar-dependent, as well as the BCA beneficial effects. Indeed, *Bs* PTA-271 was effective on the protection of Chardonnay against Np-Bt67, while *Ta* SC1 alone or combined with *Bs* PTA-271 was effective to protect Tempranillo against Np-Bt67 (80 and 90%, respectively). Authors additionally highlighted a common metabolic feature for both protected cultivars and suggested that plant metabolism conditions both pathogen infection and the beneficial effects of BCA.

In the present study, the same leaf samples as those used by Leal et al. (2021b) were deeply analyzed by RNA-seq, to further study the plant molecular changes associated with both (1) the infection by Np-Bt67, and (2) the protection induced by *Bs* PTA-271 and/or *Ta* SC1.

In **Chardonnay plants infected with Np-Bt67**, **2** up-regulated genes encoding for a **carotenoid cleavage dioxygenase** and a putative receptor-like protein kinase are associated to Chardonnay disease expression. In good accordance, the predominant functions (GO terms) impacted in the leaves of Np-Bt67 infected Chardonnay plants involved dioxygenase and oxidoreductase activities, in relationship with pigment production (carotene and carotenoid biosynthesis), hormonal balance (terpene /

isoprenoid pathway and cellular lipidic catabolic processes) and hydrocarbon metabolic processes (among which carbon-oxygen lyase activity, acting on phosphatases). Indeed, carotenoids in plants are responsible for the biosynthesis of some phytohormones such as abscisic acid (ABA) and the strigolactones through the isoprenoid pathway (Walter and Strack 2011). The oxidative cleavage of carotenoids is catalyzed by enzymes from the dioxygenase family (CCD, carotenoid cleavage dioxygenase), that later initiate the first step of ABA biosynthesis pathway (Zhang et al. 2015). The ABA phytohormone is not only important to mediate plant adaptation to abiotic stress, but it is also described as playing roles in plant immunity (Cao et al. 2011). The second category of upregulated genes upon Np-Bt67 infection in Chardonnay, involved a putative receptor-like protein kinase. **Receptor-like kinases (RLKs)** play critical roles in the regulation of plant developmental processes, signaling networks and disease resistance (Ye et al. 2017). As membrane-localized receptors, RLKs perceive extracellular stimuli through an extracellular ligand-binding domain, then transduce the signal by phosphorylating substrates through a cytoplasmic kinase domain (Jose et al. 2020). Interestingly, among the GO terms impacting leaves of Chardonnay plants infected with Np-Bt67 are hydrocarbon metabolic processes that involve a carbon-oxygen lyase activity acting on **phosphatases**. Indeed, ABA signaling pathways is initiated by a physical inactivation of phosphatases by ABA, allowing further ABA signal transduction through auto-phosphorylation processes (Umezawa et al. 2009). **In summary, ABA signaling appears to be involved in disease expression of BD on Chardonnay plants** since the two upregulated genes associated with Chardonnay disease expression lead to both ABA production and ABA signaling. Similar results were observed with the red cultivar Cabernet Sauvignon trunk when exposed to esca-associated fungal pathogens (Romeo-Olivan et al. 2022). In this study we further propose that the two genes encoding for a carotenoid cleavage dioxygenase and a putative receptor-like protein kinase could represent useful dieback markers of Chardonnay leaves exposed to *Np*-Bt67. They could also be targets to consider to better protect Chardonnay plants against Np-Bt67 since these genes are both repressed in the leaves of plants protected by *Bs* PTA-271.

In infected Chardonnay plants protected with *Bs* PTA-271, GO terms analyses indicate that the *Bs* PTA-271 protection involves changes in the phenylpropanoid biosynthetic process, aromatic amino acid family metabolic process, and secondary metabolic process. Compared to infected diseased plants, only **15** genes are

downregulated in protected plants, encoding for : an uncharacterized LOC104882538, an aldehyde oxidase GLOX, a subtilisin-like protease SBT1.5, a glucose-6-phosphate/phosphate translocator 2 chloroplastic, a phenylalanine ammonia-lyase like, a fasciclin-like arabinogalactan protein 2, a subtilisin like protease SBT1.9, a LDOX, a limonoid UDP-glucosyltransferase, NCED1, a serine carboxypeptidase-like 16, a 3-deoxy-D-arabino-heptulosonate-7-phosphate synthase, an uncharacterized protein At4g06744, GRIP4, and an oligopeptide transporter 4. Since the downregulation of these genes by a BCA is correlated with *Vitis vinifera* protection against *Np*-Bt67, we suggest that these genes could be additional targets to consider to better protect Chardonnay against Np-Bt67. Some of them encode for a key enzyme involved in **ABA biosynthesis** (He et al. 2018; Yao et al. 2022), namely *NCED1* (*9-cis-epoxycarotenoid dioxygenase*), whose repression directly prevents the ABA production, previously suggested to favour disease expression. Another gene also potentially related to ABA signaling is the s*ubtilin-like protease SBT1.5*, a serine protease (or subtilase) described to contribute to the regulation of cell wall structure, plant immune responses, and cell-to-cell signaling during symbiosis by suppressing host defense (Schaller et al. 2017; Xu et al. 2019). Proteases are also described to recycle the receptors required to ABA signaling (Irigoyen et al. 2014), receptors themselves stabilized by ABA (Irigoyen et al.,2014). Thus, decreasing their expression level would seriously interfere with ABA signaling. Genes linked to the **phenylpropanoid pathways and derivatives** are: the *phenylalanine ammonia-lyase-like* (*PAL*) that encodes for an enzyme involved in the biosynthesis of many phenolic compounds such as flavonoids and stilbenes (Urban et al. 2018); The *3-deoxy-D-arabino-heptulosonate-7-phosphate synthase* (*DHAP*) is the first enzyme in a series of metabolic reactions that are responsible for the biosynthesis of amino acids, like phenylalanine (substrate of PAL) (Ganson et al. 1986); *Serine carboxypeptidase-like 16* is involved in the synthesis of flavonoids, facilitating the transacylation reaction of a large variety of phenolics, acids, saponins, and other compounds (Ahmad et al. 2020); *Leucoanthocyanidin dioxygenase* (*LDOX*) is involved in the flavonoid pathway, catalyzing hydroxylation to protect plants against abiotic stress (Wang et al. 2021). Thus, a decrease in the expression level of these genes could possibly prevent the production of flavonoids, in favor of stilbenes that are described as useful secondary metabolites with antimicrobial properties to consider against Np-Bt67 (El Kattab et al. 2021). **Secondary metabolites** include terpenes, phenolic compounds and alkaloids, which activities can be modified by glycosylation, acetylation, hydroxylation, redox changes, etc. Therefore, the

contribution of *Bs* PTA-271 to repress the expression of enzymes involved in such processes could contribute to activate useful plant molecules once treated with *Bs* PTA-271, unless their repression aims to inactivate damaging molecules produced by the pathogen Np-Bt67. Genes encoding for such enzymes are: *Glyoxal oxidases* described as genes encoding for the extracellular H_2O_2-generating enzymes GLOX (Daou and Faulds 2017). The ubiquist *oligopeptide transporter 4* (*OPT4*) known to transport tetra- and penta-peptides, and peptide-like substrates such as glutathione (Pike et al. 2009); Glycosyltransferases, like *limonoid UDP-glucosyltransferase*, involved in hormone homeostasis, defense responses such as detoxification processes, but also biosynthesis and modification of secondary metabolites (Huang and Hou 2009). *Fasciclin-like arabinogalactan proteins* (*FLAs*) are a subclass of arabinogalactan proteins (AGPs), which are described as plant cell wall hydroxyproline-rich glycoproteins (HRGPs) post-translationally modified by glycosylation (Showalter and Basu 2016). To date, HRGPs are designated as important to strengthen plant cell walls and contribute to plant defense reactions (Deepak et al. 2010). But the decrease in the expression level of *FLA* genes in Chardonnay plants treated with *Bs* PTA-271 suggests that a less rigid cell wall structure could favor the beneficial effects of BCA against Np-Bt67. The GO terms analyses, when comparing the infected plants protected with *Bs* PTA-271 to control plants, also point out that the beneficial effect of this BCA requires changes in macromolecules and carbohydrate metabolic processes, impacting on the biogenesis and organization of the **cell wall structure**. Looking at genes involved in carbohydrate metabolism, the *glucose-6-phosphate/phosphate translocator 2* is described to regulate and stabilize photosynthetic electron transport and carbon metabolism, and to accumulate in the plant leaves that collect sugars (Li et al. 2019). Therefore, the decrease in the expression level of this gene in infected plant protected with *Bs* PTA-271 could contribute to prevent sugar accumulation that would be more favorable to pathogen development or aggressiveness (Leal et al. 2022, review submitted to Phytopathology). **In summary, *Bs* PTA-271 beneficial effect on Chardonnay plants against BD** correlates with the downregulation of genes involved in ABA biosynthesis and phenylpropanoid pathway, especially flavonoid derivatives, as well as a downregulation of genes encoding for post-translational modifications of secondary metabolites whatever their origin. Changes in the biogenesis and organization of the plant cell wall structure also appear to assert *Bs* PTA-271 beneficial effect against Np-Bt67, in relationship with carbohydrate metabolism that require much more consideration.

Tempranillo plants infected with Np-Bt67 present much more molecular changes in their leaves (567 differentially expressed genes) than in Chardonnay plants (2 upregulated genes). GO term analyses of Tempranillo data indicate predominant transcriptomic changes for **amino acid import**, **chloroplast and photosystem related processes**, plant **responses to biotic stimulus**, and biosynthesis of **secondary metabolites**. In particular, the upregulation of ***early-nodulin-75-like*** in diseased plants, compared to control and protected plants, suggests that protein transporters are critical for disease expression. Indeed, protein transporters can redirect or control the flow of nutrients, amino acids, hormones, and many other solutes such as carbohydrates, within the plant and/or towards the pathogen to reinforce its fitness or aggressiveness due to phytotoxin production (Trotel-Aziz et al. 2019, Leal et al. Review to Phytopathology 2022). Therefore, ***early-nodulin-75-like*** represents a useful early-marker associated with Np-Bt67 disease expression in Tempranillo plants. **Altogether**, despite much more consistent changes in the infected Tempranillo cultivars compared to the Chardonnay plants, our whole data on the two infected cultivars are in agreement with several recent studies indicating that grapevine infection with a GTD pathogen induces a profound reprogramming of defense gene expression in the plant trunk and leaves to better serve pathogen expansion and/or aggressiveness (Pierron et al., 2016; Massonnet et al., 2017; Gonçalves et al., 2019; Trotel-Aziz et al., 2019; Labois et al., 2020).

In infected Tempranillo protected with *Ta* SC1, GO terms analyses indicate that *Ta* SC1 protection also correlates with changes in **cell wall formation** (syncytium formation, pectin catabolic process, cell wall modification, plant-type cell wall organization, galacturonan and pectin metabolic process), **protein quenching and expression silencing**, **lipid transport**, and **carbohydrate/polysaccharide catabolism**. GO terms analyses comparing infected plants protected with *Ta* SC1 and control plants, additionally highlighted that *Ta* SC1 beneficial effect requires changes in chloroplast related processes such as **photosynthesis and photorespiration**, and biosynthesis of **secondary metabolites**. RNA-seq analysis reveals **7 DOWNREGULATED GENES**, among which: 2 genes encoding for early-nodulin-75-like proteins, a galactinol-sucrose glucosyltransferase, a major allergen Pru av1-like, a pectin esterase 2, a basic proline-rich protein-like, and another gene encoding for a hypothetical protein. **Silencing** of transporters such as *early-nodulin-75-like proteins* is described to be linked to a

suppression of plant defense signals to allow a better colonization by beneficial microorganisms such as BCAs (Tripathi et al. 2019). **Transporters** can also redirect or control the flow of many nutrients (e.g. amino acids, hormones and many other solutes) to favor pathogen fitness and aggressiveness, instead of that of the host. Silencing the *galactinol-sucrose galactosyltransferase* involved in the production of galactinol and raffinose, could also enable to prevent their use as **nutrients** for pathogens (Meyer et al. 2018). The encoding allergen *Pru av1-like* is described as a lipid transfer protein (Scheurer et al. 2001) whose silencing by *Ta* SC1 is suggested to decrease Tempranillo **susceptibility to pathogen** infection. *Proline rich proteins* (*PRPs*) are other indispensable plant proteins that support several developmental processes from germination to plant death. Downregulating *PRP* genes is described as helpful to suppress **pathogen induced cell death** and to enhance the plant resistance to diseases (Yeom et al. 2012; Gujjar et al. 2019). *Pectin esterase* genes encode for proteins that catalyze the hydrolysis of pectin into pectate and methanol. In plants, they are described to play important roles in cell wall metabolism during fruit ripening, cell wall extension during pollen germination and can vary in plant response to pathogens (Liu et al. 2018). The silencing of *pectin esterase* genes by *Ta* SC1 is suggested to preserve **cell wall integrity** and avoid the use of cell wall components (e.g., lipid, carbohydrates, etc.) as nutrients able to favor pathogen fitness or aggressiveness. RNA-seq analysis also reveals 16 upregulated genes **in infected Tempranillo protected with *Ta* SC1**, among which: two non-specific lipid-transfer protein (nsLTPs such as P5), two expansin-like (as A4), two GDSL esterase/lipase (as At1g29670 and APG), the aspartic proteinase A1, PL1, DNA-damage-repair / toleration protein DRT100-like, organ-specific protein P4-like, probable pectate lyase 5, protein SCARECROW, PR10.7, alkane hydroxylase MAH1, homeobox-leucine zipper protein ATHB-13, and pectin esterase. Most of these genes encode for substances that confer resistance to biotic and abiotic stresses, with antifungal and antimicrobial potential. For instance, gene encoding for non-specific Lipid Transfer Proteins (*nsLTPs*) are small basic proteins able to (1) bind and transport a variety of hydrophobic molecules, and to (2) work in synergy with other antimicrobial peptides such as defensins and thionines, thus taking part to a greater a **network of immunologically active proteins** (Missaoui et al. 2022). Genes encoding for GDSL esterase/lipases (GELPs) are also overexpressed by *Ta* SC1 (*GDSL esterase/lipase At1g29670* and *GDSL esterase/lipase APG*). GELP proteins represent a variety of lipolytic enzymes that hydrolyze diverse lipidic substrates including thioesters, aryl esters, and phospholipids.

They play an important role in vegetative and reproductive development, plant metabolism, and especially plant-environment interactions, like **microbiome interactions** (Chen et al. 2022). Other proteins encoded by *expansin like* genes can be produced by *Trichoderma species* to rapidly induce the **extension of plant cell walls** (Brotman et al. 2008; Marowa et al. 2016); Bacteriocins, such as putidacin L1 (encoded by *PL1*) are **proteic toxins**, that, when over-expressed *in planta*, provide an effective resistance against microbial pathogens (Rooney et al. 2019, 2020); **PR-10 proteins** are suggested as small non-specific binders to different kind of ligands such as a plant hormone, but also to several ligands creating then another molecule in its conformation, in order to promote plant development or defense systems (Lebel et al. 2010). Aspartic proteinase A1 functions are still unclear, however, their involvement in **protein turn-over** could be useful **to control hormonal signaling pathways** and improve defenses against phytopathogens (Simões and Faro 2004; Cheung et al. 2020). Similarly, the *homeobox-leucine zipper protein ATHB-13* encodes for a **transcription factor** (TF) whose function in development is largely unknown, despite the fact that TFs are known as proteins controlling molecular regulations (Ribone et al. 2015). **Relationship with hormones** needs further investigation since proteins encoded by *scarecrow* genes are involved in the complex regulation of hormone biosynthesis, that largely contribute to plant defense against pathogens, herbivores, and weeds (Wang et al. 2019, Yang et al. 2021; Sanchez et al. 2019). **Cytochrome P450s** (CYPs) are other **versatile enzymes involved in multiple processes** of plant growth and development, thus playing an essential role in stress response. CYPs can protect plants from stresses through the biosynthesis and regulation of hormones, fatty acids, sterols, cell wall components, biopolymers, and several other defense compounds (terpenoids, alkaloids, flavonoids, furanocoumarins, glucosinolates, allelochemicals) (Pandian et al. 2020; Samuels et al. 2008). For instance, *Alkane hydroxylase MAH1* encodes for a CYP450 involved in the formation of secondary alcohols and ketones in stem **cuticular wax**, to better protect the plant tissues from environmental stresses. Tempranillo plants protected with *Ta* SC1 can also induced-changes in **cell wall composition** (i.e. cellulose, hemicellulose, pectin and lignin) by over-expressing a gene encoding for P4-like organ-specific protein (Wan et al. 2021). Finally, *Ta* SC1 upregulates both the DRT100-like proteins suspected to have significant roles in **DNA-damage-repair/toleration** (Fujimori et al. 2014), and gene encoding for the probable pectate lyase 5 proteins (*Pectate lyase gene*) mediating the maintenance of normal **cell division through auxin signaling** pathway (Sun et al. 2018;

Leng et al. 2017). **In summary, *Ta* SC1 beneficial effect on Tempranillo plants against BD** correlates with: (1) the **silencing of many transporters** suggested to prevent the use of nutrients by pathogens as reported by Esparza-Reynoso et al. (2021); (2) the **preservation of cell wall integrity and extension** suggested (2a) to prevent the use of cell wall components as nutrients to favor pathogen fitness or aggressiveness, but also (2b) to better protect the plant tissues from environmental stresses (hormonal production of cuticular wax, changes in cell wall composition); (3) the **preservation of cell division** (possibly through auxin signaling) suggested to suppress pathogen induced cell death ; (4) **a network of immunologically active proteins**, among which nsLTPs, proteic toxins, proteinases, but also different TF or assimilated (PR-10 proteins), whose relationship needs further investigations with hormone signalling pathways and DNA-damage-repair/toleration as reported by Moran-Diez et al. (2021); (5) **microbiome interactions.** Compared to *Bs* PTA-271 beneficial effect on Chardonnay plants against BD, **much more changes are thus induced** by the beneficial effect of *Ta* SC1 in the leaves of infected Tempranillo, **probably because of the endophytic location of *Ta* SC1, forced thus to exploit the same "ecological niche" as the pathogen *N. parvum* Bt67.** They are thus **suspected to compete for the same space and nutrients**, which induce a highest number of systemic molecular changes inside Tempranillo leaves.

4.5. Conclusion

This study reports the transcriptomic analyses of artificially infected grapevine cultivars differentially protected by distinct BCA, simultaneously. Compared to recent publications investigating too BCA effects against GTD pathogens, our results provide new insight on the molecular changes associated with either (1) the infection by Np-Bt67 in Chardonnay and Tempranillo, or (2) their BCA-protection against this pathogen.

Considering the infection side, Chardonnay plants infected with *Np*-Bt67 over-expressed genes involved in ABA production or signaling, while the changes in infected Tempranillo plants concern amino acid import, chloroplast and photosystem related processes, plant responses to biotic stimulus, and biosynthesis of secondary metabolites.

Our study also provides deep insights on the protection induced by *Bs* PTA-271 in Chardonnay, and *Ta* SC1 in Tempranillo. Protection with *Bs* PTA-271 in Chardonnay targets genes related to ABA biosynthesis, phenylpropanoid pathways and secondary metabolites, and cell wall structure/organization in relationship with carbohydrate

metabolism that requires much more consideration. Protection with *Ta* SC1 in Tempranillo requires a larger number of changes, probably because of *Ta* SC1 location in the same "ecological niche" as the pathogen Np-Bt67, thus forcing them to compete in order to ensure each actor survival. In brief, *Ta* SC1 beneficial effect on Tempranillo plants against BD correlates with many changes related to transporters, cell wall integrity and extension, cell division and pathogen induced cell death, multidirectional active proteins, and microbiome interactions.

Comparative studies with other cultivars and pathogens, might help to better decipher *Ta* SC1 beneficial effect and to better distinguish the effects of BCA from those of the plant resistance/susceptibility to infections. Further work remains now to be done on the microbiome/microbiota quality and dynamic evolution in relationship with each scenario involving our key players (1 BCA, 1 pathogen, 1 cultivar). Finally, as GTD infection are still very recurrent in vineyards, and can be undetected for years, the insight on the molecular changes in infections by GTD pathogens, as well as the changes with the application of BCAs, will become increasingly important.

Chapter V

Evaluation of *Bacillus subtilis* PTA-271 and *Trichoderma atroviride* SC1 to control Botryosphaeria dieback and black-foot pathogens in grapevine propagation material

5.1. Introduction

Grapevine trunk diseases (GTDs), despite having been extensively studied since the early 20th century, are still considered one of the most relevant challenges for viticulture, leading to important economic losses all around the world (Bertsch et al. 2013; Gramaje et al. 2018; Mondello et al. 2018). Botryosphaeria (BOT) and Eutypa diebacks, and Esca, Petri, and black foot (BF) diseases, are the predominant GTDs currently found in vineyards (Bertsch et al. 2013; Gramaje et al. 2018; Patanita et al. 2022).

The control of GTDs is a major challenge for grape growers, nurserymen, and scientists, mostly because of their complexity compared to other grapevine diseases. It is well known that more than one GTD can be expressed within the same plant, and one of the most problematic aspects of the fungal pathogens associated with GTDs is their indeterminate latency (endophytic status) (Hrycan et al. 2020). By the time the first external symptoms appear, the grapevine wood may already be extensively damaged (Calzarano et al. 2007; Mondello et al. 2018), leaving viticulturists with few options to reduce the impact of GTDs in vineyard (Gramaje et al. 2018). Latent infections are also dangerous during nursery propagation processes, as asymptomatic planting material infected by GTDs pathogens during the various steps of nursery plant production (hydration, cold storage, grafting, callus formation, etc.) can preserve and then transmit the infections to newly planted vineyards (Gramaje et al. 2018). The nursery grapevine material is very susceptible to GTDs infections due to the several cuts and wounds made during the nursery steps (Waite et al. 2018), and there may be an unsuspected spread of infected plants if these infections are not controlled at an early stage, first in the nursery and then in the vineyard (Aroca et al. 2010; Gramaje et al. 2011, 2015, 2018; Waite et al. 2018). In this sense, the most important aspects to be covered for the sustainable management of GTDs are the improvement of the phytosanitary quality of the vines produced in nursery, and the subsequent prevention of pruning wound infections in the vineyard from the time of planting (Berbegal et al. 2020).

Investigation of biocontrol agents (BCAs) capable to forestall or at least to minimize the impact of GTDs is viewed as a research priority. In the past 10 years, many efforts have been made to develop new microbial antagonists, including fungi, bacteria and oomycetes (Andreolli et al. 2019; Berbegal et al. 2020; Daraignes et al. 2018; Halleen and Fourie 2016; Leal et al. 2021b; Mondello et al. 2019; Pertot et al. 2016; Pilar Martínez-Diz et al. 2021; Santos et al. 2016; Trotel-Aziz et al. 2019). *Trichoderma* spp. currently represent

one of the most studied fungal-based BCAs used in agriculture. *Trichoderma* have a broad range of benefits for plants (Pollard-Flamand et al. 2022; Sood et al. 2020). They can parasitize and suppress other fungi (mycoparasitism) (Ghazanfar et al. 2018; Poveda 2021), and produce several secondary metabolites, such as antibiotics (Ghazanfar et al. 2018; Sood et al. 2020) that help to control fungal pathogens. Besides pathogen control, *Trichoderma* can increase both plant and root growth by enhancing nutrient and nitrogen uptake and inducing plant systemic defenses (Poveda 2021; Sood et al. 2020). In grapevine, *T. atroviride* strains USPP-T1, USPP-T2, I-1237 and SC1 have shown good performances in the protection of grapevine against GTDs, as well as other *Trichoderma* spp. like the *T. harzianum*, *T. asperellum* and *T. gamsii* strains (Berbegal et al. 2020; Leal et al. 2021b; Pilar Martínez-Diz et al. 2021; Reis et al. 2020, 2022).

Bacillus subtilis strains have also been widely tested to be used as BCAs against fungal pathogens (Bolivar-Anillo et al. 2021; Bouchard-Rochette et al. 2022; Leal et al. 2021b; Trotel-Aziz et al. 2008, 2019). They are well known for their ability to enhance the systemic defenses of the plant against subsequent biotic stresses and promote plant growth by mobilizing nutrients, increasing their availability to the plant (Fira et al. 2018; Leal et al. 2021a, 2021b). *Bacillus subtilis* strains can also directly suppress pathogens due to the production of several secondary metabolites such as antimicrobial molecules, siderophores, lytic enzymes, and lipopeptides (Fira et al. 2018; Leal et al. 2021a, 2021b; Miljaković et al. 2020). *B. subtilis* PTA-271(Leal et al. 2021b), *B. subtilis* F62 (Russi et al. 2020) and *B. subtilis* BBG127 and BBG131 (Farace et al. 2015), have been studied and shown potential to protect grapevines against GTDs.

When performing field experiments with BCAs, the most common methods to study the quality of BCA application, are the re-isolations in petri dishes. Although these methods are relatively easy, show visually fast results, and can be cheaper than molecular techniques, they cannot ensure that the re-isolated strain corresponds to the inoculated one, and rely on molecular techniques to do so. Moreover, with these methodologies, it is not possible to accurately quantify BCAs. By using molecular techniques, especially qRT-PCR, it is possible to, not only detect BCAs presence, but also quantify the microorganism. qRT-PCR technique also allows us to distinguish between bioaugmented inoculated strains and the low-density native ones, even in complex samples such as root or soil samples (Sanzani et al. 2014; Schena et al. 2004).

Thus, the objectives of this work were (i) to assess the biocontrol effect of *Trichoderma atroviride SC1* and *Bacillus subtilis PTA-271*, alone and in simultaneous application,

against BOT and BF associated pathogens during the grapevine propagation process, and (ii) to evaluate the success of the BCA inoculation during the grapevine propagation process, using qRT-PCR methods.

5.2. Material and methods

Grapevine scion and rootstock material

Two independent nursery trials (A and B) were performed using scions of cv. Tempranillo and cuttings of 110 Richter rootstock from a commercial nursery located in Valencia province, Spain in 2021. In each trial, prior to the grafting process, 25 scion fragments and 25 rootstock fragments were randomly selected from the plant material and analyzed for the presence of GTDs pathogens. To do so, in each material type, isolations were performed from 3 cm long sections. The sections were washed with tap water, surface-disinfested using 70% ethanol and passed in a flame. Then, ten internal wood fragments per section were placed on malt extract agar (MEA) complemented with 0.5 g L^{-1} of streptomycin sulfate (Sigma-Aldrich, St. Louis, MO, USA) (MEAS) (five fragments per two Petri dishes). Plates were incubated for 10–15 days at 25 ∘C in the dark, and all evolving colonies were then transferred to potato dextrose agar (PDA). For confirmation of species identity, fungal mycelium and conidia from pure cultures grown on PDA for 15-20 days at 25 ∘C in the dark were scraped and mechanically disrupted using FastPrep-24™5G (MP Biomedicals, Santa Ana, CA, USA). Total DNA was extracted using the E.Z.N.A. Plant Miniprep Kit (Omega Bio-tek, Doraville, USA) following manufacturer's instructions. The quality and integrity of the DNA was visualized on 1% agarose gels stained with REALSAFE (Durviz S.L., Valencia, Spain). All DNA samples were stored at −20 ∘C. The identification of all isolates was performed by analysis of the internal transcribed spacer (ITS) region amplified using the fungal universal primers ITS1F and ITS4 (Gardes and Bruns 1993; White et al. 1990). Further molecular identification was then conducted for specific groups of pathogens. *Cadophora* and *Phaeoacremonium* spp. were identified by sequence analysis of the β-tubulin gene, with the primers BTCadF and BTCadR and T1 and Bt2b respectively (Glass and Donaldson 1995; O'Donnell and Cigelnik 1997; Travadon et al. 2015). Identification of Botryosphaeriaceae spp. was confirmed by analysis of the translation elongation factor *1-*α gen amplified using EF1F and EF2R primers (Jacobs et al. 2004). Identification of *Cylindrocarpon*-like asexual

morphs was confirmed by sequencing part of the *histone H3* gene with primers CYLH3F and CYLH3R.48 (Crous et al. 2004).

Biological control agent's preparation

Bacillus subtilis PTA-271

Bacillus subtilis PTA-271 (GenBank Nucleotide EMBL Accession No. AM293677 for 16S rRNA and DDBJ/ENA/GenBank Accession No. JACERQ000000000 for the whole genome), therefore *Bs* PTA-271, was isolated in 2001 from the rhizosphere of healthy Chardonnay grapevines on a vineyard located in Champagne (Marne, France) (Leal et al. 2021b; Trotel-Aziz et al. 2008). Bacterial growth started with addition of 1 ml of glycerol stock suspension to sterile Luria Bertani (LB) medium and incubating at 25-28°C. Experiments were performed when the bacterial culture was at the exponential growth phase. After centrifugation (5,000 g, 10 min), the pellet was resuspended with a sterile 10 mM MgSO4 medium adjusting the density to 10^6 cfu mL^{-1}.

Trichoderma atroviride SC1

Trichoderma atroviride SC1 (Vintec®, Belchim Crop Protection, Bi-PA; 10^{10} conidia per gram of formulated product), therefore *Ta* SC1, was suspended in water at 2g L^{-1} as indicated by the producer. The viability of the conidia in the commercial product was checked to be at a minimum of 85% before each trial, as described by Pertot et al. (2016). A serial dilution of the conidia suspension was plated on PDA (Biokar-Diagnostics, Zac de Ther, France) and the colony forming units were counted after 24-48 h incubation at room temperature.

Nursery experiments

Grapevine propagating material (cuttings of 110 R rootstock subsequently grafted with Tempranillo cultivar) were treated with *T. atroviride* SC1, *B. subtilis* PTA-271 or the simultaneous application of both BCAs at three stages of the grapevine propagating process as performed by Berbegal et al. (2020): (i) 1-day soak in suspension prior to grafting, (ii) 20-days application of suspension in sawdust at stratification, and (iii) 1-h soak of the basal parts of the plants in a BCA suspension before planting in the rooting field (Fig. 1). All propagation material was subjected to the three treatments, and the

untreated control was treated with water at all stages. Two separate experiments were performed at different times and corresponding grafted plants were transferred to different rooting fields, using four replicates per treatment with 50 plants in each replicate. The two experiments were managed separately with plant material coming from different mother blocks (Fig. 1).

Grafted plants were transfered in two different nursery-rooting fields separated by more than 10 km (experiment A was located at Llanera de Ranes and experiment B was located at Rotglà i Corberà, both in Valencia province) in 19th of May 2021 and 28th of May 2021, respectively. Both fields were arranged in a randomized complete block design with four replicates per treatment (200 plants in total). Cultural practices were performed according to the integrated pest management (IPM) guidelines and only copper compounds and wettable sulphur were applied at label dosages to control downy and powdery mildew, respectively, when required. Plants were uprooted in November 2021 and wrapped in individual perforated plastic bags to avoid cross-contamination, but also to prevent oxygen deprivation and fermentation, without exposing the cuttings to dehydration.

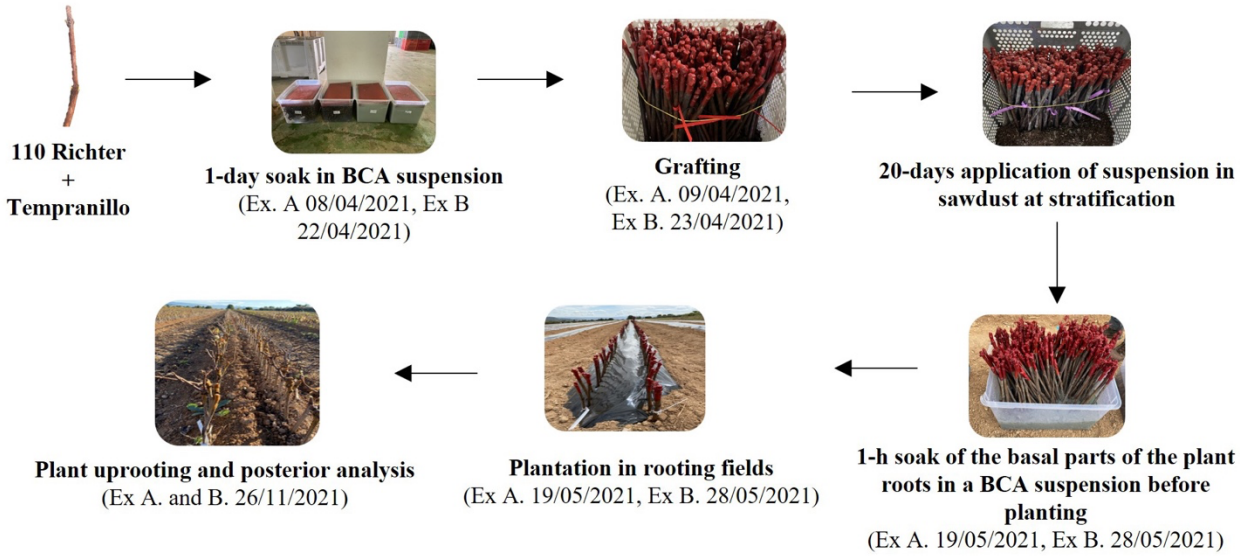

Figure 1. Process scheme of nursery experiments A and B, and BCA inoculations of all treatments (control, *Bs* PTA-271, *Ta* SC1, and both BCAs).

Fungal isolation at the end of the experiments

In each trial, 20 plants per treatment and replicate were selected randomly for fungal isolation analyses. Isolations were made from 3 cm long sections cut from three different areas: the grafting point, the basal end of the rootstock cuttings and the root system. These materials were washed, surface-sterilized and isolations were performed as described in section 2.1. Ten wood fragments per each type of area (five fragments per two Petri dishes) were analysed (30 wood fragments per plant). The 3 cm sections were washed with tap water, surface-disinfested using 70% ethanol and passed in a flame. Then, ten internal wood fragments per section were placed on malt extract agar (MEA) complemented with 0.5 g L^{-1} of streptomycin sulfate (Sigma-Aldrich, St. Louis, MO, USA) (MEAS) (five fragments per two Petri dishes). Plates were incubated for 10–15 days at 25 ∘C in the dark, and all evolving colonies were transferred to PDA petri dishes. All GTDs pathogens were identified using the techniques explained in section 2.1, and a selection of *Trichoderma* colonies (10%) were analyzed using PCR (Broeders et al. 2014) to confirm the specific *Trichoderma* strain.

Quantification of biological control agents on plant material by qRT-PCR

From the 20 plants selected for fungal isolation, 10 were randomly selected for Quantitative Reverse-Transcription Polymerase Chain Reaction (qRT-PCR) analysis of *Bs* PTA-271 and *Ta* SC1. Thus, after fungal isolation, the remaining wood tissues of the 3 cm long sections from the rootstock base were grinded in liquid nitrogen and stored at -20 °C. DNA was extracted from 200 mg of powdered wood, according to the protocol from Alfonzo et al. (2012). DNA quality was checked by agarose gel electrophoresis, and total DNA concentration was measured for each sample using the NanoDrop One spectrophotometer (Ozyme) and adjusted to 50 ng/µl. Both *Ta* SC1 and *Bs* PTA-271 were tracked by qRT-PCR using specific primers. For *Ta* SC1, *endochitinase* gene (*ech42*) primers described in Savazzinni et al. (2008) was used. For *Bs* PTA-271, a set of primers were designed targeting the *DNA polymerase III* (*dnaE*) gene. The *DNA polymerase III* gene sequence of *Bs* PTA-271 full genome was aligned with other *Bacillus dnaE* sequences retrieved from GenBank nucleotide database using Clustal W (1.82) Multiple Alignment Program. A set of primers was designed (5' – TGGATGAAGCGAGACAGCAG – 3', 3'- TCTTCACTCAGGACAACGCC- 5'), using NCBI primer designer tool (Ye et al. 2012). A standard curve was prepared to calculate

the efficiency of the primers. The curve was constructed using 7 consecutive 1:5 dilutions from genomic DNA from a *Bs* PTA-271 culture in LB medium starting with 50 ng/µl. One millilitre from each bacterial concentration was subjected to DNA extraction by means of the Wizard® Genomic DNA purification kit (Promega). Average Ct values (from duplicates) and standard deviations were calculated for each dilution. The threshold cycle (Ct) value was plotted against the log concentration of the template DNA, and the slope of the obtained regression line was used for calculating the efficiency (E) with the following equation: E = [10(−1/slope)]–1*100 (Klein 2002). The primers presented an efficiency of 99.8%.

QRT-PCR reactions were carried out in duplicate in 96-well plates in a 15 µl final volume containing Absolute Blue SYBR Green ROX mix including Taq polymerase ThermoPrime, dNTPs, buffer, and $MgCl_2$ (Thermo Fisher Scientific, Inc., Waltham, MA, United States), 280 nM forward and reverse primers, and 10 ng μL^{-1} gDNA according to the manufacturer's protocol. Cycling parameters were 15 min of Taq polymerase activation at 95°C, followed by 40 two-step cycles composed of 5 s of denaturation at 95°C and 20 s of annealing and elongation at 60°C. Melting curve assays were performed from 60 to 95°C at 0.5°C s^{-1}, and melting peaks were visualized to check amplification specificity. Elongation factor *1-alpha* (*EF1*) gene was used as reference (5'-AACCAAAATATCCGGAGTAAAAGA-3', 3'GAACTGGGTGCTTGATAGGC-5')[18]. Relative gene expression was determined with the formula fold induction: 2(−11Ct), where 11Ct = [Ct TG (US) − Ct RG (US)] − [Ct TG (RS) − Ct RG (RS)], where Ct is cycle threshold, Ct value is based on the threshold crossing point of individual fluorescence traces of each sample, TG is target gene, RG is reference gene, the US is an unknown sample, and RS is reference sample. Integration of the formula was performed by the CFX Manager 3.1 software (Bio-Rad).

Statistical analyses

The isolation of pathogens belonging to the family Botryosphaeriaceae, causal agents of BOT disease, and *Cylindrocarpon*-like asexual morphs, causal agents of BF disease, from the grafted plants was expressed as the mean percentage of infected plants and the mean percentage of positive fungal isolation from wood fragments per each group of pathogens. Statistical analyses were carried out using JASP 0.16.1 (JASP team 2022). For treatment effect, mean values were analysed using Kruskal-Wallis test. When differences in the

means were significant, Dunn post hoc test ($\alpha = 0.05$) was applied to determine which treatments were significantly different from others.

5.3. Results

Pre-existing latent infection at the nursery entrance

In the experiment A, it was not possible to detect any infection by GTDs pathogens on the 25 scions of cv Tempranillo and the 25 cuttings of 110 Richter rootstocks collected prior to the grafting process. In the experiment B, only two rootstock cuttings showed infection by *Neofusicoccum vitifusiforme,* proving that the initial infection level was very low (data not shown).

***Ta* SC1 commercial viability, recovery from trial plants and compatibility with *Bs* PTA-271**

In both trials, the percentage recovery of this strain was close to 100% (90-98%) on treated plants and wood fragments colonized by *Ta* SC1, and it was not recovered from untreated plants (data not shown). Moreover, the presence of *Bs* PTA-271 did not alter wood colonization by *Ta* SC1, since they were both > 90% (data not shown).

Impact of BCA treatments on fungal pathogen recovery at the end of the nursery process

At the end of both experiments, fungal pathogens associated with BOT (Botryosphaeriaceae spp.) and BF (*Cylindrocarpon*-like asexual morphs) were recovered from the grafted plants. Pathogens associated with Petri disease were recovered only in very few plants, thus, they were considered insufficient for statistical analysis. Pathogens associated with BF were preferably found on the roots, while those associated with BOT were preferably found on the grafting point. Therefore, the statistical comparison of treated and untreated plants was performed grouping the results of the different pathogens associated with BOT and BF diseases and their preferred areas for infection.

Impact of BCA treatments on the percentage of infected plants and percentage of fungal isolation from wood fragments at the end of the propagation process

Experiment A

At the end of the propagation process Botryosphaeriaceae isolated fungi were *N. parvum, Lasiodiplodia citricola, Diplodia seriata, N. luteum* and *L. pseudotheobromae*, and isolated *Cylindrocarpon*-like asexual morphs were *Ilyonectria liriodendri, Dactylonectria novozelandica* and *D. torresensis*. Data from the different pathogens were grouped according to the two main GTDs considered in figures 2 and 3.

The percentage of plants infected with BOT (Fig. 2) and BF (Fig. 3) associated fungi in untreated plants was 33.75% (BOT) and 18.75% (BF), in plants treated with *Ta* SC1 it was 13.75% and 11.25%, in plants treated with *Bs* PTA-271 it was 37.5% and 7.5%, and in plants treated simultaneously with both BCAs 7.5% and 2.5%, respectively. Regarding the percentage of fungal isolation from wood fragments, untreated plants presented 13.75% (BOT) and 4.25% (BF), plants treated with *Ta* SC1 8.5% and 2.75%, plants treated with *Bs* PTA-271 20.25% and 0%, and plants treated simultaneously with both BCAs 3.75% and 0.75%, respectively (Figs. 2, Fig.3). The analyses of variance revealed a significant reduction of the percentage of infected plants and the isolation from wood fragments of BOT associated pathogens in plants treated with *Ta* SC1 and plants treated simultaneously with both BCAs (Fig. 2). Plants treated simultaneously with *Bs* PTA-271 and *Ta* SC1 presented the lowest percentage of BOT infected plants and isolation from wood fragments, although this difference was not statistically different from *Ta* SC1 alone. Plants treated with *Bs* PTA-271 showed no significant differences when compared to untreated plants. Regarding fungi associated with BF, plants treated simultaneously with both BCAs was the only treatment that showed significantly lower percentage of infected plants and isolation from wood fragments, than untreated plants (Fig. 3). However, the values were not significantly different from the treatments with one BCA alone.

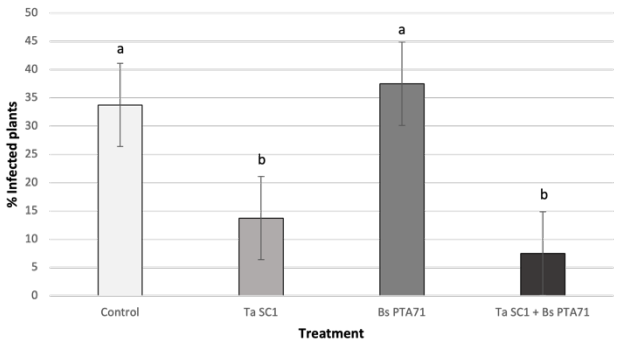

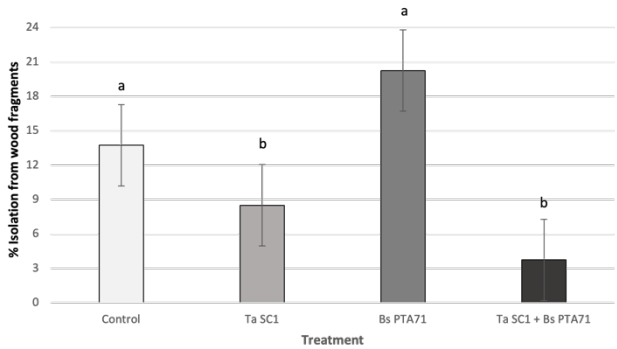

Figure 2. Percentages of plants infected with Botryosphaeriaceae spp., and percentage of isolations of Botryosphaeriaceae spp. from wood fragments observed in plants treated with *Bs* PTA-271, *Ta* SC1, simultaneously with both BCAs and untreated plants (control) in the nursery experiment A. Mean percentages are based on four replicates of 20 plants per treatment and 10 wood fragments per plant. Letters a and b represent significant differences (P-value <0.05) between treatments.

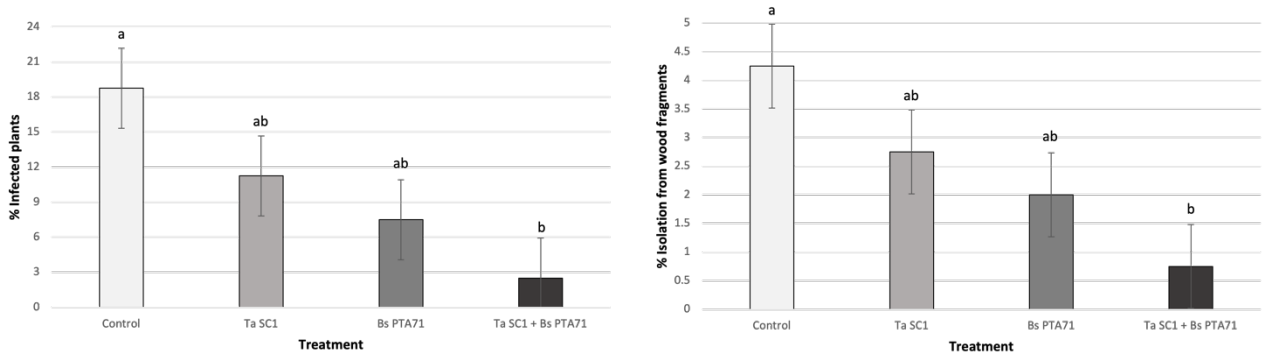

Figure 3. Percentages of plants infected with *Cylindrocarpon*-like asexual morphs, and percentage of isolations of *Cylindrocarpon*-like asexual morphs from wood fragments observed in plants treated with *Bs* PTA-271, *Ta* SC1, simultaneously with both BCAs and untreated plants (control) in the nursery experiment A. Mean percentages are based on four replicates of 20 plants per treatment and 10 wood fragments per plant. Letters a and b represent significant differences (P-value <0.05) between treatments.

Experiment B

At the end of the propagation process, Botryosphaeriaceae isolated fungi were *N. parvum, L. pseudotheobromae, D. seriata* and *N. algeriense*, and isolated *Cylindrocarpon*-like asexual morphs were *I. liriodendri, D. novozelandica* and *D. torresensis*. As for the experiment A, data from the different pathogens were grouped according to the two main GTDs considered in figures 4 and 5.

The percentage of plants infected with BOT (Fig 4.) and BF (Fig. 5) associated pathogens in untreated plants was 37.5% (BOT) and 10% (BF), in plants treated with *Ta* SC1 7.5% and 9.25%, in plants treated with *Bs* PTA-271 33.75% and 8.75%, and in plants treated

plants treated simultaneously with both BCAs 10% and 6.25%, respectively. Regarding the percentage of fungal isolation from wood fragments, untreated plants presented 17.5% (BOT) and 2% (BF), plants treated with *Ta* SC1 2.25% and 2.5%, plants treated with *Bs* PTA-271 16.5% and 1.75%, and plants treated plants treated simultaneously with both BCAs 3% and 2%, respectively (Fig. 4 and Fig. 5). The analyses of variance revealed significant reduction of the percentage of infected plants and the fungal isolations from wood fragments of BOT associated fungi in plants treated with *Ta* SC1 and plants treated simultaneously with both BCAs. Plants treated with *Ta* SC1 presented the lowest percentage of BOT infected plants and isolation from wood fragments. Plants treated with *Bs* PTA-271 showed no significant differences when compared to untreated plants (Fig. 4). Regarding fungi associated with BF, there was not a statistically significant reduction of the percentage of infected plants or the percentage of fungal isolation from wood fragments with any treatment (Fig. 5).

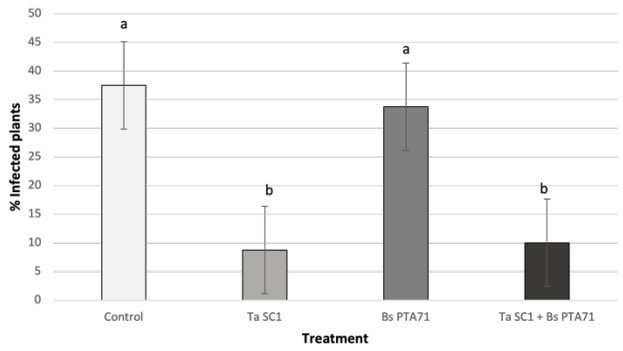

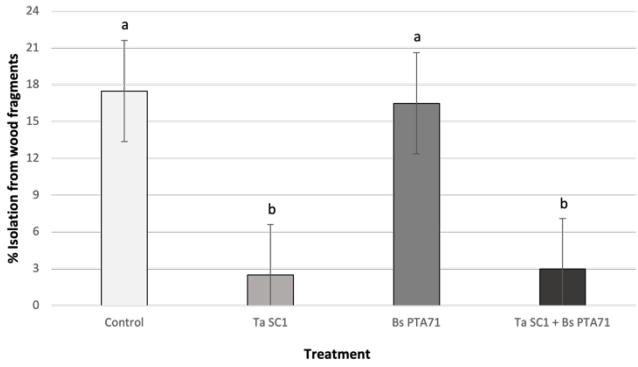

Figure 4. Percentages of plants infected with Botryosphaeriaceae spp., and percentage of isolations of Botryosphaeriaceae spp. from wood fragments observed in plants treated with *Bs* PTA-271, *Ta* SC1, simultaneously with both BCAs and untreated plants (control) in the nursery experiment B. Mean percentages are based on four replicates of 20 plants per treatment and 10 wood fragments per plant. Letters a and b represent significant differences (P-value <0.05) between treatments.

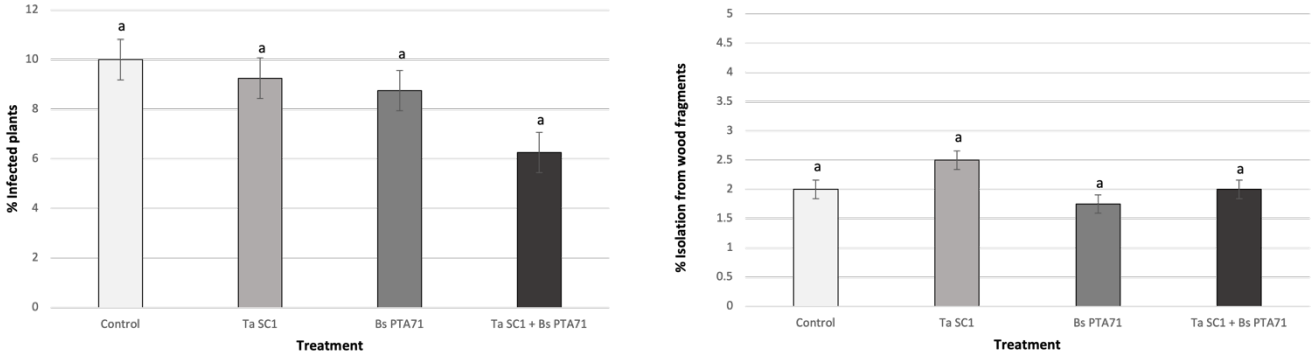

Figure 5. Percentages of plants infected with *Cylindrocarpon*-like asexual morphs, and percentage of isolations of *Cylindrocarpon*-like asexual morphs from wood fragments observed in plants treated with *Bs* PTA-271, *Ta* SC1, simultaneously with both BCAs and untreated plants (control) in the nursery experiment B. Mean percentages are based on four replicates of 20 plants per treatment and 10 wood fragments per plant. Letters a and b represent significant differences (P-value <0.05) between treatments.

BCA detection by qRT-PCR at the end of the propagation process

Since *Bs* PTA-271 is more often recovered from roots, and *Ta* SC1 more often recovered from the rootstock and grafting point, the molecular analysis was performed with wood sections from the base of the rootstock, in order to facilitate the simultaneous detection of both BCAs. In both experiments, *Ta* SC1 and *Bs* PTA-271 were detected in every treated plant, and in untreated plants, neither *Ta* SC1 nor *Bs* PTA-271 were detected (Fig. 6 and Fig. 7).

Experiment A

In experiment A (Figure 6), plants treated with *Bs* PTA-271 presented 2.65-fold more *Bs* PTA-271 than the untreated plants, and plants treated simultaneously with both BCAs presented 3.96-fold more *Bs* PTA-271 than the untreated plants. Plants treated only with *Ta* SC1 showed similar quantity of *Bs* PTA-271 as the control, showing no signs of crossed contamination. Regarding *Ta* SC1, plants treated with *Ta* SC1 presented 13.1-fold *Ta* SC1 than the untreated plants, and the plants treated simultaneously with both BCAs showed 12.2-fold *Ta* SC1 than the untreated plants. Plants treated with only *Bs* PTA-271 showed similar quantity of *Ta* SC1 as the control, showing no signs of crossed contamination.

Experiment B

In experiment B (Figure 7), plants treated with *Bs* PTA-271 presented 2.5-fold more *Bs* PTA-271 than the untreated plants, and plants treated simultaneously with both BCAs presented 3.2-fold more *Bs* PTA-271 than the untreated plants. Plants treated only with *Ta* SC1 showed similar quantity of *Bs* PTA-271 as the control, showing no signs of crossed contamination. Regarding *Ta* SC1, plants treated with *Ta* SC1 presented 29.09-fold more *Ta* SC1 than the untreated plants, and the plants treated simultaneously with both BCAs showed 12.48-fold more *Ta* SC1 than the untreated plants (Fig. 7). Plants treated only with *Bs* PTA-271 showed similar quantity of *Ta* SC1 as the control, showing no signs of crossed contamination (Fig. 7).

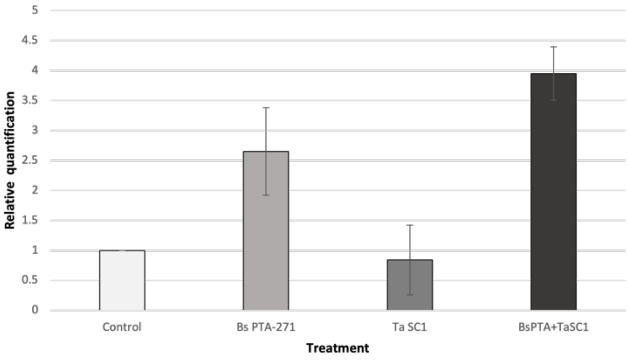

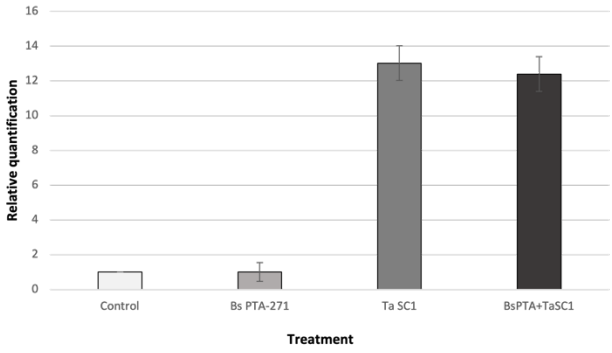

Figure 6. Relative quantification of *Bs* PTA-271 (a) and *Ta SC1* (b), in experiment A on plants treated with *Bs* PTA-271, *Ta* SC1 and simultaneously with both BCAs. The quantification of each BCA is in comparison with untreated plants (Control) that represents 1x.

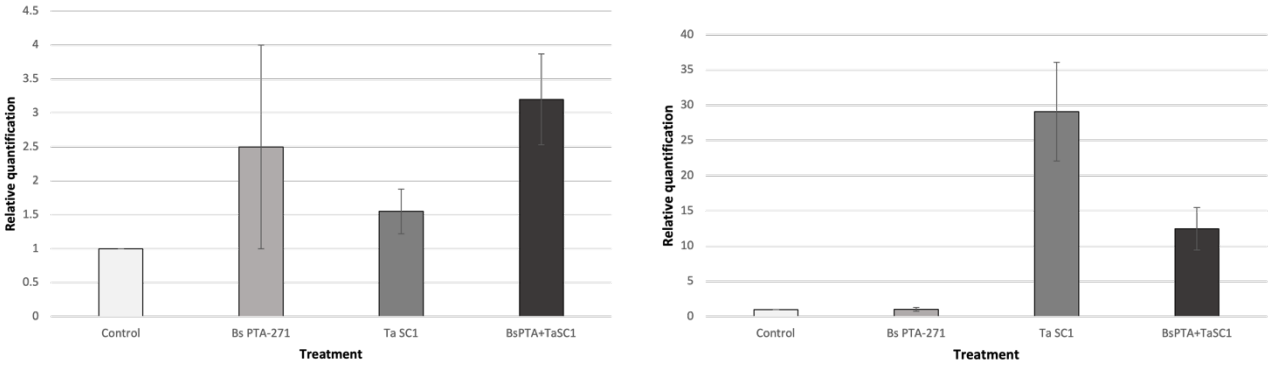

Figure 7. Relative quantification of *Bs* PTA-271 (a) and *Ta SC1* (b), in experiment B on plants treated with *Bs* PTA-271, *Ta* SC1 and simultaneously with both BCAs. The quantification of each BCA is in comparison with untreated plants (Control) that represents 1x.

5.4. Discussion

The aim of the current study was to investigate the biocontrol effect of *Ta* SC1 and *Bs* PTA-271, in single and simultaneous application, against BOT and BF associated pathogens, during the grapevine propagation process. Leal et al. (2021b) already evaluated the biocontrol effect of *Ta* SC1 and *Bs* PTA-271, in single and simultaneous application, against *N. parvum* Bt67 in Chardonnay and Tempranillo grapevines in controlled greenhouse conditions. Although the layout of both works can be somewhat related, nursery experiments enabled us to work upon much more realistic environmental conditions, including natural infections with GTDs pathogens, and additional microorganism interactions, delivering much more truthful results.

It is well known that the grapevine grafting process leads to an increased risk of infection by GTDs pathogens due to the several cuts and wounds produced during this process, by the use of grafting machines and scissors infected with pathogen spores, and during callusing (subjected to high temperature and humidity) and field rooting phases (Gramaje

and Armengol 2011; Gramaje et al. 2018; Waite et al. 2018). It is also during the propagation process that grapevine acquires the first GTDs pathogens infections, that will progress in the plant, leading to the appearance of GTDs symptoms, years later (Fontaine et al. 2016). For this reason, when performing experiments with nursery grapevines, it is not possible to detect GTDs symptoms, since the infections are recently acquired (Gramaje and Armengol 2011). In fact, in our nursery experiments, prior to the grafting process, the infection levels of GTDs in the plant material were zero or almost negligible, with only one pathogen, *N. vitifusiforme* found in experiment B. However, at the end of the propagation process, the diversity of GTDs pathogens recovered from untreated plants increased significantly. Gramaje et al. 2022 studied the temporal dynamics of fungal microbiome in rootstocks during the propagation process, and concluded that during the process, the abundance of plant pathogens largely increases, and *Neofusicoccum* genus was found as a persistent taxon in different plant material, in agreement with our results. In both experiments, BOT and BF associated pathogens were prevalent, emphasizing the importance of trying to contain these early infections in the propagation process, to avoid BOT and BF symptoms development later in the vineyard, which have been reported as some of the most common GTDs worldwide (Gramaje and Armengol 2011; Gramaje et al. 2018; Guerin-Dubrana et al. 2019; Mondello et al. 2018).

The colonization of the BCAs *Ta* SC1 and *Bs* PTA-271, alone or simultaneously, in treated plants, was successful in both experiments, with higher quantities of the BCAs in treated plants, compared to untreated plants. This was concluded using, for the first time in nursery field experiments, the qRT-PCR methodology, applied to wood samples collected from the rootstock base. qRT-PCR has the sensitivity and accuracy necessary to detect specific bioaugmented strains of microorganisms, lacking in the traditional PCR technique, and can be used to monitor BCA population changes over a period of time, representing the future of pathogens and BCA detection (Farace et al. 2015; Russi et al. 2020).

In both experiments, plants treated with *Ta* SC1 presented significantly less percentage of infected plants and percentage of fungal isolations from wood fragments, of BOT associated pathogens, compared with untreated plants. Berbegal et al. (2019), also proved this effect during the propagation process. Concerning BF associated pathogens, plants treated with *Ta* SC1 showed no significant differences in neither the percentage of infected plants nor the percentage of isolation from wood fragments, when compared to the untreated plants. In experiment B, this is most likely, due to the initial lower

percentage of infected plants (untreated plants presented 10%, compared to 18% in experiment A). However, it is known that *Trichoderma* spp., as any other BCA present inconsistencies in its biocontrol effect, depending not only on the types of pathogens, but also on the environmental conditions (temperatures, relative humidity, surface wetness, gases, and air movement), plant cultivar metabolism, and other present microorganisms. In fact, several studies have shown the lack of effect of *Trichoderma* spp. against BF associated pathogens (Berbegal et al. 2020; Berlanas et al. 2018; Pilar Martínez-Diz et al. 2021; Van Jaarsveld et al. 2021).

Focusing now on *Bs* PTA-271 effect, several authors have previously pointed out a positive effect of *B. subtilis* to control infections by BOT associated fungi (Alfonzo et al. 2009; Bertsch et al. 2013; Ferreira et al. 1991; Russi et al. 2020). More specifically, Trotel-Aziz et al. (2019) and Leal et al. (2021b) had already shown the beneficial effect of *Bs* PTA-271 in reducing the symptoms of one BOT associated fungus (*N. parvum*) in grapevine cv. Chardonnay but could not detect the same positive effect in the cv. Tempranillo. Corroborating with the previous findings, the treatments with *Bs* PTA-271 did not reduce either the percentage of infected plants or the percentage of fungal isolation from wood fragments of BOT associated fungi.

In contrast, it is noteworthy to highlight that *Bs* PTA-271 showed promising effects against BF associated fungi. Indeed, in experiment A, plants treated with *Bs* PTA-271 presented a reduced percentage of infected plants, and percentage of isolation from wood fragments of BF associated fungi, when compared with untreated plants, although in experiment B it was not possible to detect any significant difference. These results are promising when considering that BF pathogens are particularly difficult to manage due to many parameters influencing its development, such as soil nature, but also environmental and plant stress factors such as the soil mineral deficiency, poor drainage, soil compaction, heavy crop loads on young plants, poorly prepared soil, and improper plant holes (Halleen and Crous 2006). More importantly, during the grapevine propagation process and especially at the time of planting, the susceptible basal ends of most of the nursery cuttings are partly or even fully exposed, since the young callus roots easily break during the planting process, resulting in additional wounds susceptible to infection by soilborne pathogens (Agusti-Brisach and Armengol 2013). The grapevine roots are therefore an area of intense infection where BF soil-borne pathogens establish a parasitic relationship with the plant. But to succeed to infect the root tissues, BF pathogens must compete with the beneficial microorganisms that make up the complex

rhizosphere microbiome for nutrients and ecological niches (Chapelle et al. 2016), explaining why this disease is so unpredictable and hard to control (Darriaut et al. 2022). Currently, no curative control measures are available to eradicate BF pathogens in nurseries, and the management of this disease involves improving the quality of grapevine planting material by maintaining healthy microbiome, but also good hygiene and wound protection. During the last decades, several studies have been carried out to find effective strategies to manage BF pathogens in nursery and established vineyard (Pilar Martínez-Diz et al. 2021; Guerin-Dubrana et al. 2019; Fourie and Halleen 2001, 2006; Halleen et al. 2007), and a treatment with *Bs* PTA-271 could be a potential effective way to reduce the infection by BF associated fungi during the grapevine propagation process.

For both BOT and BF associated pathogens, one BCA (*Ta SC1* or *Bs* PTA-27), when well selected, could be the basic and simplest way to reduce infections caused by these fungi. However, both BCAs presented inconsistencies, and only showed a beneficial effect against Botryosphaeriaceae spp. (*Ta* SC1) or *Cylindrocarpon*-like asexual morphs (*Bs* PTA-271). The simultaneous application of *Ta SC1* and *Bs* PTA-271 presented a significant decrease in the percentage of infected plants and the percentage of isolation from wood fragments, for both Botryosphaeriaceae spp., and *Cylindrocarpon*-like asexual morphs, when compared to untreated plants, but only observed in experiment A. Simultaneous applications of BCAs have already been indicated as a possible effective strategy to overcome inconsistent control of plant pathogens in vineyards (Magnin-Robert et al. 2013; Pilar Martínez-Diz et al. 2021; Xu et al. 2011), and literature has been reporting that the interaction of more than one BCA can improve specific disease management and promote plant development and therefore resistance (Guetsky 2002; El-Tarabily and Sivasithamparam 2006; Leal et al. 2021b; Magnin-Robert et al. 2013; Weller 1988; Yobo et al. 2011). However, further research is necessary to recommend the benefits of the simultaneous applications of *Ta* SC1 and *Bs* PTA-271 in grapevine nurseries.

5.5. Conclusion

The results obtained in this study showed a promising biocontrol potential of treatments with *Bs* PTA-271 and *Ta* SC1 against BOT and BF pathogen infections during the grapevine propagation process of cv. Tempranillo. Alone, *Ta* SC1 confirmed its effectiveness to reduce the percentage of infected plants with BOT associated pathogens

and the percentage of isolation from wood fragments, and *Bs* PTA-271 demonstrated, for the first time, effectiveness to reduce infections caused by BF associated pathogens during the propagation process. In one of the experiments, the simultaneous application of both BCAs presented a significant decrease in the number of infected plants and the number of infected wood fragments for both groups of pathogens.

In our study, qRT-PCR techniques were used for the first time in grapevine nursery experiments, enabling accurate quantification of the inoculated BCAs, confirming the successful colonization by BCAs in treated plants, and the lack of crossed contaminations between treatments.

Since the pathogen inoculum of GTDs pathogens can be strongly affected by environmental factors, further research is still needed to cover as many changing conditions as possible in order to finally erase the variability of such beneficial results in field conditions. Nevertheless, these beneficial biological treatments, may be a relevant component of an integrated approach, using complementary management strategies to limit infection by GTDs pathogens.

Chapter VI

Effect of *Bacillus subtilis* PTA-271 and *Trichoderma atroviride* SC1 on grapevine defenses and temporal dynamics of fungal and bacterial microbiome in grapevine rhizosphere

6.1. Introduction

The rhizosphere (narrow zone of soil around plant roots and influenced by root secretions) is where soil-borne pathogens and plant beneficial microorganisms exert influences on the growth and health of plant hosts (Raaijmakers et al. 2009; Liu et al. 2014). Soilborne plant pathogens can be a major limitation in yield production more recalcitrant to management and control compared to pathogens attacking the above-ground parts of the plant (Bruehl 1987). Microorganisms that adversely affect plant growth and health are the pathogenic fungi, oomycetes, bacteria, and nematodes (Raaijmakers et al. 2009; Li et al. 2021). Bacteria require wounds or natural openings to penetrate the plant and cause infections, and most nematodes in soil are free-living, although some can parasitize plant roots (Siddiqui et al. 2012; Perri and Moens 2006). Fungi and oomycetes are designated as the most important soilborne pathogens. They are described to penetrate in plant roots by using cell wall-degrading enzymes and mechanical turgor pressure to colonize the root cortex (Knogge 1996). Several plant diseases and symptoms are attributed to fungal soilborne pathogens, such as a plant size reduction, stunting, drought stress and nutrient deficiencies (Raaijmakers et al. 2009). These diseases are difficult to diagnose because these symptoms mostly occur below ground (Raaijmakers et al. 2009).

Plant-associated microbiomes are diverse and complex, and there is still a limited understanding (i) of the mechanisms and factors that maintain specific plant-associated microbial communities, and (ii) of the factors that stimulate the appropriate balance microbiomes (Reinhold-Hurek et al. 2015). The grapevine is considered an excellent model plant system deeply research on fungal and bacterial microbiota (Gramaje et al. 2022), using new technologies of sequencing such as the massive next generation sequencing (NGS) that provide powerful tools to characterize and quantify microbial communities fastly with reliable identifications (Azevedo-Nogueira et al. 2022). The main benefit of such methods is the wide microbiome analysis, for each sample simultaneously, without the need to isolate the detected agents (Azevedo-Nogueira et al. 2022). These methodologies also allow to identify and relatively quantify the presence of each microbial agent (Eichmeier et al. 2018; Morales-Cruz et al. 2018; Nerva et al. 2022) and can be performed without destroying and endangering the sampled vines.

Grapevine trunk diseases (GTDs) represent one of the biggest challenges in viticulture nowadays, as there is no current control. GTDs (i.e., Eutypa dieback, Botryosphaeria

dieback, Esca complex, Cytospora canker, Phomopsis dieback, Black foot disease and Petri disease) affect mainly the perennial part of grapevines, from the trunk to shoots, and down to the root system (Nogueira-Azevedo et al. 2022). Infections happen trough pruning wounds and propagation material, with pathogen inoculum present in the soil and traveling by air. To date, the most common treatments for GTDs include few chemicals that are applied on pruning wounds in vineyards to prevent dissemination of the conidia of fungal pathogens (Sosnowski et al. 2004), associated to cultural practices in vineyard (Mondello et al. 2018) and sanitation methods in nurseries (Gramaje and Armengol 2011; Gramaje et al. 2018). However, these types of treatments cannot eradicate the pathogens once established in a vineyard or in nurseries (Calzarano et al. 2004; Gramaje and Armengol 2011).

An interesting alternative and complement to the previously cited GTD control methods in vineyard is the use of biological control agents (BCAs) such as *Trichoderma* and *Bacillus subtilis* (Mondello et al. 2018; Trotel-Aziz et al. 2019; Berbegal et al. 2020; Leal et al. 2021). *Trichoderma* species are the most used fungal-based BCA in viticulture (Harman 2006; Muckherjee et al. 2012; Waghunde et al. 2016) and are described to directly antagonize GTD pathogens aggressiveness by competition for nutrients and space, mycoparasitism, cell-wall degrading enzymes, and antibiosis (Harman 2006; Van Wees et al. 2008; Vinale et al. 2008; Pieterse et al. 2014; Waghunde et al. 2016). *Trichoderma* spp. have also been described as plant growth and defense stimulators (Harman 2006; Van Wees et al. 2008; Vinale et al. 2008; Pieterse et al. 2014; Waghunde et al. 2016; Romeo-Olivan et al. 2022; Leal et al. 2021b). *B. subtilis* spp. are also among the most frequently bacterial microorganisms tested against GTDs (Mondello et al. 2018), that produce a broad range of beneficial molecules, both to induce or elicit plant defenses (as with phytohormones precursors, lipopolysaccharides, siderophores, etc.) and to directly compete, antagonize, or alter plant pathogens or their aggressiveness (Kloepper et al. 2004; Ongena and Jacques 2008; Leal et al. 2021).

Over the years, studies have focused on the effects that inoculating plants with beneficial microorganisms has on plant health and/or plant pathogens, but few studies have looked at the impact of introducing a new biocontrol organism in rhizosphere, on the indigenous soil microbial communities (Gao et al. 2012; Gramaje et al. 2022, Kozdrój et al. 2004). In this study, we therefore investigated: 1) the effect of *B. subtilis* PTA 271 (*Bs* PTA-271) and *T. atroviride* SC1 (*Ta* SC1) inoculations in the grapevine rhizosphere microbiome;

2) the survival capacity of *Bs* PTA-271 and *Ta* SC1 over time; and finally, 3) the effect of *Bs* PTA-271 and *Ta* SC1 inoculations in grapevine defenses.

6.2. Materials and Methods

Planting Material

Dormant grapevine cuttings of rootstocks 110 Richter (110 R) were obtained from commercial nursery mother fields in Larraga (Navarra, northern Spain). Two stocks of 32 cuttings were used. Each stock was collected in different mother fields separated by 800 m. Rootstock mother vines were 12-year-old and were cultivated along the ground from a self-supporting crown approximately 40 cm above the soil surface. Within each mother field, the 16 cuttings were randomly collected from 32 plants (one cutting per plant) near the crown of the mother vine. All rootstock cuttings were 40 cm long and 1.5 cm in diameter.

Biological control agent's preparation

Bacillus subtilis PTA-271

Bacillus subtilis PTA-271 (GenBank Nucleotide EMBL Accession No. AM293677 for 16S rRNA and DDBJ/ENA/GenBank Accession No. JACERQ000000000 for the whole genome), thereafter *Bs* PTA-271, was isolated in 2001 from the rhizosphere of healthy Chardonnay grapevines on a vineyard located in Champagne (Marne, France) (Trotel-Aziz et al. 2008). Bacterial growth started with addition of 1 ml of glycerol stock suspension to sterile Luria Bertani (LB) medium and incubating at 25-28°C. Experiments were performed when the bacterial culture was at the exponential growth phase. After centrifugation (5,000 g, 10 min), the pellet was resuspended with a sterile 10 mM MgSO4 medium adjusting the density to 10^9 cfu mL^{-1}.

Trichoderma atroviride SC1

Trichoderma atroviride SC1 (Vintec®, Belchim Crop Protection, Bi-PA; 1010 conidia per gram of formulated product), therefore *Ta* SC1, was suspended in water at 2g L^{-1} as indicated by the producer. The viability of the conidia in the commercial product was checked to be at a minimum of 85% before each trial, as described by Pertot et al. (2016). A serial dilution of the conidia suspension was plated on Potato Dextro Agar (Biokar-Diagnostics, Zac de Ther, France) and the colony forming units were counted after 24-48 h incubation at room temperature.

Experiment layout

Rootstock 110R cuttings were placed in individual pots with one of two types of soil: limestone soil (8 plants) or sandy soil (8 plants). The soils were collected from vineyards with a history of severe Black-foot disease incidence in Logroño, (La Rioja, northern Spain) (Berlanas et al. 2017). Cuttings were placed in the greenhouse for 12 months to allow plant natural infections and watered every 48h. Before BCA application, rhizosphere samples were collected from all plants (T1). Plants were then inoculated with a soil drench with *Bs* PTA-271 (2 plants per type of soil), *Ta* SC1 (2 plants per type of soil), or *Bs* PTA-271 and *Ta* SC1 (2 plants per type of soil). Control plants were treated with a water soil drench. Twenty-four hours (24 hpi) and four days after the inoculation (4 dpi), leaf samples were collected from all plants to analyze expression of plant defense genes. Rhizosphere of every plant was also collected 30 days after the inoculation (T2, 30 dpi), and 90 days after inoculation (T3, 90 dpi) for microbiome analysis.

RNA Extraction and Quantitative Reverse-Transcription Polymerase Chain Reaction Analysis

Leaf samples were collected 48h post-inoculation of BCAs, ground in liquid nitrogen, and then stored at −80°C. Total RNA was extracted from 50 mg of leaf powder with Plant RNA Purification Reagent according to manufacturer instructions (Invitrogen, Pontoise, France), and DNase treated as described by the manufacturer's instructions (RQ1 RNase-Free DNase, Promega). RNA quality was checked by agarose gel electrophoresis, and total RNA concentration was measured at 260 nm for each sample using the NanoDrop One spectrophotometer (Ozyme) and adjusted to 100 ng μl^{-1}. First-strand cDNA was

synthesized from 150 ng of total RNA using the Verso cDNA synthesis kit (Thermo Fisher Scientific, Inc., Waltham, MA, United States). Polymerase chain reaction (PCR) conditions were the ones described by Gruau et al. (2015). Quantitative reverse-transcription polymerase chain reaction (qRT-PCR) was performed with Absolute Blue qPCR SYBR Green ROX Mix according to manufacturer instructions (Thermo Fisher Scientific, Inc., Waltham, MA, United States), in a BioRad C1000 thermocycler using the Bio-Rad manager software CFX96 Real-Time PCR (BioRad, Hercules, CA, United States). A set of six defense-related genes, selected for their responsiveness to pathogen or priming state induced by beneficial microorganisms (Trotel-Aziz et al. 2019), was tracked by qRT-PCR using specific primers (Table 1). Quantitative RT-PCR reactions were carried out in duplicate in 96-well plates in a 15-µl final volume containing Absolute Blue SYBR Green ROX mix including Taq polymerase ThermoPrime, dNTPs, buffer, and MgCl2 (Thermo Fisher Scientific, Inc., Waltham, MA, United States), 280 nM forward and reverse primers, and 10-fold diluted cDNA according to the manufacturer's protocol. Cycling parameters were 15 min of Taq polymerase activation at 95°C, followed by 40 two-step cycles composed of 10 s of denaturation at 95°C and 45 s of annealing and elongation at 60°C. Melting curve assays were performed from 65 to 95°C at 0.5°C s^{-1}, and melting peaks were visualized to check amplification specificity. EF1 and 60RSP genes were used as references and experiments were repeated five times. Relative gene expression was determined with the formula fold induction: 2(−11Ct), where 11Ct = [Ct TG (US) − Ct RG (US)] − [Ct TG (RS) − Ct RG (RS)], where Ct is cycle threshold, Ct value is based on the threshold crossing point of individual fluorescence traces of each sample, TG is target gene, RG is reference gene, the US is an unknown sample, and RS is reference sample. Integration of the formula was performed by the CFX Manager 3.1 software (Bio-Rad). Although the genes analyzed were considered significantly up- or down-regulated when changes in their expression were >2-fold or <0.5-fold, respectively, we still performed a statistical analysis. Control samples are cDNA from leaves of untreated plants (1× expression level).

Table 1. Primer sequences used for qRT-PCR analysis of defense-related genes (Trotel-Aziz et al. 2019).

Gene	Name	Accession number[1]	Forward primer (5′-3′)	Reverse primer (5′-3′)	Annealing temperature (°C)	Amplicon size (bp)	Efficiency of primers pairs (%)
60RSP	60S ribosomal protein L18	XM_002270599[1]	ATCTACCTCAAGCTCCTAGTC	CAATCTTGTCCTCCTTTCCT	60	166	100.0
EF1	Elongation factor 1-alpha	XM_002284888[1]	AACCAAAATATCCGGAGTAA AAGA	GAACTGGGTGCTTGATAGGC	60	164	100.0
LOX9	Lipoxygenase	NM_001281249[1]	CCCTTCTTGGCATCTCCCTTA	TGTTGTGTCCAGGGTCCATTC	60	101	90.0
PR1	Pathogenesis-related protein 1	XM_002273752[1]	GGAGTCCATTAGCACTCCTTTG	CATAATTCTGGGCGTAGGCAG	60	168	90.0
PR2	Class I beta-1,3-glucanase	NM_0012809671	TCAATGGCTGCAATGGTGC	CGGTCGATGTTGCGAGATTTA	60	155	97.2
GST1	Glutathione-*S*-transferase	NM_001281248[1]	TGCATGGAGGAGGAGTTCGT	CAAGGCTATATCCCCATTTTCTTC	60	98	90.0
PAL	Phenylalanine ammonia lyase	XM_003635637[1]	TCCTCCCGGAAAACAGCTG	TCCTCCAAATGCCTCAAATCA	60	101	92.9
STS	Stilbene synthase	NM_001281117[1]	AGGAAGCAGCATTGAAGGCTC	TGCACCAGGCATTTCTACACC	60	101	94.3

[1] *NCBI accession number.*

DNA Extraction, Sequencing and Data Analysis of the High-Throughput Amplification Assay

Genomic rhizosphere DNA was extracted from 0.5 g sample using the DNeasy PowerSoil Kit (Qiagen, Hilden, Germany), following the kit protocol. DNA yields were quantified using the Invitrogen Qubit 4 Fluorometer with Qubit dsDNA HS (High Sensitivity) Kit (Thermo Fisher Scientific, Waltham, MA, USA) and the extracts were adjusted to 10-15 ng/μL.

For fungal library preparation, the complete fungal ITS2 region was amplified using the primers ITS86F (Turenne et al. 1999) and ITS4 (White et al. 1990). Primers were modified to include the Illumina sequencing primers. PCR reactions were carried out in a final volume of 25 μL, containing 2.5 μL of template DNA, 0.5 μM of the primers, 12.5 μL of Supreme NZYTaq 2× Green Master Mix (NZYTech), and ultrapure water up to 25 μL. PCR amplifications consisted of an initial denaturation step at 95 °C for 5 min,

followed by 35 cycles of 95 °C for 30 s, 49 °C for 30 s, 72 °C for 30 s, and a final extension step at 72 °C for 10 min. Libraries were purified using the Mag-Bind RXNPure Plus magnetic beads (Omega Biotek, Norcross, GE, USA), following the instructions provided by the manufacturer. The purified libraries were pooled in equimolar amounts according to the quantification data provided by the Qubit dsDNA HS Assay (Thermo Fisher Scientific, Waltham, MA, USA). Samples were sequenced in the MiSeq platform (Illumina, San Diego, CA, USA) at the AllGenetics and Biology SL (Galicia, Spain), using a paired-end 2 × 300 bp (PE 300) sequencing and the MiSeq Reagent Kit v3 (Illumina, San Diego, CA, USA). Negative controls during library preparation and DNA extraction, and a positive control containing DNA of a grapevine rhizosphere sample (Berlanas et al. 2019) were included.

Fungal and bacterial Diversity, Taxonomy Distribution and Statistical Analysis

Alpha-diversity was calculated by analyzing the Chao1 richness and Shannon diversity in Phyloseq package. Differences in fungal alpha-diversity among stocks and nursery stages were inferred by multiple mean comparisons using Tukey's honestly significant difference range test ($p \leq 0.05$). PERMANOVA was used to infer which OTUs significantly differed in relative abundance among experimental factors after Bonferroni corrections. The relationship in OTUs composition among samples was investigated by calculating Bray Curtis metrics and visualized in PCoA plots. Good's coverage values and rarefaction curves were also calculated. All diversity analyses were made using MicrobiomeAnalyst (Chong et al. 2020). Persistent and transient microbiota were inferred using TIME (Baksi et al. 2018). Persistent fungal microbiota was defined as those taxa observed in 20% or more of the sampling times but with at least 90% of those observations being consecutive (Caporaso et al. 2011). Transient fungal microbiota was defined as those taxa observed in at least 60% of the samples, but with at most 75% of those observations being consecutive (stages of sample development) (Caporaso et al. 2011).

The identification of fungal taxa that differed in relative abundance among sampling times was performed by computing the Linear Discriminant Analysis Effect Size (LEfSe) algorithm in MicrobiomeAnalyst. The Linear Discriminant Analysis (LDA) threshold

score was set up at 1.0 and Wilcoxon p-value at 0.05. The results are displayed in a dot plot. The fungal OTUs shared among sampling times were visualized by Venn-diagram analysis (https://bioinformatics.psb.ugent.be/webtools/Venn/, accessed on: 13 January 2021). Correlation networks were computed with the SparCC algorithm to identify potential interactions between fungal genera that could represent parasitic, commensal, mutualistic or competitive relationships, using MicrobiomeAnalyst. *p*-value threshold was set up at 0.05 with 120 permutations, and the correlation threshold at 0.6.

Heatmaps were employed to visualize the abundances of GTD fungi at each sampling time using MicrobiomeAnalyst, with Euclidean as distance measure and Ward as a clustering algorithm. An ANOVA with log transforms was performed to compare the percentage abundance of each fungal genus associated with GTDs among sampling times. Normality of residuals was checked by Shapiro-Wilk's test, and homogeneity of the variance by Levene's test. Means were compared using Tukey's test ($p \leq 0.05$).

6.3. Results

Microorganisms Abundance

Fungi

Regarding the rhizosphere fungal microbiome of plants inoculated with *Bs* PTA-271, *Ta* SC1, both BCAs, and control plants, differences were found according to the applied treatment, and the time of sampling (Figure 1).

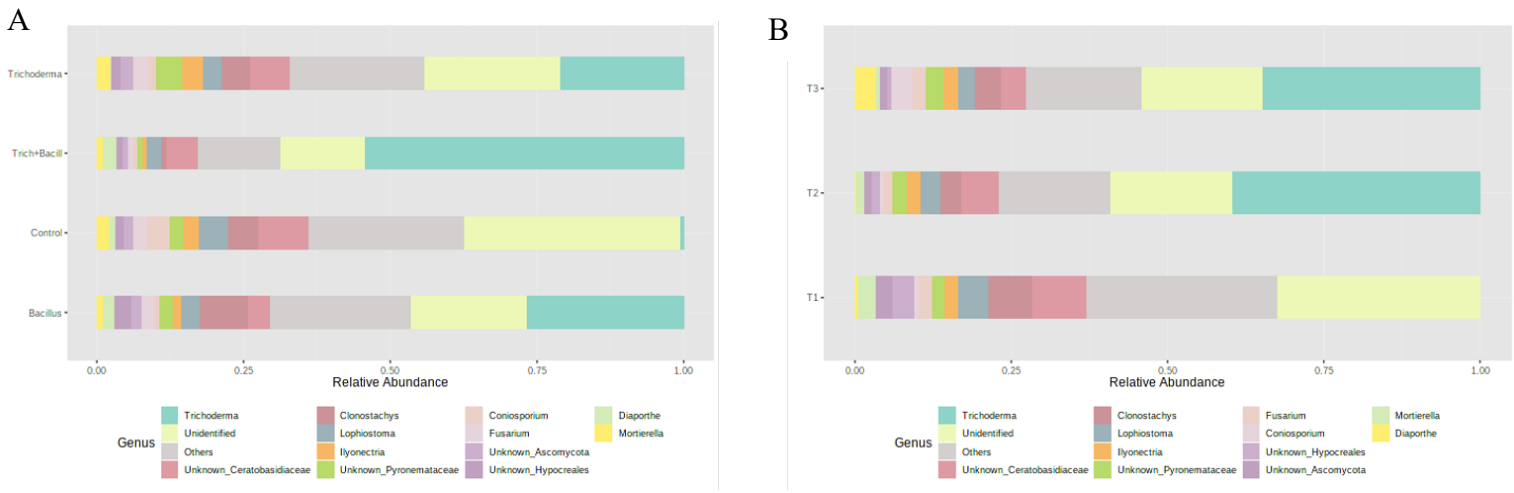

Figure 1. Fungal relative abundance comparison between (A) applied treatments (Control, *Bs* PTA-271, *Ta* SC1, *Bs* PTA-271 + *Ta* SC1), and (B) sampling times (T1, T2, T3).

As indicated by the Figure 1A, the main changes concerns *Trichoderma* spp., for which control plants presented a significant lower abundance, when compared to other treatments. However, plants inoculated with *Bs* PTA-271 alone had a considerable abundance of *Trichoderma* spp., similar to the treatment with *Ta* SC1 alone. The treatment with both BCAs showed a significantly higher abundance of *Trichoderma* spp. than the treatments with only one BCA.

Concerning sampling time (Figure 1B), *Trichoderma* spp. was undetected at T1 (before inoculation), while its abundance increased significantly at both T2 and T3. However, the abundance of *Trichoderma* spp. decreased at T3, since samples presented less *Trichoderma* spp. abundance compared to T2 samples (Figure 1B).

Bacteria

The bacterial microbiome of the rhizosphere presented more microorganisms, when compared to the fungal microbiome (Figure 2). Unlike *Trichoderma* spp., *Bacillus* spp. is not the most abundant groups of bacteria. Globally, *Rudobacte*r spp. was the most abundant bacterial group in the rhizosphere (Figure 2A). Looking at *Bacillus* spp., control plants presented a significant abundance of *Bacillus* spp., and there were no significant

differences on *Bacillus* spp. abundance, according to the treatments (Figures 2A) and the sampling times (Figure 2C). However, *Bacillus* spp. was more abundant in sandy soil, compared with limestone soil samples (Figure 2B).

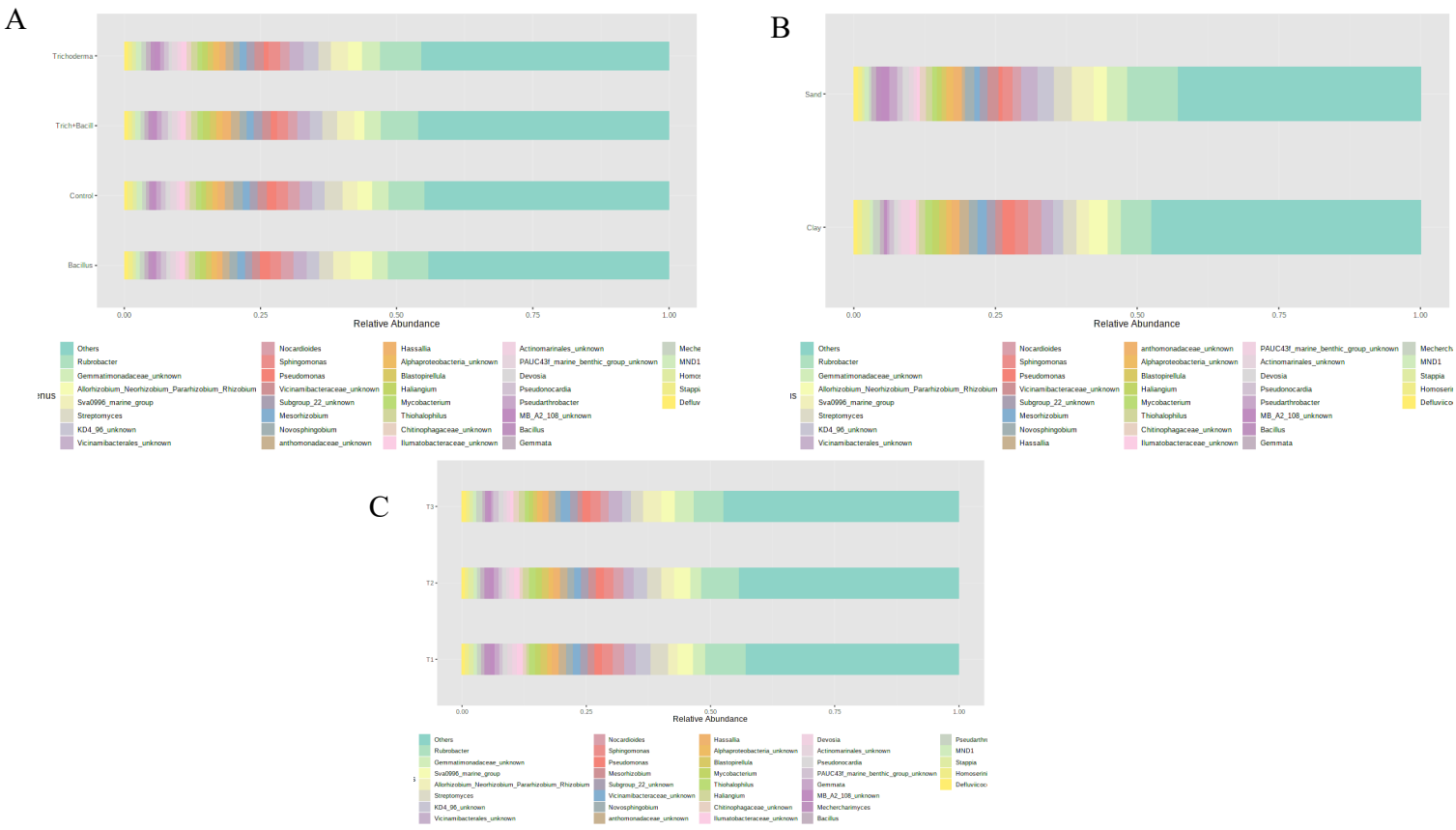

Figure 2. Bacterial relative abundance comparison between applied treatments (Control, *Bs* PTA-271, *Ta* SC1, *Bs* PTA-271 + *Ta* SC1) (A), type of soil (B) (sandy and limestone), and sampling times (T1, T2, T3) (C).

Alpha diversity

Fungi

On sandy soil there were significant differences on the diversity between the 2 compartments, roots, and rhizosphere. In case of rhizosphere, there were significant

differences between treatments and sampling time, therefore we focused our further analysis on rhizosphere only (Table 2).

Table 2. Statistical analysis of fungal alpha diversity in sandy soil samples, using Chao1 index and Shannon index. p: p-value, F: F statistics.

Sandy soil			
Dataset	Factor	Indexes	
		Chao1	Shannon
Sandy soil	Treatment	p: 0.97885; F: 0.06377	p: 0.013127; F: 3.7815
	Compartement	p: 1.0881e-36; F: 21.601	p: 3.8454e-07; F: 5.5378
	Sampling	p: 0.7041; F: 0.35216	p: 0.5345; F: 0.63066
	Treatment_Sampling	P: 0.99942; F: 0.14286	p: 0.063168; F: 1.8196
Sandy soil/Rhizosphere	Treatment	p: 0.68457; F: 0.49948	p: 0.00012458; F: 8.6653
	Sampling	p: 0.15655; F: 1.933	p: 0.025993; F: 3.9626
	Treatment_Sampling	p: 0.86101; F: 0.54219	p: 1.4285e-08; F: 11.115
Sandy soil/Root	Treatment	p: 0.13665; F: 1.9425	p: 0.68432; F: 0.49985
	Sampling	p: 0.47012; F: 0.76758	p: 0.010596; F: 5.0393
	Treatment_Sampling	p: 0.20794; F: 1.4164	p: 0.29356; F: 1.247

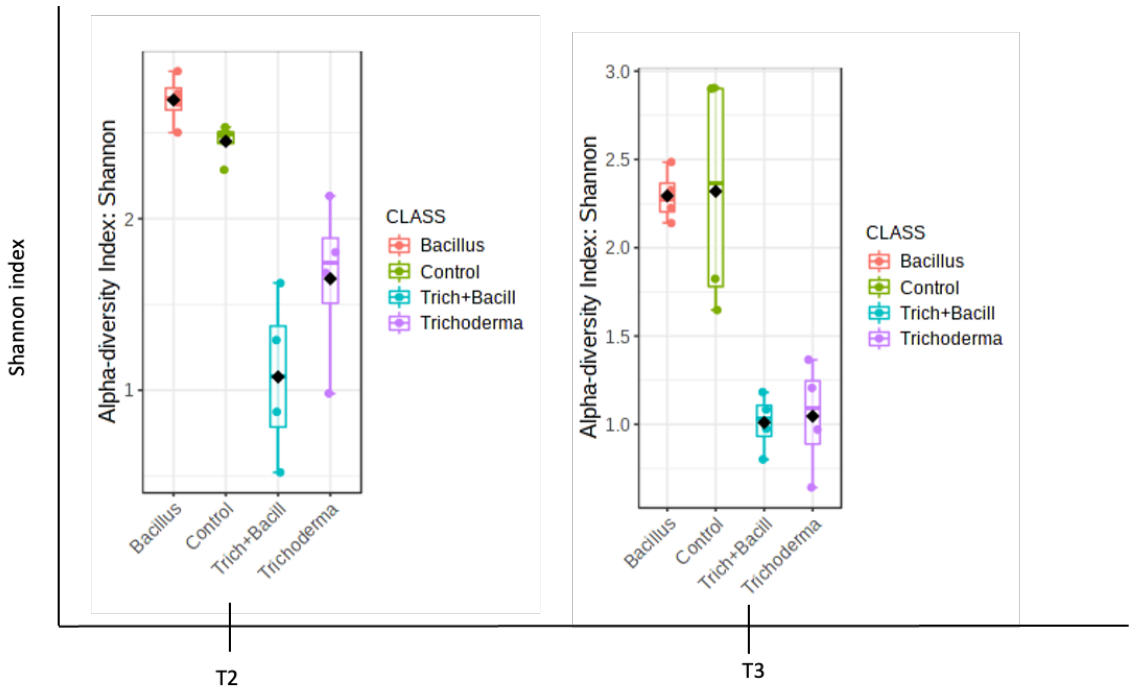

Figure 3. Differences in fungal alpha-diversity in sandy soil samples, between treatment applied (Control, *Bs* PTA-271 (*Bacillus*), *Ta* SC1 (*Trichoderma*), and *Trich* + *Bacill* (*Bs* PTA-271 + *Ta* SC1)), in sampling time T2 and T3, using Shannon index.

On sandy soil, at the sampling times T2 and T3, the treatments with *Ta* SC1 and both BCAs, presented significant lower fungal diversity than non-inoculated treatments (Figure 3).

On limestone soil there were significant differences on diversity between compartments (roots and rhizosphere). In case of rhizosphere, there were significant differences between treatments and sampling time, therefore we focused further analysis on the rhizosphere only (Table 3).

Table 3. Statistical analysis of fungal alpha diversity in limestone soil samples, using Chao1 index and Shannon index. p: *p*-value, F: F statistics.

Limestone soil			
Dataset	Factor	Indexes	
		Chao1	Shannon
Limestone soil	Treatment	p: 0.92065; F: 0.16355	p: 0.0011323; F: 5.7928
	Compartement	p: 1.7327e-37; F: 22.989	p: 4.4596e-08; F: 6.2158
	Sampling	p: 0.6081; F: 0.50009	p: 0.022458; F: 3.9554
	Treatment_Sampling	p: 0.99576; F: 0.21976	p: 0.0017627; F: 3.0531
Limestone soil/Rhizosphere	Treatment	p: 0.33803; F: 1.154	p: 7.1432e-06; F: 12.008
	Sampling	p: 7.4878e-05; F: 11.82	p: 0.018984; F: 4.3348
	Treatment_Sampling	p: 0.017008; F: 2.5468	p: 2.4087e-08; F: 10.673
Limestone soil/Root	Treatment	p: 0.19994; F: 1.6131	p: 0.31083; F: 1.2281
	Sampling	p: 0.55562; F: 0.5954	p: 0.33492; F: 1.1209
	Treatment_Sampling	p: 0.16228; F: 1.5336	p: 0.59129; F: 0.85294

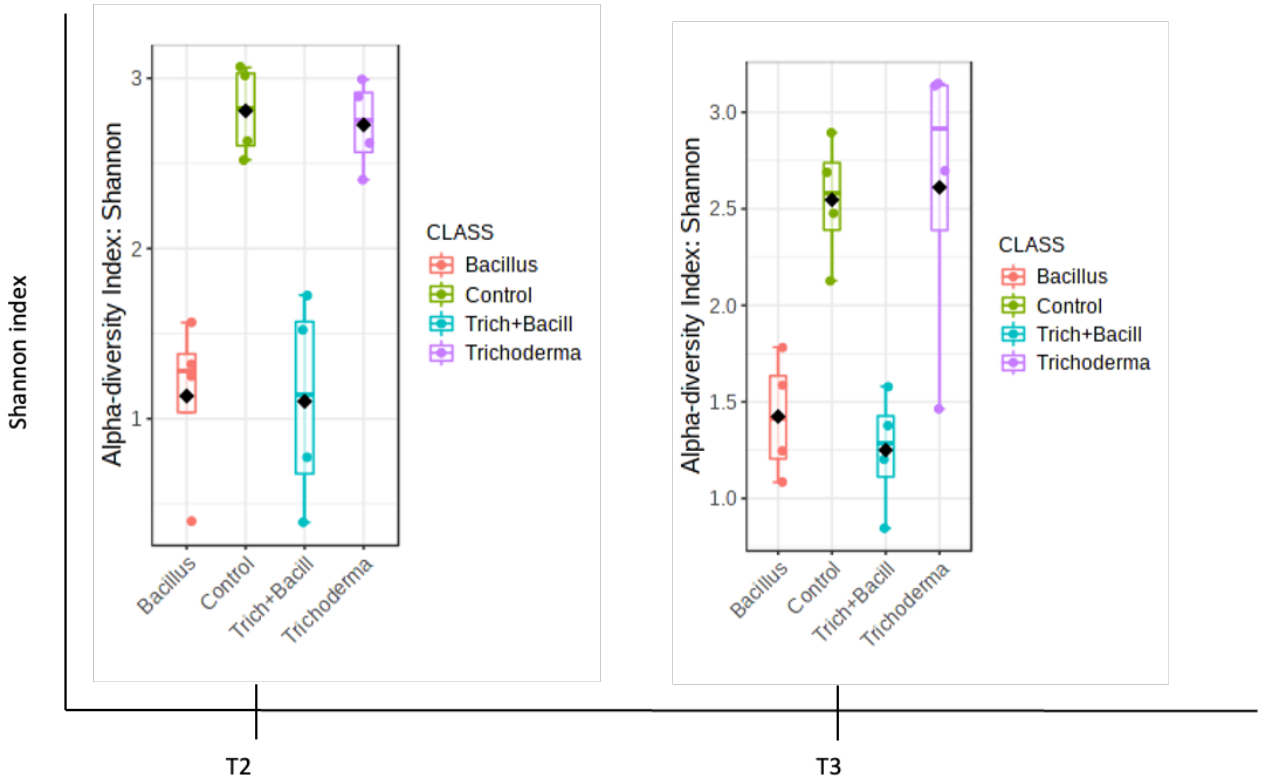

Figure 4. Differences in fungal alpha-diversity of limestone soil samples, between treatment applied (Control, *Bs* PTA-271 (*Bacillus*), *Ta* SC1 (*Trichoderma*), and *Trich* + *Bacill* (*Bs* PTA-271 + *Ta* SC1)), in sampling times T2 and T3, using Shannon index.

On limestone soil, at the sampling times T2 and T3, plants inoculated with *Bs* PTA-271 and both BCAs, presented significantly lower diversity than plants inoculated with *Ta* SC1 alone, and control plants (Figure 4.).

Bacteria

On sandy soil there were significant differences on diversity between compartments (roots and rhizosphere). In case of rhizosphere, there were significant differences between sampling times, therefore we focused further analysis on rhizosphere only (Table 4.).

Table 4. Statistical analysis of bacterial alpha diversity in sandy soil samples, using Chao1 index and Shannon index. p: p-value, F: F statistics.

Sandy soil			
Dataset	Factor	Indexes	
		Chao1	Shannon
Sandy soil	Treatment	p: 0.93156; F: 0.1467	p: 0.66954; F: 0.52005
	Sampling	p: 0.26353; F: 1.3529	p: 0.34303; F: 1.0823
	Compartement	p: 1.8697e-26; F: 21.636	p: 1.1661e-24; F: 16.964
	Treatment_Sampling	p: 0.98753; F: 0.28295	p: 0.97168; F: 0.34782
Sandy soil/Rhizosphere	Treatment	p: 0.34341; F: 1.14	p: 0.4937; F: 0.81274
	Sampling	p: 0.0039894; F: 6.2613	p: 0.0073146; F: 5.4967
	Treatment_Sampling	p: 0.059909; F: 1.986	p: 0.24222; F: 1.3425
Sandy soil/Root	Treatment	p: 0.79329; F: 0.34446	p: 0.15545; F: 1.831
	Sampling	p: 0.00024413; F: 10.064	p: 0.07751; F: 2.7083
	Treatment_Sampling	p: 0.075435; F: 1.8829	p: 0.35822; F: 1.1442

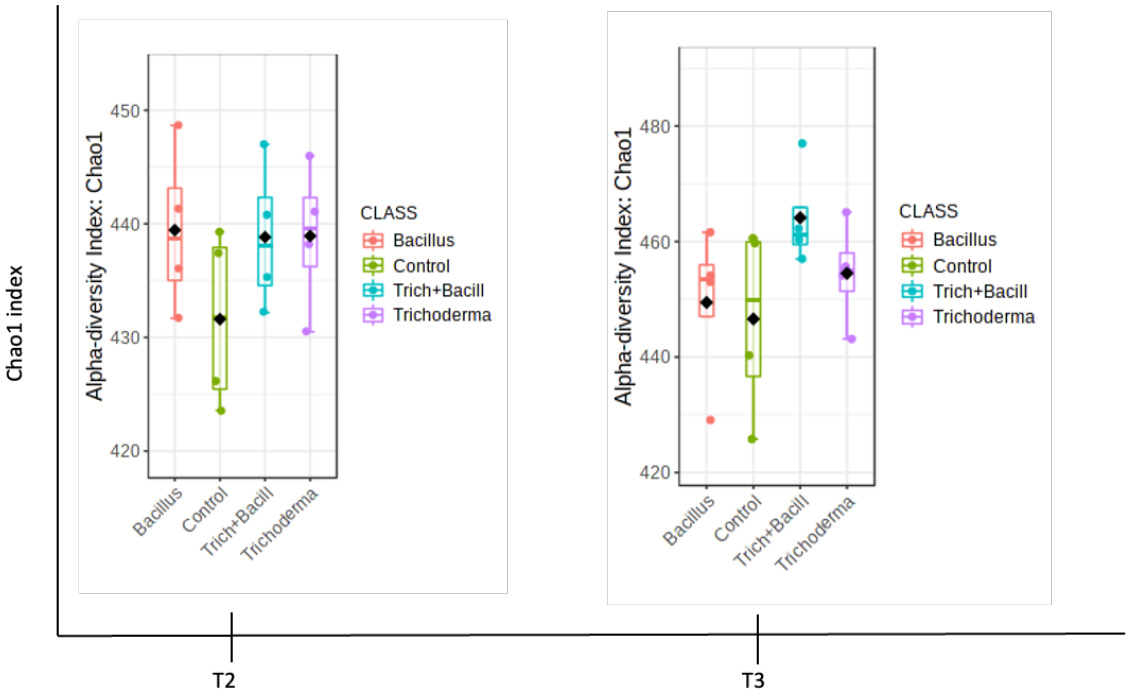

Figure 5. Differences in bacterial alpha-diversity of sandy soil samples, between treatment applied (Control, *Bs* PTA-271 (*Bacillus*), *Ta* SC1 (*Trichoderma*), and *Trich* + *Bacill* (*Bs* PTA-271 + *Ta* SC1)), in sampling times T2 and T3, using Chao1 index.

On sandy soil, at the sampling times T2 and T3, plants inoculated with any BCA presented higher bacterial diversity than control plants. Moreover, at T3, plants inoculated with both BCAs presented higher diversity than other treated plants (Figure 5).

On limestone soil there were significant differences on diversity between compartments (roots and rhizosphere). In case of rhizosphere, there were significant differences between sampling times, therefore we focused further analysis on rhizosphere only (Table 5).

Table 5. Statistical analysis of bacterial alpha diversity in limestone soil samples, using Chao1 index and Shannon index. p: *p*-value, F: F statistics.

Limestone soil			
Dataset	Factor	Indexes	
		Chao1	Shannon
Limestone soil	Treatment	p: 0.99973; F: 0.0033513	p: 0.84411; F: 0.27386
	Sampling	p: 0.58565; F: 0.53813	p: 0.22722; F: 1.5057
	Compartement	p: 3.8175e-29; F: 25.174	p: 8.9455e-22; F: 16.694
	Treatment_Sampling	p: 0.99863; F: 0.17128	p: 0.92856; F: 0.44911
Limestone soil/Rhizosphere	Treatment	p: 0.7099; F: 0.4625	p: 0.26051; F: 1.3829
	Sampling	p: 0.061759; F: 2.9641	p: 0.014797; F: 4.6336
	Treatment_Sampling	p: 0.13058; F: 1.6342	p: 0.07506; F: 1.8852
Limestone soil/Root	Treatment	p: 0.89202; F: 0.20554	p: 0.41773; F: 0.96504
	Sampling	p: 0.03358; F: 3.6632	p: 0.00012811; F: 11.01
	Treatment_Sampling	p: 0.45059; F: 1.0185	p: 0.003698; F: 3.242

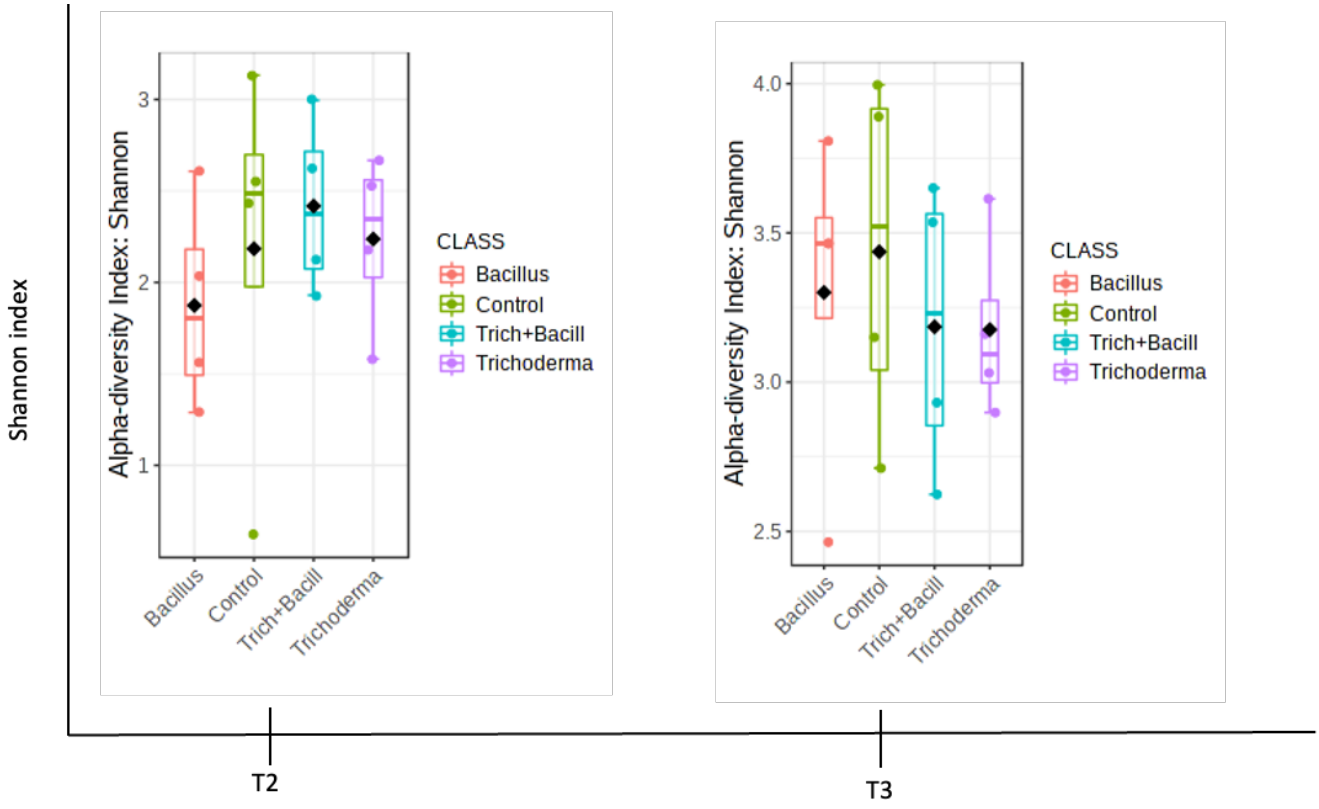

Figure 6. Differences in bacterial alpha-diversity of limestone soil samples, between treatment applied (Control, *Bs* PTA-271 (*Bacillus*), *Ta* SC1 (*Trichoderma*), and *Trich* + *Bacill* (*Bs* PTA-271 + *Ta* SC1)), in sampling times T2 and T3, using Shannon index.

On limestone soil, few differences were observed in bacterial diversity between sampling times according to the treatment. However, at T3, plants inoculated with *Ta* SC1 alone and both BCAs seem to present lower diversity when compared to control plants, and plants treated with *Bs* PTA-271 alone (Figure 6).

Microbial relationships in rhizosphere

Fungi

In sandy soil, the control plants reduced all positive relationships over time, as well as plants inoculated with *Bs* PTA-271 alone. In plants inoculated with *Ta* SC1, this reduction was not so prominent. In limestone soil, control plants presented an increase of positive relationships very accentuated at 30 dpi, however at 90 dpi both positive and negative relationships were reduced. Plants treated with *Bs* PTA-271 presented a very significant increase of positive relationships and a significant decrease of negative relationships overtime. Plants treated with *Ta* SC1 presented an increase of positive relationships at 30 dpi which then reduce at 90 dpi. Negative relationships reduced initially, were then stabilized 90 dpi. Plants treated with both BCAs had the most significant increase in positive relationships and reduction in negative relationships that improved 90 dpi (Table 6).

In sandy soil, the plants rhizosphere was mainly colonized by fungi from the genus *Clonostachys* (Out 85) and Ceratobasidiaceae (Otu 536). The genus *Fusarium* (Out 165) and Ascomycota (Otu 638) were also presented in higher quantities. Over time, control plants rhizosphere was mainly colonized by fungi from the family Ceratobasidiaceae and the genus *Fusarium*. At 30 dpi, plants inoculated with *Bs* PTA-271 did not present any dominant genus of fungi, however, at 90 dpi, the rhizosphere of these plants were mainly colonized by *Clonostachys*. In plants inoculated with *Ta* SC1 and both BCAs, *Trichoderma* (Out 490) was the main genus colonizing rhizosphere both at 30 and 90 dpi (Figure 7).

In limestone soil, the plants rhizosphere was mainly colonized by fungi from the family Ceratobasidiaceae (out 536), and the genera *Mortierella* (Out 287), *Lophiostoma* (Otu 253), and *Clonostachys* (Out 85). Control plants did not present any dominant genus at 30 dpi, while at 90 dpi they were mainly colonized by *Coniosporium* (Otu 91). Plants inoculated with *Bs* PTA-271 and both BCAs became colonized mainly with *Trichoderma* at 30 dpi, that is maintained at 90 dpi. Plants inoculated only with *Ta* SC1 did not show any dominant genus at 30 dpi, and at 90 dpi, plants were mainly colonized with *Coniosporium* (Figure 8).

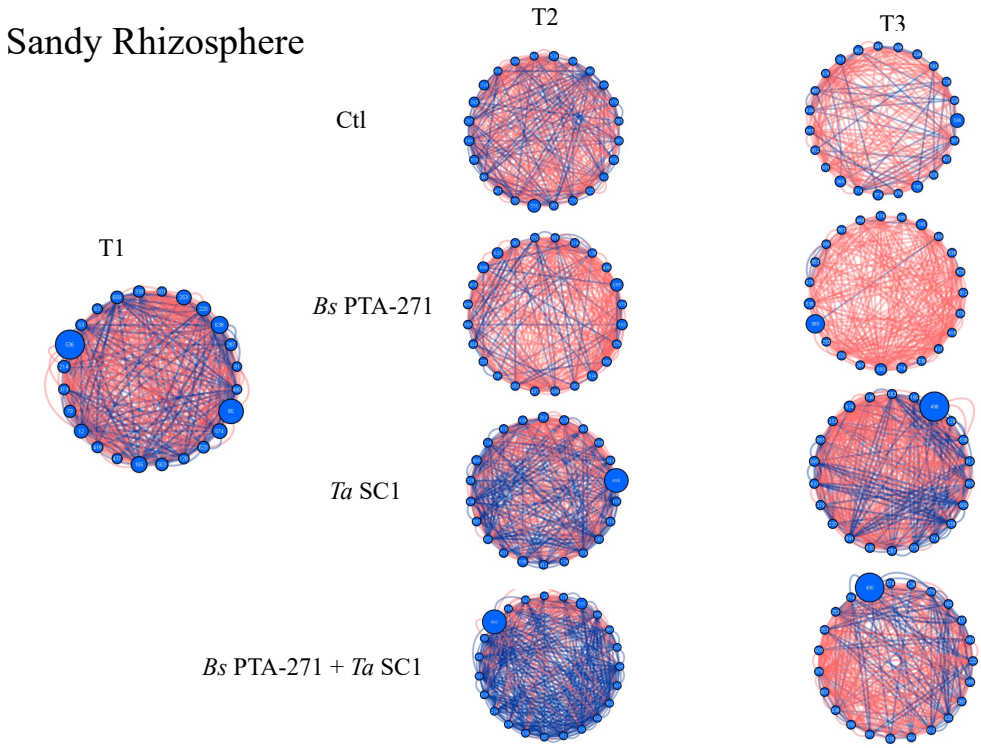

Figure 7. Co-occurrence networks from fungal rhizosphere structural communities in sandy rhizosphere samples, inoculated with *Bs* PTA-271, *Ta* SC1, *Bs* PTA-271 + *Ta* SC1, and control plants (CTL), on sampling times 1, 2 and 3 (T1, T2, T3). Numbers correspond to the OTU numbers, and abundance of each module is sorted by size. Red lines represent negative correlations, and blue lines represent positive correlations.

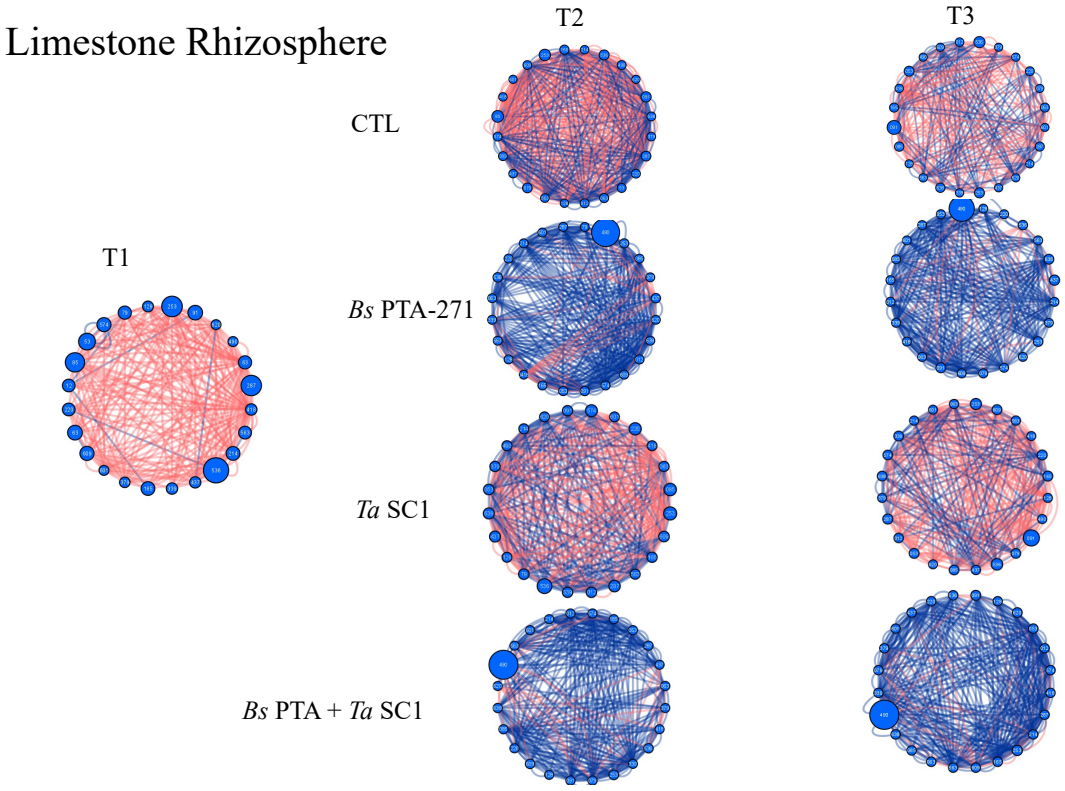

Figure 8. Co-occurrence networks from fungal rhizosphere structural communities in limestone rhizosphere samples, inoculated with *Bs* PTA-271, *Ta* SC1, *Bs* PTA-271 + *Ta* SC1, and control plants (CTL), on sampling times 1, 2 and 3 (T1, T2, T3). Numbers correspond to the OTU numbers, and abundance of each module is sorted by size. Red lines represent negative correlations, and blue lines represent positive correlations.

Table 6. Number of positive (blue) and negative (red) fungal correlations between sandy and limestone soil samples, between treatments (Control, *Bs* PTA-271, *Ta* SC1, and *Bs* PTA-271 + *Ta* SC1), in sampling times 1, 2 and 3 (T1, T2, T3).

	Sandy soil				Limestone soil			
	Ctl	***Bs* PTA-271**	***Ta* SC1**	***Bs* PTA-271 + *Ta SC1***	**Ctl**	***Bs* PTA-271**	***Ta* SC1**	***Bs* PTA-271 + *Ta SC1***
T1			183/259				11/207	
T2	124/205	73/245	184/164	286/104	181/268	315/40	138/178	271/27
T3	41/160	8/235	163/226	105/210	126/136	260/26	107/178	309/39

Bacteria

In sandy soil, plants tended to increase positive relationships over time. However, plants inoculated with *Bs* PTA-271 and both BCAs decreased positive relationships and increased negative ones at 90 dpi.

In limestone soil, plants decreased positive relationships at 30 dpi, and increased them again at 90 dpi while negative relationships are increased at 30 dpi and maintained at 90 dpi. Plants inoculated with *Bs* PTA-271 decreased positive relationships and increased negative relationships over time. Plants inoculated with *Ta* SC1 maintained positive relationships at 30 dpi, but highly decreased them at 90 dpi. For plants treated with both BCAs, positive relationships strongly decreased at 30 dpi, but highly increase at 90 dpi (Table 7).

In both, sandy and limestone soils, plants rhizosphere was mainly colonized by bacteria from the genus *Rubrobacter* (Otu 660) that was maintained over time. No treatment caused any changes in the bacterial microbiome on any type of soil (Figures 9 and 10).

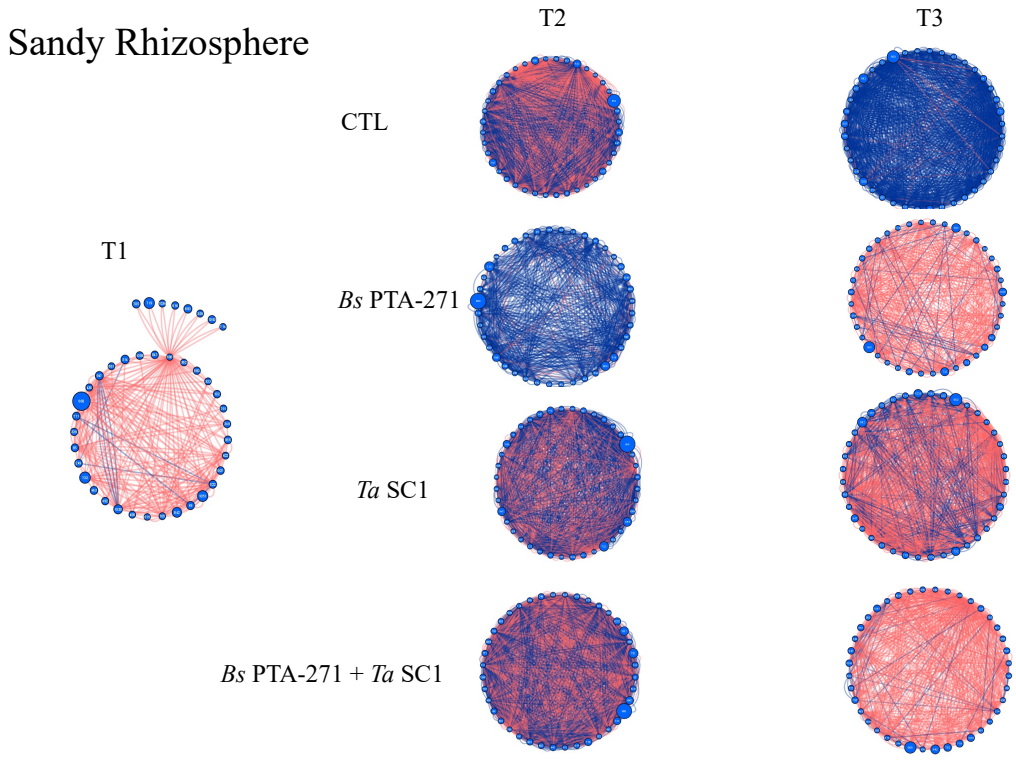

Figure 9. Co-occurrence networks from bacterial rhizosphere structural communities in sandy rhizosphere samples, inoculated with *Bs* PTA-271, *Ta* SC1, *Bs* PTA-271 + *Ta* SC1, and control plants (CTL), on sampling times 1, 2 and 3 (T1, T2, T3). Numbers correspond

to the OTU numbers, and abundance of each module is sorted by size. Red lines represent negative correlations, and blue lines represent positive correlations.

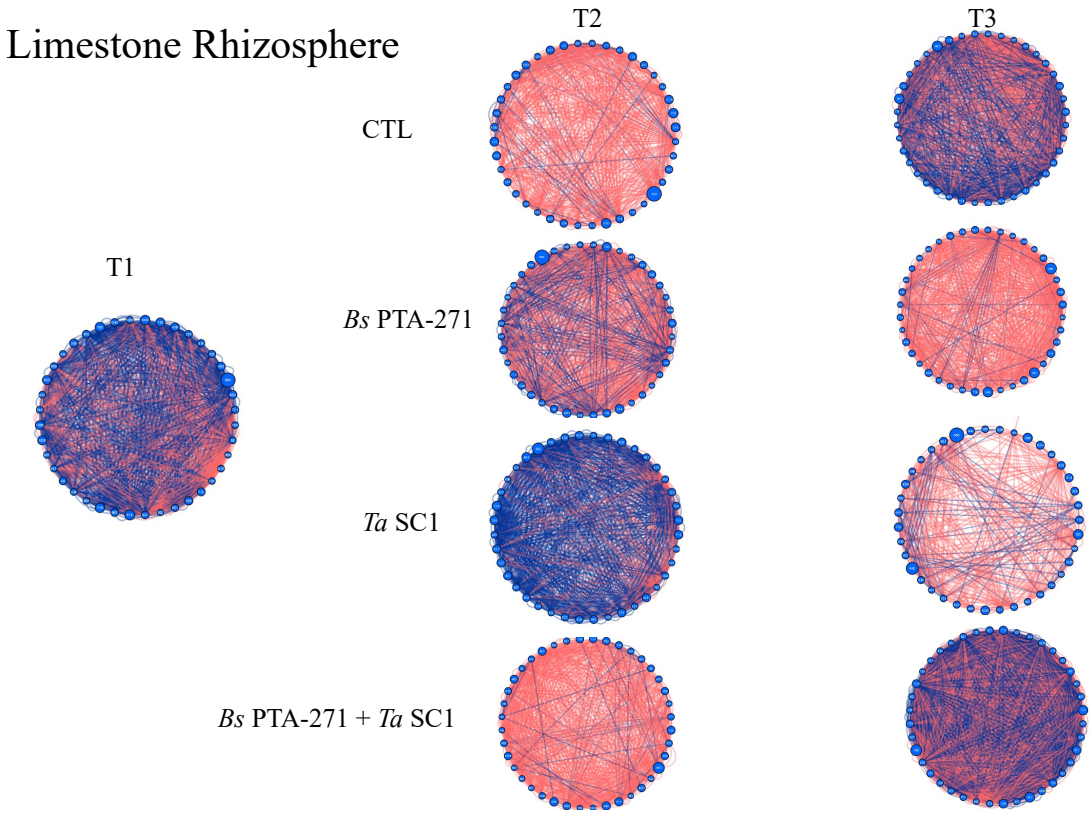

Figure 10. Co-occurrence networks from bacterial rhizosphere structural communities in limestone rhizosphere samples, inoculated with *Bs* PTA-271, *Ta* SC1, *Bs* PTA-271 + *Ta* SC1, and control plants (CTL), on sampling times 1, 2 and 3 (T1, T2, T3). Numbers correspond to the OTU numbers, and abundance of each module is sorted by size. Red lines represent negative correlations, and blue lines represent positive correlations.

Table 7. Number of positive (blue) and negative (red) bacterial correlations between sandy and limestone soil samples, between treatments (Control, *Bs* PTA-271, *Ta* SC1, and *Bs* PTA-271 + *Ta* SC1), in sampling times 1, 2 and 3.

	Sandy soil				Limestone soil			
	Ctl	*Bs* PTA-271	*Ta* SC1	*Bs* PTA-271 + *Ta SC1*	Ctl	*Bs* PTA-271	*Ta* SC1	*Bs* PTA-271 + *Ta SC1*
T1			9/229				615/397	
T2	763/785	584/40	708/554	820/696	63/525	293/567	680/224	49/685
T3	1083/41	58/424	326/704	52/518	564/552	56/672	74/284	919/773

Plant defense gene expression

According to the selected plant defense markers followed, plant leaving on sandy soil appeared much more impacted by BCA inoculation than plants in limestone soil. In sandy soil, plants inoculated with *Ta* SC1 and both BCAs presented a strong repression in almost all tested genes expression at 24hpi (except *PR1*). On the opposite, plants treated with *Ta* SC1 at 4dpi had an overexpression on all tested genes (*PR1* and *PR2* in a lesser extent), while the treatment with both BCAs presented the strongest overexpression for *LOX9*, *GST1*, *PAL* and *STS*. Interestingly, while *Bs* PTA-271 did not significantly affect the expression of the plant defense genes at 24hpi, plants inoculated with *Bs* PTA-271 showed a slight repression of *PR1, PAL* and *STS* expression at 4dpi (Figure 11).

In limestone soil, except for *PR1*, plants inoculated with *Bs* PTA-271 presented an overexpression of all selected genes (*LOX9, PR2, GST1, PAL* and *STS*) at 24hpi, that intensified at 4 dpi (except for *GST1*). Plants treated with *Ta* SC1 showed similar trends than with *Bs* PTA-271 (despite less marked at 24hpi, but also intensified at 4dpi). In contrast, plants inoculated with both BCAs showed a repression of *LOX9*, *PR1*, and *GST1* expression at 24hpi, that persist only for *GST1* at 4 dpi (Figure 12). Indeed, the sole slight overexpression observed with the treatment combining BCA are for *STS* at 24hpi, then for *LOX9*, *PR2* and *PAL* at 4dpi.

	Sandy Soil							
	24h after inoculation				4 days after inoculation			
	Ctl	*Bs* PTA-271	*Ta* SC1	*Bs* PTA-271 + Ta SC1	Ctl	*Bs* PTA-271	*Ta* SC1	*Bs* PTA-271 + Ta SC1
LOX9	1.00	1.29	0.13	0.16	1.00	1.03	53.80	11.71
PR1	1.00	1.71	0.35	0.94	1.00	0.91	11.25	4.35
PR2	1.00	2.27	0.02	0.01	1.00	1.45	17.76	3.32
GST1	1.00	1.33	0.09	0.07	1.00	1.47	48.07	11.86
PAL	1.00	1.52	0.00	0.00	1.00	0.84	264.26	92.17
STS	1.00	1.24	0.00	0.00	1.00	0.39	108.82	57.08

Figure 11. Induced differential expression of defense-related genes in leaves of sandy soil plants. Samples were collected 24h and 4 days after inoculation with four treatments (Control, *Bs* PTA-271, *Ta* SC1, and *Bs* PTA-271 + *Ta* SC1). Heatmaps represent changes in the transcript expression levels as indicated by the color shading. Data are the means from three representative replicates. Different letters indicate statistically significant differences between the treatments (ANOVA, Fisher's LSD post hoc test, $\alpha = 0.1$). Legends for genes are *LOX9*, lipoxygenase 9; *PR1*, pathogenesis-related protein 1; *PR2*, class I β-1,3-glucanase; *GST1*, glutathione-S-transferase 1; *PAL*, phenylalanine ammonia lyase; *STS*, stilbene synthase.

	Limestone soil							
	24h after inoculation				4 days after inoculation			
	Ctl	*Bs* PTA-271	*Ta* SC1	*Bs* PTA-271 + Ta SC1	Ctl	*Bs* PTA-271	*Ta* SC1	*Bs* PTA-271 + Ta SC1
LOX9	1.00	3.03	1.55	0.22	1.00	13.35	15.39	1.88
PR1	1.00	1.13	1.20	0.50	1.00	1.22	1.48	0.93
PR2	1.00	2.48	2.26	1.11	1.00	13.26	43.90	2.51
GST1	1.00	2.69	2.10	0.62	1.00	1.21	1.36	0.12
PAL	1.00	4.80	2.32	1.52	1.00	47.97	67.64	2.64
STS	1.00	5.98	3.01	3.27	1.00	38.77	35.44	1.53

Figure 12. Induced differential expression of defense-related genes in leaves of limestone soil plants. Samples were collected 24h and 4 days after inoculation with four treatments

(Control, *Bs* PTA-271, *Ta* SC1, and *Bs* PTA-271 + *Ta* SC1). Heatmaps represent changes in the transcript expression levels as indicated by the color shading. Data are the means from three representative replicates. Different letters indicate statistically significant differences between the treatments (ANOVA, Fisher's LSD post hoc test, $\alpha = 0.1$). Legends for genes are *LOX9*, lipoxygenase 9; *PR1*, pathogenesis-related protein 1; *PR2*, class I β-1,3-glucanase; *GST1*, glutathione-S-transferase 1; *PAL*, phenylalanine ammonia lyase; *STS*, stilbene synthase.

6.4. Discussion

In this study, we examined the temporal dynamics of the fungal and bacterial microbiome in 110R rootstocks naturally infected with black-foot pathogens and inoculated with *Bacillus subtilis* PTA 271 (*Bs* PTA-271) and *Trichoderma atroviride* SC1 (*Ta* SC1), in two different types of soil (sandy and limestone soils). Samples were collected from rhizosphere in 3 different times (before inoculations, 30dpi, and 90dpi), using a non-destructive method.

Generally, research on grapevine microbiome is predominantly focused on the scion cultivar, the visible half-part of the vine that produces grapes. However, more than 80% of the vineyards worldwide are currently grafted onto rootstocks (Ollat et al. 2016), which have a significantly effect on grape yield and quality and contribute to confer protection against pathogens (Marín et al. 2021).

Microorganisms abundance

When analyzing the fungal microbiota, the rhizosphere is initially colonized mainly by Ascomycota (Cloronostachys and Lophiostoma) and Basidiomycota (Ceratobasideaceae). These fungi are commonly found in soil and dead wood tissues in all geographic locations (Jacquemyn et al. 2017; Sun et al. 2020; Hashimoto et al. 2018). Genera of pathogenic fungi related with GTDs were also detected in the studied plants, such as *Ilyonectria* (black-foot disease pathogen) (Probst et al. 2019), and *Diaporthe* (Phomopsis dieback pathogen) (Dissanayake et al. 2015). In our experiments, control plants did not have a significant abundance of *Trichoderma* spp., showing no contamination with *Ta* SC1. In contrast, when plants are inoculated with *Bs* PTA-271

they presented a considerable abundance of *Trichoderma* spp., and similarly with plants inoculated with both BCAs that contain more *Trichoderma* than plants inoculated with only *Ta* SC1. This indicate that *Bacillus* species can recruit other microorganisms towards the plant rhizosphere to modulate the microbiome activity. Sabaté and Brandán (2022) already demonstrated that soil inoculation with *Bacillus amyloliquefaciens* B14 improves the *Trichoderma* spp. soil abundance. Interestingly, we observed that *Trichoderma* spp. abundance decreases from 30dpi to 90dpi, showing that this BCA had problems to maintain after inoculation. This could happen due to the complex nature of the rhizosphere and root microbiome (Berendsen et al. 2012), or due to abiotic factors that can change the interaction between micoorganisms (Niu et al. 2020). Martinez-Diz et al. (2018) also observed a decrease in *Trichoderma* recovery in grapevine rhizosphere over time.

The bacterial microbiota described in the sampled plants was much more complex and abundant than the fungal microbiota. The plant rhizosphere was mainly colonized by *Rubrobacter*, *Streptomyces*, *Rhizobium* and Vicinamibacterales, as well as *Bacillus* spp. that, although present did not present a significant abundance. These bacterial genera are commonly found in grapevine soil and rhizosphere (Darriaut et al. 2022; Mocali et al. 2020; Dries et al. 2021). Looking at *Bacillus* spp. evolution overtime, no significant differences were observed between the rhizosphere of BCA treated plants, probably because *Bacillus* spp. is not the main bacterial genera detected in these conditions (BCA treated plants). To contrast with *Trichoderma* spp., control plants already presented a significant abundance of *Bacillus* spp., that could lead to an impossibility of detecting differences in *Bacillus* spp. evolution overtime.

Alpha diversity

Our results indicated that the fungal alpha diversity fluctuated very differently over time according to the soil samples. In sandy soil, treatments with *Ta* SC1 showed a lower diversity compared with the control plants and plants treated with *Bs* PTA-271 at 30dpi. The *Ta* SC1 successful inoculation leads to a generalized colonization of this microorganism in rhizosphere and soil, giving less space and nutrients for other fungi, therefore reducing the fungal diversity. Li et al. (2022) reported a decrease in fungal diversity in soil of plants inoculated with *Trichoderma atroviride* strain HB 20111. On limestone soil, plants inoculated with *Bs* PTA-271 presented a much lower fungal diversity than control plants and plants treated with *Ta* SC1. Garbeva et al. (2004)

reported that the two main factors affecting the soil microbial community structure are plant type and soil type, due to the complex interactions between microorganisms, soil, and plants. Therefore, physicochemical characteristics of the soil used in this experiment could lead to secondary metabolites production by *Bs* PTA-271 that may lead to a decrease in fungal diversity. Moreover, limestone soils are denser and heavier than sandy soils, creating complications for microorganisms to colonize plant roots (Marshal 1975). However, without further analysis on the soil composition, it is not possible to confirm this theory. The bacterial alpha diversity also varied depending on the type of soil. In sandy soil, the BCAs inoculation improved bacterial diversity in grapevine rhizosphere, and at 90dpi, the treatment with both BCAs presented higher bacterial diversity than plants inoculated with only one BCA. Previous studies pointed the BCA inoculation as a factor that can increase microbiome diversity (Gadhave et al. 2018; Li et al. 2011). In limestone soil, as in the fungal diversity, plants inoculated with *Ta* SC1 show less bacterial diversity. Environmental heterogeneity, such as the soil physicochemical properties and moisture content have been identified as major factors shaping the spatial scaling of the rhizosphere microbiome in many previous studies (Costa et al. 2006; Tan et al. 2013; Schreiter et al. 2014), including grapevine (Fernández-Calviño et al. 2010; Corneo et al. 2014; Burns et al. 2015; Zarraonaindia et al. 2015; Holland et al. 2016).

Microbial relationships in rhizosphere

Network analysis of taxon co-occurrence patterns provides new insight into the structure of complex microbial communities, patterns that are otherwise more difficult to reveal using standard alpha/beta diversity measures widely used in microbial ecology (Barberán et al. 2012), and also used in this study. It has been suggested that complex soil microbial community networks (networks with high number of nodes, number of links, and average connectivity), rather than the simple ones, benefit plants (Jiemeng et al. 2018). Indeed, complex networks contribute to better cope with environmental changes or to suppress soilborne pathogens. For instance, tobacco plants associated with rhizosphere microbial communities exhibiting complex networks showed lower incidence of bacterial wilt disease compared to plants associated with communities displaying less connections in their networks (Yang et al. 2017). Our results show that the correlation networks of bacterial taxa are more complex than the fungal networks. The study of the fungal taxa correlations in rhizosphere revealed that, in sandy soil, positive relationships is reduced

over time, although in plants inoculated with *Ta* SC1 and both BCAs the reduction on positive correlations is subtler. Sui et al. (2022) also observed a reduction in correlations in wheat rhizosphere of plants inoculated with *T. atroviride,* probably due to the direct confrontation between *Trichoderma* and other fungi, possibly pathogenic. In limestone soil, plants treated with *Bs* PTA-271 have a very significant increase of positive relationships while negative relationships significantly decrease. As mentioned before, *Bacillus* species can recruit specific microorganisms into the microbiome, improving its quality (positive correlations).

In our study, bacterial microbiome tended to stabilize overtime, increasing positive relationships, and reducing negative relationships. However, unexpectedly, plants inoculated with *Bs* PTA-271 and both BCAs decreased positive relationships and increased negative ones at 90 dpi. This could be explained by the high amount of *Bs* PTA-271 present in the rhizosphere, leading to an increase of negative correlations with other bacteria. Again, plants treated with both BCAs increased positive correlations at 90dpi, showing the potential of inoculating a combination of these BCAs, already pointed by Leal et al. (2021).

Concurring our previous works, a study on grapevine systemic immunity was performed, aiming six selected defense genes in leaves: the lipoxygenase *LOX9* involved in oxylipin synthesis and described as dependent to JA/ET; *PR1* described to be regulated by SA; the β-1,3-glucanase *PR2* described to be regulated by various phytohormones such as SA, JA, and ET; the glutathione-S-transferase *GST1* putatively involved in the detoxification process; the phenylalanine ammonia-lyase *PAL* catalyzing the first step in the phenylpropanoid pathway; and the stilbene synthase *STS* involved in the synthesis of phytoalexins (Leal et al. 2021; Trotel-Aziz et al. 2019). Interestingly, induced defenses were different in sandy soil plants and limestone soil plants. In sandy soil plants at 24 hpi with *Ta* SC1 and combined BCAs, we observed a strong suppression of both SA and JA/ET–dependent defense genes. These findings suggest that *Ta* SC1 must cope with the plant defense responses during its initial stages of the interaction, and thus by suppressing elements regulating the broad-spectrum of plant innate immunity, *Ta* SC1 ensure its own colonization of grapevine roots (Jacobs et al. 2011). After 4 dpi, plants inoculated with *Ta* SC1 and *Ta* SC1+ *Bs* PTA-271 showed stimulated defenses, with a significant overexpression of *PAL* and *STS* (through many possible hormonal inducing paths, such as SA, but also JA/ET, etc.), well known to be involved in the production of antimicrobial compounds such as phytoalexins. This would suggest that the plant finally succeed to

detect *Ta* SC1 as a foreigner, and it could constitute an interesting pre-priming state for the plant. Plants inoculated with *Bs* PTA-271 do not induce any changes in plant defenses during the first 24hpi, while at 4dpi a slight repression of *PAL* and *STS* is observed. This could indicate that these experimental conditions did not favor *Bs* PTA-271 in its ability to stimulate its host defenses, compared to *Ta* SC1, unless *Bacillus spp.* are already detected as non-threatening beneficial microorganisms by the plants at the selected experimental time. In limestone soil plants, results were slightly different from the sandy soil plants. In this study, our results showed that *Bs* PTA-271 or *Ta* SC1 treated-plants at 24hpi, show a slight increase in the expression of all selected genes (*LOX9, PR2, GST1, PAL* and *STS*), that intensified at 4 dpi (except for *GST1*). *Ta* SC1 effect being less marked at 24hpi, but also intensified at 4dpi. In contrast, plants inoculated with both BCAs also showed a slight overexpression for *STS* at 24hpi, then for *LOX9*, *PR2* and *PAL* at 4dpi. Since limestone soils are high in nutrients (Marshal 1975), one can thus assume, that colonization of plant roots by BCAs in limestone soil is less stressful for the plant in sandy soils (Vose 1982). Thus, contrary to sandy soil plants, all treatments stimulate the plant defenses, even weakly and lately, but as expected from a biocontrol agent that is not pathogenic to the plant (thus only leading to defense corresponding to a pre-priming state, not to a disease state). The late changes when using combined BCA doesn't exclude a direct confrontation between BCAs, until they find their balance.

6.5. Conclusion

Altogether, our results provide evidence that the success of *T. atroviride* SC1 and *B. subtilis* PTA-271 inoculations in grapevine rhizosphere microbiome is soil-dependent. Sandy soil seems to favor *Ta* SC1 implantation in the rhizospheric microbiome, consistent with its fungal nature (better adapted to acidic pH), while *Bs* PTA-271 thrives in a limestone soil. These results were corroborated with the study of plant defense gene expression.

The inoculation of *Ta* SC1 and *Bs* PTA-271 demonstrated a positive effect in rhizosphere correlation networks, improving positive correlations and reducing negative ones. In addition, we report the beneficial effect on grapevine rhizosphere microbiome of

combining the two BCAs in the same application. This is a promising result to reduce inconsistencies observed with the use of only one BCA.

Droplet digital PCR (ddPCR) analysis are being carried out to specifically quantify *Ta* SC1 and *Bs* PTA-271 to better understand the success of the inoculations. Finally, further studies are needed to associate soil physicochemical properties with BCA beneficial effect to determine the best BCA depending on several factors (cultivar, physicochemical parameters of the soil, wine region, meteorological conditions, etc.).

Concluding remarks and Perspectives

Finding sustainable management approaches for GTDs is of utmost importance, as the present treatments are either not effective to eliminate these diseases completely or rely on the use of arch chemicals that are harmful for the environment. It is also imperative to better understand the relationships between GTDs pathogens, grapevines, and BCAs that can be added as treatments, to better treat GTDs. In this context, the overall findings of this thesis documented the importance to deeply study biological microorganisms, their modes of action, and their interactions with plants and pathogens, as they can be the answer to control GTDs, but due to their nature, they can also be unpredictable and inconsistent on their biocontrol potential.

Firstly, this work unrevealed the biocontrol potential of a new *Bacillus subtilis* strain (*Bs* PTA-271) to be used against GTDs. With a full genomic analysis, this study highlighted the genes encoding for biocontrol related processes. The most relevant predicted genes encode for: (1) a functional swarming motility system highlighting advantageous colonizing capacity of host and a strong interacting capacity within plant microbiota; (2) a strong survival capacity, due to sporulation but also to complex detoxifying systems, auto-inducing metabolic paths and recruiting capacities for adding microbiota values; and (3) the delivery of many bioactive substances (hormones, elicitors, effectors and quenchers, siderophores and lytic enzymes, etc.), facilitating the stimulation of plant growth or defenses, or else, disturbing pathogen fitness or aggressiveness. Interestingly, the putative capacity of *B. subtilis* PTA-271 to produce a wide range of phytohormone analogous (SA, ET precursor, ABA etc.), as well as diverse direct effectors and lytic enzymes against plant pathogens, highlight a significant potential for biocontrol strategies.

This study also provide evidence of the biocontrol potential of *Bs* PTA-271 and *Ta* SC1 against *N.parvum* BT67, *in vitro*, and in two grapevine cultivars (*in planta*). Our results provide evidence that grapevine susceptibility to *Np*-BT67 is cultivar-dependent, as well as the BCA beneficial effects. *Bs* PTA-271 was confirmed as an effective protector for Chardonnay against *Np*-Bt67, and *Ta* SC1 was shown for the first time as a good protector for Tempranillo. This study also reports for the first time the biocontrol potential of the combination of *Bs* PTA-271 and *Ta* SC1 against *Np*-Bt67 in Tempranillo. This is a promising result for an improved efficiency of sustainable biological control in a proven context of lack of effective chemicals to manage GTDs.

Endowed with aggressive molecules, *Bs* PTA-271 and *Ta* SC1 can antagonize each other, but *Bs* PTA-271 inhibits *Np*-Bt67 development with a greater efficiency in a three-way

confrontation. This beneficial BCA collaboration against *Np*-Bt67 still operates in Tempranillo and confirms the interest of using both BCAs in combination to optimize the direct fight against *Np*-Bt67. These results are of great interest for effective curative treatments to obtain healthy mother plants in the nursery and to control BOT in vineyard. However, the direct beneficial effect of combined BCAs did not operate to protect Chardonnay, suggesting that Chardonnay itself probably alters the fine-tuned orchestrated cooperation of BCAs that drives such direct beneficial effect. Plant systemic immunity is also affected by each BCA. Our findings suggest a common feature for the two cultivars: the defenses that are greatly diminished in BCA-protected plants appear to be those that are responsive to SA, in contrast to symptomatic plants. For Tempranillo, the high basal expression of SA-dependent defenses may thus explain the highest susceptibility to BOT and the ineffectiveness of *Bs* PTA-271 in our experimental conditions. In transcriptomic analysis from these experiments, our results provide a new insight of molecular changes associated with the infection by Np-Bt67 in Chardonnay and Tempranillo. In Chardonnay, plants infected with *Np*-Bt67 present overexpressed genes that are implicated on ABA signaling pathways. In Tempranillo, the infection with *Np*-Bt67 leads to expression changes in more than 200 genes, related mostly with amino acid import, chloroplast and photosystem related processes, plant responses to biotic stimulus, and biosynthesis of secondary metabolites. Our study also provides deep insights of the protection induced by *Bs* PTA-271 in Chardonnay, and *Ta* SC1 in Tempranillo. Protection from *Bs* PTA-271 in Chardonnay involves genes related to ABA biosynthesis, phenylpropanoid pathways, secondary metabolites and cell wall structure and organization. Protection of *Ta* SC1 in Tempranilllo plants involves a larger number of changes, that cover both primary and secondary metabolism, related to changes in hormonal signals, such as with ABA.

One of the most important approaches to GTDs integrated management is the improvement of the phytosanitary quality of the nursery produced grapevines, as this can prevent future pathogen dissipations. This study, especially the work conducted in chapter V, reveals how promising these BCAs can be to reduce pathogen infections during the grapevine propagation process, but how inconsistent these treatments can sometimes be. These results showed a promising biocontrol potential of treatments with *Bs* PTA-271 and *Ta* SC1 against Botryosphaeria dieback and black foot pathogen infections during the grapevine propagation process of cv. Tempranillo. Alone, *Ta* SC1 confirmed its

effectiveness to reduce the percentage of infected plants with BOT associated pathogens and the percentage of isolation from wood fragments, and *Bs* PTA-271 demonstrated, for the first time, effectiveness to reduce infections caused by BF associated pathogens during the propagation process. In one of the experiments, the simultaneous application of both BCAs presented a significant decrease in the number of infected plants and the number of infected wood fragments for both groups of pathogens. In this study, qRT-PCR techniques were used for the first time in grapevine nursery experiments, enabling accurate quantification of the inoculated BCAs, confirming the successful colonization by BCAs in treated plants, and the lack of crossed contaminations between treatments. Complement to the work on chapter V, the work conducted to test the effect of *Bs* PTA-271 and *Ta* SC1 in the grapevine rhizosphere microbiome, also highlights the potential of this microorganisms to be integrated in sustainable disease management in grapevines. Our results provide evidence that the success of *Ta* SC1 and *Bs* PTA-271 inoculations in grapevine rhizosphere microbiome is soil-dependent. Sandy soil seems to favor *Ta* SC1 implantation in the rhizospheric microbiome, consistent with its fungal nature (better adapted to acidic pH), while *Bs* PTA-271 thrives in a limestone soil. These results were corroborated with the study of plant defense gene expression. The inoculation of *Ta* SC1 and *Bs* PTA-271 demonstrated a positive effect in rhizosphere correlation networks, improving positive correlations and reducing negative ones. In addition, we report the beneficial effect on grapevine rhizosphere microbiome of combining the two BCAs in the same application. This is a promising result to reduce inconsistencies observed with the use of only one BCA.

Although the outcomes of this thesis provide new knowledge on the grapevine interactions with pathogens and BCAs, and the potential of using more than one BCA to treat grapevine GTDs, there are still unanswered questions that need further clarification. The first question, related to the contribution of an BCAs in a non-sterile environment, raises the question of the origin of the protection: is it BCA-dependent or is it the result of a change induced by the BCA on the microbiome of the vine? This is a crucial point to investigate further, whether it involves intermediate physiological changes in the host plant.

The living conditions of plants and microorganisms such as BCAs also deserve more attention, especially the quality of their support, which is the soil. Depending on the

geographical location, the nature of the soil fluctuates depending on the nature of the bedrock on which it rests and the climatic conditions of the station where it is located. The key elements to consider having a quality soil conducive to the good physiological state of plants and microorganisms that it carries are among others: its porosity (structure conditioned by its texture or granulometry), its pH, and its organic matter content. The use of a sandy substrate and a limestone substrate are the two extremes on the texture scale. The sandy soil offers a microporosity not very favorable to a good biological activity, but on the contrary, it is favorable to the development of an acid pH and to a bad degradation of the organic matter (if however, this one was retained). The limestone soil is rich in nutrients but can be denser and heavier than sandy soils, which complicates the colonization of plant roots by micro-organisms.

The way the vineyard is cultivated must also be considered, in particular its irrigation, which can influence the development or not of a particular pathogen likely to infect the plant, or modulate the pressure of pathogens, etc. Further research on these aspects is still needed. This would allow us to cover as many changing conditions as possible in order to better channel/erase the variability that may be observed in the protection induced by our BCAs when transferring the results obtained to field conditions. The combined use of a larger number of BCAs is also desired, in an attempt to ensure effective protection despite fluctuations in environmental factors.

Finally, the differential effects of Bs PTA-271 and Ta SC1 against Np-Bt67 in two different grapevine varieties also revealed grapevine effects on their sensitivities to pathogens, but also to BCAs, and potentially to other environmental factors not yet understood. It is therefore necessary to further open our molecular/genetic investigations to grapevines, for example by comparing the genomes and defense responses of grapevines from very different climatic regions. The idea is to discover potential genes for tolerance or resistance to GTDs in grapevines since: (i) the diversity of genotypes within grapevine varieties, grapevines or even clones, and (ii) the distribution and pressure of pathogens responsible for GTDs, are both conditioned by the geographical area.

Bibliography

Abou-Mansour E, Debieux J L, Ramírez-Suero M, Bernard-Gellon M, Magnin-Robert M, Spagnolo A, Chong J, Farine S, Bertsch C, L'Haridon F, Serrano M, Fontaine F, Rego C, Larignon P. 2015. Phytotoxic metabolites from Neofusicoccum parvum, a pathogen of Botryosphaeria dieback of grapevine. Phytochem. 115:207−215.

Abuzinadah R, Finlay R, Read D. 1986. The role of proteins in the nitrogen nutrition of ectomycorrhizal plants. New Phytol. 103(3):495-506.

Adams G, Roux, J, Wingfield MJ. 2006. Cytospora species (*Ascomycota, Diaporthales, Valsaceae*): introduced and native pathogens. Australas. Plant Dis. Notes 35(5):521-548.

Adie A., Pérez-Pérez J, Pérez-Pérez M, Godoy M, Sánchez-Serrano JJ, Schmelz EA, Solano R. 2007. ABA is an essential signal for plant resistance to pathogens affecting JA biosynthesis and the activation of defenses in Arabidopsis. The Plant Cell 19(5):1665-1681.

Agustí-Brisach C, Armengol J. 2013. Black-foot disease of grapevine: an update on taxonomy, epidemiology and management strategies. Phytopathol. Mediterr. 52:245–261.

Agustí-Brisach C, Cabral A, González-Domínguez E, Pérez-Sierra A, León M, Abad-Campos P, Armengol J. 2016. Characterization of *Cylindrodendrum, Dactylonectria and Ilyonectria* isolates associated with loquat decline in Spain, with description of Cylindrodendrum alicantinum sp. nov. Eur. J. Plant Pathol. 145(1):103–118.

Ahmad MZ, Li P, She G, Xia E, Benedito VA, Wan XC, Zhao J. 2020. Genome-wide analysis of serine carboxypeptidase-like acyltransferase gene family for evolution and characterization of enzymes involved in the biosynthesis of galloylated catechins in the tea plant (Camellia sinensis). Front. Plant Sci. 11:848.

Akgül S, Yildi M, Güngör Savas N, Bülbül I, Özarslandan M, León M, Armengol J. 2022 Occurrence and diversity of black-foot pathogens on asymptomatic nursery-produced grapevines in Turkiye. Eur. J. Plant Pathol. 164(1):21-32.

Akram W, Anjum T, Ali B. 2015. Searching ISR determinant/s from Bacillus subtilis IAGS174 against Fusarium wilt of tomato. BioControl. 60(2):271-280.

Alexander A, Phin CK. 2014. Combination of biological agents in suppressing colonization of *Ganoderma boninense* of basal stem rot. Am-Eurasian J. Sustain. Agric. 8:1-7.

Alfiky A, Weisskopf L. 2021. Deciphering Trichoderma–plant–pathogen interactions for better development of biocontrol applications. J. Fungus. 7(1):61.

Alfonzo A, Conigliaro G, Moschetti G, Burruano S, Barone A. 2012. A simple and rapid DNA extraction method from leaves of grapevine suitable for polymerase chain reaction analysis. Afr .J. Biotechnol. 11(45):10305-10309.

Alfonzo A, Conigliaro G, Torta L, Burruano S, Moschetti G. 2009. Antagonism of *Bacillus subtilis* strain AG1 against vine wood fungal pathogens. Phytopathol. Mediterr. *48*(1):155-158.

Alström S. 1991. Induction of disease resistance in common bean susceptible to halo blight bacterial pathogen after seed bacterization with rhizosphere pseudomonads. The Journal of General and Appl. Microbiol. 37(6):495-501.

Álvarez-Pérez JM, González-García S, Cobos R, Olego MÁ, Ibañez A, Díez-Galán A, Garzón-Jimeno E, Coque JJR. 2017. Use of endophytic and rhizosphere actinobacteria from grapevine plants to reduce nursery fungal graft infections that lead to young grapevine decline. Appl. Environ. Microbiol. 83(24):01564-17.

Anderson PK, Cunningham AA, Patel NG, Morales FJ, Epstein PR, Daszak P. 2004. Emerging infectious diseases of plants: pathogen pollution, climate change and agrotechnology drivers. Trends Ecol. Evol. 19(10):535-544.

Andolfi A, Maddau L, Cimmino A, Linaldeddu BT, Franceschini, Serra S, Basso S, Melck D, Evidente A. 2012. Cyclobotryoxide, a phytotoxic metabolite produced by the plurivorous pathogen *Neofusicoccum australe*. J. Nat. Prod. 75:1785−1791.

Andreini L, Caruso G, Bertoll C, Scalabrelli G, Viti R, Gucci R. 2009. Gas exchange, stem water potential and xylem flux on some grapevine cultivars affected by esca disease. S. Afr. J. Enol. Vitic. 30:142-147.

Andreolli M, Zapparoli G, Angelini E, Lucchetta G, Silvia Lampis S, Vallini G. 2019. Pseudomonas protegens MP12: A plant growth-promoting endophytic bacterium with broad-spectrum antifungal activity against grapevine phytopathogens. Microbiol. Res. 219:123-131.

Andrews S. 2010. FastQC: A Quality Control Tool for High Throughput Sequence Data. Available online: https://www.bioinformatics.babraham.ac.uk/projects/fastqc (accessed on 1 July 2020).

Andrews SC, Robinson AK, Rodríguez-Quiñones F. 2003. Bacterial iron homeostasis. FEMS Microbiol. Rev. 27(2-3):215-237.

Arkhipova TN, Veselov SU, Melentiev AI, Martynenko EV, Kudoyarova GR. 2005. Ability of bacterium *Bacillus subtilis* to produce cytokinins and to influence the growth and endogenous hormone content of lettuce plants. Plant Soil 272:201-209.

Armijo G, Schlechter R, Agurto M, Muñoz D, Nuñez C, Arce-Johnson P. 2016. Grapevine pathogenic microorganisms: understanding infection strategies and host response scenarios. Front. Plant Sci. 7:382.

Aroca A, Gramaje D, Armengol , García-Jiménez J, Raposo R. 2010. Evaluation of grapevine nursery process as a source of *Phaeoacremonium* spp. and *Phaeomoniella chlamydospora* and occurrence of trunk disease pathogens in rootstock mother vines in Spain. Eur. J. Plant Pathol. 126:165-174.

Arzanlou M, Narmani A. 2015. ITS sequence data and morphology differentiate *Cytospora chrysosperma* associated with trunk disease of grapevine in northern Iran. J. Plant Prot. Res. 55(2):117–125.

Audrain B, Farag MA, Ryu C-M, Ghigo J-M. 2015. Role of bacterial volatile compounds in bacterial biology. FEMS Microbiology Reviews 39(2):222-233.

Azevedo-Nogueira F, Rego C, Gonçalves HM, Fortes M, Gramaje D, Martins-Lopes P. 2022. The road to molecular identification and detection of fungal grapevine trunk diseases. Front. Plant Sci. 13.

Aziz A, Martin-Tanguy J, Larher F. 1997. Plasticity of polyamine metabolism associated with high osmotic stress in rape leaf discs and with ethylene treatment. Plant Growth Regul. 21(2):153-163.

Aziz A, Perazzolli M, Gramaje D, Zyprian EM, Cantu D. 2020. Recent Advances on Grapevine-Microbe Interactions: From Signal Perception to Resistance Response. Front. Plant Sci. 11:1164.

Bais HP, Fall R, Vivanco JM. 2004. Biocontrol of *Bacillus subtilis* against infection of *Arabidopsis* roots by *pseudomonas syringae* is facilitated by biofilm formation and surfactin production. Plant. Physiol. 134(1):307-319.

Baksi KD, Kuntal BK, Mande SS. 2018. 'TIME': A web application for obtaining insights into microbial ecology using longitudinal microbiome data. Front. Microbiol. 9:36.

Baltrus DA, McCann HC, Guttman DS. 2017. Evolution, genomics and epidemiology of *Pseudomonas syringae*: challenges in bacterial molecular plant pathology. Mol. Plant Pathol. 18(1):152-168.

Bankevich A, Nurk S, Antipov D, Gurevich AA, Dvorkin M, Kulikov AS, et al. 2012. SPAdes: a new genome assembly algorithm and its applications to single-cell sequencing. J. Comput. Biol. 19(5):455-477.

Barberán A, Bater ST, Casamayor EO, Fierer N. 2012. Using network analysis to explore co-occurrence patterns in soil microbial community. ISME J. 6:343–51.

Baskaratheva J, Jaspers MV, Jones EE, Cruickshank RH, Ridgway HJ. 2012. Genetic and pathogenic diversity of *Neofusicoccum parvum* in New Zealand vineyards. Fungal Biology 116(2):276-288.

Bass D, Stentiford GD, Wang HC, Koskella B, Tyler CR. 2019. The pathobiome in animal and plant diseases. Trends Ecol. Evol. 34(11):996-1008.

Baumgartner K, Fujiyoshi PT, Travadon R, Castlebury LA, Wilcox WF. Rolshausen PE. 2013. Characterization of species of *Diaporthe* from wood cankers of grape in eastern North American vineyards. Plant Dis. 97: 912-920.

Bednare P. 2012. Sulfur-containing secondary metabolites from Arabidopsis thaliana and other Brassicaceae with function in plant immunity. ChemBioChem 13(13):1846-1859.

Berendsen RL, Pieterse CM, Bakker PA. 2012. The rhizosphere microbiome and plant health. Trends Plant Sci. 17(8):478-486.

Berbegal M, Ramón-Albalat A, León M, Armengol J, 2020. Evaluation of long-term protection from nursery to vineyard provided by *Trichoderma atroviride* SC1 against fungal grapevine trunk pathogens. Pest Manag. Sci. 76(3): 967-977.

Berlanas C, Andrés-Sodupe M, López-Manzanares B, Maldonado-González MM, Gramaje D. 2018. Effect of white mustard cover crop residue, soil chemical fumigation and *Trichoderma* spp. root treatment on black-foot disease control in grapevine. Pest Manag. Sci. 74(12):2864-2873.

Berlanas C, Berbegal M, Elena G, Laidani M, Cibriain JF, Sagües A, Gramaje D. 2019. The fungal and bacterial rhizosphere microbiome associated with grapevine rootstock genotypes in mature and young vineyards. Front. Microbiol. 10:1142.

Berlanas C, López-Manzanares B, Gramaje D. 2017. Estimation of viable propagules of black-foot disease pathogens in grapevine cultivated soils and their relation to production systems and soil properties. Plant and Soil 417(1):467-479.

Berlanas C, Ojeda S, López-Manzanares B, Andrés-Sodupe M, Bujanda R, Pilar Martínez-Diz M, Díaz-Losada E, Gramaje D. 2020. Occurrence and diversity of

black-foot disease fungi in symptomless grapevine nursery stock in Spain. Plant Dis. 104(1):94-104.

Bertsch C, Ramírez-Suero M, Magnin-Robert M, Larignon P, Chong J, Abou-Mansour E, Sapgnolo A, Clément C, Fontaine F. 2013. Grapevine trunk diseases: complex and still poorly understood. Plant Pathol. 62(2):243-265.

Bettenfeld P, Canal JC, Jacquens L, Fernandez, Fontaine F, van Schaik E, Courtie P, Trouvelot S. 2021. The microbiota of the grapevine holobiont: A key component of plant health. J. Adv. Res.

Bettenfeld P, Fontaine F, Trouvelot S, Fernandez O, Court PE. 2020. Woody plant declines. What's wrong with the microbiome?. Trends Plant Sci. 25(4):381-394.

Biggs AR. 1989. Integrated approach to control Leucostoma canker of peach in Ontario. Plant Dis. 73(11):869–874.

Billar de Almeida A, Concas J, Campos M, Materatski P, Varanda C, Patanita M. et al. 2020. Endophytic fungi as potential biological control agents against grapevine trunk diseases in alentejo region. Biology 9(12):420.

Billones-Baaijens R, Savocchia S. 2019. A review of Botryosphaeriaceae species associated with grapevine trunk diseases in Australia and New Zealand. Australas. Plant Dis. 48(1):3-18.

Bitas V, Kim H-S, Bennett JW, Kang S. 2013. Sniffing on microbes: diverse roles of microbial volatile organic compounds in plant health. Mol. Plant Microbe Interact. 26(8):835-843.

Blake C, Christensen MN, Kovács ÁT. 2021. Molecular aspects of plant growth promotion and protection by *Bacillus subtilis*. Mol. Plant Microbe Interact. 34(1):15-25.

Blundell R, Arreguin M, Eskalen A. 2021. In vitro evaluation of grapevine endophytes, epiphytes and sap micro-organisms for potential use to control grapevine trunk disease pathogens. bioRxiv.

Bohn-Courseau I. 2010. Auxin: a major regulator of organogenesis. C. R. Biol. 333(4):290-296.

Bois B, Zito S, Calonnec A. 2017. Climate vs grapevine pests and diseases worldwide: the first results of a global survey. OENO one 51(2-3):133-139.

Bokulich NA, Thorngate JH, Richardson PM, Mills DA. 2014. Microbial biogeography of wine grapes is conditioned by cultivar, vintage, and climate. Proc. Natl. Acad. Sci. U.S.A. 111(1):e139-e148.

Bolger AM, Lohse M, Usadel B. 2014. Trimmomatic: A flexible trimmer for illumina sequence data. Bioinformatics 30:2114–2120.

Bolger AM, Lohse M, Usadel B. 2014. Trimmomatic: a flexible trimmer for Illumina sequence data. Bioinformatics. 30(15):2114-2120.

Bolivar-Anillo HJ, González-Rodríguez VE, Cantoral JM, García-Sánchez D, Collado IG, and Garrido C. 2021. Endophytic bacteria Bacillus subtilis, isolated from Zea mays, as potential biocontrol agent against Botrytis cinerea. Biology 10(6):492.

Booth IR, Louis P. 1999. Managing hypoosmotic stress: aquaporins and medianosensitive channels in Escherichia coli. Curr. Opin. Microbiol. 2(2):166-169.

Borgo M, Pegoraro G, Sartori E. 2016. Susceptibility of grape varieties to esca disease. BIO Web of Conferences 7:0104.

Borriss R. 2011. Use of plant-associated *Bacillu*s strains as biofertilizers and biocontrol agents in agriculture. Bacteria in agrobiology: Plant growth responses. In: Maheshwari DK (ed.) Bacteria in agrobiology: Plant growth responses. Springer-Verlag, Berlin Heidelberg. 41-76.

Bottini R, Cassán F, Piccoli P. 2004. Gibberellin production by bacteria and its involvement in plant growth promotion and yield increase. Appl. Microbiol. Biotechnol. 65(5):497-503.

Bouchard-Rochette M, Machrafi Y, Cossus L, Nguyen TTA, Antoun H, Droit A, Tweddell RJ. 2022. *Bacillus pumilus* PTB180 and *Bacillus subtilis* PTB185: production of lipopeptides, antifungal activity, and biocontrol ability against Botrytis cinerea. Biol. Control 170:104-925.

Boutrot F, Zipfel C. 2017. Function, discovery, and exploitation of plant pattern recognition receptors for broad-spectrum disease resistance. Annu. Rev. Phytopathol. 55:257-286.

Boyd LA, Ridout C, O'Sullivan DM, Leach JE, Leung H. 2013. Plant–pathogen interactions: disease resistance in modern agriculture. Trends in genetics 29(4):233-240.

Brader G, Compant S, Vesci K, Mitter B, Trognitz F, Ma LJ, Sessitsch A. 2017. Ecology and genomic insights into plant-pathogenic and plant-nonpathogenic endophytes. Annu. Rev. Phytopathol. 55(1).

Broberg M, Doonan J, Mundt F. Denman S,McDonald JE. 2018. Integrated multi-omic analysis of host-microbiota interactions in acute oak decline. Microbiome 6(1):1-15.

Broeders S, Huber I, Grohmann L, Berben G, Taverniers I, Mazzara M, et al. 2014. Guidelines for validation of qualitative real-time PCR methods. Trends Food Sci. Technol. 37(2):115-126.

Brotman Y, Briff E, Viterbo A, Chet I. 2008. Role of swollenin, an expansin-like protein from Trichoderma, in plant root colonization. Plant Physiol. 147(2):779-789.

Brue E, Haidar, Alou MT, Vallance, Bertsch C, Mazet F, Fermaud M Deschamps A, Guerin-Dubrana G, Compant S, Rey P. 2015. Bacteria in a wood fungal disease: characterization of bacterial communities in wood tissues of esca-foliar symptomatic and asymptomatic grapevines. Front. Microbiol. 6:1137.

Brue E, Lecomte P, Grosman J, Doublet B, Bertsch, Fontaine F, Ugaglia A, Teissedre P, Da Costa P, Guerin-Dubrana L, Rey P. 2013. Overview of grapevine trunk diseases in France in the 2000s. Phytopathol. Mediterr. 262-275.

Bruez E, Vallance J, Gautie, Laval V, Compant S, Maurer W, Sessitsch A, Lebrun M, Rey P. 2020. Major changes in grapevine wood microbiota are associated with the onset of esca, a devastating trunk disease. Environ. Microbiol. 22(12):5189-5206.

Brunner PC, Torriani SF, Croll D, Stukenbrock EH, McDonald BA. 2013. Coevolution and life cycle specialization of plant cell wall degrading enzymes in a hemibiotrophic pathogen. Mol. Biol. Evol. 30(6):1337-1347.

Buensanteai N, Mukherjee PM, Horwitz BA, Cheng C. 2010. Expression and purification of biologically active *Trichoderma virens* proteinaceous elicitor Sm1 in Pichia pastoris. Protein Express. Purif. 72:131-138.

Caarls L, Pieterse CM, Van Wees SC. 2015. How salicylic acid takes transcriptional control over jasmonic acid signaling. Front. Plant Sci. 6:170.

Calzarano F, Di Marco S, Cesari A. 2004. Benefit of fungicide treatment after trunk renewal of vines with different types of esca necrosis. Phytopathol. Mediterr. 43, 116–23.

Calzarano F, Di Marco S. 2007. Wood discoloration and decay in grapevines with esca proper and their relationship with foliar symptoms. Phytopathol. Mediterr. 46(1):96-101.

Cane DE, Walsh CT, Khosla C. 1998. Harnessing the biosynthetic code: combinations, permutations, and mutations. Science 282(5386):63-68.

Cao FY, Yoshioka K, Desveaux D. 2011. The roles of ABA in plant–pathogen interactions. J. Plant Res. 124(4):489-499.

Caporaso JC, Lauber CL, Costello EK, Berg-Lyons D, Gonzalez A, Stombaugh J, Knights D, Gajer P, Ravel J, Fierer N, et al. 2011. Moving pictures of the human microbiome. Genome Biol. 12:R50.

Cardoza RE, Vizcaino JA, Hermosa MR, Gonzalez FJ, Llobell A, Monte M, Gutierrez S. 2006. Cloning and characterization of the erg1 gene of *Trichoderma harzianum*: Effect of the erg1 silencing on ergosterol biosynthesis and resistance to terbinafine. Fungal Genet. Biol. 43:164-178.

Carlucci, Francesco L, Mostert L, Halleen F, Raimondo ML. 2017. Occurrence fungi causing black foot on young grapevines and nursery rootstock plants in Italy. Phytopathol. Mediterr. 56(1):10–39.

Carter MV. 1991. The status of *Eutypa lata* as a pathogen. Monogr. Phytopathol. Pap. No 32. Commonwealth Agricultural Bureau, International Mycological Institute, Wallingford, Oxfordshire, U.K.

Caulier S, Nannan C, Gillis A, Licciardi F, Bragard C, Mahillon J. 2019. Overview of the antimicrobial compounds produced by members of the Bacillus subtilis group. Front. microbiol. 10, 302.

Chacon JL, Gramaje D, Izquierdo PM, Martínez J, Mena A. 2020. Evaluation of six red grapevine cultivars inoculated with Neofusicoccum parvum. Eur. J. Plant Pathol. 158,811–815

Chacón JL, Gramaje D, Izquierdo PM, Martínez J, Mena A. 2020. Evaluation of six red grapevine cultivars inoculated with *Neofusicoccum parvum*. Eur. J. Plant Pathol. 158(3):811-815.

Chacón-Vozmediano JL, Gramaje D, León, Armengol J, Moral J, Izquierdo-Cañas PM, and Martínez-Gascueña J. 2021. Cultivar Susceptibility to Natural Infections Caused by Fungal Grapevine Trunk Pathogens in La Mancha Designation of Origin (Spain). Plants 10(6):1171.

Chacón-Vozmediano JL, Martínez-Gascueña J, Ramos MC. 2021. Projected effects of climate change on Tempranillo and Chardonnay varieties in La Mancha Designation of Origin. Agron. Sustain. Dev. 41(2):1-14.

Chapelle E, Mendes R, Bakker PAH, Raaijmakers JM. 2016. Fungal invasion of the rhizosphere microbiome. ISME J 10(1):265-268.

Chen F, Gao Y, Chen X, Yu Z, Li X. 2013. Quorum quenching enzymes and their application in degrading signal molecules to block quorum sensing-dependent infection. Int. J. Mol. Sci. 14(9):17477-17500.

Chen G, Wu P, Wang J, Zhang P, Jia Z. 2022. Ridge–furrow rainfall harvesting system helps to improve stability, benefits and precipitation utilization efficiency of maize production in Loess Plateau region of China. Agric. Water Manag. 261:107360.

Chen H, Xiao X, Wang J, Wu L, Zheng Z, Yu Z. 2008. Antagonistic effects of volatiles generated by *Bacillus subtilis* on spore germination and hyphal growth of the plant pathogen, Botrytis cinerea. Biotechnol. 30:919-923.

Chen L, Shi H, Heng J, Wang D, Bian K. 2019. Antimicrobial, plant growth-promoting and genomic properties of the peanut endophyte *Bacillus velezensis* LDO2. Microbiol. Res. 218:41-48.

Chen Y, Yan F, Chai Y, Liu H, Kolter R, Losick R, Guo JH. 2013. Biocontrol of tomato wilt disease by *Bacillus subtilis* isolates from natural environments depends on conserved genes mediating biofilm formation. Environ. Microbiol. 15:848-864.

Chet I, Harman GE, Baker R. 1981. *Trichoderma hamatum*: Its hyphal interactions with *Rhizoctonia solani* and *Pythium* spp. Microb. Ecol. 7(1):29-38.

Cheung LK, Dupuis JH, Dee DR, Bryksa BC, Yada RY. 2020. Roles of plant-specific inserts in plant defense. Trends Plant Sci. 25(7):682-694

Chong J, Liu P, Zhou G, Xia J. 2020. Using MicrobiomeAnalyst for comprehensive statistical, functional, and meta-analysis of microbiome data. Nat. Protoc. 15:799–821.

Chooi YH, Krill C, Barrow RA, Chen S, Trengove R, Oliver RP, Solomon PS. 2015. An in planta-expressed polyketide synthase produces (R)-mellein in the wheat pathogen *Parastagonospora nodorum.* Appl. Environ. Microbiol. 81(1):177-186.

Choudhary DK, Prakash A, Johri BN. 2007. Induced systemic resistance (ISR) in plants: mechanism of action. Indian J. Microbiol. 47(4):289-297.

Christen, Schönmann, S, Jermini M, Strasser RJ, Défago G. 2007. Characterization and early detection of grapevine (*Vitis vinifera*) stress responses to esca disease by *in situ* chlorophyll fluorescence and comparison with drought stress. Environ. Exp. Bot. 60(3):504-514.

Chun J, Yang HE, Kim DH. 2018. Identification of a novel partitivirus of *Trichoderma harzianum* NFCF319 and evidence for the related antifungal activity. Front. Plant Sci. 9:1699.

Ciesla WM, Donaubauer E. 1994. Decline and dieback of trees and forests: a global overview.

Claverie M, Notaro M, Fontaine F, Wéry J. 2020. Current knowledge on Grapevine Trunk Diseases with complex etiology: A systemic approach. Phytopathol. Mediterr. 59(1), 29-53.

Cloete M, Fischer M, Mostert L, Halleen F. 2015. Hymenochaetales associated with esca-related wood rots on grapevine with a special emphasis on the status of esca in South African vineyards. Phytopathol. Mediterr. 299-312.

Cobos ME, Peterson AT, Barve N, Osorio-Olvera L. 2019. kuenm: an R package for detailed development of ecological niche models using Maxent. PeerJ 7:e6281.

Cobos R, Calvo-Peña C, Álvarez-Pérez JM, Ibáñez A, Diez-Galán A, González-García S, et al. 2019. Necrotic and cytolytic activity on grapevine leaves produced by Nep1-like proteins of *Diplodia seriata*. Front. Plant Sci. 10, 1282.

Compant S, Brader G, Muzammil S, Sessitsch A, Lebrihi A, Mathieu F. 2013. Use of beneficial bacteria and their secondary metabolites to control grapevine pathogen diseases. BioControl. 58(4), 435-455.

Compant S, Mathieu F. 2017. Biocontrol of major grapevine diseases: leading research, 231 CABI, Wallingford, UK, 160–170.

Conrath U, Beckers GJ, Langenbach CJ, Jaskiewicz MR. 2015. Priming for enhanced defense Annu. Rev. Phytopathol. 53, 97-119.

Conrath U, Thulke O, Katz V, Schwindling S, Kohler A. 2001. Priming as a mechanism in induced systemic resistance of plants. Eur. J. Plant Pathol. 107(1), 113-119.

Cordovez V, Dini-Andreote F, Carrión VJ, Raaijmakers JM. 2019. Ecology and evolution of plant microbiomes. Annu. Rev. Microbiol. 73:69-88.

Corso, M., Vannozzi, A., Maza, E., Vitulo, N., Meggio, F., Pitacco, A., et al. (2015). Comprehensive transcript profiling of two grapevine rootstock genotypes contrasting in drought susceptibility links the phenylpropanoid pathway to enhanced tolerance. J. Exp. Bot. 66(19), 5739-5752.

Crous PW, Groenewald JZ, Risede JM and Hywel-Jones NL, Calonectria species and their Cylindrocladium anamorphs: species with sphaeropedunculate vesicles. Stud Mycol 50:415–429 (2004)

Dakin N, White D, Hardy GESJ, Burges TI. 2010. The opportunistic pathogen, *Neofusicoccum australe*, is responsible for crown dieback of peppermint (*Agonis flexuosa*) in Western Australia. Australas. Plant Pathol. 39(2):202-206.

Daou M, Faulds CB. 2017. Glyoxal oxidases: their nature and properties. World J. Microbiol. Biotechnol. 33(5):1-11.

Daraignes L, Gerbore J, Yacoub A, Dubois L, Romand C, Zekri O, Roudet J, Chambon P, Fermaud M. 2018. Efficacy of *P. oligandrum* affected by its association with bacterial BCAs and rootstock effect in controlling grapevine trunk diseases. Biol Control 119:59-67.

Darriaut R, Lailheugue V, Masneuf-Pomarède I, Marguerit E, Martins G, Compans S, et al. 2022. Grapevine rootstock and soil microbiome interactions: Keys for a resilient viticulture. Hortic Res 9.

Davey ME, O'toole GA. 2000. Microbial biofilms: from ecology to molecular genetics. Microbiol. Mol. Biol. Rev. 64(4):847-867.

De Andrés M, Benito A, Pérez-Rivera G, Ocete R, Lopez MA, Gaforio L, et al. 2012. Genetic diversity of wild grapevine populations in Spain and their genetic relationships with cultivated grapevines. Mol. Ecol. 21(4):800-816.

De Vleesschauwer D, Höfte M. 2009. Rhizobacteria-induced systemic resistance. Adv. Bot. Res. 51, 223-281.

Del Frari G, Gobbi A, Aggerbeck MR, Oliveira H, Hansen LH, Ferreira RB. 2019. Characterization of the wood mycobiome of *Vitis vinifera* in a vineyard affected by esca. Spatial distribution of fungal communities and their putative relation with leaf symptoms. Front. Plant Sci. 10:910.

Devendra J, De SS, Indra P, Arul S, Udayasuriya V. 2007. Cloning of cry2Ab gene from a new indigenous isolate of *Bacillus thuringiensis*. In Recent trends in horticultural biotechnology, Vol. II. ICAR national symposium on biotechnological interventions for improvement of horticultural crops: issues and strategies, Vellanikkara, Kerala, India, 10-12 January. 699-702.

Deyett E, Rolshausen PE. 2020. Endophytic microbial assemblage in grapevine. FEMS Microbiol. Ecol. 96(5):53.

Di Marco S, Cesari A.Osti, F. 2004. Experiments on the Control of Esca by" *Thricoderma*". 1000-1008.

Di Marco S, Osti F, Cesari A, Calzarano F, Roberti R. 2002. Vol. 2: Funghi, batteri e virus: Attività di specie di" *trichoderma*" nei confronti di" *Phaeomoniella chlamydospora*", patogeno associato al mal dell'esca della vite. 2:1000-1006.

Di Marco S, Osti F, Cesari A. 2004. Experiments on the control of esca by Trichoderma. Phytopathol. Mediterr. 43, 108–15.

Di Marco S, Osti F, Roberti R, Calzarano F, Cesari A. 2002. Attivita` di specie di 412 Trichoderma nei confronti di Phaeomoniella chlamydospora, patogeno associato al mal delll'esca 413 della vite. Atti Soc. Ital. Sci. Nat. 2, 419–424.

Dissanayake A, Purahong, W, Wubet T, Hyd KD, Zhang W, Xu H, Xing Q, Li X, Yan J. 2018. Direct comparison of culture-dependent and culture-independent molecular approaches reveal the diversity of fungal endophytic communities in stems of grapevine (*Vitis vinifera*). Fungal Divers. 90(1):85-107.

Dissanayake AJ, Liu M, Zhang W, Chen Z, Udayanga D, Chukeatirote E, Li H, Yan JY, Hyde KD. 2015. Morphological and molecular characterisation of Diaporthe species associated with grapevine trunk disease in China. Fungal Biol. 119:283-294.

Dixit P, Mukherjee PK, Ramachandran V, Eapen S. 2011. Glutathione transferase from *Trichoderma virens* enhances cadmium tolerance without enhancing its accumulation in transgenic *Nicotiana tabacum*. PLoSONE 6(1):1-15.

Djoukeng JD, Polli S, Larignon P, Abou-Mansour E. 2009. Identification of phytotoxins from *Botryosphaeria obtusa*, a pathogen of black dead arm disease of grapevine. Eur. J. Plant Pathol. 124(2):303-308.

Dries L, Bussotti S, Pozzi, Kunz R, Schnell S, Löhnertz O, Vortkamp A. 2021. Rootstocks shape their microbiome—bacterial communities in the rhizosphere of different grapevine rootstocks. Microorganisms 9(4):822.

Duanis-Assaf D, Steinberg D, Chai Y, Shemesh M. 2016. The LuxS based quorum sensing governs lactose induced biofilm formation by Bacillus subtilis. Front. Microbiol. 6:1517.

Dufour MC, Druelle L, Corio-Costet MF. 2013. BioMolChem tools used in the vineyard to predict grapevine protection against downy mildew after elicitation. Working Group “Induced resistance in plants against insects and diseases” 89:462.

Dufour MC, Lambert, Bouscaut J, Mérillon JM, Corio-Costet MF. 2013. Benzothiadiazole-primed defence responses and enhanced differential expression of

defence genes in *Vitis vinifera* infected with biotrophic pathogens Erysiphe necator and Plasmopara viticola. Plant Pathol. 62(2), 370-382.

Durrant WE, Dong X. 2004. Systemic acquired resistance. Ann. review phytopathol. 42(1):185-209.

Dutta S, Kundu A, Chakraborty M, Ojha S, Chakrabarti J, Chatterjee N. 2006. Production and optimization of Fe (III) specific ligand, the siderophore of soil inhabiting and wood rotting fungi as deterrent to plant pathogens. Acta Phytopathol. Entomol. Hung. 41(3-4):237-248.

Ebeed HT, Hassan NM, Aljarani AM. 2017. Exogenous applications of Polyamines modulate drought responses in wheat through osmolytes accumulation, increasing free polyamine levels and regulation of polyamine biosynthetic genes. Plant Physiol. Biochem. 118:438-448.

Edwards J, Laukart N, Pasco IG. 2001. In situ sporulation of *Phaeomoniella chlamydospora* in the vineyard. Phytopathol. Mediterr. 40:61-66.

Edwards J, Pascoe IG. 2004. Occurrence of *Phaeomoniella chlamydospora* and *Phaeoacremonium aleophilum* associated with Petri disease and esca in Australian grapevines. Aust. Plant Pathol. 33:273-279.

Edwards, Constable F, Wiechel T, Salib S. 2007. Comparison of the molecular tests-single PCR, nested PCR and quantitative PCR (SYBR Green and TaqMan)—for detection of *Phaemoniella chlamydospora* during grapevine nursery propagation. Phytopathol. Mediterr. 46:58–72.

Eichmeie A, Peèenka J, Peòázová E, Baránek M, Català-García S, León M, et al. 2018. High-throughput amplicon sequencing-based analysis of active fungal communities inhabiting grapevine after hot-water treatments reveals unexpectedly high fungal diversity. Fungal Ecol. 36:26–38.

El-Tarabily KA, Sivasithamparam K. 2006. Non-streptomycete actinomycetes as biocontrol agents of soil-borne fungal plant pathogens and as plant growth promoters. Soil Biol Biochem 38(7), 1505-1520.

El-Tarabily KA. 2006. Rhizosphere-competent isolates of streptomycete and non-streptomycete actinomycetes capable of producing cell-wall-degrading enzymes to control Pythium aphanidermatum damping-off disease of cucumber. Botany. 84(2), 211-222.

Elad Y. 2000. Biological control of foliar pathogens by means of Trichoderma harzianum and potential modes of action. Crop Prot. 19, 709–714.

Elena G, Luque J. 2016. Pruning debris of grapevine as a potential inoculum source of *Diplodia seriata*, causal agent of Botryosphaeria dieback. Eur. J. Plant Pathol. 144(4):803-810.

Elkoca E, Kantar F, Sahin F. 2007. Influence of nitrogen fixing and phosphorus solubilizing bacteria on the nodulation, plant growth, and yield of chickpea. J. Plant Nutr. 31:157-171.

Eltlbany N, Baklawa M, Ding G-C, Nassal, Weber N., Kandeler E. 2019. Enhanced tomato plant growth in soil under reduced P supply through microbial inoculants and microbiome shifts. FEMS Microbiol. Ecol. 95:124.

endophytes: diversity and functional roles. New phytologist 182(2):314-330.

Erbs G. Newmann MA. 2003. The role of lipopolysaccharides in induction of plant defense responses. Mol. Plant Pathol. 4:421–425.

Errington J. 1993. *Bacillus subtilis* sporulation: regulation of gene expression and control of morphogenesis. Microbiol. Rev. 57(1):1-33.

Eskalen A, Gubler D. 2001. Association of spores of *Phaeomoniella chlamydospora, Phaeoacremonium inflatipes, and Pm. aleophilum* with grapevine cordons in California. Phytopathol. Mediterr. 40S:429-432.

Evidente A, Punzo B, Andolfi A, Cimmino A, Melck D, Luque J. 2010. Lipophilic phytotoxins produced by *Neofusicoccum parvum*, a grapevine canker agent. Phytopathol. Mediterr. 49(1):74-79.

Farace G, Fernandez O, Jacquens L, Coutte F, Krier F, Jacques P, Dorey S. 2015. Cyclic lipopeptides from B acillus subtilis activate distinct patterns of defence responses in grapevine. Mol Plant Pathol 16(2):177-187.

Felix G, Duran JD, Volko S, Boller T. 1999. Plants have a sensitive perception system for the most conserved domain of bacterial flagellin. Plant J. 18(3):265-276.

Ferreira JHS, Matthee FN, Thomas AC. 1991. Biological control of Eutypa lata on grapevine by an antagonistic strain of Bacillus subtilis. Phytopathology 81:283–7.

Field D, Garrity G, Gray T, Morrison N, Selengut J, Sterk P, et al. 2008. The minimum information about a genome sequence (MIGS) specification. Nat. Biotechnol. 26(5):541-547.

Finking R, Marahiel MA. 2004. Biosynthesis of nonribosomal peptides. Annu. Rev. Microbiol. 58:453-488.

Finn RD, Coggill P, Eberhardt RY, Eddy SR, Mistry J, Mitchell AL, et al. 2016. The Pfam protein families database: towards a more sustainable future. Nucleic Acids Res. 44(1):279-285.

Fira D, Dimkić I, Berić T, Lozo J, Stanković S. 2018. Biological control of plant pathogens by Bacillus species. J Biotechnol 285:44-55.

Fischer M. 2002. A new wood-decaying basidiomycete species associated with esca of grapevine: *Fomitiporia mediterranea* (Hymenochaetales). Mycol. Prog. 1:315-324.

Flor HH. 1971. Current status of the gene-for-gene concept. Annu. Rev. Phytopathol. 9(1):275-296.

Fontaine F, Gramaje D, Armengol J, Smart R, Nagy ZA., Borgo M, Rego C, Corio-Costet MF. 2016a. Grapevine trunk diseases. A review. OIV Publications, 24:979.

Fontaine F, Pinto C, Vallet J, Clément C, Gome AC, Spagnolo A. 2016b. The effects of grapevine trunk diseases (GTDs) on vine physiology. Eur. J. Plant Pathol. 144(4):707-721.

Fotio B. Sotirios V, Elena P, Anastasios S, Stefanos T, Danae G, Tavlaki G, Tzima A, Paplomatas E, Markakis E, Karaoglanidis G, Papadupoulou K, Dimitrios KG. 2021. Grapevine wood microbiome analysis identifies key fungal pathogens and potential interactions with the bacterial community implicated in grapevine trunk disease appearance. Environ. microbiome 16(1):1-17.

Fotouhifar KB, Hedjaroude GA, Leuchtmann A. 2010. ITS rDNA phylogeny of Iranian strains of *Cytospora* and associated teleomorphs. Mycologia 102:1369–82.

Fourie PH, Halleen F. 2001. Diagnosis of fungal diseases and their involvement in 13 dieback disease of young vines. Wynboer 149 1:19-23.

Fourie PH, Halleen F. 2004. Occurrence of grapevine trunk disease pathogens in rootstock mother plants in South Africa. Aust. Plant Pathol. 33:313-315.

Fourie PH, Halleen F. 2006 Chemical and biological protection of grapevine propagation material from trunk disease pathogens. Eur J Plant Pathol 116:255-265.

Franks T, Botta R, Thomas MR, Franks J. 2002. Chimerism in grapevines: implications for cultivar identity, ancestry and genetic improvement. Theor. Appl. Genet. 104(2):192-199.

Fujimori N, Suzuki N, Nakajima Y, Suzuki S. 2014. Plant DNA-damage repair/toleration 100 protein repairs UV-B-induced DNA damage. DNA repair 21:171-176.

Fussler, Kobes, N, Bertrand F, Maumy , Grosman J, Savary S. 2008. A characterization of grapevine trunk diseases in France from data generated by the National Grapevine Wood Diseases Survey. Phytopathol. 98(5):571-579.

Gadhave KR, Devlin PF, Ebertz, Ross A, Gange AC. 2018. Soil inoculation with Bacillus spp. modifies root endophytic bacterial diversity, evenness, and community composition in a context-specific manner. Microbial Ecology 76(3):741-750.

Gadoury DM, CADLE-DAVIDSON LANCE, Wilcox WF, Dry IB, Seem RC, Milgroom MG. 2012. Grapevine powdery mildew (Erysiphe necator): a fascinating system for the study of the biology, ecology and epidemiology of an obligate biotroph. Mol. plant pathol. 13(1):1-16.

Gamir J, Darwiche R, Van't Hof P, Choudhary V, Stumpe M, Schneiter R, Mauch F. 2017. The sterol-binding activity of PATHOGENESIS-RELATED PROTEIN 1 reveals the mode of action of an antimicrobial protein. The Plant Journal 89(3):502-509.

Ganson RJ, d'Amato TA, Jensen RA. 1986. The two-isozyme system of 3-deoxy-D-arabino-heptulosonate 7-phosphate synthase in Nicotiana silvestris and other higher plants. Plant Physiol. 82(1):203-210.

Gao G, Yin, Chen S, Xia F, Yang J, Li Q, Wang W. 2012. Effect of biocontrol agent Pseudomonas fluorescens 2P24 on soil fungal community in cucumber rhizosphere using T-RFLP and DGGE. PLoS One 7:e31806.

Garcia-Brugger A, Lamotte O, Vandelle E, Bourque S, Lecourieux D, Poinssot B, et al. 2006. Early signaling events induced by elicitors of plant defenses. Mol. Plant Microbe Interact.19(7):711-724.

Garcia JF, Lawrence D, Morales-Cruz A, Travadon R, Minio A, Hernandez-Martinez R, Roulshausen P, Baumgartener K, Cantu D. 2021. Phylogenomics of plant-associated Botryosphaeriaceae species. Front. Microbiol. 12:652-802.

Gardes M, Bruns TD. 1993. ITS primers with enhanced specificity for basidiomycetes: application to the identification of mycorrhizae and rusts. Mol Ecol 2:113–118.

Garbeva P, Van Veen JA, Van Elsas JD. 2004. Microbial diversity in soil: selec- tion microbial populations by plant and soil type and implications for disease suppressiveness. Annu. Rev. of Phytopathol. 42:243–270.

Gessler C, Pertot I, Perazzolli M. 2011. Plasmopara viticola: a review of knowledge on downy mildew of grapevine and effective disease management. Phytopathol. Mediterr. 50(1):3-44.

Ge SX, Jung D, Ya R. 2020. ShinyGO: a graphical gene-set enrichment tool for animals and plants. Bioinformatics 36(8):2628-2629.

Ghazanfar MU, Raza M, Raza W, Qamar MI. 2018. Trichoderma as potential biocontrol agent, its exploitation in agriculture: a review. Int J Plant Prot 2(3):109-135.

Gindro K, Pezet R, Viret O. 2003. Histological study of the responses of two *Vitis vinifera* cultivars (resistant and susceptible) to Plasmopara viticola infections. Plant Physiol. Biochem. 41(9):846-853.

Giovannoni M, Gramegna G, Benedetti M, Mattei B. 2020. Industrial use of cell wall degrading enzymes: the fine line between production strategy and economic feasibility. Front. bioeng. biotechnol. 8:356.

Gkiz D, Poulaki EG, Tjamos SE. 2021. Towards Biological Control of Aspergillus carbonarius and Botrytis cinerea in Grapevine Berries and Transcriptomic Changes of Genes Encoding Pathogenesis-Related (PR) Proteins. Plants 10(5):970.

Glass NL, Donaldson GC. 1995. Development of primer sets designed for use with the PCR to amplify conserved genesfrom filamentous infection due to Phaeoacremonium spp. J Clin Microbiol 41:1332–1336.

Glick BR. 2012. Plant growth-promoting bacteria: mechanisms and applications. Scientifica. 2012(5):963401.

Glick BR. 2014. Bacteria with ACC deaminase can promote plant growth and help to feed the world. Microbiol. Res. 169(1):30-39.

Gómez-Góme L. 2004. Plant perception systems for pathogen recognition and defense. Mol. Immunol. 41:1055–1062.

Gonzalez V, Tello ML. 2011. The endophytic mycota associated with *Vitis vinifera* in central Spain. Fungal Divers. 47:29–42.

Gordon J, Knowlton N, Relman DA, Rohwer F, Youle M. 2013. Superorganisms and holobionts. Microbe 8(4):152-153.

Gramaj D, Urbez-Torres JR, Sosnowski MR. 2018. Managing grapevine trunk diseases with respect to etiology and epidemiology: current strategies and prospects. Plant Dis. 102(1):12-39.

Gramaje D, Armengol J. 2011. Fungal trunk pathogens in the grapevine propagation process: potential inoculum sources, detection, identification, and management strategies. Plant Dis 95(9): 1040-1055.

Gramaje D, Armengol J. 2011. Fungal trunk pathogens in the grapevine propagation process: potential inoculum sources, detection, identification, and management strategies. Plant Dis. 95(9):1040-1055.

Gramaje D, Baumgartner K, Halleen F, Mostert L, Sosnowski MR, Úrbez-Torres R, Armengol J. 2016. Fungal trunk diseases: a problem beyond grapevines?. Plant Pathol. 65(3):355-356.

Gramaje D, Di Marco S. 2015. Identifying practices likely to have impacts on grapevine trunk disease infections: a European nursery survey. Phytopathol. Mediterr. 313-324.

Gramaje D, Eichmeier A, Spetik M, Carbone MJ, Bujanda R, Vallance J, Rey P. 2022. Exploring the temporal dynamics of the fungal microbiome in rootstocks, the lesser-known half of the grapevine crop. J. Fungus 8(5):421.

Gruau C, Trotel-Aziz P, Villaume S, Rabenoelina F, Clément C, Baillieul F, et al. 2015. Pseudomonas fluorescens PTA-CT2 triggers local and systemic immune response against Botrytis cinerea in grapevine. Mol. Plant Microbe Interact. 28, 1117–1129.

Guan X, Essakhi S, Laloue H, Nick P, Bertsch C, Chong J. 2016. Mining new resources for grape resistance against Botryosphaeriaceae: a focus on *Vitis vinifera subsp. sylvestris*. Plant Pathol. 65(2):273-284.

Guarnaccia, Groenewald JZ, Woodhall J, Armengol J, Cinelli T, Eichmeier A, Crous PW. 2018. Diaporthe diversity and pathogenicity revealed from a broad survey of grapevine diseases in Europe. Pers. Mol. Phylogenet. Evol. 40:135–153.

Guerin-Dubrana L, Fontaine F, Mugnai L. 2019. Grapevine trunk disease in European and Mediterranean vineyards: occurrence, distribution and associated disease-affecting cultural factors. Phytopathol. Mediterr. 58(1):49-71.

Guetsky R, Shtienberg D, Elad Y, Fischer E, Dinoor A. 2002. Improving biological control by combining biocontrol agents each with several mechanisms of disease suppression. Phytopathology. 92: 976-985.

Guetsky R., Shtienberg D, Elad Y, Dinoor A. 2001. Combining biocontrol agents to reduce the variability of biological control. Phytopathol. 91(7):621-627.

Gujjar RS, Pathak AD, Karkute SG, Supaibulwatan K 2019. Multifunctional proline rich proteins and their role in regulating cellular proline content in plants under stress. Biol. Plant 63:448-454.

Gurevich A, Saveliev V, Vyahhi N, Tesler G. 2013. QUAST: quality assessment tool for genome assemblies. Bioinformatics. 29(8):1072-1075.

Haft DH, Selengut JD, White O. 2003. The TIGRFAMs database of protein families. Nucleic Acids Res. 31(1):371-373.

Haidar R, Deschamps, Roudet J, Calvo-Garrido C, Bruez E, Rey P, Fermaud M. 2016. 451 Multi-organ screening of efficient bacterial control agents against two major pathogens of 452 grapevine. Biological Control. 92: 55–65.

Haidar R, Fermaud M, Calvo-Garrido C, Roudet J, Deschamps A. 2016. Modes of action for biological control of *Botrytis cinerea* by antagonistic bacteria. Phytopathol. Mediterr. 301-322.

Halleen F, Crous PW. 2006. A review of black foot disease of grapevine. A Review of Black Foot Disease of Grapevine 1:1000-1013.

Halleen F, Fouri PH, Lombard PJ. 2010. Protection of grapevine pruning wounds against *Eutypa lata* by biological and chemical methods. S. Afr. J. Enol. Vitic. 31(2):125-132.

Halleen F, Fourie PH, Crous PW. 2007. Control of black foot disease in grapevine nurseries. Plant Pathol 56:637-645.

Halleen F, Fourie PH. 2016. An integrated strategy for the proactive management of grapevine trunk disease pathogen infections in grapevine nurseries. S. Afr. J. Enol. Vitic. 37(2):104-114.

Hamiduzzaman MM, Jakab G, Barnavon L, Neuhaus JM, Mauch-Mani B. 2005. β-Aminobutyric acid-induced resistance against downy mildew in grapevine acts through the potentiation of callose formation and jasmonic acid signaling. Mol Plant Microbe Interact. 18(8):819-829.

Hamon MA, Lazazzera BA. 2001. The sporulation transcription factor Spo0A is required for biofilm development in Bacillus subtilis. Mol. Microbiol. 42(5):1199-1209.

Harman GE. 2006. Overview of Mechanisms and Uses of *Trichoderma s*pp. Phytopathol. 96(2):190-194.

Hashem A, Tabassum B, ABOTallah EF. 2019. *Bacillus subtilis*: A plant-growth promoting *rhizobacterium* that also impacts biotic stress. Saudi J. Biol. Sci. 26(6):1291-1297.

Hashimoto A, Hirayama K, Takahashi H, Matsumura M, Okada G, Chen CY, et al. 2018. Resolving the Lophiostoma bipolare complex: Generic delimitations within Lophiostomataceae. Stud. Mycol. 90(1):161-189.

Hayat R, Ali S, Amara U, Khalid R, Ahmed I. 2010. Soil beneficial bacteria and their role in plant growth promotion: a review. Ann. Microbiol. 60(4):579-598.

He R, Zhuang Y, Cai Y, Agüero CB, Liu S, Wu J, et al. 2018. Overexpression of 9-cis-epoxycarotenoid dioxygenase cisgene in grapevine increases drought tolerance and results in pleiotropic effects. Front. Plant Sci. 9:970.

Heloir MC, Adrain M, Brulé D, Claverie M, Cordelier S, Daire X, Dorey S, Gauthier A, Lemaître-Guillier C, Negrel J, Trdá L, Trouvelot S, Vandelle E, Poinssot B. 2019. Recognition of Elicitors in Grapevine: From MAMP and DAMP Perception to Induced Resistance. Front. Plant Sci. 10:1117.

Henrichsen J. 1972. Bacterial surface translocation: a survey and a classification. Bacteriol Rev. 36(4):478.

Hermosa R, Botella L, Keck M, Jimenez JA, MonteroBarrientos M, Arbona V, GomezCadenas A, Monte E, Nicolas C. 2011. The overexpression in *Arabidopsis thaliana* of a *Trichoderma harzianum* gene that modulates glucosidase activity, and enhances tolerance to salt and osmotic stresses. J. Plant Physiol. 168:1295-1302.

Hermosa R, Viterbo A, Chet I, Monte E. 2012. Plant-beneficial effects of Trichoderma and of its genes. Microbiol. 158(1):17-25.

Hofstetter V, Buyck B, Croll D, Viret O, Couloux A, Gindro K. 2012. What if esca disease of grapevine were not a fungal disease?. Fungal Divers. 4:51–67.

Horbach R, Navarro-Quesada AR, Knogge W, Deising HB. 2011. When and how to kill a plant cell: infection strategies of plant pathogenic fungi. J. Plant Physiol. 168(1):51-62.

Horton NJ, Kleinma K. 2015. Using R and RStudio for data management, statistical analysis, and graphics. CRC Press.

Hou Y, Zhai YI, Feng LI, Karimi HZ, Rutter BOT, Zeng L, Gu W, Chen X, Ye W, Innes R, Zhai J, Ma W. 2019. A Phytophthora effector suppresses trans-kingdom RNAi to promote disease susceptibility. Cell Host Microb. 25(1):153-165.

Hrycan J, Hart M, Bowen P, Forge T, Urbez-Torres JR. 2020. Grapevine trunk disease fungi: their roles as latent pathogens and stress factors that favour disease develop-ment and symptom expression. Phytopathol. Mediterr. 59:395-424.

Huang X-F, Chaparro JM, Reardon KF, Zhang R, Shen Q, Vivanco JM. 2014. Rhizosphere interactions: root exudates, microbes, and microbial communities. Botany. 92(4):267-275.

Hunt JS, Gale DSJ, Harvey IC. 2001. Evaluation of Trichoderma as bio-control for protection against wood-invading fungi implicated in grapevine trunk diseases. Phytopathol. Mediterr. 40:S485–6.

Hunter JJ, Volschenk CG, Le Roux DJ, Fouché GW, Adams L. 2004. Plant Material Quality, a compilation of research. Research Reports, ARC Infruitec-Nietvoorbij, Stellenbosch, South Africa.

Hyatt D, Chen G, Locascio P, Land M, Larimer F, Hauser L. 2010. BMC bioinformatics [electronic resource]. BMC Bioinform. 11:119-119.

Imazio S, Maghradze D, De Lorenzis G, Bacilieri R, Laucou V, This P, et al. 2013. From the cradle of grapevine domestication: molecular overview and description of Georgian grapevine (*Vitis vinifera* L.) germplasm. Tree Genet. Genomes. 9(3):641-658.

Jacobs K, Bergdahl DR, Wingfield MJ, Halik S, Seifert KA, Bright DE et al. 2004. Leptographium wingfieldii introduced into North America and found associated with exotic Tomicus piniperda and native bark beetles. Mycol. Res 108:411–418.

Jacquemyn H, Duffy KJ, Selosse MA. 2017. Biogeography of orchid mycorrhizas. In Biogeography of mycorrhizal symbiosis 159-177. Springer, Cham.

Jaroszuk-Ściseł J, Tyśkiewicz R, Nowak A, Ozimek E, Majewska M, Hanaka A, Tyśkiewicz K, Pawlik A, Janusz G. 2019. Phytohormones (auxin, gibberellin) and ACC deaminase in vitro synthesized by the mycoparasitic *Trichoderma* DEMTkZ3A0 strain and changes in the level of auxin and plant resistance markers in wheat seedlings inoculated with this strain conidia. nt. J. Mol. Sci. 20(19):4923.

Jiemeng T, Meng D, Qin C, Liu X, Liang Y, Xiao Y, et al. 2018. Integrated network analysis reveals the importance of microbial interaction for maize growth. Appl. Microbiol. Biotechnol. 102(8):3805–18.

John S, Scott ES Wicks T, Hunt J. 2004. Interactions between Eutypa lata and Trichoderma harzanium. Phytopathol. Mediterr. 43:95–104.

John S, Wicks TJ, Hunt JS, Lorimer MF, Oakey H, Scott ES. 2005. Protection of grapevine pruning wounds from infection by *Eutypa lata* using *Trichoderma harzianum* and *Fusarium lateritium*. Australas. Plant Pathol. 34(4):569-575.

John S, Wicks TJ, Hunt JS, Scott ES. 2008. Colonization of grapevine wood by *Trichoderma harzianum* and *Eutypa lata*. Aust. J. Grape Wine Res. 14(1):18-24.

Johnson JA, Zineh I, Puckett BJ, McGorray SP, Yarandi HN, Pauly DF. 2003. β1-Adrenergic receptor polymorphisms and antihypertensive response to metoprolol. Clin. Pharm. Therap. 74(1):44-52.

Jones JD, Dangl JL. 2006. The plant immune system. Nature 444(7117):323-329.

Jose J, Ghantasala S, Roy Choudhury S. 2020. Arabidopsis transmembrane receptor-like kinases (RLKs): a bridge between extracellular signal and intracellular regulatory machinery. Int. J. Mol. Sci. 21(11):4000.

Kanehisa M, Sato Y, Furumichi M, Morishima K, Tanabe M. 2019. New approach for understanding genome variations in KEGG. Nucleic Acids Res. 47(1):590-595.

Karlovsky P. 1999. Biological detoxification of fungal toxins and its use in plant breeding, feed and food production. Natural Toxins. 7:1-23.

Kenfaoui J, Radouane N, Mennani M, Tahiri A, El Ghadraoui L, Belabess Z, Fontaine F, Hams H, Amiri S, Lahladi R, Barka EA. 2022. A Panoramic View on Grapevine Trunk Diseases Threats: Case of Eutypa Dieback, Botryosphaeria Dieback, and Esca Disease. J. Fungi 8(6):595.

Khattab IM, Sahi VP, Baltenweck , Maia-Grondard A, Hugueney P, Bieler E, Dürrenberger M, Riemann M, Nick P. 2021. Ancestral chemotypes of cultivated grapevine with resistance to Botryosphaeriaceae-related dieback allocate metabolism towards bioactive stilbenes. New Phytol. 229(2):1133-1146.

Klein D. 2002. Quantification using real-time PCR technology: applications and limitations. Trends Mol Med0 8(6):257-260.

Kloepper JW, Ryu C-M, Zhang S. 2004. Induced systemic resistance and promotion of plant growth by Bacillus spp. Phytopathology. 94(11):1259-1266.

Knogge W. 1996. Fungal infection of plants. The Plant Cell 8(10):1711.

Kogel KH, Franken P, Hückelhoven R. 2006. Endophyte or parasite–what decides?. Curr. Opin. Plant Biol. 9(4):358-363.

Köhl J, Booij K, Kolnaar R, Ravensberg WJ. 2019. Ecological arguments to reconsider data requirements regarding the environmental fate of microbial biocontrol agents in the registration procedure in the European Union. BioControl 64(5):469-487.

Konietzny U, Greiner R. 2004. Bacterial phytase: potential application, in vivo function and regulation of its synthesis. Braz. J. Microbiol. 35(1-2):12-18.

Koo B, Adriano D, Bolan N, Barton C. 2005. Root exudates and microorganisms. In: Hillel D (ed.) Encyclopedia of Soils in the Environment. Elsevier Ltd., UK, Oxford. 421-428.

Kotze RG, Van der Merwe CF, Crampton BG, Kritzinger Q. 2019. A histological assessment of the infection strategy of Exserohilum turcicum in maize. Plant Patho. 68(3):504-512.

Kourelis J, Van Der Hoorn RA. 2018. Defended to the nines: 25 years of resistance gene cloning identifies nine mechanisms for R protein function. The Plant Cell 30(2):285-299.

Kozdrój J, Trevors J, Van Elsas J. 2004. Influence of introduced potential biocontrol agents on maize seedling growth and bacterial community structure in the rhizosphere. Soil Biol. Biochem. 36:1775-1784.

Kumar. 2013. Trichoderma: a biological weapon for managing plant diseases and promoting sustainability, Int. J. Agrl. Sc. & Vet. Med. 1(3):106-121.

Kuntzmann P, Villaume S, Larignon P, Bertsch C. 2010. Esca, BOTA and Eutypiosis: foliar symptoms, trunk lesions and fungi observed in diseased vinestocks in two vineyards in Alsace. Vitis 49(2):71-76.

Kusari S, Hertweck C, Spiteller M. 2012. Chemical ecology of endophytic fungi: origins of secondary metabolites. Chem. Biol. 19(7):792-798.

Kuzmanovska B, Rusevski R, Jankulovska M, Oreshkovikj KB. 2018. Antagonistic activity of Trichoderma asperellum and Trichoderma harzianum against genetically diverse Botrytis cinerea isolates. Chil. J. Agric. Res. 78(3):391-399.

Lade SB, Štraus D, Oliva J. 2022. Variation in Fungal Community in Grapevine (*Vitis vinifera*) Nursery Stock Depends on Nursery, Variety and Rootstock. J. Fungi 8(1):47.

Lakkis, Trotel-Aziz P, Rabenoelina F, Schwarzenberg A, Nguema-Ona E, Clément C, Aziz A. 2019. Strengthening grapevine resistance by Pseudomonas fluorescens PTA-CT2 relies on distinct defense pathways in susceptible and partially

resistant genotypes to downy mildew and gray mold diseases. Front. Plant Sci. 10:1112.

Lambert C, Bisson J, Waffo-Téguo P, Papastamoulis Y, Richard T, Corio-Costet MF, Cluzet S. 2012. Phenolics and their antifungal role in grapevine wood decay: focus on the Botryosphaeriaceae family. J. Agric. Food Chem., 60(48):11859-11868.

Landum MC, Félix MR, Alho J, Garcia R, Cabrita MJ, Rei F, Varanda CMR. 2016 Antagonistic activity of fungi of Olea europaea L. against Colletotrichum acutatum. Microbiol. Res. 183:100–108.

Larach, Torres, C, Riquelme N, Valenzuela M, Salgado E, Seeger M, Besoain X. 2020. Yield loss estimation and pathogen identification from Botryosphaeria dieback in vineyards of Central Chile over two growing seasons. Phytopathol. Mediterr. 59(3): 537-548.

Larignon P, Dubos B. 1997. Fungi associated with esca disease in grapevine. Eur. J. Plant Pathol. 103(2):147-157.

Larignon P, Fontaine F, Farine S, Clement C, Bertsch C. 2009. Esca and Black Dead Arm: two major actors of grapevine trunk diseases. C R Biol. 332(9):765-783.

Larignon P, Fulchic R, Cere L, Dubos B. 2001. Observation on black dead arm in French vineyards. Phytopathol. Mediterr. S336-S342.

Larignon P. 2004. La constitution d'un groupe international de travail sur les maladies du bois et les premiers résultats des expérimentations menées par l'ITV en laboratoire et en pépinières. Les Maladies du Bois en Midi-Pyrénées. 122:24-27.

Larignon PFR, Cere L, Dubos B. 2001. Observation on black dead arm in French vineyards. Phytopathol. Mediterr. 40S(3):336–342.

Lawrence DP, Travadon R, Pouzoulet J, Rolshausen PE, Wilco WF, Baumgartner K. 2017. Characterization of Cytospora isolates from wood cankers of declining grapevine in North America, with the descriptions of two new Cytospora species. Plant Pathol. 66(5):713–725.

Lazazzara V, Vicelli B, Bueschl C, Parich A, Pertot I, Schuhmacher R, Perazzolli M. 2021. *Trichoderma* spp. volatile organic compounds protect grapevine plants by activating defense-related processes against downy mildew. Physiol. Plant. 172(4):1950-1965.

Leal C, Fontaine F, Aziz A, Ega C, Clémen C, Trotel-Aziz P. 2021a. Genome sequence analysis of the beneficial *Bacillus subtilis* PTA-271 isolated from a *Vitis*

vinifera (cv. Chardonnay) rhizospheric soil: assets for sustainable biocontrol. Environ. microbiome 16(1):1-14.

Leal C, Richet N, Guis, JF, Gramaje D, Armengol J, Fontaine F, Trotel-Aziz P. 2021b. Cultivar contributes to the beneficial effects of Bacillus subtilis PTA-271 and Trichoderma atroviride SC1 to protect grapevine against Neofusicoccum parvum. Front Microbiol 12:2889.

Leão PCDS, Chaves ARDM. 2019. Training systems and rootstocks on yield and agronomic performance of 'Syrah'grapevine in the Brazilian semiarid. Ciência e Agrotecnologia, 43.

Lebel S. 2010. Caractérisation des gènes PR10 chez *Vitis vinifera* et étude de leur expression durant l'embryogenèse somatique (Doctoral dissertation, Université de Haute Alsace-Mulhouse).

Lebon G, Duchêne E, Brun O, Clément C. 2005. Phenology of flowering and starch accumulation in grape (*Vitis vinifera* L.) cuttings and vines. Ann. Bot. 95:943–948.

Leng Y, Yang Y, Ren D, Huang L, Dai L, Wang Y, et al. 2017. A rice PECTATE LYASE-LIKE gene is required for plant growth and leaf senescence. Plant Physiol.174(2):1151-1166.

Levadoux L. 1956. Les populations sauvages et cultivées des Vitis vinifera L (Vol. 1, pp. 59-118). Institut national de la recherche agronomique.

Levina N, Tötemeyer S, Stokes NR, Louis P, Jones MA, Booth IR. 1999. Protection of Escherichia coli cells against extreme turgor by activation of MscS and MscL mechanosensitive channels: identification of genes required for MscS activity. EMBO J. 18(7):1730-1737.

Li CW, Bae Y, Lee SC. 2022. Differential role of Capsicum annuum FANTASTIC FOUR-like gene CaFAF1 on drought and salt stress responses. Environ. Exp. Bot. 199:104887.

Li H, Toh R, We Y, Wang, Hu J, An S, et al. 2022. Microbiomes across root compartments are shaped by inoculation with a fungal biological control agent. App. Soil Ecol. 170:104230.

Li J, Wang C, Liang W, Liu S. 2021. Rhizosphere microbiome: The emerging barrier in plant-pathogen interactions. Front. Microbiol. 12:772420.

Li Y, Wang L, Zhang W, Wang H, Fu X, Le Y. 2011. The variability of soil microbial community composition of different types of tidal wetland in Chongming Dongtan and its effect on soil microbial respiration. Ecol. Engin. 37(9):1276-1282.

Li J, Weraduwage SM, Preiser AL, Tietz S, Weise SE, Stran DD, et al. 2019. A cytosolic bypass and G6P shunt in plants lacking peroxisomal hydroxypyruvate reductase. Plant Physiol. 180(2):783-792.

Li M, Yang Q. 2007. Isolation and characterization of a β-tubulin gene from *Trichoderma harzianum*. Biochem. Genet. 45(7):529-534.

Li P, Lu YJ, Chen H, Day B. 2020. The lifecycle of the plant immune system. Crit. Rev. Plant. Sci. 39(1):72-100.

Liminan J, Pacreau, Boureau F, Menard E, David S, Himonnet C, Fermau M., Goutouly, J, Lecomte P, Dumot V. 2009. Inner necrosis in grapevine rootstock mother plants in the Cognac area (Charentes, France). Phytopathol. Mediterr. 48(1):92-100.

Liu B, Xue X, Cui S, Zhang X, Han Q, Zhu L, et al. 2010. Cloning and characterization of a wheat β-1, 3-glucanase gene induced by the stripe rust pathogen Puccinia striiformis f. sp. Mol. Biol. Rep. 37(2):1045.

Liu N, Sun Y, Pei Y, Zhang X, Wang P, Li X, et al. 2018. A pectin methylesterase inhibitor enhances resistance to Verticillium wilt. Plant Physiol. 176(3):2202-2220.

Liu X, Hou X. 2018. Antagonistic regulation of ABA and GA in metabolism and signaling pathways. Front. Plant Sci. 9:251.

Liu Y, Tao J, Yan Y, Li B, Li H, Li C. 2011. Biocontrol efficiency of Bacillus subtilis SL-13 and characterization of an antifungal chitinase. Chin. J. Chem. Eng. 19:128-134.

Liu Y, Zhang N, Qiu , Feng H, Vivanco JM, Shen Q, Zhang R. 2014. Enhanced rhizosphere colonization of beneficial Bacillus amyloliquefaciens SQR9 by pathogen infection. FEMS Microbiol. Lett. 353(1):49-56.

Lucas Espadas A. 2009. Phytosanitary situation of grapevine crop in Murcia Region Spain. *Vida Rural (España)*.

Lugtenberg B, Kamilova F. 2009. Plant-growth-promoting rhizobacteria. Annu. Rev. Microbiol. 63:541-556.

Luque J, Martos S, Aroca , Raposo R, Garcia-Figueres F. 2009. Symptoms and fungi associated with declining mature grapevine plants in northeast Spain. J. Plant Pathol. 381-390.

Lyagin I, Efremenko E. 2019. Enzymes for detoxification of various mycotoxins: origins and mechanisms of catalytic actions. Molecules. 24:2362.

Magnin-Robert M, Quantinet D, Couderchet M, Azi A, Trotel-Aziz P. 2013. Differential induction of grapevine resistance and defense reactions against Botrytis cinerea by bacterial mixtures in vineyards. BioControl. 58(1):117-131.

Magnin-Robert M, Trotel-Aziz P, Quantinet, Biagianti S, Aziz A. 2007. Biological control of *Botrytis cinerea* by selected grapevine-associated bacteria and stimulation of chitinase and β-1, 3 glucanase activities under field conditions. Eur. J. Plant Pathol. 118(1):43–57.

Magris G, Jurman I, Fornasiero A, Paparelli, Schwope R, Marroni F, Di Gaspero G, Morgante M. 2021. The genomes of 204 *Vitis vinifera* accessions reveal the origin of European wine grapes. Nat. Commun. 12(1):1-12.

Mahoney N, Molyneux RJ, Smith LR, Schoch TK, Rolshausen PE, Gubler WD. 2005. Dying-arm disease in grapevines: diagnosis of infection with Eutypa lata by metabolite analysis. J. Agric. Food Chem. 53:8148-8155.

Manjula K, Podile AR. 2005. Production of fungal cell wall degrading enzymes by a biocontrol strain of Bacillus subtilis AF 1. Indian J. Exp. Biol. 43(10):892-898.

Mannaa M, Han G, Seo YS, Park I. 2021. Evolution of food fermentation processes and the use of multi-omics in deciphering the roles of the microbiota. Foods 10(11):2861.

Manter D, Delgado A, Holm G, Stong A. 2010. Pyrosequencing reveals a highly diverse and cultivar-specific bacterial endophyte community in potato roots. Microb. Ecol. 60:157–166.

Marasc R, Rolli E, Fusi, Michoud G, Daffonchio D. 2018. Grapevine rootstocks shape underground bacterial microbiome and networking but not potential functionality. Microbiome 6(1):1-17.

Marchi G. 2001. Susceptibility to Esca of Various Grapevine (" *Vitis vinifera*") Cultivars Grafted on DIfferent Rootstock in a Vineyard in the Province of Siena (Italy). Susceptibility to Esca of Various Grapevine (" Vitis vinifera") Cultivars Grafted on DIfferent Rootstock in a Vineyard in the Province of Siena (Italy) 1000-1010.

Marín D, Armengol J, Carbonell-Bejerano P, Escalona JM, Gramaje D, Hernández-Montes E, Intrigliolo DS, Martínez-Zapater JM, Medrano H, Mirás-Ávalos JM, Palomares-Rius JE, Romero-Azorín P, Savé R, Santesteban LG, De Herralde F.

2021. Challenges of viticulture adaptation to global change: tackling the issue from the roots. Aust. J. Grape Wine Res. 27:8-25.

Marowa P, Ding A, Kong Y. 2016. Expansins: roles in plant growth and potential applications in crop improvement. Plant Cell Rep.35(5):949-965.

Martínez-Diz M, Díaz-Losada E, Díaz-Fernández Á, Bouzas-Cid Y, Gramaje D. 2021b. Protection of grapevine pruning wounds against *Phaeomoniella chlamydospora* and *Diplodia seriata* by commercial biological and chemical methods. Crop Prot. 143:105465.

Martínez-Diz, M. P., Díaz-Losada, E., Barajas, E., Ruano-Rosa, D., Andrés-Sodupe, M., and Gramaje, D. 2019. Screening of Spanish *Vitis vinifera* germplasm for resistance to Phaeomoniella chlamydospora. Sci. Hort. 246:104–109.

Martínez-Diz M, Díaz-Losada E, Andrés-Sodupe M, Bujanda R, Maldonado-González MM, Ojeda S, Yacoub A, Rey P, Gramaje D. 2021a. Field evaluation of biocontrol agents against black-foot and Petri diseases of grapevine. Pest Manag. Sci. 77(2):697-708.

Masi M, Nocera P, Boari A, Cimmino A, Zonn MC, Infantino A, Vurro M, Evidente A. 2018. Lathyroxins A and B, phytotoxic monosubstituted phenols isolated from *Ascochyta lentis* var. lathyri, a fungal pathogen of grass pea (*Lathyrus sativus*). J. Nat. Prod. 81(4):1093-1097.

Massonnet M, Fasoli , Tornielli GB, Altieri M, Sandri M, Zuccolotto P, et al. 2017. Ripening transcriptomic program in red and white grapevine varieties correlates with berry skin anthocyanin accumulation. Plant physio. 174(4):2376-2396.

Meier-Kolthoff JP, Klenk H-P, Göker M. 2014. Taxonomic use of DNA G+ C content and DNA–DNA hybridization in the genomic age. Int. J. Syst. Evol. Microbiol. 64(2):352-356.

Meyer SL, Roberts DP. 2002. Combinations of biocontrol agents for management of plant-parasitic nematodes and soilborne plant-pathogenic fungi. J. Nematol. 34(1):1.

Meyer T, Vigouroux A, Aumont-Nicaise M, Comte G, Vial L, Lavir C, Moréra S. 2018. The plant defense signal galactinol is specifically used as a nutrient by the bacterial pathogen Agrobacterium fabrum. J. Biol. Chem.293(21):7930-7941.

Meziane H, Vander SI, Van Loon LC, Höfte M, Bakker M. 2005. Determinants of *P. putida* WCS 358 involved in induced systemic resistance in plants. Mol. Plant Pathol. 6:177–185.

Miljaković D, Marinković J, Balešević-Tubić S. 2020. The significance of Bacillus spp. in disease suppression and growth promotion of field and vegetable crops. Microorganisms 8(7):1037.

Mimiague F, Le Gall D. 1994. Bilan sur les enquetes eutypiose dans le vignoble europeen. In: Quatrieme Conference Internationale sur les Maladies des Plante. Bordeaux, France: Annales ANPP 1265–76.

Missaoui K, Gonzalez-Klein Z, Pazos-Castro D, Hernandez-Ramirez G, Garrido-Arandia M, Brini, F, et al. J. 2022. Plant non-specific lipid transfer proteins: An overview. Plant Physiol. Biochem.171:115-127.

Mocali S, Kuramae EE, Kowalchuk GA, Fornasier F, Priori S. 2020. Microbial functional diversity in vineyard soils: sulfur metabolism and links with grapevine plants and wine quality. Front. Environme. Sci. 8:75.

Molyneux RJ, Mahoney N, Bayman P, Wong RY, Meyer K, Irelan N. 2002. Eutypa dieback in grapevines: differential production of acetylenic phenol metabolites by strains of *Eutypa lata*. J. Agric. Food Chem. 50:1393-1399.

Monaghan J, Zipfel C. 2012. Plant pattern recognition receptor complexes at the plasma membrane. Curr. Opin. Plant Biol. 15(4):349-357.

Mondello V, Songy A, Battiston E, Pinto C, Coppin C, Trotel-Aziz P, Clément C, Maugnai L, Fontaine F. 2018. Grapevine trunk diseases: a review of fifteen years of trials for their control with chemicals and biocontrol agents. Plant Dis. 102(7):1189-1217.

Mondello V, Spagnolo A, Larignon P, Clemen C. Fontaine F. 2019. Phytoprotection potential of Fusarium proliferatum for control of Botryosphaeria dieback pathogens in grapevine. Phytopathol. Mediterr. 58(2).

Monteiro F, Sebastiana M, Pais MS, Figueiredo A. 2013. Reference gene selection and validation for the early responses to downy mildew infection in susceptible and resistant *Vitis vinifera* cultivars. PloS one 8(9):e72998.

Montero-Barrientos M, Hermosa R, Nicolás C, Cardoza RE, Gutiérrez S, Monte E. 2008. Overexpression of a *Trichoderma* HSP70 gene increases fungal resistance to heat and other abiotic stresses. Fungal Genet. Biol. 45(11):1506-1513.

Morales-Cruz A, Figueroa-Balderas R, García JF, Tran E, Rolshausen PE, Baumgartner K, et al. 2018b. Profiling grapevine trunk pathogens in planta: A case for community-targeted DNA metabarcoding. BMC Microbiol. 18:214.

Mostert L, Crous PW, Fourie P, Halleen F. 2006. A review of "*Phaeoacremonium*" Species Involved in Petri Disease and Esca of Grapevines. Phytopathol. Mediterr. 45:S12-S29.

Mou S, Liu Z, Guan D, Qiu A, Lai Y, He S. 2013. Functional analysis and expressional characterization of rice ankyrin repeat-containing protein, Os PIANK1, in basal defense against Magnaporthe oryzae attack. PloS one 8(3):e59699.

Moyo P, Allsopp E, Roets F, Mostert L, Halleen F. 2014. Arthropods vector grapevine trunk disease pathogens. Phytopathol. 104:1063-1069.

Muckherjee M, Muckherjee PK, Horwitz A, Zachow, Berg G, et al. 2012. Trichoderma–plant–pathogen interactions: advances in genetics of biological control. Indian J Microbiol. 52:522–529.

Mugnai L, Granit A, Surico G. 1999. Esca (black measles) and brown wood-streaking: two old and elusive diseases of grapevines. Plant Dis. 83(5):404-418.

Murolo S, Romanazzi G. 2014. Effects of grapevine cultivar, rootstock and clone on esca disease. Australas. Plant Pathol. 43(2):215-221.

Mutawila C, Fourie P, Halleen F, Mostert L. 2011. Grapevine cultivar variation to pruning wound protection by Trichoderma species against trunk pathogens. Phytopathol. Mediterr. 50:S264-S276.

Naito K, Taguchi F, Suzuki T, Inagaki Y, Toyoda K, Shiraishi T, Ichinose Y. 2008. Amino acid sequence of bacterial microbe-associated molecular pattern flg22 is required for virulence. Mol. Plant Microbe Interact. 21(9):1165-1174.

Naznin HA, Kiyohara D, Kimura M, Miyazawa M, Shimizu M, Hyakumachi M. 2014. Systemic resistance induced by volatile organic compounds emitted by plant growth-promoting fungi in *Arabidopsis thaliana*. PLoS One 9(1):e86882.

Nerva L, Garcia JF, Favaretto F, Giudice G, Moffa L, Sandrini M, et al. 2022. The hidden world within plants: Metatranscriptomics unveils the complexity of wood microbiomes. J. Exp. Bot. 73:2682–2697.

Nerva L, Giudice G, Quiroga G, Belfiore N, Lovat L, Perria R, Volpe M, Moffa L, Sandrini M, Gaiotti F, Balestrini R, Chitarra W. 2022. Mycorrhizal symbiosis balances rootstock-mediated growth-defence tradeoffs. Biol. Fertil. Soils. 58(1):17-34.

Nerva L, Turina M, Zanzotto A, Gardiman M, Gaiotti F, Gambino G, Chitarra W. 2019. Isolation, molecular characterization and virome analysis of culturable

wood fungal endophytes in esca symptomatic and asymptomatic grapevine plants. Environ. Microbiol. 21(8):2886-2904.

Newton J, Fray R. 2004. Integration of environmental and host-derived signals with quorum sensing during plant–microbe interactions. Cell. microbiol. 6(3):213-224.

Nguyen NH, Trotel-Aziz P, Villaume S, Rabenoelina F, Schwarzenberg A, Nguema-Ona E, et al. 2020. Bacillus subtilis and Pseudomonas fluorescens Trigger Common and Distinct Systemic Immune Responses in Arabidopsis thaliana Depending on the Pathogen Lifestyle. Vaccines. 8(3):503.

Ni DD, Liu HX, Jiang CH, Wang YP, Wang QY, Jin HL, Guo JH. 2011. The plant growth–promoting rhizobacterium Bacillus cereus AR156 induces systemic resistance in Arabidopsis thaliana by simultaneously activating salicylate-and jasmonate/ethylene-dependent signaling pathways. Mol Plant Microbe Interact. 24(5): 533-542.

Nicholson WL, Munakata N, Horneck G, Melosh HJ, Setlow P. 2000. Resistance of Bacillus endospores to extreme terrestrial and extraterrestrial environments. Microbiol. Mol. Biol. Rev. 64(3):548-572.

Nie P, Li, Wang S, Guo J, Zhao H, Niu D. 2017. Induced systemic resistance against Botrytis cinerea by Bacillus cereus AR156 through a JA/ET-and NPR1-dependent signaling pathway and activates PAMP-triggered immunity in Arabidopsis. Front. Plant Sci. 8:238.

Niu B, Wang W, Yuan Z, Sederoff RR, Sederoff, H., Chiang, V. L., & Borriss, R. (2020). Microbial interactions within multiple-strain biological control agents impact soil-borne plant disease. Frontiers in Microbiology, 11, 585404.

O'Brien, Philip A. 2017. Biological control of plant diseases. Australas. Plant Pathol. 46(4): 293-304.

O'Donnell K, Cigelnik E. 1997. Two divergent intragenomic rDNA ITS2 types within a monophyletic lineage of the fungus Fusarium are nonorthologous. Mol Phylog Evol 7:103–116.

Oksal E, Çelik Y, Özer G. 2020. First report of canker and dieback caused by *Cytospora viticola* on grapevine in Turkey. J. Plant Pathol. 102(1):239-239.

Olishevska S, Nickzad A, Déziel E. 2019. Bacillus and Paenibacillus secreted polyketides and peptides involved in controlling human and plant pathogens. Appl. Microbiol. Biotechnol. 103(3):1189-1215.

Ollat N, Bordenave L, Tandonnet JP, Boursiquot JM, Marguerit E. 2014. Grapevine rootstocks: origins and perspectives. In I International Symposium on Grapevine Roots 1136:11-22.

Ollat N, Peccoux A, Papura D, Esmenjaud D, Marguerit E, Tandonnet JP, Bordenave L, Cookson SJ, Barrieu F, Rossdeutsch L, et al. 2016. Rootstocks as a component of adaptation to environment. In Grapevine in a Changing Environment; Gerós, H., Chaves, M.M., Gil, H.M., Delrot, S., Eds.; John Wiley: Chichester, UK. 68–108.

Ongena M, Jacques P. 2008. *Bacillus* lipopeptides: Versatile weapons for plant disease biocontrol. Trends Microbiol. 16:115-125.

Ongena M, Jourdan E, Adam A, Paquot M, Brans A, Joris B, et al. 2007. Surfactin and fengycin lipopeptides of Bacillus subtilis as elicitors of induced systemic resistance in plants. Environ. Microbiol. 9(4):1084-1090.

Oono R, Lefevre E, Simha A, Lutzoni FA. 2015. Comparison of the community diversity of foliar fungal endophytes between seedling and adult loblolly pines (Pinus taeda). Fungal Biol. 119,:917–928.

Ortíz-Castro R, Contreras-Cornejo HA, Macías-Rodríguez L, López-Bucio J. 2009. The role of microbial signals in plant growth and development. Plant. Signal. Behav. 4(8):701-712.

Pacifico, Squartin A, Crucitti D, Barizza E, Lo Schiavo F, Muresu R, Carimi F, Zottini M. 2019. The role of the Endophytic microbiome in the grapevine response to environmental triggers. Front. Plant Sci. 10:1256.

Pancher M, Ceol M, Corne PE, Long CMO, Yousaf S, Pertot I, Campisano A. 2012. Fungal endophytic communities in grapevines (*Vitis vinifera L.*) respond to crop management. Appl. Environ. Microbiol. 78(12):4308-4317.

Pandey S, Ranade S, Nagar P, Kumar N. 2000. Role of polyamines and ethylene as modulators of plant senescence. J. Biosci. 25(3):291-299.

Pandian BA, Sathishraj R, Djanaguiraman M, Prasad PV. Jugulam M. 2020. Role of cytochrome P450 enzymes in plant stress response. Antioxidants 9(5):454.

Parker CT, Tindall BJ, Garrity GM. 2019. International code of nomenclature of prokaryotes: Prokaryotic code (2008 revision). Int. J. Syst. Evol. Microbiol. 69(1A):S1-S111.

Parks DH, Imelfort M, Skennerton CT, Hugenholtz P, Tyson GW. 2015. CheckM: assessing the quality of microbial genomes recovered from isolates, single cells, and metagenomes. Genome Res. 25(7):1043-1055.

Pasco IG, Cottral EH. 2000. Developments in grapevine trunk diseases research in Australia. Phytopathol. Mediterr. 39:68-75.

Patanita M, Albuquerque A, Campos MD, Materatski P, Varanda CM, Ribeiro JA, Félix MDR. 2022 Metagenomic Assessment Unravels Fungal Microbiota Associated to Grapevine Trunk Diseases. Horticulturae 8:288.

Pedruzzi I, Rivoire C, Auchincloss AH, Coudert E, Keller G, De Castro E, et al. 2015. HAMAP in 2015: updates to the protein family classification and annotation system. Nucleic Acids Res. 43(1):1064-1070.

Pen Y, Li SJ, Yan J, Tang Y, Cheng JP, Gao AJ, Yao , Ruan J, Xu BL. 2021. Research progress on phytopathogenic fungi and their role as biocontrol agents. Front. Microbiol. 1209.

Perry RN, Moens M, 2006. Plant nematology. CABI, Cambridge, MA.

Pertot I, Giovannini O, Benanchi M, Caffi T, Rossi V, Mugnai L. 2017. Combining biocontrol agents with different mechanisms of action in a strategy to control *Botrytis cinerea* on grapevine. Crop Prot. 97:85-93.

Pertot I, Prodorutti D, Colombini A, Pasini L. 2016. Trichoderma atroviride SC1 prevents Phaeomoniella chlamydospora and Phaeoacremonium aleophilum infection of grapevine plants during the grafting process in nurseries. BioControl. 61(3):257-267.

Petzoldt CH, Sall MA, Moller WJ. 1983. Factors determining the relative number of ascospores released by Eutypa armeniacae in California. Plant Dis. 67:857-860.

Pezet R, Jermini M. 1989. Black rot of grapevine: symptoms, epidemiology and control. Revue Suisse de Viticulture, d'Arboriculture et d'Horticulture 21(1):27-34.

Phillips AJ, Fonseca F, Povoa V, Castilh R, Nolasco G. 2002. A reassessment of the anamorphic fungus *Fusicoccum luteum* and description of its teleomorph *Botryosphaeria lutea* sp nov. Sydowia 54(1):54-77.

Pieters CM, Van der Does D, Zamioudis C, Leon-Reyes A,Van Wees SC. 2012. Hormonal modulation of plant immunity. Annu. Rev. Cell Dev. Biol. 28:489-521.

Pieterse CM, Leon-Reyes A, Van der Ent S, Van Wees SC. 2009. Networking by small-molecule hormones in plant immunity. Nat. Chem. Biol. 5(5):308-316.

Pieterse CM, Ton, J, Van Loon LC. 2002. Cross-talk between plant defense signaling pathways: boost or burden? Agri. Biotech. Net. 3:1–18.

Pieterse CM, Van Pelt JA, Van Wees SC, Ton J, Léon-Kloosterziel KM, Keurentjes JJ, et al. 2001. Rhizobacteria-mediated induced systemic resistance: triggering, signalling and expression. Eur. J. Plant Pathol. 107(1):51-61.

Pieterse CM, Zamioudis C, Berendsen RL, Welle DM, Van Wees C, Bakker PA. 2014. Induced systemic resistance by beneficial microbes. Annu. Rev. Phytopathol. 52:347–75.

Pike S, Patel A, Stacey G, Gassmann W. 2009. Arabidopsis OPT6 is an oligopeptide transporter with exceptionally broad substrate specificity. Plant Cell Physiol. 50(11):1923-1932.

Pilar Martínez-Diz M, Díaz-Losada E, Andrés-Sodupe M, Bujanda R, Maldonado-González MM, Ojeda S, et al. 2021. Field evaluation of biocontrol agents against black-foot and Petri diseases of grapevine. Pest Manag. Sci. 77(2):697-708.

Pineda A, Zheng SJ, van Loon JJ, Pieterse CM, Dicke M. 2010. Helping plants to deal with insects: the role of beneficial soil-borne microbes. Trends Plant Sci. 15(9):507-514.

Pinto C, Sousa S, Froufe H, Egas C, Clément C, Fontaine F, Gomes AC. 2018. Draft genome sequence of *Bacillus amyloliquefaciens subsp. plantarum* strain Fito_F321, an endophyte microorganism from *Vitis vinifera* with biocontrol potential. Stand. Genom. Sci. 13(1):1-12.

Pollard-Flamand J, Boulé J, Hart M, Úrbez-Torres JR. 2022. Biocontrol Activity of Trichoderma Species Isolated from Grapevines in British Columbia against Botryosphaeria Dieback Fungal Pathogens. Journal of Fungi 8(4):409.

Pouzoulet J, Pivovaroff AL, Santiago LS, Rolshausen PE. 2014. Can vessel dimension explain tolerance toward fungal vascular wilt diseases in woody plants? Lessons from Dutch elm disease and esca disease in grapevine. Front. Plant Sci. 5:253.

Poveda J. 2021. Trichoderma as biocontrol agent against pests: New uses for a mycoparasite. Biol. Control 159:104-634.

Powell P, Szaniszlo P, Cline G, Reid C. 1982. Hydroxamate siderophores in the iron nutrition of plants. J. Plant Nutr. 5(4–7):653–73.

Pozo MJ, Slezack-Deschaumes S, Dumas-Gaudot E, Gianinazzi S, Azcón-Aguilar C. 2002. Plant defense responses induced by arbuscular mycorrhizal fungi. Mycorrhizal technology in agriculture 103-111. Birkhäuser, Basel.

Pradhan N, Sukla L-B. 2005. Solubilization of inorganic phosphates by fungi isolated from agriculture soil. Afr. J. Biotechnol. 5(10):850-854.

Pradhan S, Durgam M, Mailapalli DR. 2021. Urea loaded hydroxyapatite nanocarrier for efficient delivery of plant nutrients in rice. Arch. Agron. Soil Sci. 67(3):371-382.

Probst CM, Ridgway HJ, Jaspers MV, Eirian Jones E. 2019. Pathogenicity of Ilyonectria liriodendri and Dactylonectria macrodidyma propagules in grapevines. Eur. J. Plant Pathol. 154(2):405-421.

Qin W, Yu Y, Jin Y, Wang X, Liu J, Xi J, et al. 2018. Genome-wide analysis elucidates the role of CONSTANS-like genes in stress responses of cotton. Int. J. Mol. Sci. 199;2658.

Raaijmakers JM, Paulitz TC, Steinberg C, Alabouvette C, Moënne-Loccoz Y. 2009. The rhizosphere: a playground and battlefield for soilborne pathogens and beneficial microorganisms. Plant and soil 321(1):341-361.

Rajarammohan S. 2021. Redefining plant-necrotroph interactions: the thin line between hemibiotrophs and necrotrophs. Front. Microbiol. 12:673518.

Ramírez-Suero M, Bénard-Gellon M, Chong J, Laloue H, Stempien E, Abou-Mansour E, Fontaine F, Larignon P, Mazet-Kieffer F, Farine S, Bertsch, C. 2014. Extracellular compounds produced by fungi associated with *Botryosphaeria dieback* induce differential defence gene expression patterns and necrosis in *Vitis vinifera* cv. Chardonnay cells. Protoplasma 251(6):1417-1426.

Ramsin CK, Gramaje D, Mocholí S, Agustí J, de Santa María FCS, Armengol J, Berbegal M. 2021. Relationship between the xylem anatomy of grapevine rootstocks and their susceptibility to *Phaeoacremonium minimum* and *Phaeomoniella chlamydospora*. Front. Plant Sci. 12.

Rawlings ND, Barrett AJ, Finn R. Bettenfeld P, Canal JC, Jacquens L, Fernandez , Fontaine F, van Schaik E, Courtie P, Trouvelot S. 2021. The microbiota of the grapevine holobiont: A key component of plant health. J. Adv. Res.

Regner F, Stadlhuber A, Eisenheld C, Kaserer HAHI. 1998. Considerations about the evolution of grapevine and the role of Traminer. VII International Symposium on Grapevine Genetics and Breeding 528:179-184.

Reinhold-Hurek B, Bunger W, Burbano CS, Sabale M, Hurek T. 2015. Roots shaping their microbime: global hotspots for microbial activity. Annu. Rev. Phytopathol. 53:403-424.

Reis P, Mondello V, Diniz I, Alves A, Rego C, Fontaine F. 2022. Effect of the Combined Treatments with LC2017 and Trichoderma atroviride Strain I-1237 on Disease Development and Defense Responses in Vines Infected by Lasiodiplodia theobromae. Agronomy 12(5):996.

Reis P, Pierron R, Larignon P, Lecomte P, Abou-Mansour E, Farine S, et al. 2019. Vitis methods to understand and develop strategies for diagnosis and sustainable control of grapevine trunk diseases. Phytopathology. 109(6):916-931.

Reis, Gaspar A, Alves A, Fontaine F, Lourenço I, Saramago J, et al. 2020. Early season symptoms on stem, inflorescences and flowers of grapevine associated with Botryosphaeriaceae species. Plants 9(11):1427 (2020).

Reithner B, Brunner K, Schuhmacher R, Peissl I, Seidl V, Krska R, Zeilinger S. 2005. The G protein α subunit Tga1 of *Trichoderma atroviride* is involved in chitinase formation and differential production of antifungal metabolites. Fungal Genet. Biol. 42:749-760.

Revegli P, Savocchia S, Billones-Baaijens R, Masi M, Cimmino A, Evidente A. 2019. Phytotoxic metabolites by nine species of Botryosphaeriaceae involved in grapevine dieback in Australia and identification of those produced by *Diplodia mutila, Diplodia seriata, Neofusicoccum australe* and *Neofusicoccum luteum*. Nat. Prod. Res. 33(15):2223-2229.

Reveglia P, Billones-Baaijens R, Millera Niem J, Masi M, Cimmino A, Evidente A, Savocchia S. 2021. Production of Phytotoxic Metabolites by Botryosphaeriaceae in Naturally Infected and Artificially Inoculated Grapevines. Plants. 10(4):802.

Reveglia P, Masi M, Evidente A. 2020. Melleins—Intriguing natural compounds. Biomolecules 10(5):772.

Reveglia P, Pacetti A, Masi M, Cimmino A, Carella G, Marchi G, Mugnai L, Evidente A. 2021. Phytotoxic metabolites produced by *Diaporthe eres* involved in cane blight of grapevine in Italy. Nat. Prod. Res. 35(17):2872-2880.

Reynolds AG, Heuvel JEV. 2009. Influence of grapevine training systems on vine growth and fruit composition: a review. Am. J. Enol. Vitic. 60(3):251-268.

Rezgui C, Ghnaya-Chakroun AB, Vallance J, Bruez E, Hajlaoui MR, Sadfi-Zouaoui N, Rey P. 2016. Endophytic bacteria with antagonistic traits inhabit the wood tissues of grapevines from Tunisian vineyards. Biol. Cont. 99:28-37.

Rezgui C, Trinsoutrot-Gattin I, Benoit M Laval K,Wassila RA. 2021. Linking changes in the soil microbial community to C and N dynamics during crop residue decomposition. J. Integr. Agric. 20(11):3039-3059.

Riaz S, Garrison KE, Dangl GS, Boursiquot JM, Meredith CP. 2002. Genetic divergence and chimerism within ancient asexually propagated winegrape cultivars. J. Am. Soc. Hortic. Sci. 127(4):508-514.

Ribone PA, Capella M, Chan RL. 2015. Functional characterization of the homeodomain leucine zipper I transcription factor AtHB13 reveals a crucial role in Arabidopsis development. J. Exp. Bot.66(19):5929-5943.

Ricca E, Henriques AO, Cutting SM. 2004. Bacterial spore formers: probiotics and emerging applications. Biosci. Horiz.

Richter M, Rosselló-Móra R. 2009. Shifting the genomic gold standard for the prokaryotic species definition. Proc. Natl. Acad. Sci. 106(45):19126-19131.

Rodríguez-Gacio MdC, Matilla-Vázquez MA, Matilla AJ. 2009. Seed dormancy and ABA signaling: the breakthrough goes on. Plant Signal Behav. 4(11):1035-1048.

Rolshausen PE, Urbez-Torres JR, Rooney-Latham S, Eskalen A, Smith RJ, Gubler WD. 2010. Evaluation of pruning wound susceptibility and protection against fungi associated with grapevine trunk diseases. Am. J. Enol. Vitic. 61: 113-119.

Romeo-Olivá , Chervin J, Breton C, Lagravèr T, Daydé J, Dumas B, Jacques A. 2022. Comparative Transcriptomics Suggests Early Modifications by Vintec® in Grapevine Trunk of Hormonal Signaling and Secondary Metabolism Biosynthesis in Response to Phaeomoniella chlamydospora and Phaeoacremonium minimum. Front. Microbiol. 13.

Rooney WM, Chai R, Milner JJ, Walke D. 2020. Bacteriocins targeting Gram-negative phytopathogenic bacteria: Plantibiotics of the future. Front. Microbiol. 11:575981.

Rooney-Latham S, Eskalen A, Gubler WD. 2005. Occurrence of *Togninia minima* perithecia in esca-affected vineyards in California. Plant Dis. 89(8):867-871.

Rouxe T, Balesdent MH. 2017. Life, death and rebirth of avirulence effectors in a fungal pathogen of *B. rassica* crops, *L. eptosphaeria* maculans. New Phytol. 214(2):526-532.

Rouxel T, Grandaubert J, Hane JK, Hoede C, Van de Wouw A, Couloux A, et al. 2011. Effector diversification within compartments of the *Leptosphaeria maculans* genome affected by Repeat-Induced Point mutations. Nat. comm. 2(1):1-10.

Rubio MB, Hermosa R, Reino J, Collado IG, Monte E. 2009. Thctf1 transcription factor of *Trichoderma harzianum* is involved in 6-pentyl2H-pyran-2-one production and antifungal activity. Fungal Genet. Biol. 46:17-27.

Rueden CT, Schindelin J, Hiner MC, DeZonia BE, Walter AE, Arena ET, Eliceiri KW. 2017. ImageJ2: ImageJ for the next generation of scientific image data. BMC bioinformatics. 18(1):1-26.

Russi A, Almança MAK, Grohs DS, Schwambach J. 2020. Biocontrol of black foot disease on grapevine rootstocks using Bacillus subtilis strain F62. Trop Plant Pathol 45(2):103-111.

Sabaté DC, Brandán CP. 2022. Bacillus amyloliquefaciens strain enhances rhizospheric microbial growth and reduces root and stem rot in a degraded agricultural system. Rhizosphere 100544.

Saha J, Brauer EK, Sengupta A, Popescu SC, Gupta K, Gupta B. 2015. Polyamines as redox homeostasis regulators during salt stress in plants. Front. Environ. Sci. 3:21.

Saiprasad GVS, Mythili JB, Anand L, Suneetha C, Rashmi HJ, Naveena C, Ganeshan, G. 2009. Development of *Trichoderma harzianum* gene construct conferring antifungal activity in transgenic tobacco. Ind. J. Biotechnol. 8:199-206.

Salvatore MM, Alve A, Andolfi A. 2021. Secondary metabolites produced by Neofusicoccum species associated with plants: A review. Agriculture 11(2):149.

Samuels L, Kunst L, Jetter R. 2008. Sealing plant surfaces: cuticular wax formation by epidermal cells. Annu. Rev. Plant Biol.59(1):683-707.

Sanchez-Corrionero A, Perez-Garcia P, Cabrer J, Silva-Navas J, Perianez-Rodriguez J, Gude I, et al. 2019. Root patterning and regeneration are mediated by the quiescent center and involve Bluejay, Jackdaw and Scarecrow regulation of vasculature factors. bioRxiv 803973.

Sánchez-Vicente I, Fernández-Espinosa MG, Lorenzo O. 2019. Nitric oxide molecular targets: reprogramming plant development upon stress. J. Exp. Bot. 70(17):4441-4460.

Santos RF, Heckler LI, Lazarotto M, Garrido LR, Rego C Blume E. 2016. Trichoderma spp. and Bacillus subtilis for control of Dactylonectria macrodidyma in grapevine. Phytopathol Mediterr 55:293-300.

Santoyo G, Moreno-Hagelsieb G, del Carmen Orozco-Mosqueda M, Glick BR. 2016. Plant growth-promoting bacterial endophytes. Microbiological research. 183:92-99.

Sanzani S M, Li Destri Nicosia MG, Faedda R, Cacciola SO, Schena L. 2014. Use of quantitative PCR detection methods to study biocontrol agents and phytopathogenic fungi and oomycetes in environmental samples. J Phytopathol 162(1):1-13.

Sato T, Kobayashi Y. 1998. The ars Operon in the skinElement of Bacillus subtilis Confers Resistance to Arsenate and Arsenite. J. Bacteriol. 180(7):1655-1661.

Savazzini F, Longa CMO, Pertot I, Gessler C. 2008. Real-time PCR for detection and quantification of the biocontrol agent Trichoderma atroviride strain SC1 in soil. J Microbiol Methods 73(2):185-194.

Schena L, Nigro F, Ippolito A, Gallitelli D. 2004. Real-time quantitative PCR: a new technology to detect and study phytopathogenic and antagonistic fungi. Eur J Plant PathoL 110(9):893-908.

Schirmböck M, Lorito M, Wang YL, Hayes CK, Arisan-Atac I, Scala F, Harma GE, Kubicek CP. 1994. Parallel formation and synergism of hydrolytic enzymes and peptaibol antibiotics, molecular mechanisms involved in the antagonistic action of *Trichoderma harzianum* against phytopathogenic fungi. Appl. Environ. Microbiol. 60(12):4364-4370.

Schmid CS, Lorenz D, Wolf GA. 2001. Biological control of the grapevine dieback fungus Eutypa lata I: screening of bacterial antagonists. Phytopathol. 149(7-8):427-435.

Schmidt CS, Alavi M, Cardinale M, Müller H, Berg G. 2012. *Stenotrophomonas rhizophila* DSM14405 T promotes plant growth probably by altering fungal communities in the rhizosphere. Biol. Fertil. Soils 48:947–960.

Schmidt R, Köberl M, Mostafa A, Ramadan EM, Monschein M, Jensen KB, Bauer R, Berg G. 2014. Effects of bacterial inoculants on the indigenous microbiome and secondary metabolites of chamomile plants. Front.Microbiol. 5:64.

Schmidt SM, Panstruga R. 2011. Pathogenomics of fungal plant parasites: what have we learnt about pathogenesis? Curr. Opin. Plant Biol. 14(4):392-399.

Schrecke K, Staroń A, Mascher T. 2012. Two-component signaling in the Gram-positive envelope stress response: intramembrane-sensing histidine kinases and accessory membrane proteins. In: Gross R, Beier D (eds) Two component systems in bacteria. Caister Academic Press, Germany, Würzburg. 199-229.

Seemann T. 2014. Prokka: rapid prokaryotic genome annotation. Bioinformatics. 30(14):2068-2069.

Seong SY, Matzinger P. 2004. Hydrophobicity: an ancient damage-associated molecular pattern that initiates innate immune responses. Nat. Rev. Immunol. 4(6):469-478.

Shang Y, Xiao G, Zheng P, Cen K, Zhan S, Wang C. 2016. Divergent and convergent evolution of fungal pathogenicity. Genome Biol. Evol. 8(5):1374-1387.

Sharifi R, Ryu C-M. 2018. Revisiting bacterial volatile-mediated plant growth promotion: lessons from the past and objectives for the future. Ann. Bot. 122(3):349-358.

Sharma P, Kumar V, Ramesh R, Saravanan K, Deep S, Sharma M, Mahesh S, Dinesh S. 2011. Biocontrol genes from Trichoderma species: a review. Afr. J. Biotechnol. 10(86):19898-19907.

Shine MB, Xiao X, Kachroo P, Kachroo A. 2019. Signaling mechanisms underlying systemic acquired resistance to microbial pathogens. Plant science 279:81-86.

Siddiqui ZA, Nesha R, Singh N, Alam S. 2012. Interactions of plant-parasitic nematodes and plant-pathogenic bacteria. In Bacteria in agrobiology: Plant probiotics (pp. 251-267). Springer, Berlin, Heidelberg.

Simões I, Faro C. 2004. Structure and function of plant aspartic proteinases. European journal of biochemistry 271(11):2067-2075.

Sinclai WA, Lyon HH, Johnson WT. 1987. Diseases of Trees and Shrubs. Ithaca, NY, USA: Cornell University Press.

Sivasakthi S, Usharani G, Saranraj P. 2014. Biocontrol potentiality of plant growth promoting bacteria (PGPR)-Pseudomonas fluorescens and Bacillus subtilis: A review. Afr. J. Agric. Res. 9(16):1265-1277.

Slippers B, Wingfield MJ. 2007. Botryosphaeriaceae as endophytes and latent pathogens of woody plants: diversity, ecology and impact. Fungal Biol. Rev. 21(2-3):90-106.

Sonenshein AL, Hoch JA, Losick R. 2002. *Bacillus subtilis* and its closest relatives: from genes to cells. eds. Sonenshein AL, Hoch JA, and Losick R, ASM press, Washington, DC, 129-150.

Songy A, Fernandez O, Clément C, Larignon P, Fontaine F. 2019. Grapevine trunk diseases under thermal and water stresses. Planta 249(6):1655-1679.

Sood M, Kapoor D, Kumar V, Sheteiwy MS, Ramakrishnan M, Landi M, Araniti F, Sharma A. 2020. Trichoderma: The "secrets" of a multitalented biocontrol agent. Plants 9(6):762.

Sosnowski MR, Creaser M, Wicks T. 2004. Evaluating fungicides as pruning wound treatments to control Eutypa dieback. Aust. N.Z. Grapegrow. Winemak. 485:51–3.

Sosnowski MR, Lardner R, Wicks TJ, Scott ES. 2007. The influence of grapevine cultivar and isolate of *Eutypa lata* on wood and foliar symptoms. Plant Dis. 91(8):924-931.

Soyer JL, Hamiot A, Ollivier B, Balesdent MH, Rouxel T, Fudal I. 2015. The APSES transcription factor LmStuA is required for sporulation, pathogenic development and effector gene expression in *L. eptosphaeria maculans*. Mol. Plant Pathol. 16(9):1000-1005.

Spagnolo A, Magnin-Robert M, Alayi TD, Cilindre C, Schaeffer-Reiss C, Van Dorsselaer A, Clément C, Larignon P, Ramirez-Suero M, Chong J, Bertsch C, Abou-Mansor E, Fontaine F. 2014. Differential responses of three grapevine cultivars to Botryosphaeria dieback. Phytopathol. 104(10):1021-1035.

Srivastava M, Shahid M, Pandey S, Singh A, Kumar V, Gupta S, Maurya M. 2014. Trichoderma genome to genomics: a review. J. Data Min. Genom. Proteom. 5(162):2153-0602.

Stamp JA. 2003. Pathogenic Status of High Quality Grapevine Nursery Stock. Wine Business Monthly 10(2):30-35.

Stempien E, Goddard ML, Wilhelm K, Tarnus C, Bertsch C, Chong J. 2017. Grapevine Botryosphaeria dieback fungi have specific aggressiveness factor repertory involved in wood decay and stilbene metabolization. PloS one 12(12):e0188766.

Stempien E, Jean R, Pierron G, Adendorff I, Van Jaarsveld J, Halleen F, Mostert L. 2020. Host defence activation and root colonization of grapevine rootstocks by the biological control fungus Trichoderma atroviride. Phytopathol. Mediterr. 59(3):615-626.

Stepanova A N, Yun J, Likhacheva AV, Alonso JM. 2007. Multilevel interactions between ethylene and auxin in Arabidopsis roots. The Plant Cell 19(7):2169-2185.

Stopnisek N, Zühlke D, Carlier A, Barberán A, Fierer N, Becher D, Riedel K, Eberl L, Weisskopf L. 2016. Molecular mechanisms underlying the close association between soil Burkholderia and fungi. The ISME J. 10(1):253-264.

Stot HU, Mitrousia GK, de Wit PJ, Fitt BOT. 2014. Effector-triggered defence against apoplastic fungal pathogens. Trends Plant Sci. 19(8):491-500.

Stothard P, Wishart DS. 2005. Circular genome visualization and exploration using CGView. Bioinformatics. 21(4):537-539.

Sukchawalit R, Loprasert S, Atichartpongkul S, Mongkolsuk S. 2001. Complex Regulation of the Organic Hydroperoxide Resistance Gene (ohr) from XanthomonasInvolves OhrR, a Novel Organic Peroxide-Inducible Negative Regulator, and Posttranscriptional Modifications. J. Bacteriol. 83(15):4405-4412.

Sun H, Hao PM, Zhang, M, Qin Y, Wei H, et al. 2018. Genome-wide identification and expression analyses of the pectate lyase (PEL) gene family in cotton (Gossypium hirsutum L.). BMC genomics 19(1):1-14.

Sun ZB, Li SD, Ren Q, Xu JL, Lu X, Sun MH. 2020. Biology and applications of Clonostachys rosea. J. Appl. Microbiol. 129(3):486-495.

Surico G. 2009. Towards a redefinition of the diseases within the esca complex of grapevine. Phytopathol. Mediterr. 48(1):5-10.

Tao C, Li R, Xiong W, Shen Z, Liu S, Wang B, Ruan Y, Geisen S, Shen Q, Kowalchuk GA. 2020. Bio-organic fertilizers stimulate indigenous soil Pseudomonas populations to enhance plant disease suppression. Microbiome 8(1):1-14.

Terral JF, Tabard , Bouby L, Ivorra S, Pastor T, Figueiral I, et al. 2010. Evolution and history of grapevine (Vitis vinifera) under domestication: new

morphometric perspectives to understand seed domestication syndrome and reveal origins of ancient European cultivars. Ann. botany 105(3):443-455.

Tey-Rulh P, Philippe I, Renaud JM, Tsoupras G, De Angelis P, Fallot J,Tabacchi R. 1991. Eutypine, a phytotoxin produced by Eutypa lata the causal agent of dying-arm disease of grapevine. Phytochemistry 30:471-473.

Thambugala KM, Daranagama DA, Phillips AJ, Kannangara SD, Promputtha I. 2020. Fungi vs. fungi in biocontrol: An overview of fungal antagonists applied against fungal plant pathogens. Front. Cell Infect. Microbiol. 10.

Tian J, Wang L-P, Yang Y-J, Sun J, Guo S-R. 2012. Exogenous spermidine alleviates the oxidative damage in cucumber seedlings subjected to high temperatures. J. Am. Soc. Hortic. Sci. 137(1):11-19.

Tijerino A, Cardoz R, Moraga J, Malmierca MG, Vicente F Aleu , Collado IG, Gutierrez S, Monte E, Hermosa R. 2011. Overexpression of the trichodiene synthase gene tri5 increases trichodermin production and antimicrobial activity in *Trichoderma brevicompactum.* Fungal Genet. Biol. 48:285-296.

Tiwari S, Verma T. 2019. Cellulose as a Potential Feedstock for Cellulose Enzyme Production. Approaches to Enhance Industrial Production of Fungal Cellulases. Springer. 89-116.

Toyama H, Chistoserdova L, Lidstrom ME. 1997. Sequence analysis of pqq genes required for biosynthesis of pyrroloquinoline quinone in Methylobacterium extorquens AM1 and the purification of a biosynthetic intermediate. Microbiology. 143(2):595-602.

Travadon R, Lawrence DP, Rooney-Latham S, Gubler WD, Wilcox WF, Rolshausen PE et al. 2015. Cadophora species associated with wood-decay of grapevine in North America. Fungal Biol 119:53–66.

Travadon R, Rolshausen PE, Gubler WD, Cadle-Davidson L, Baumgartner K. 2013. Susceptibility of cultivated and wild *Vitis spp*. to wood infection by fungal trunk pathogens. Plant Dis. 97(12):1529-1536.

Trese AT, Burton CL, Ramsdell DC. 1980. *Eutypa armeniacae* in Michigan vineyards: Ascospore production and survival, host infection, and fungal growth at low temperatures. Phytopathol. 70:788-793.

Tripathi, Tripathi JN, Shah T, Muiruri KS, Katari M. 2019. Molecular basis of disease resistance in banana progenitor Musa balbisiana against Xanthomonas campestris pv. musacearum. Sci. Rep.9(1):1-17.

Trotel-Aziz P, Abou-Mansour E, Courteaux B, Rabenoelina F, Clément C, Fontaine F, Aziz A. 2019. *Bacillus subtilis* PTA-271 counteracts Botryosphaeria dieback in grapevine, triggering immune responses and detoxification of fungal phytotoxins. Front. Plant Sci. 10:25.

Trotel-Aziz P, Couderchet M, Biagianti S, Aziz A. 2008. Characterization of new bacterial biocontrol agents Acinetobacter, *Bacillus*, *Pantoea* and *Pseudomonas* spp. mediating grapevine resistance against Botrytis cinerea. Environ. Exp. Bot. 64(1):21–32.

Trotel-Aziz P, Robert-Siegwald G, Fernandez O, Leal C, Villaume S, Guise JF, Abou-Mansour E, Lebrun M, Fontaine F. 2022. Diversity of *Neofusicoccum parvum* for the Production of the Phytotoxic Metabolites (-)-Terremutin and (R)-Mellein. J. Fungi 8(3):319.

Turenne CY, Sanche SE, Hoban DJ, Karlowsky JA, Kabani AM. 1999. Rapid identification of fungi by using the ITS2 genetic region and an automated fluorescent capillary electrophoresis system. J. Clin. Microbiol. 37:1846–1851.

Tyagi S, Mulla SI, Lee K-J, Chae J-C, Shukla P. 2018. VOCs-mediated hormonal signaling and crosstalk with plant growth promoting microbes. Crit. Rev. Biotechnol. 38(8):1277-1296.

Umezawa T, Sugiyama N, Mizoguchi M, Hayashi S, Myouga F, Yamaguchi-Shinozaki K, Ishihama, Y, Hirayama T, Shinozaki K. 2009. Type 2C protein phosphatases directly regulate abscisic acid-activated protein kinases in Arabidopsis. Prod. Natl. Acad. Sci. USA 106:17588-17593.

Urban L, Sari DC, Orsal B, Lopes MMDA, Miranda R, Aarrouf J. 2018. UV-C light and pulsed light as alternatives to chemical and biological elicitors for stimulating plant natural defenses against fungal diseases. Sci. Hortic.235:452-459.

Urbez-Torres JR, Bruez E, Hurtado J, Gubler WD. 2010. Effect of temperature on conidial germination of Botryosphaeriaceae species infecting grapevines. Plant Dis. 94:1476-1484.

Urbez-Torres JR, Gubler WD. 2011. Susceptibility of grapevine pruning wounds to infection by *Lasiodiplodia theobromae* and *Neofusicoccum parvum*. Plant Pathol. 60:261-270.

Urbez-Torres JR, Leavitt GM, Voegel T, Gubler WD. 2006. Identification and distribution of Botryosphaeria species associated with grapevine cankers in California. Plant Dis. 90:1490-1503.

Urbez-Torres JR, Peduto F, Smith RJ, Gubler WD. 2013. Phomopsis dieback: A grapevine trunk disease caused by *Phomopsis viticola* in California. Plant Dis. 97:1571-1579.

Úrbez-torres JR, Tomaselli E, Pollard-Flamand J, Boulé J, Gerin D, Pollastro S. 2020. Characterization of Trichoderma isolates from southern Italy, and their potential biocontrol activity against grapevine trunk disease fungi. Phytopathol. Mediterr. 59(3):425-439.

Úrbez-Torres JR. 2011. The status of Botryosphaeriaceae species infecting grapevines. Phytopathol. Mediterr. 50(4):5-45.

Vaillancourt FH, Bolin JT, Eltis LD. 2006. The ins and outs of ring-cleaving dioxygenases. Crit. Rev. Biochem. Mol. Biol. 41(4):241-267.

Van der Does D, Leon-Reyes A, Koornneef A, Van Verk MC, Rodenburg N, Pauwels L, Goossense A, Korbes A, Memelink J, Ritsema T, Van Wees S, Pieterse CM. 2013. Salicylic acid suppresses jasmonic acid signaling downstream of SCFCOI1-JAZ by targeting GCC promoter motifs via transcription factor ORA59. The Plant Cell 25(2):744-761.

Van der Ent S, Van Wees SC, Pieterse CM. 2009. Jasmonate signaling in plant interactions with resistance-inducing beneficial microbes. Phytochemistry 70(13-14):1581-1588.

Van Jaarsveld WJ, Halleen F, Bester MC, Pierron RJ, Stempien E, Mostert L. 2021. Investigation of Trichoderma species colonization of nursery grapevines for improved management of black foot disease. Pest Manag. Sci. 77(1):397-405.

Van Loon L, Bakker P, Pieterse C. Systemic resistance induced by rhizosphere bacteria. Annu. Rev. Phytopath. 1998;36(1):453-483.

Van Loon LC, Geraats BP, Linthorst HJ. 2006. Ethylene as a modulator of disease resistance in plants. Trends Plant Sci.11(4):184-191.

Van Loon LC, Van Kammen A. 1970. Polyacrylamide disc electrophoresis of the soluble leaf proteins from Nicotiana tabacum var.'Samsun'and 'Samsun NN': II. Changes in protein constitution after infection with tobacco mosaic virus. Virology 40(2):199-211.

Van Loon LC. 2000. Systemic induced resistance. In: Mechanisms of resistance to plant diseases. Slusarenko AJ, Fraser RSS & van Loon LC eds. Kluwer: Dordrechet 521–574.

Van Niekerk JM, Calitz FJ, Halleen F, Fourie PH. 2010. Temporal spore dispersal patterns of grapevine trunk pathogens in South Africa. Eur. J. Plant Pathol. 127:375-390.

Van Niekerk JM, Crous P, Hallenn F, Fourie PH. 2006. " *Botryosphaeria*" spp. as Grapevine Trunk Disease Pathogens. Phytopathol. Mediterr. 45:S43–S54.

Van Peer R, Niemann GJ, Schippers B. 1991. Induced resistance and phytoalexin accumulation in biological control of Fusarium wilt of carnation by Pseudomonas sp. strain WCS 417 r. Phytopathol. 81(7):728-734.

Van Schie B, De Mooy O, Linton J, Van Dijken J, Kuenen J. 1987. PQQ-dependent production of gluconic acid by Acinetobacter. Agrobacterium and Rhizobium species Microbiology. 133(4):867–75.

Van Schie CC, Takken FL. 2014. Susceptibility genes 101: how to be a good host. Annu. Rev. Phytopathol. 52:551-581.

Van Wees SC, Van der Ent S, Pieterse CM. 2008. Plant immune responses triggered by beneficial microbes. Curr. Opin. Plant Biol. 11:443–448.

Velásquez AC, Castroverde CDM, He SY. 2018. Plant–pathogen warfare under changing climate conditions. Curr. Biol. 28(10):R619-R634.

Verbeke F, De Craemer S, Debunne N, Janssens Y, Wynendaele E, Van de Wiele C, et al. 2017. Peptides as quorum sensing molecules: measurement techniques and obtained levels in vitro and in vivo. Front. Neurosci. 11:183.

Verhagen BW, Glazebrook J, Zhu T, Chang HS, Van Loon LC, Pieterse CM. 2004. The transcriptome of rhizobacteria-induced systemic resistance in Arabidopsis. Mol Plant Microbe Interact. 17(8):895-908.

Viaene T, Langendries , Beirinckx S, Maes M, Goormachtig S. 2016. Streptomyces as a plant's best friend?. FEMS Microbio. Ecol. 92(8).

Villena J, Kitazawa H, Van Wees S, Pieterse CM, Takahashi H. 2018. Receptors and signaling pathways for recognition of bacteria in livestock and crops: prospects for beneficial microbes in healthy growth strategies. Front. Immunol. 9:2223.

Vinale F, Sivasithamparam K, Ghisalberti EL, Marra R, Barbetti MJ, Li H, Woo SL, Lorito M. 2008. A novel role for Trichoderma secondary metabolites in the interactions with plants. Physiol. Mol. Plant Pathol. 72:80–86.

Viterbo A, Chet I. 2007. TasHyd1, a new hydrophobin gene from the biocontrol agent *Trichoderma asperellum*, is involved in plant root colonization. Mol. Plant Pathol. 7:249–258.

Viterbo A, Landau U, Ki S, Chernin L, Chet I. 2010. Characterization of ACC deaminase from the biocontrol and plant growth-promoting agent *Trichoderma asperellum* T203. FEMS Microbiol. Lett. 305(1):42-48.

Vizcain JA, Cardoza RA, Hauser M, Hermosa R, Rey M, Lobell A, Becker JM, Gutierrez S, Monte E. 2006. ThPTR2, a di/tri-peptide transporter gene from *Trichoderma harzianum*. Fungal Genet. Biol. 43:234-246.

Vorholt J. 2012. Microbial life in the phyllosphere. Nat. Rev. Microbiol. 10:828–840.

Vose PB. 1982. Iron nutrition in plants: a world overview. J. Plant Nutr. 5(4-7):233-249.

Waghunde RR, Shelake RM, Sabalpara AN. 2016. Trichoderma: a significant fungus for agriculture and environment. Afr. J. Agric. Res. 11:1952–1965.

Waghunde RR, Shelake RM, Shinde MS, Hayashi H. 2017. Endophyte microbes: a weapon for plant health management. In Microorganisms for green revolution 303-325. Springer, Singapore.

Wahl V, Brand LH, Guo YL, Schmid M. 2010. The FANTASTIC FOUR proteins influence shoot meristem size in Arabidopsis thaliana. BMC Plant Biol. 10(1):1-12.

Waite H, Armengol J, Billones-Baaijens R, Gramaje D, Halleeen F, Di Marco S, Smart R. 2018. A protocol for the management of grapevine rootstock mother vines to reduce latent infections by grapevine trunk pathogens in cuttings. Phytopathol. Mediterr. 57:384-398.

Waite H, Armengol J, Billones-Baaijens R, Gramaje D, Halleen F, Di Marco S, Smart R. 2018. A protocol for the management of grapevine rootstock mother vines to reduce latent infections by grapevine trunk pathogens in cuttings. Phytopathol. Mediterr. 57(3):384-398.

Waite H, Morton L. 2007. Hot water treatment, trunk diseases and other critical factors in the production of high-quality grapevine planting material. Phytopathol. Mediterr. 46:5-17.

Wan J, He M, Hou Q, Zou L, Yan, Y, Wei Y, Chen X. 2021. Cell wall associated immunity in plants. Stress Biology 1(1):1-15.

Wang XQ, Zhao DL, Shen LL, Jing CL, Zhang CS. 1988. Application and mechanisms of *Bacillus subtilis* in biological control of plant disease. In: Meena VS, editor. Role of rhizospheric microbes in soil. Singapore Pte Ltd: Springer Nature 225–50.

Wang Y, Shi Y, Li K, Yang D, Liu N, Zhang L, et al. 2021. Roles of the 2-Oxoglutarate-Dependent Dioxygenase Superfamily in the Flavonoid Pathway: A Review of the Functional Diversity of F3H, FNS I, FLS, and LDOX/ANS. Molecules 26(21):6745.

Wei G, Kloepper JW, Tuzun S. 1991. Induction of systemic resistance of cucumber to Colletotrichum orbiculare by select strains of plant growth-promoting rhizobacteria. Phytopathol. 81(11):1508-1512.

Weller DM. 1988. Biological control of soilborne plant pathogens in the rhizosphere with bacteria. Annu. Rev. Phytopathol. 26:379–407.

White TJ, Bruns TD, Lee SB Taylor JW. 1990. Amplification sand direct sequencing of fungal ribosomal RNA genes for phylogenetics. PCR Protoc. 18:315–322.

Williams B, Kabbage M, Kim HJ, Britt R, Dickman MB. 2011. Tipping the balance: Sclerotinia sclerotiorum secreted oxalic acid suppresses host defenses by manipulating the host redox environment. PLoS Patho. 7(6):e1002107.

Wise RP, Moscou MJ, Bogdanove AJ, Whitham SA. 2007. Transcript profiling in host-pathogen interactions.

Woo OG, Kim H, Kim JS, Keum HL, Lee KC, Sul WJ, Lee JH. 2020. *Bacillus subtilis* strain GOT9 confers enhanced tolerance to drought and salt stresses in Arabidopsis thaliana and Brassica campestris. Plant Physiol. Biochem. 148:359-367.

Woo SL, Donzelli B, Scala F, Mach R, Harman GE, Kubicek CP, Sorbo GD, Lorito M. 1999. Disruption of the ech42 (endochitinaseencoding) gene affects biocontrol activity in *Trichoderma harzianum* P1. Am. Phytopathol. Soc. 12(5):219-229.

Wu L, Wu HJ, Qiao J, Gao X, Borriss R. 2015. Novel routes for improving biocontrol activity of Bacillus based bioinoculants. Front. Microbiol. 6:1395.

Wu Y, Zhou JM. 2013. Receptor-L ike Kinases in Plant Innate Immunity. J. Integr. Plant Biol. 55(12):1271-1286.

Xie S-S, Wu H-J, Zang H-Y, Wu L-M, Zhu Q-Q, Gao X-W. 2014. Plant growth promotion by spermidine-producing Bacillus subtilis OKB105. Mol. Plant Microbe Interact. 27(7):655-663.

Xie X, Zhang H, Pare P. 2009. Sustained growth promotion in Arabidopsis with long-term exposure to the beneficial soil bacterium Bacillus subtilis (GB03). Plant. Signal. Behav. 4(10):948-953.

Xu , Wang, S, Li L, Sahu SK, Petersen M, Liu X, et al. 2019. Molecular evidence for origin, diversification and ancient gene duplication of plant subtilases (SBTs). Sci. Rep. 9(1):1-10.

Xu L, Xing S-T, Sun X-Z, Guo J-E, Xu D-H. 2014. Effects of polyamines on hormones contents and the relationship with the flower bud differentiation in chrysanthemum. Plant Physiol. J. 50(8):1195-1202.

Xu XM, Jeffries P, Pautass, M, Jeger MJ. 2011. Combined use of biocontrol agents to manage plant diseases in theory and practice. Phytopathol. 101(9):1024-1031.

Yacoub A, Gerbore J, Magnin N, Chambon P, Dufour MC, Corio-Costet MF, et al. 2016. Ability of *Pythium oligandrum* strains to protect *Vitis vinifera L*., by inducing plant resistance against *Phaeomoniella chlamydospora*, a pathogen involved in Esca, a grapevine trunk disease. Biol. Control 92:7-16.

Yacoub A, Magnin N, Gerbore J, Haidar R, Bruez E, Compant S, Guyoneaud R, Rey P. 2020. The biocontrol root-oomycete, Pythium Oligandrum, triggers grapevine resistance and shifts in the transcriptome of the trunk pathogenic fungus, Phaeomoniella chlamydospora. Int. J. Mol. Sci. 21:6876-6183.

Yang C, Marillonnet S, Tissier A. 2021. The scarecrow-like transcription factor SlSCL3 regulates volatile terpene biosynthesis and glandular trichome size in tomato (Solanum lycopersicum). Plant J.107(4):1102-1118.

Yang H, Li Y, Xiao Y, Gu Y, Liu H, Liang Y, et al. 2017. An integrated insight into the relationship between soil microbial community and tobacco bacterial wilt disease. Front Microbiol. 8:2179.

Yang H, Mu, Chen L, Feng J, Hu J, Li L, et al. 2015. S-nitrosylation positively regulates ascorbate peroxidase activity during plant stress responses. Plant Physiol. 167(4):1604-1615.

Yang L, Li B, Zhen XY, Li J, Yang M, Dong X, He G, An C, Deng XW. 2015. Salicylic acid biosynthesis is enhanced and contributes to increased biotrophic pathogen resistance in Arabidopsis hybrids. Nat. Commun. 6(1):1-12.

Yao C, Li W, Liang X, Ren C, Liu W, Yang G, et al. 2022. Molecular Cloning and Characterization of MbMYB108, a Malus baccata MYB Transcription Factor Gene, with Functions in Tolerance to Cold and Drought Stress in Transgenic Arabidopsis thaliana. Int. J. Mol. Sci. 23(9):4846.

Ye Y, Ding Y, Jiang Q, Wang F, Sun J, Zhu C. 2017. The role of receptor-like protein kinases (RLKs) in abiotic stress response in plants. Plant Cell Rep.36(2):235-242.

Ye, Coulouris G, Zaretskaya I, Cutcutache I, Rozen S, Madden TL. 2012. Primer-BLAST: a tool to design target-specific primers for polymerase chain reaction. BMC Bioinform. 13(1):1-11.

Yeom KH, Ariyoshi W, Okinaga T, Washio A, Morotomi T, Kitamura C, Nishihara T. 2016. Platelet-rich plasma enhances the differentiation of dental pulp progenitor cells into odontoblasts. Int. Endod. J. 49(3):271-278.

Yin D, Wang N, Xia F, Li Q, Wang W. 2013. Impact of biocontrol agents *Pseudomonas fluorescens* 2P24 and CPF10 on the bacterial community in the cucumber rhizosphere. Eur. J. Soil Biol. 59:36–42.

Yin Y, Mao X, Yang J, Chen X, Mao F, Xu Y. 2012. dbCAN: a web resource for automated carbohydrate-active enzyme annotation. Nucleic Acids Res. 40(1):445-451.

Yin YY, Li T, Lu X, Fang Q, Ding M, Zhan ZK. 2016. First report of capsicum chlorosis virus infecting tomato in yunnan, southwest of china. Plant Dis. 100(1):230-230.

Yıldırım K, Yağcı A, Sucu S, Tunç S. 2018. Responses of grapevine rootstocks to drought through altered root system architecture and root transcriptomic regulations. Plant Physiol. Biochem. 127:256-268.

Yobo KS, Laing MD, Hunter CH. 2011. Effects of single and combined inoculations of selected Trichoderma and Bacillus isolates on growth of dry bean and biological control of *Rhizoctonia solani* damping-off. Afr. J. Biotechnol. 10(44):8746-8756.

Yoon S-H, Ha S-m, Lim J, Kwon S, Chun J. 2017. A large-scale evaluation of algorithms to calculate average nucleotide identity. Anton. Leeuw. Int. J. G. 110(10):1281-1286.

Yu X, Ai C, Xin L, Zhou G. 2011. The siderophore-producing bacterium, Bacillus subtilis CAS15, has a biocontrol effect on Fusarium wilt and promotes the growth of pepper. Eur. J. Soil Biol.;47(2):138-145.

Zahavi T, Reuveni M, Scheglo D, Lavee S. 2001. Effect of grapevine training systems on development of powdery mildew. Eur. J. Plant Pathol. 107(5):495-501.

Zaidi A, Khan MS, Rizvi A, Saif S, Ahmad B, Shahid M. 2017. Role of phosphate-solubilizing bacteria in legume improvement. In: Zaidi A, Khan M, Musarrat J (eds) Microbes for Legume Improvement Springer,Cham. 175-197.

Zamioudis C, Korteland J, Van Pelt JA, van Hamersveld M, Dombrowski N, Bai Y, et al. 2015. Rhizobacterial volatiles and photosynthesis-related signals coordinate MYB 72 expression in Arabidopsis roots during onset of induced systemic resistance and iron-deficiency responses. Plant J. 84(2):309-322.

Zarraonaindia I, Eouzan I, Muñoz AM, Neves C, Legout H, Delalande D, Estonba A. 2016. Apis mellifera gut and head virome/microbiome survey: a spatio-temporal approach. In TIBEES, Scientific Bee Health Symposium.

Zeilinger S, Gupta VK, Dahms TE, Silva R, Singh HB, Upadhyay RS, Vieira Gomes E, Tsui C, Nayak SC. 2016. Friends or foes? Emerging insights from fungal interactions with plants. FEMS Microbiol. Rev. 40(2):182-207.

Zentella R, Zhang Z-L, Park M, Thomas SG, Endo A, Murase K, et al. 2007. Global analysis of DELLA direct targets in early gibberellin signaling in Arabidopsis. Plant Cell. 19(10):3037-3057.

Zhang B, Liu C, Wang Y, Yao X, Wang F, Wu J, et al. 2015. Disruption of a CAROTENOID CLEAVAGE DIOXYGENASE 4 gene converts flower colour from white to yellow in Brassica species. New Phytol. 206(4):1513-1526.

Zhang H, Kim M-S, Krishnamachari V, Payton P, Sun Y, Grimson M, Fet al. 2007. Rhizobacterial volatile emissions regulate auxin homeostasis and cell expansion in Arabidopsis. Planta. 2007;226(4):839.

Zhang H, Murzello C, Sun Y, Kim MS, Xie X, Jeter M, Zak JC, Dowd SE, Paré PW. 2010. Choline and osmotic-stress tolerance induced in Arabidopsis by the soil microbe Bacillus subtilis (GB03). Mol. Plant-Microbe Inter. 23:1097-1104.

Zhang Z, J R, Li H, Zhao T, Liu J, Lin C, Liu B. 2014. CONSTANS-LIKE 7 (COL7) is involved in phytochrome B (phyB)-mediated light-quality regulation of auxin homeostasis. Mol. Plant 7(9):1429-1440.

Zhou, Minio, A, Massonnet M, Solares E, Lv Y, Beridze T, Cantu D, Gaut BS. 2019. The population genetics of structural variants in grapevine domestication. Nat. Plants 5(9):965-979.

Zipfel C, Robatzek S. 2010. Pathogen-associated molecular pattern-triggered immunity: veni, vidi? Plant physiol. 154(2):551-554.

Ziv C, Zhao Z, Gao YG, Xia Y. 2018. Multifunctional roles of plant cuticle during plant-pathogen interactions. Front. plant sci. 9:1088.

Appendix

Support to chapter II

Table s1. *Bacillus subtilis* PTA-271 encoding genes for motility, adhesion and plant root colonizing capacity.

Locus tag ID	Gene	Function		
Motility (swarming), biofilm and root colonization				
S19-40_00277	*ylxH*	Flagellum site-determining protein		
S19-40_00278	*flhF*	Flagellar biosynthesis protein		
S19-40_00279	*flhA*	Flagellar biosynthesis protein		
S19-40_00280	*flhB*	Flagellar biosynthetic protein		
S19-40_00283	*fliP*	Flagellar biosynthetic protein		
S19-40_00286	*fliN*	Flagellar motor switch protein		
S19-40_00287	*fliM*	Flagellar motor switch protein		
S19-40_00289	*flgG*	Flagellar basal-body rod protein		
S19-40_00293	*fliJ*	Flagellar protein		
S19-40_00296	*fliG*	Flagellar motor switch protein		
S19-40_00297	*fliF*	Flagellar M-ring protein		
S19-40_00298	*fliE*	Flagellar hook-basal body complex protein		
S19-40_00299	*flgC*	Flagellar basal-body rod protein		
S19-40_00300	*flgB*	Flagellar basal body rod protein		
S19-40_00290	*flgD*	Basal-body rod modification protein		
S19-40_00310	*flhB*	Flagellar biosynthetic protein		
S19-40_00890	*flgK*	Flagellar hook-associated protein 1		
S19-40_00891	*flaB3*	Flagellar filament 31 kDa core protein		
S19-40_00893	*fliW*	Flagellar assembly factor		
S19-40_00895	*hag*	Flagellin		
S19-40_00897	*fliD*	B-type flagellar hook-associated protein 2		
S19-40_00898	*fliS*	Flagellar protein		
S19-40_00557	*motB*	Motility protein B		
S19-40_02745	*cheR*	Chemotaxis protein methyltransferase		
S19-40_00115	*cheY*	Chemotaxis protein		
S19-40_00272	*cheD*	Chemoreceptor glutamine deamidase		
S19-40_00273	*cheC*	CheY-P phosphatase		
S19-40_00274	*cheW*	Chemotaxis protein		
S19-40_00275	*cheA*	Chemotaxis protein		
S19-40_00276	*cheB*	Chemotaxis response regulator protein-glutamate methylesterase		
S19-40_00285	*cheY*	Chemotaxis protein		
S19-40_00519	*cheV*	Chemotaxis protein		
S19-40_02745	*cheR*	Chemotaxis protein methyltransferase		
S19-40_03165	*swrC*	Swarming motility protein		
S19-40_00882	*spo0A*	Response regulator receiver domain protein		

Table s2. *Bacillus subtilis* PTA-271 encoding genes for some Transcriptional regulators and Operons.

	Gene	Function
		Transcriptional regulators
S19-40_00006	purR	LacI family transcriptional regulator, purine nucleotide synthesis repressor
S19-40_00012	immR	HTH-type transcriptional regulator ImmR
S19-40_00023	gltC	HTH-type transcriptional regulator GltC
S19-40_00025	sinR	XRE family transcriptional regulator, master regulator for biofilm formation
S19-40_00049	slyA	Transcriptional regulator SlyA
S19-40_00060	gltC	HTH-type transcriptional regulator GltC
S19-40_00064	yofA	HTH-type transcriptional regulator YofA
S19-40_00173	glnR	HTH-type transcriptional regulator GlnR
S19-40_00212	betI	HTH-type transcriptional regulator BetI
S19-40_00255	infB	Translation initiation factor IF-2
S19-40_00268	tsf	Elongation factor Ts
S19-40_00374	dksA	RNA polymerase-binding transcription factor DksA
S19-40_00374	yocK	General stress protein 16O
S19-40_00405	mraZ	Transcriptional regulator MraZ
S19-40_00506	argP	HTH-type transcriptional regulator ArgP
S19-40_00516	ykuD	Putative L,D-transpeptidase YkuD
S19-40_00529	splA	Transcriptional regulator protein (SplA)
S19-40_00549	ytcD	putative HTH-type transcriptional regulator YtcD
S19-40_00558	mhqR	HTH-type transcriptional regulator MhqR
S19-40_00593	mhqR	HTH-type transcriptional regulator MhqR
S19-40_00596	tnrA	HTH-type transcriptional regulator TnrA
S19-40_00599	splA	Transcriptional regulator protein (SplA)
S19-40_00614	ohrR	Organic hydroperoxide resistance transcriptional regulator
S19-40_00667	yusO	putative HTH-type transcriptional regulator YusO
S19-40_00690	crp	CRP/FNR family transcriptional regulator, cyclic AMP receptor protein
S19-40_00758	ywnA	Putative HTH-type transcriptional regulator YwnA
S19-40_00761	zntR	Zn(II)-responsive transcriptional regulator
S19-40_00768	hipB	Transcriptional regulator, y4mF family
S19-40_00779	-	putative HTH-type transcriptional regulator/GBAA_1941/BAS1801
S19-40_00794	ulaR	HTH-type transcriptional regulator UlaR
S19-40_00809	gltR	HTH-type transcriptional regulator GltR
S19-40_00814	lrpC	HTH-type transcriptional regulator LrpC
S19-40_00823	hdfR	HTH-type transcriptional regulator HdfR
S19-40_00834	scrR	LacI family transcriptional regulator, sucrose operon repressor
S19-40_00841	ywtF	Putative transcriptional regulator YwtF

S19-40_00865	lytR	Transcriptional regulator LytR
S19-40_00879	yvhJ	Putative transcriptional regulator YvhJ
S19-40_00882	degU	Transcriptional regulatory protein DegU
S19-40_00882	*spo0A*	Response regulator receiver domain protein
S19-40_00912	betI	HTH-type transcriptional regulator BetI
S19-40_00924	zitR	Transcriptional regulator ZitR
S19-40_00927	adcR	Transcriptional regulator AdcR
S19-40_00929	nanR	Transcriptional regulator NanR
S19-40_00962	phoB	Phosphate regulon transcriptional regulatory protein PhoB
S19-40_00987	yvdT	putative HTH-type transcriptional regulator YvdT
S19-40_00997	sinR	HTH-type transcriptional regulator SinR
S19-40_01016	lutR	HTH-type transcriptional regulator LutR
S19-40_01017	lacR	HTH-type transcriptional regulator LacR
S19-40_01028	desR	Transcriptional regulatory protein DesR
S19-40_01035	hdfR	HTH-type transcriptional regulator HdfR
S19-40_01050	opcR	HTH-type transcriptional regulator, osmoprotectant uptake regulator
S19-40_01060	opcR	HTH-type transcriptional regulator, osmoprotectant uptake regulator
S19-40_01067	yodB	HTH-type transcriptional regulator YodB
S19-40_01068	rghR	HTH-type transcriptional repressor RghR
S19-40_01069	rghR	HTH-type transcriptional repressor RghR
S19-40_01078	tetR	Mycofactocin system transcriptional regulator
S19-40_01084	csoR	Copper-sensing transcriptional repressor CsoR
S19-40_01118	walR	Transcriptional regulatory protein WalR
S19-40_01132	liaR	Transcriptional regulatory protein LiaR
S19-40_01138	ethR	HTH-type transcriptional regulator EthR
S19-40_01140	cssR	Transcriptional regulatory protein CssR
S19-40_01148	gltR	HTH-type transcriptional regulator GltR
S19-40_01152	yusO	putative HTH-type transcriptional regulator YusO
S19-40_01185	yurK	putative HTH-type transcriptional regulator YurK
S19-40_01273	comA	Transcriptional regulatory protein ComA
S19-40_01288	dcuR	Transcriptional regulatory protein DcuR
S19-40_01325	ulaR	HTH-type transcriptional regulator UlaR
S19-40_01340	opcR	HTH-type transcriptional repressor OpcR

S19-40_01355	-	Transcriptional regulator, Acidobacterial, PadR-family
S19-40_01359	tetR	Tetracycline repressor protein class B from transposon Tn10
S19-40_01367	csoR	Copper-sensing transcriptional repressor CsoR
S19-40_01369	tipA	HTH-type transcriptional activator TipA
S19-40_01375	gltR	HTH-type transcriptional regulator GltR
S19-40_01379	gltR	HTH-type transcriptional regulator GltR
S19-40_01398	cmpR	HTH-type transcriptional activator CmpR
S19-40_01412	adhR	HTH-type transcriptional regulator AdhR
S19-40_01421	dgaR	Transcriptional regulatory protein DagR
S19-40_01424	-	Sugar-specific transcriptional regulator TrmB
S19-40_01430	bm3R1	HTH-type transcriptional repressor Bm3R1
S19-40_01468	cymR	HTH-type transcriptional regulator CymR
S19-40_01482	comN	Post-transcriptional regulator ComN
S19-40_01499	yebC	putative transcriptional regulatory protein YebC
S19-40_01559	yusO	putative HTH-type transcriptional regulator YusO
S19-40_01574	betI	HTH-type transcriptional regulator BetI
S19-40_01606	infC	Translation initiation factor IF-3
S19-40_01618	nrdR	Transcriptional repressor NrdR
S19-40_01621	ytcD	putative HTH-type transcriptional regulator YtcD
S19-40_01629	phoP	Alkaline phosphatase synthesis transcriptional regulatory protein PhoP
S19-40_01660	cmpR	HTH-type transcriptional activator CmpR
S19-40_01683	yttP	putative HTH-type transcriptional regulator YttP
S19-40_01722	ytzE	putative HTH-type transcriptional regulator YtzE
S19-40_01733	yesS	HTH-type transcriptional regulator YesS
S19-40_01744	lacR	HTH-type transcriptional regulator LacR
S19-40_01764	ytrA	HTH-type transcriptional repressor YtrA
S19-40_01802	dksA	RNA polymerase-binding transcription factor DksA
S19-40_01845	gmuR	HTH-type transcriptional regulator GmuR
S19-40_01860	rspR	HTH-type transcriptional repressor RspR
S19-40_01863	slyA	Transcriptional regulator SlyA
S19-40_01866	tcaR	HTH-type transcriptional regulator TcaR
S19-40_01872	betI	HTH-type transcriptional regulator BetI
S19-40_01894	cmtR	HTH-type transcriptional regulator CmtR

S19-40_01896	norG	HTH-type transcriptional regulator NorG
S19-40_01900	aseR	HTH-type transcriptional repressor AseR
S19-40_01901	-	putative HTH-type transcriptional regulator
S19-40_01904	yybR	putative HTH-type transcriptional regulator YybR
S19-40_01906	yybR	putative HTH-type transcriptional regulator YybR
S19-40_01909	gabR	HTH-type transcriptional regulatory protein GabR
S19-40_01921	rhaS	HTH-type transcriptional activator RhaS
S19-40_01923	carD	RNA polymerase-binding transcription factor CarD
S19-40_01927	-	Transcriptional regulator, y4mF family
S19-40_01969	dcuR	Transcriptional regulatory protein DcuR
S19-40_01990	lrpC	HTH-type transcriptional regulator LrpC
S19-40_01999	mtlR	Transcriptional regulator MtlR
S19-40_02005	kipR	HTH-type transcriptional regulator KipR
S19-40_02028	gabR	HTH-type transcriptional regulatory protein GabR
S19-40_02044	srrA	Transcriptional regulatory protein SrrA
S19-40_02058	benM	HTH-type transcriptional regulator BenM
S19-40_02064	gabR	HTH-type transcriptional regulatory protein GabR
S19-40_02082	hpr	HTH-type transcriptional regulator Hpr
S19-40_02087	yciB	Putative L,D-transpeptidase YciB
S19-40_02114	mhqR	HTH-type transcriptional regulator MhqR
S19-40_02148	natR	Transcriptional regulatory protein NatR
S19-40_02154	yxaF	putative HTH-type transcriptional regulator YxaF
S19-40_02167	walR	Transcriptional regulatory protein WalR
S19-40_02172	lutR	HTH-type transcriptional regulator LutR
S19-40_02207	-	Transcriptional regulator SlyA
S19-40_02257	ybbH	putative HTH-type transcriptional regulator YbbH
S19-40_02291	xre	HTH-type transcriptional regulator Xre
S19-40_02305	exuR	putative HTH-type transcriptional repressor ExuR
S19-40_02344	manR	Transcriptional regulator ManR
S19-40_02402	spxA	Transcriptional regulator, Spx/MgsR family
S19-40_02449	-	Transcriptional regulator, Acidobacterial, PadR-family
S19-40_02468	norG	HTH-type transcriptional regulator NorG
S19-40_02472	degA	HTH-type transcriptional regulator DegA

S19-40_02497	sgrR	HTH-type transcriptional regulator SgrR
S19-40_02539	bm3R1	HTH-type transcriptional repressor Bm3R1
S19-40_02555	hpr	HTH-type transcriptional regulator Hpr
S19-40_02602	gabR	HTH-type transcriptional regulatory protein GabR
S19-40_02607	cysL	HTH-type transcriptional regulator CysL
S19-40_02612	nsrR	HTH-type transcriptional repressor NsrR
S19-40_02617	liaR	Transcriptional regulatory protein LiaR
S19-40_02643	ytrA	HTH-type transcriptional repressor YtrA
S19-40_02786	srrA	Transcriptional regulatory protein SrrA
S19-40_02834	xre	HTH-type transcriptional regulator Xre
S19-40_02872	ykuD	Putative L,D-transpeptidase YkuD
S19-40_02880	-	Zn(II)-responsive transcriptional regulator
S19-40_02904	argR	Arginine repressor
S19-40_02924	efp	Elongation factor P
S19-40_02931	mntR	Transcriptional regulator MntR
S19-40_02940	sinR	HTH-type transcriptional regulator SinR
S19-40_02959	spxA	Transcriptional regulator, Spx/MgsR family
S19-40_02992	zur	Fur family transcriptional regulator, zinc uptake regulator
S19-40_03061	marR	MarR family transcriptional regulator, multiple antibiotic resistance protein MarR
S19-40_03147	lrpC	HTH-type transcriptional regulator LrpC
S19-40_03152	trpR	TrpR family transcriptional regulator, trp operon repressor
S19-40_03164	kstR2	HTH-type transcriptional repressor KstR2
S19-40_03183	-	putative transcriptional regulatory protein
S19-40_03199	yesS	HTH-type transcriptional regulator YesS
S19-40_03219	mprA	Transcriptional repressor MprA
S19-40_03221	IF5B	translation initiation factor 5B
S19-40_03237	yfmP	HTH-type transcriptional regulator YfmP
S19-40_03254	citT	Transcriptional regulatory protein CitT
S19-40_03272	treR	HTH-type transcriptional regulator TreR
S19-40_03308	glvR	HTH-type transcriptional regulator GlvR
S19-40_03316	degU	Transcriptional regulatory protein DegU
S19-40_03325	yusO	putative HTH-type transcriptional regulator YusO
S19-40_03379	-	Transcriptional regulator PadR-like family protein

S19-40_03402	liaR	Transcriptional regulatory protein LiaR
S19-40_03450	mgrA	HTH-type transcriptional regulator MgrA
S19-40_03463	cynR	HTH-type transcriptional regulator CynR
S19-40_03472	slrA	Transcriptional regulator SlrA
S19-40_03472	slrA	Transcriptional regulator SlrA
S19-40_03494	-	Transcriptional regulator, Acidobacterial, PadR-family
S19-40_03530	cysL	HTH-type transcriptional regulator CysL
S19-40_03537	iscR	HTH-type transcriptional regulator IscR
S19-40_03547	btr	HTH-type transcriptional activator Btr
S19-40_03554	czrA	HTH-type transcriptional repressor CzrA
S19-40_03562	desR	Transcriptional regulatory protein DesR
S19-40_03567	dksA	RNA polymerase-binding transcription factor DksA
S19-40_03599	yodB	HTH-type transcriptional regulator YodB
S19-40_03634	yusO	putative HTH-type transcriptional regulator YusO
S19-40_03677	kdgR	HTH-type transcriptional regulator KdgR
S19-40_03703	tcrX	putative transcriptional regulatory protein TcrX
S19-40_03711	walR	Transcriptional regulatory protein WalR
S19-40_03729	yybR	putative HTH-type transcriptional regulator YybR
S19-40_03734	mta	HTH-type transcriptional activator mta
S19-40_03739	gltC	HTH-type transcriptional regulator GltC
S19-40_03743	slyA	Transcriptional regulator SlyA
S19-40_03753	-	putative HTH-type transcriptional regulator
S19-40_03760	purR	HTH-type transcriptional repressor PurR
S19-40_03790	yydK	putative HTH-type transcriptional regulator YydK
S19-40_03799	gntR	putative D-xylose utilization operon transcriptional repressor
S19-40_03804	nicR	MarR family transcriptional regulator, lower aerobic nicotinate degradation pathway
S19-40_03806	yxaF	putative HTH-type transcriptional regulator YxaF
S19-40_03815	dhaS	HTH-type dhaKLM operon transcriptional activator DhaS
S19-40_03885	infA	Translation initiation factor IF-1
S19-40_03911	tuf	Elongation factor Tu
S19-40_03912	fusA	Elongation factor G
S19-40_03940	ctsR	Transcriptional regulator CtsR
S19-40_03944	-	Transcriptional regulator, y4mF family

S19-40_00023	cysL	LysR family transcriptional regulator, transcriptional activator of the cysJI operon
S19-40_00049	HpaR	homoprotocatechuate degradation operon regulator, HpaR
S19-40_00060	gltC	LysR family transcriptional regulator, transcription activator of glutamate synthase o
S19-40_00271	fliA	RNA polymerase sigma factor for flagellar operon FliA
S19-40_00371	pyrR	pyrimidine operon attenuation protein / uracil phosphoribosyltransferase
S19-40_00482	fruR2, fruR	DeoR family transcriptional regulator, fructose operon transcriptional repressor
S19-40_00506	cysL	LysR family transcriptional regulator, transcriptional activator of the cysJI operon
S19-40_00529	splA	transcriptional regulator of the spore photoproduct lyase operon
S19-40_00533	glcT	PtsGHI operon antiterminator
S19-40_00558	HpaR	HpaR: homoprotocatechuate degradation operon regulator, HpaR
S19-40_00593	HpaR	HpaR: homoprotocatechuate degradation operon regulator, HpaR
S19-40_00599	splA	transcriptional regulator of the spore photoproduct lyase operon
S19-40_00614	HpaR	HpaR: homoprotocatechuate degradation operon regulator, HpaR
S19-40_00779	HpaR	HpaR: homoprotocatechuate degradation operon regulator, HpaR
S19-40_00823	hcaR	Hca operon transcriptional activator HcaR
S19-40_00834	scrR	LacI family transcriptional regulator, sucrose operon repressor
S19-40_00884	comFA	ComF operon protein 1
S19-40_00885	comFB	ComF operon protein 2
S19-40_00887	YvyF	YvyF: flagellar operon protein
S19-40_00912	mexL	TetR/AcrR family transcriptional regulator, mexJK operon transcriptional repressor
S19-40_00927	HpaR	HpaR: homoprotocatechuate degradation operon regulator, HpaR
S19-40_01035	gltC	LysR family transcriptional regulator, transcription activator of glutamate synthase o
S19-40_01037	araR	GntR family transcriptional regulator, arabinose operon transcriptional repressor
S19-40_01078	acrR	TetR/AcrR family transcriptional regulator, multidrug resistance operon repressor
S19-40_01106	btr	AraC family transcriptional regulator, transcriptional activator for feuABC-ybbA op
S19-40_01116	fliA	RNA polymerase sigma factor for flagellar operon FliA
S19-40_01138	nemR	TetR/AcrR family transcriptional regulator, transcriptional repressor for nem operon
S19-40_01152	HpaR	HpaR: homoprotocatechuate degradation operon regulator, HpaR
S19-40_01185	frlR	GntR family transcriptional regulator, frlABCD operon transcriptional regulator
S19-40_01325	srlR	Glucitol operon repressor
S19-40_01365	pspE	phageshock_pspE: phage shock operon rhodanese PspE
S19-40_01421	gfrR	sigma-54 dependent transcriptional regulator, gfr operon transcriptional activator

S19-40_01430	fatR, bscR	TetR/AcrR family transcriptional regulator, repressor of fatR-cypB operon
S19-40_01559	HpaR	HpaR: homoprotocatechuate degradation operon regulator, HpaR
S19-40_01660	ytlI	LysR family transcriptional regulator, regulator of the ytmI operon
S19-40_01683	fatR, bscR	TetR/AcrR family transcriptional regulator, repressor of fatR-cypB operon
S19-40_01695	cytR	LacI family transcriptional regulator, repressor for deo operon, udp, cdd, tsx, nupC,
S19-40_01733	btr	AraC family transcriptional regulator, transcriptional activator for feuABC-ybbA op
S19-40_01744	cytR	LacI family transcriptional regulator, repressor for deo operon, udp, cdd, tsx, nupC,
S19-40_01764	-	trehalos_R_Bsub: trehalose operon repressor
S19-40_01771	caiE	Carnitine operon protein CaiE
S19-40_01845	-	trehalos_R_Bsub: trehalose operon repressor
S19-40_01860	rspR	GntR family transcriptional regulator, rspAB operon transcriptional repressor
S19-40_01901	mexL	TetR/AcrR family transcriptional regulator, mexJK operon transcriptional repressor
S19-40_01911	fatR, bscR	TetR/AcrR family transcriptional regulator, repressor of fatR-cypB operon
S19-40_01921	rhaS	AraC family transcriptional regulator, L-rhamnose operon regulatory protein RhaS
S19-40_01984	bcsB	cellulose synthase operon protein B
S19-40_01999	mtlR	mannitol operon transcriptional antiterminator
S19-40_02105	gltC	LysR family transcriptional regulator, transcription activator of glutamate synthase o
S19-40_02114	HpaR	HpaR: homoprotocatechuate degradation operon regulator, HpaR
S19-40_02154	lmrA, yxaF	TetR/AcrR family transcriptional regulator, lmrAB and yxaGH operons repressor
S19-40_02186	-	trehalos_R_Bsub: trehalose operon repressor
S19-40_02202	rhaS	AraC family transcriptional regulator, L-rhamnose operon regulatory protein RhaS
S19-40_02233	arsR	Arsenical resistance operon repressor
S19-40_02262	btr	AraC family transcriptional regulator, transcriptional activator for feuABC-ybbA op
S19-40_02263	btr	AraC family transcriptional regulator, transcriptional activator for feuABC-ybbA op
S19-40_02344	manR	activator of the mannose operon, transcriptional antiterminator
S19-40_02472	cytR	LacI family transcriptional regulator, repressor for deo operon, udp, cdd, tsx, nupC,
S19-40_02473	araC	Arabinose operon regulatory protein
S19-40_02500	cytR	LacI family transcriptional regulator, repressor for deo operon, udp, cdd, tsx, nupC,
S19-40_02539	fatR, bscR	TetR/AcrR family transcriptional regulator, repressor of fatR-cypB operon
S19-40_02594	merR1	Mercuric resistance operon regulatory protein
S19-40_02623	glpP	Glycerol uptake operon antiterminator regulatory protein
S19-40_02649	HpaR	HpaR: homoprotocatechuate degradation operon regulator, HpaR
S19-40_02717	birA	BirA family transcriptional regulator, biotin operon repressor / biotin---[acetyl-CoA

S19-40_02933	pspE	phageshock_pspE: phage shock operon rhodanese PspE
S19-40_02946	comGG	ComG operon protein 7
S19-40_02950	comGC	ComG operon protein 3
S19-40_02952	comGA	ComG operon protein 1
S19-40_03041	comEC	ComE operon protein 3
S19-40_03042	comEB	ComE operon protein 2
S19-40_03043	comEA	ComE operon protein 1
S19-40_03075	nemR	TetR/AcrR family transcriptional regulator, transcriptional repressor for nem operon
S19-40_03104	gutR	LuxR family transcriptional regulator, glucitol operon activator
S19-40_03152	trpR	TrpR family transcriptional regulator, trp operon repressor
S19-40_03199	btr	AraC family transcriptional regulator, transcriptional activator for feuABC-ybbA op
S19-40_03219	emrR, mprA	MarR family transcriptional regulator, negative regulator of the multidrug operon en
S19-40_03237	yfmP	MerR family transcriptional regulator, repressor of the yfmOP operon
S19-40_03272	-	trehalos_R_Bsub: trehalose operon repressor
S19-40_03300	acoR	Acetoin dehydrogenase operon transcriptional activator AcoR
S19-40_03308	glvR	RpiR family transcriptional regulator, glv operon transcriptional regulator
S19-40_03325	HpaR	HpaR: homoprotocatechuate degradation operon regulator, HpaR
S19-40_03357	perR	Peroxide operon regulator
S19-40_03384	licT, bglG	beta-glucoside operon transcriptional antiterminator
S19-40_03432	licR	putative licABCH operon regulator
S19-40_03450	HpaR	HpaR: homoprotocatechuate degradation operon regulator, HpaR
S19-40_03453	sacY	Levansucrase and sucrase synthesis operon antiterminator
S19-40_03463	gltC	LysR family transcriptional regulator, transcription activator of glutamate synthase o
S19-40_03473	acrR, smeT	TetR/AcrR family transcriptional regulator, acrAB operon repressor
S19-40_03488	sacY	Levansucrase and sucrase synthesis operon antiterminator
S19-40_03530	cysL	LysR family transcriptional regulator, transcriptional activator of the cysJI operon
S19-40_03547	btr	AraC family transcriptional regulator, transcriptional activator for feuABC-ybbA op
S19-40_03634	HpaR	HpaR: homoprotocatechuate degradation operon regulator, HpaR
		sigma-54 dependent transcriptional regulator, acetoin dehydrogenase operon transcr
S19-40_03642	acoR	AcoR
S19-40_03677	kdgR	LacI family transcriptional regulator, kdg operon repressor
S19-40_03739	gltC	LysR family transcriptional regulator, transcription activator of glutamate synthase o
S19-40_03760	scrR	LacI family transcriptional regulator, sucrose operon repressor

S19-40_03790	-	trehalos_R_Bsub: trehalose operon repressor
S19-40_03799	gntR	putative D-xylose utilization operon transcriptional repressor
S19-40_03804	HpaR	HpaR: homoprotocatechuate degradation operon regulator, HpaR
S19-40_03806	lmrA, yxaF	TetR/AcrR family transcriptional regulator, lmrAB and yxaGH operons repressor
S19-40_03815	dhaS	HTH-type dhaKLM operon transcriptional activator DhaS
S19-40_03823	srlR	Glucitol operon repressor
S19-40_03839	btr	AraC family transcriptional regulator, transcriptional activator for feuABC-ybbA op
S19-40_03856	lsrR	lsr operon transcriptional repressor
S19-40_03865	hutP	Hut operon positive regulatory protein
S19-40_03979	purR	Pur operon repressor

Table s3. *Bacillus subtilis* PTA-271 encoding genes for antimicrobial molecules, other effectors and lytic enzymes.

Table s4. *Bacillus subtilis* PTA-271 encoding genes for sporulation.

Locus tag ID	Gene	Function
		Bacteriocin/Bacteriocin-like-peptides
S19-40_00081	menE	AMP-binding enzyme
S19-40_00234	albE	Antilisterial bacteriocin subtilosin biosynthesis protein AlbE
S19-40_00679	albG	Antilisterial bacteriocin subtilosin biosynthesis protein AlbG
S19-40_00681	albE	Antilisterial bacteriocin subtilosin biosynthesis protein AlbE
S19-40_00682	alBOT	Antilisterial bacteriocin subtilosin biosynthesis protein AlBOT
S19-40_00683	btuD	Lantibiotic protection ABC transporter, ATP-binding subunit
S19-40_00684	albB	Antilisterial bacteriocin subtilosin biosynthesis protein AlbB
S19-40_00685	albA	Antilisterial bacteriocin subtilosin biosynthesis protein AlbA
S19-40_00690	crp	CRP/FNR family transcriptional regulator, cyclic AMP receptor protein
S19-40_00726	ywlC	Threonylcarbamoyl-AMP synthase
S19-40_00946	hisI	Phosphoribosyl-AMP cyclohydrolase
S19-40_00964	btuD	Putative bacteriocin export ABC transporter, lactococcin 972 group
S19-40_01244	dhbE	2,3-dihydroxybenzoate-AMP ligase

S19-40_01246	-	AMP-binding enzyme
S19-40_01575	-	AMP-binding enzyme
S19-40_01689	-	AMP-binding enzyme
S19-40_01755	bceB	Bacitracin export permease protein BceB
S19-40_01756	bceA	Bacitracin export ATP-binding protein BceA
S19-40_01915	-	Bacteriocin-protection, YdeI or OmpD-Associated
S19-40_01966	nukF, mcdF, sboF	lantibiotic transport system ATP-binding protein
S19-40_01998	-	AMP-binding enzyme
S19-40_01998	-	AMP-binding enzyme
S19-40_02046	btuD	Putative bacteriocin export ABC transporter, lactococcin 972 group
S19-40_02071	licA	lichenysin synthetase A
S19-40_02165	btuD	lantibiotic protection ABC transporter, ATP-binding subunit
S19-40_02198	-	Trypsin
S19-40_02227	skfF	Putative bacteriocin-SkfA transport system permease protein SkfF
S19-40_02641	btuD	Lantibiotic protection ABC transporter, ATP-binding subunit
S19-40_03432	licR	lichenan operon transcriptional antiterminator
S19-40_03433	licB	Lichenan-specific phosphotransferase enzyme IIB component
S19-40_03434	licC	Lichenan permease IIC component
S19-40_03435	licA	Lichenan-specific phosphotransferase enzyme IIA component
S19-40_03456	licC	Lichenan permease IIC component
S19-40_03706	-	Trypsin-like peptidase domain protein
S19-40_03836	btuD	Putative bacteriocin export ABC transporter, lactococcin 972 group
		Other effectors
S19-40_00073	fenC	fengycin family lipopeptide synthetase A
S19-40_00074	fenD	fengycin family lipopeptide synthetase B
S19-40_00075	-	fengycin family lipopeptide synthetase C
S19-40_00076	fenA	fengycin family lipopeptide synthetase D
S19-40_00077	fenB	fengycin family lipopeptide synthetase E
S19-40_00208	pksD	bacillaene synthase trans-acting acyltransferase
S19-40_00567	bacF	Transaminase BacF
S19-40_00679	albG	Antilisterial bacteriocin subtilosin biosynthesis protein AlbG
S19-40_00681	albE	Antilisterial bacteriocin subtilosin biosynthesis protein AlbE
S19-40_00682	alBOT	Antilisterial bacteriocin subtilosin biosynthesis protein AlBOT

S19-40_00684	albB	Antilisterial bacteriocin subtilosin biosynthesis protein AlbB
S19-40_00684	albB	Antilisterial bacteriocin subtilosin biosynthesis protein AlbB
S19-40_00685	albA	Antilisterial bacteriocin subtilosin biosynthesis protein AlbA
S19-40_00686	sboA	Subtilosin-A
S19-40_02068	srfAD	Surfactin synthase thioesterase subunit
S19-40_02069	srfAC	Surfactin synthase subunit 3
S19-40_02070	srfAB	Surfactin synthase subunit 2
S19-40_02071	srfAA	Surfactin synthase subunit 1
S19-40_03525	bacE	Putative bacilysin exporter BacE
S19-40_03526	bacF	Transaminase BacF
S19-40_03527	bacG	NADPH-dependent reductase BacG
		Siderophores
S19-40_01242	dhbA	2,3-dihydro-2,3-dihydroxybenzoate dehydrogenase
S19-40_01243	dhbC	Isochorismate synthase DhbC
S19-40_01244	dhbE	2,3-dihydroxybenzoate-AMP ligase
S19-40_01245	dhbB	Isochorismatase
S19-40_01246	dhbF	Dimodular nonribosomal peptide synthase
		Lytic enzymes
S19-40_00094	-	Cellulase (glycosyl hydrolase family 5)
S19-40_00541	sleB	Spore cortex-lytic enzyme
S19-40_00651	sleB	spore cortex-lytic enzyme
S19-40_01400	csn	Chitosanase
S19-40_02204	sleB	spore cortex-lytic enzyme
S19-40_02296	sleB	spore cortex-lytic enzyme
S19-40_02768	sleB	Spore cortex-lytic enzyme
S19-40_03055	sleB	spore cortex-lytic enzyme
S19-40_03077	sleB	spore cortex-lytic enzyme
S19-40_03385	bglS	Beta-glucanase
		Proteases
S19-40_00020	ydeA	putative protease YdeA
S19-40_00164	-	CAAX protease self-immunity
S19-40_00193	aprX	Serine protease AprX
S19-40_00233	albF	Putative zinc protease AlbF

S19-40_00239	clpP	ATP-dependent Clp protease proteolytic subunit
S19-40_00247	-	putative zinc protease
S19-40_00262	rasP	Regulator of sigma-W protease RasP
S19-40_00302	clpY	ATP-dependent protease ATPase subunit ClpY
S19-40_00303	clpQ	ATP-dependent protease subunit ClpQ
S19-40_00414	lon	Lon protease
S19-40_00475	-	Thermophilic metalloprotease (M29)
S19-40_00555	clpE	ATP-dependent Clp protease ATP-binding subunit ClpE
S19-40_00578	htpX	Protease HtpX
S19-40_00609	isp	Major intracellular serine protease
S19-40_00640	htrA	Serine protease Do-like HtrA
S19-40_00669	rip2	Putative zinc metalloprotease Rip2
S19-40_00680	albF	Putative zinc protease AlbF
S19-40_00908	ctpB	Carboxy-terminal processing protease CtpB
S19-40_00980	clpP	ATP-dependent Clp protease proteolytic subunit
S19-40_01141	htrB	Serine protease Do-like HtrB
S19-40_01229	paiB	Protease synthase and sporulation protein PAI 2
S19-40_01403	lasA	LasA protease
S19-40_01404	lasA	LasA protease
S19-40_01415	yraA	Putative cysteine protease YraA
S19-40_01448	ydcP	putative protease YdcP
S19-40_01449	ydcP	putative protease YdcP
S19-40_01512	-	Cysteine protease Prp
S19-40_01538	lon1	Lon protease 1
S19-40_01539	lon2	Lon protease 2
S19-40_01540	clpX	ATP-dependent Clp protease ATP-binding subunit ClpX
S19-40_01953	gluP	Rhomboid protease GluP
S19-40_02198	mpr	Extracellular metalloprotease
S19-40_02280	-	Putative phage serine protease XkdF
S19-40_02300	ftsH	ATP-dependent zinc metalloprotease FtsH
S19-40_02446	nprB	Neutral protease B
S19-40_02479	wprA	Cell wall-associated protease
S19-40_02527	htpX	Protease HtpX

S19-40_02732	bepA	Beta-barrel assembly-enhancing protease
S19-40_02769	prsW	Protease PrsW
S19-40_02776	-	CAAX protease self-immunity
S19-40_02969	gluP	Rhomboid protease GluP
S19-40_03037	gpr	Germination protease
S19-40_03091	tsaD	Glycoprotease family protein
S19-40_03093	tsaD	Glycoprotease family protein
S19-40_03100	-	CAAX protease self-immunity
S19-40_03218	yccA	modulator of FtsH protease
S19-40_03275	pfpL	Intracellular protease, PfpI family
S19-40_03413	htpX	Protease HtpX
S19-40_03455	epr	Minor extracellular protease Epr
S19-40_03486	vpr	Minor extracellular protease vpr
S19-40_03605	ctpA	Carboxy-terminal processing protease CtpA
S19-40_03706	htrA	Serine protease Do-like HtrA
S19-40_03756	-	CAAX protease self-immunity
S19-40_03937	clpX	ATP-dependent Clp protease ATP-binding subunit ClpX
S19-40_03955	ftsH	ATP-dependent zinc metalloprotease FtsH
S19-40_03982	yabG	Sporulation-specific protease YabG

Table s5. *Bacillus subtilis* PTA-271 encoding genes for some CYP450 and for Transferases.

Locus tag ID	Gene	Function
		Bacteriocin/Bacteriocin-like-peptides
S19-40_00081	menE	AMP-binding enzyme
S19-40_00234	albE	Antilisterial bacteriocin subtilosin biosynthesis protein AlbE
S19-40_00679	albG	Antilisterial bacteriocin subtilosin biosynthesis protein AlbG
S19-40_00681	albE	Antilisterial bacteriocin subtilosin biosynthesis protein AlbE
S19-40_00682	alBOT	Antilisterial bacteriocin subtilosin biosynthesis protein AlBOT
S19-40_00683	btuD	Lantibiotic protection ABC transporter, ATP-binding subunit
S19-40_00684	albB	Antilisterial bacteriocin subtilosin biosynthesis protein AlbB
S19-40_00685	albA	Antilisterial bacteriocin subtilosin biosynthesis protein AlbA
S19-40_00690	crp	CRP/FNR family transcriptional regulator, cyclic AMP receptor protein
S19-40_00726	ywlC	Threonylcarbamoyl-AMP synthase
S19-40_00946	hisI	Phosphoribosyl-AMP cyclohydrolase
S19-40_00964	btuD	Putative bacteriocin export ABC transporter, lactococcin 972 group
S19-40_01244	dhbE	2,3-dihydroxybenzoate-AMP ligase
S19-40_01246	-	AMP-binding enzyme
S19-40_01575	-	AMP-binding enzyme
S19-40_01689	-	AMP-binding enzyme
S19-40_01755	bceB	Bacitracin export permease protein BceB
S19-40_01756	bceA	Bacitracin export ATP-binding protein BceA
S19-40_01915	-	Bacteriocin-protection, YdeI or OmpD-Associated
S19-40_01966	nukF, mcdF, sboF	lantibiotic transport system ATP-binding protein
S19-40_01998	-	AMP-binding enzyme
S19-40_01998	-	AMP-binding enzyme
S19-40_02046	btuD	Putative bacteriocin export ABC transporter, lactococcin 972 group
S19-40_02071	licA	lichenysin synthetase A
S19-40_02165	btuD	lantibiotic protection ABC transporter, ATP-binding subunit
S19-40_02198	-	Trypsin
S19-40_02227	skfF	Putative bacteriocin-SkfA transport system permease protein SkfF
S19-40_02641	btuD	Lantibiotic protection ABC transporter, ATP-binding subunit
S19-40_03432	licR	lichenan operon transcriptional antiterminator
S19-40_03433	licB	Lichenan-specific phosphotransferase enzyme IIB component
S19-40_03434	licC	Lichenan permease IIC component
S19-40_03435	licA	Lichenan-specific phosphotransferase enzyme IIA component
S19-40_03456	licC	Lichenan permease IIC component
S19-40_03706	-	Trypsin-like peptidase domain protein
S19-40_03836	btuD	Putative bacteriocin export ABC transporter, lactococcin 972 group

		Other effectors
S19-40_00073	fenC	fengycin family lipopeptide synthetase A
S19-40_00074	fenD	fengycin family lipopeptide synthetase B
S19-40_00075	-	fengycin family lipopeptide synthetase C
S19-40_00076	fenA	fengycin family lipopeptide synthetase D
S19-40_00077	fenB	fengycin family lipopeptide synthetase E
S19-40_00208	pksD	bacillaene synthase trans-acting acyltransferase
S19-40_00567	bacF	Transaminase BacF
S19-40_00679	albG	Antilisterial bacteriocin subtilosin biosynthesis protein AlbG
S19-40_00681	albE	Antilisterial bacteriocin subtilosin biosynthesis protein AlbE
S19-40_00682	alBOT	Antilisterial bacteriocin subtilosin biosynthesis protein AlBOT
S19-40_00684	albB	Antilisterial bacteriocin subtilosin biosynthesis protein AlbB
S19-40_00684	albB	Antilisterial bacteriocin subtilosin biosynthesis protein AlbB
S19-40_00685	albA	Antilisterial bacteriocin subtilosin biosynthesis protein AlbA
S19-40_00686	sboA	Subtilosin-A
S19-40_02068	srfAD	Surfactin synthase thioesterase subunit
S19-40_02069	srfAC	Surfactin synthase subunit 3
S19-40_02070	srfAB	Surfactin synthase subunit 2
S19-40_02071	srfAA	Surfactin synthase subunit 1
S19-40_03525	bacE	Putative bacilysin exporter BacE
S19-40_03526	bacF	Transaminase BacF
S19-40_03527	bacG	NADPH-dependent reductase BacG
		Siderophores
S19-40_01242	dhbA	2,3-dihydro-2,3-dihydroxybenzoate dehydrogenase
S19-40_01243	dhbC	Isochorismate synthase DhbC
S19-40_01244	dhbE	2,3-dihydroxybenzoate-AMP ligase
S19-40_01245	dhbB	Isochorismatase
S19-40_01246	dhbF	Dimodular nonribosomal peptide synthase
		Lytic enzymes
S19-40_00094	-	Cellulase (glycosyl hydrolase family 5)
S19-40_00541	sleB	Spore cortex-lytic enzyme
S19-40_00651	sleB	spore cortex-lytic enzyme
S19-40_01400	csn	Chitosanase

S19-40_02204	sleB	spore cortex-lytic enzyme
S19-40_02296	sleB	spore cortex-lytic enzyme
S19-40_02768	sleB	Spore cortex-lytic enzyme
S19-40_03055	sleB	spore cortex-lytic enzyme
S19-40_03077	sleB	spore cortex-lytic enzyme
S19-40_03385	bglS	Beta-glucanase
		Proteases
S19-40_00020	ydeA	putative protease YdeA
S19-40_00164	-	CAAX protease self-immunity
S19-40_00193	aprX	Serine protease AprX
S19-40_00233	albF	Putative zinc protease AlbF
S19-40_00239	clpP	ATP-dependent Clp protease proteolytic subunit
S19-40_00247	-	putative zinc protease
S19-40_00262	rasP	Regulator of sigma-W protease RasP
S19-40_00302	clpY	ATP-dependent protease ATPase subunit ClpY
S19-40_00303	clpQ	ATP-dependent protease subunit ClpQ
S19-40_00414	lon	Lon protease
S19-40_00475	-	Thermophilic metalloprotease (M29)
S19-40_00555	clpE	ATP-dependent Clp protease ATP-binding subunit ClpE
S19-40_00578	htpX	Protease HtpX
S19-40_00609	isp	Major intracellular serine protease
S19-40_00640	htrA	Serine protease Do-like HtrA
S19-40_00669	rip2	Putative zinc metalloprotease Rip2
S19-40_00680	albF	Putative zinc protease AlbF
S19-40_00908	ctpB	Carboxy-terminal processing protease CtpB
S19-40_00980	clpP	ATP-dependent Clp protease proteolytic subunit
S19-40_01141	htrB	Serine protease Do-like HtrB
S19-40_01229	paiB	Protease synthase and sporulation protein PAI 2
S19-40_01403	lasA	LasA protease
S19-40_01404	lasA	LasA protease
S19-40_01415	yraA	Putative cysteine protease YraA
S19-40_01448	ydcP	putative protease YdcP
S19-40_01449	ydcP	putative protease YdcP

S19-40_01512	-	Cysteine protease Prp
S19-40_01538	lon1	Lon protease 1
S19-40_01539	lon2	Lon protease 2
S19-40_01540	clpX	ATP-dependent Clp protease ATP-binding subunit ClpX
S19-40_01953	gluP	Rhomboid protease GluP
S19-40_02198	mpr	Extracellular metalloprotease
S19-40_02280	-	Putative phage serine protease XkdF
S19-40_02300	ftsH	ATP-dependent zinc metalloprotease FtsH
S19-40_02446	nprB	Neutral protease B
S19-40_02479	wprA	Cell wall-associated protease
S19-40_02527	htpX	Protease HtpX
S19-40_02732	bepA	Beta-barrel assembly-enhancing protease
S19-40_02769	prsW	Protease PrsW
S19-40_02776	-	CAAX protease self-immunity
S19-40_02969	gluP	Rhomboid protease GluP
S19-40_03037	gpr	Germination protease
S19-40_03091	tsaD	Glycoprotease family protein
S19-40_03093	tsaD	Glycoprotease family protein
S19-40_03100	-	CAAX protease self-immunity
S19-40_03218	yccA	modulator of FtsH protease
S19-40_03275	pfpL	Intracellular protease, PfpI family
S19-40_03413	htpX	Protease HtpX
S19-40_03455	epr	Minor extracellular protease Epr
S19-40_03486	vpr	Minor extracellular protease vpr
S19-40_03605	ctpA	Carboxy-terminal processing protease CtpA
S19-40_03706	htrA	Serine protease Do-like HtrA
S19-40_03756	-	CAAX protease self-immunity
S19-40_03937	clpX	ATP-dependent Clp protease ATP-binding subunit ClpX
S19-40_03955	ftsH	ATP-dependent zinc metalloprotease FtsH
S19-40_03982	yabG	Sporulation-specific protease YabG

Table s6. *Bacillus subtilis* PTA-271 encoding genes for lactonases, β-lactamases, deaminases, deacetylases.

Locus tag ID	Gene	Function
		Sporolation related genes
S19-40_00078	*yjcA*	Sporulation protein YjcA
S19-40_00117	*ynzD*	Spo0E like sporulation regulatory protein
S19-40_00119	*sirA*	Sporulation inhibitor of replication protein SirA
S19-40_00176	*spoVK*	Stage V sporulation protein K
S19-40_00177	*cwlC*	Sporulation-specific N-acetylmuramoyl-L-alanine amidase
S19-40_00222	*spoVS*	Stage V sporulation protein S
S19-40_00246	*ylmC*	Sporulation protein, YlmC/YmxH family
S19-40_00387	*spoIIGA*	Sporulation sigma-E factor-processing peptidase
S19-40_00401	*spoVD*	Stage V sporulation protein D
S19-40_00416	*ylbJ*	Sporulation integral membrane protein YlbJ
S19-40_00471	*kinA*	Sporulation kinase A
S19-40_00495	-	Sporulation protein cse15
S19-40_00522	*kinA*	Sporulation kinase A
S19-40_00539	*stoA*	Sporulation thiol-disulfide oxidoreductase A
S19-40_00540	*ykvU*	Sporulation protein YkvU
S19-40_00541	*sleB*	Spore cortex-lytic enzyme
S19-40_00545	*ydhD*	Putative sporulation-specific glycosylase YdhD
S19-40_00546	*ykvP*	Spore protein YkvP
S19-40_00547	*ykvP*	Spore protein YkvP
S19-40_00559	*kinD*	Sporulation kinase D
S19-40_00561	*spo0E*	stage 0 sporulation regulatory protein
S19-40_00573	*kinE*	Sporulation kinase E
S19-40_00649	*spoIISA*	Stage II sporulation protein SA
S19-40_00650	*spoIISB*	Stage II sporulation protein SB
S19-40_00708	*spo0F*	Sporulation initiation phosphotransferase F
S19-40_00746	*spoIID*	stage II sporulation protein D
S19-40_00766	*spoIIQ*	Stage II sporulation protein Q
S19-40_00780	*spoIIID*	Stage III sporulation protein D
S19-40_00844	*gerBB*	Spore germination protein B2
S19-40_00845	*gerBA*	Spore germination protein B1
S19-40_00958	*whiA*	Sporulation transcription regulator WhiA
S19-40_00982	*cotR*	Putative sporulation hydrolase CotR
S19-40_01032	*ydhD*	Putative sporulation-specific glycosylase YdhD
S19-40_01057	*sdpC*	Sporulation delaying protein C
S19-40_01058	*sdpB*	Sporulation-delaying protein SdpB

S19-40_01059	*sdpA*	Sporulation-delaying protein SdpA
S19-40_01133	*gerAC*	Spore germination protein A3
S19-40_01134	*gerAB*	Spore germination protein A2
S19-40_01135	*gerAA*	Spore germination protein A1
S19-40_01208	*yunB*	Sporulation protein YunB
S19-40_01211	*YhcN*	Sporulation lipoprotein, YhcN/YlaJ family
S19-40_01229	*paiB*	Protease synthase and sporulation protein PAI 2
S19-40_01261	*Ytvl*	Sporulation integral membrane protein YtvI
S19-40_01297	*kinE*	Sporulation kinase E
S19-40_01298	*kinE*	Sporulation kinase E
S19-40_01483	*spoVB*	Stage V sporulation protein B
S19-40_01500	*coxA*	Sporulation cortex protein CoxA
S19-40_01501	*safA*	SpoIVD-associated factor A
S19-40_01510	*spo0B*	Sporulation initiation phosphotransferase B
S19-40_01514	*spoIVFB*	Stage IV sporulation protein FB
S19-40_01515	*spoIVFA*	Stage IV sporulation protein FA
S19-40_01523	*spoIIB*	Stage II sporulation protein B
S19-40_01529	*spoVID*	Stage VI sporulation protein D
S19-40_01557	*gerM*	Spore germination protein GerM
S19-40_01560	*gerE*	Spore germination protein GerE
S19-40_01642	*ytrH*	Sporulation membrane protein YtrH
S19-40_01643	*ytrI*	Sporulation membrane protein YtrI
S19-40_01727	-	Sporulation protein cse60
S19-40_01859	*ydhD*	Putative sporulation-specific glycosylase YdhD
S19-40_01951	*ydcC*	Sporulation protein YdcC
S19-40_02076	*nucB*	Sporulation-specific extracellular nuclease
S19-40_02162	*cwlJ*	Spore cortex-lytic enzyme
S19-40_02177	*spo0A*	Stage 0 sporulation protein A
S19-40_02216	-	Sigma-G-dependent sporulation-specific SASP protein
S19-40_02229	*skfC*	Sporulation-killing factor biosynthesis protein SkfC
S19-40_02230	*skfB*	Sporulation killing factor maturation protein SkfB
S19-40_02231	*skfA*	Sporulation killing factor
S19-40_02296	*cwlA*	Spore cortex-lytic enzyme

S19-40_02371	*yjcA*	Sporulation protein YjcA
S19-40_02372	*cotV*	Spore coat protein V
S19-40_02373	*cotW*	Spore coat protein W
S19-40_02374	*cotX*	Spore coat protein X
S19-40_02375	*cotY*	Spore coat protein Y
S19-40_02376	*cotZ*	Spore coat protein Z
S19-40_02450	*sdpA*	Sporulation-delaying protein SdpA
S19-40_02451	*sdpB*	Sporulation-delaying protein SdpB
S19-40_02452	*sdpC*	Sporulation delaying protein C
S19-40_02483	*yisI*	Spo0E like sporulation regulatory protein
S19-40_02484	*gerPA*	Spore germination protein gerPA/gerPF
S19-40_02485	*gerPB*	Spore germination GerPB
S19-40_02486	*gerPC*	Spore germination protein GerPC
S19-40_02487	*gerPD*	Spore germination protein GerPD
S19-40_02488	*gerPE*	Spore germination protein GerPE
S19-40_02489	*gerPF*	Spore germination protein gerPA/gerPF
S19-40_02559	*yhaL*	Sporulation protein YhaL
S19-40_02674	*spo0M*	Sporulation-control protein spo0M
S19-40_02725	*YpjB*	Sporulation protein YpjB
S19-40_02753	*spoIVA*	Stage IV sporulation protein A
S19-40_02767	*ypeB*	Sporulation protein YpeB
S19-40_02768	*sleB*	Spore cortex-lytic enzyme
S19-40_02812	*spoVAF*	stage V sporulation protein AF
S19-40_02813	-	stage V sporulation protein AE
S19-40_02814	-	stage V sporulation protein AE
S19-40_02815	*spoVAD*	stage V sporulation protein AD
S19-40_02816	*spoVAC*	stage V sporulation protein AC
S19-40_02817	*spoVAB*	stage V sporulation protein AB
S19-40_02818	*spoVAA*	stage V sporulation protein AA
S19-40_02820	*spoIIAB*	stage II sporulation protein AB (anti-sigma F factor)
S19-40_02821	*spoIIAA*	stage II sporulation protein AA (anti-sigma F factor antagonist)
S19-40_02828	*spoIIM*	Stage II sporulation protein M
S19-40_02901	*spo0A*	Stage 0 sporulation protein A

S19-40_02902	*spoIVB*	SpoIVB peptidase
S19-40_02915	*spoIIIAH*	Stage III sporulation protein AH
S19-40_02918	*spoIIIAE*	Stage III sporulation protein AE
S19-40_03018	*yqfD*	Sporulation protein YqfD
S19-40_03019	*yqfC*	Sporulation protein YqfC
S19-40_03055	*cwlH*	Spore cortex-lytic enzyme
S19-40_03059	*nucB*	Sporulation-specific extracellular nuclease
S19-40_03771	*soj*	Sporulation initiation inhibitor protein Soj
S19-40_03960	*spoIIE*	Stage II sporulation protein E
S19-40_03969	*gerD*	Stage V sporulation protein B
S19-40_03970	*spoVT*	Stage V sporulation protein T
S19-40_03977	*spoVG*	Putative septation protein SpoVG
S19-40_03982	*yabG*	Sporulation-specific protease YabG

Locus tag ID	Gene	Function
		P450 mono-oxigenases
S19-40_00039	hpaB	4-hydroxyphenylacetate 3-monooxygenase
S19-40_01036	luxA	Alkanal monooxygenase alpha chain
S19-40_01390	ncd2/npd	Nitronate monooxygenase
S19-40_01651	moxC	Putative monooxygenase MoxC
S19-40_01653	camP	2,5-diketocamphane 1,2-monooxygenase
S19-40_02002	mhuD, hmoB	Antibiotic biosynthesis monooxygenase
S19-40_02030	ycnE	Putative monooxygenase YcnE
S19-40_02134	limB	Limonene 1,2-monooxygenase
S19-40_02347	-	Antibiotic biosynthesis monooxygenase
S19-40_02506	otcC	Anhydrotetracycline monooxygenase
S19-40_02544	hmoB	Heme-degrading monooxygenase HmoB
S19-40_02664	ssuD	Alkanesulfonate monooxygenase
S19-40_02844	-	Antibiotic biosynthesis monooxygenase
S19-40_03213	hmoA	Heme-degrading monooxygenase HmoA
S19-40_03220	kmo	Kynurenine 3-monooxygenase
S19-40_03485	luxB	Alkanal monooxygenase beta chain
S19-40_03847	ntaA	Nitrilotriacetate monooxygenase component A
		dioxygenases
S19-40_00125	fosB	Glyoxalase/Bleomycin resistance protein/Dioxygenase superfamily protein
S19-40_00563	mtnD	Acireductone dioxygenase
S19-40_00645	mhqA	Putative ring-cleaving dioxygenase MhqA
S19-40_00719	-	Glyoxalase/Bleomycin resistance protein/Dioxygenase superfamily protein
S19-40_01175	-	Glyoxalase/Bleomycin resistance protein/Dioxygenase superfamily protein
S19-40_01333	cdoA	Cysteine dioxygenase
S19-40_01883	mhqO	Putative ring-cleaving dioxygenase MhqO
S19-40_02093	hcaC	3-phenylpropionate/cinnamic acid dioxygenase ferredoxin subunit
S19-40_02313	hcaD	3-phenylpropionate/cinnamic acid dioxygenase ferredoxin--NAD(+) reductase componer
S19-40_02851	-	Glyoxalase/Bleomycin resistance protein/Dioxygenase superfamily protein
S19-40_02870	-	Glyoxalase/Bleomycin resistance protein/Dioxygenase superfamily protein
S19-40_03214	-	Glyoxalase/Bleomycin resistance protein/Dioxygenase superfamily protein
S19-40_03313	catE	Catechol-2,3-dioxygenase
S19-40_03371	-	2OG-Fe dioxygenase
S19-40_03457	-	Glyoxalase/Bleomycin resistance protein/Dioxygenase superfamily protein
S19-40_03602	mhqE	Putative ring-cleaving dioxygenase MhqE
S19-40_03717	-	Glyoxalase/Bleomycin resistance protein/Dioxygenase superfamily protein

S19-40_03759	-	Glyoxalase/Bleomycin resistance protein/Dioxygenase superfamily protein
S19-40_03807	qdoI	Quercetin 2,3-dioxygenase
		GST-GT-MT related genes
S19-40_00083	gcvH	Glycine cleavage system H protein
S19-40_00328	faBOT	Malonyl CoA-acyl carrier protein transacylase
S19-40_00397	ftsW	putative peptidoglycan glycosyltransferase FtsW
S19-40_00399	mraY	Phospho-N-acetylmuramoyl-pentapeptide-transferase
S19-40_00434	ftsW	putative peptidoglycan glycosyltransferase FtsW
S19-40_00547	-	Glycosyl transferases group 1
S19-40_00588	-	Glycosyl transferase family 2
S19-40_00592	ugtP	Processive diacylglycerol beta-glucosyltransferase
S19-40_00642	-	putative glycosyltransferase
S19-40_00852	-	glyco_rSAM_CFB: glycosyltransferase, GG-Bacteroidales peptide system
S19-40_00853	-	Glycosyl transferase WecB/TagA/CpsF family protein
S19-40_00856	-	Glycosyl transferase family 2
S19-40_00857	-	CDP-Glycerol:Poly(glycerophosphate) glycerophosphotransferase
S19-40_00861	-	Glycosyl transferase 1 domain A
S19-40_00862	-	Glycosyl transferases group 1
S19-40_00863	-	Glycosyl transferase family 2
S19-40_00869	-	Glycosyl transferase family 2
S19-40_00872	-	Glycosyl transferases group 1
S19-40_00876	-	Glycosyl transferase family 2
S19-40_00877	-	Glycosyl transferases group 1
S19-40_00878	-	Glycosyl transferase family 4
S19-40_01001	-	Glycosyl transferases group 1
S19-40_01002	-	Glycosyl transferase family 2
S19-40_01003	-	Glycosyl transferases group 1
S19-40_01005	-	Glycosyl transferase family 2
S19-40_01007	-	Glycosyl transferase family 2
S19-40_01589	-	Glyoxalase-like domain protein
S19-40_01806	-	Glycosyl transferases group 1
S19-40_01809	-	Glycosyl transferases group 1
S19-40_01858	-	UDP-glucoronosyl and UDP-glucosyl transferase

S19-40_01985	-	Glycosyltransferase like family 2
S19-40_01997	-	Methyltransferase domain protein
S19-40_02321	-	MGT: glycosyltransferase, MGT family
S19-40_02705	-	Transglycosylase
S19-40_02719	-	Glycosyl transferases group 1
S19-40_02740	-	Glycosyl transferase family, a/b domain
S19-40_02973	-	Glycosyl transferases group 1
S19-40_03228	-	Glycosyl transferase family 2
S19-40_03344	-	Glycosyl transferase family 2
S19-40_03391	-	Methyltransferase domain protein
S19-40_03452	-	Glycosyl transferase family 8
S19-40_03483	-	Cell cycle protein
S19-40_03497	-	Glycosyl transferase family 2
S19-40_03504	-	Glycosyl transferase family 2
S19-40_03586	-	MGT: glycosyltransferase, MGT family
S19-40_03626	-	Glycosyl transferase family 2
S19-40_03656	-	Monogalactosyldiacylglycerol (MGDG) synthase
S19-40_03859	-	Glycosyl transferase family, a/b domain
		Other transferases
S19-40_00001	araP	L-arabinose transport system permease protein AraP
S19-40_00002	araQ	L-arabinose transport system permease protein AraQ
S19-40_00053	ydaF	Putative ribosomal N-acetyltransferase YdaF
S19-40_00065	-	g_glut_trans: gamma-glutamyltransferase
S19-40_00083	-	methylmalonyl-CoA carboxyltransferase 1.3S subunit
S19-40_00089	gtaB	UTP--glucose-1-phosphate uridylyltransferase
S19-40_00090	DPM1	dolichol-phosphate mannosyltransferase
S19-40_00101	plsY	Glycerol-3-phosphate acyltransferase
S19-40_00174	pat	Putative phenylalanine aminotransferase
S19-40_00185	miaA	tRNA dimethylallyltransferase
S19-40_00207	-	Acyl transferase domain protein
S19-40_00208	-	Acyl transferase domain protein
S19-40_00219	miaB	miaB-methiolase: tRNA-i(6)A37 thiotransferase enzyme MiaB
S19-40_00456	arnB	UDP-4-amino-4-deoxy-L-arabinose--oxoglutarate aminotransferase

S19-40_00588	arnC	Undecaprenyl-phosphate 4-deoxy-4-formamido-L-arabinose transferase
S19-40_00642	arnC	Undecaprenyl-phosphate 4-deoxy-4-formamido-L-arabinose transferase
S19-40_00842	-	MFS transporter, SP family, arabinose:H+ symporter
S19-40_00856	arnC	Undecaprenyl-phosphate 4-deoxy-4-formamido-L-arabinose transferase
S19-40_00869	arnC	Undecaprenyl-phosphate 4-deoxy-4-formamido-L-arabinose transferase
S19-40_00876	arnC	Undecaprenyl-phosphate 4-deoxy-4-formamido-L-arabinose transferase
S19-40_01002	arnC	Undecaprenyl-phosphate 4-deoxy-4-formamido-L-arabinose transferase
S19-40_01005	arnC	Undecaprenyl-phosphate 4-deoxy-4-formamido-L-arabinose transferase
S19-40_01007	arnC	Undecaprenyl-phosphate 4-deoxy-4-formamido-L-arabinose transferase
S19-40_01011	arnB	UDP-4-amino-4-deoxy-L-arabinose--oxoglutarate aminotransferase
S19-40_01037	araR	Arabinose metabolism transcriptional repressor
S19-40_01038	araE	Arabinose-proton symporter
S19-40_01182	araP	L-arabinose transport system permease protein AraP
S19-40_01183	araQ	L-arabinose transport system permease protein AraQ
S19-40_01592	araQ	L-arabinose transport system permease protein AraQ
S19-40_01593	araP	L-arabinose transport system permease protein AraP
S19-40_01599	araA	L-arabinose isomerase
S19-40_01735	araQ	L-arabinose transport system permease protein AraQ
S19-40_01999	mtlR	mannitol operon transcriptional antiterminator
S19-40_02017	mtlD	Mannitol-1-phosphate 5-dehydrogenase
S19-40_02018	mtlF	Mannitol-specific phosphotransferase enzyme IIA component
S19-40_02019	mtlA	PTS system mannitol-specific EIICB component
S19-40_02074	kdsD, kpsF	arabinose-5-phosphate isomerase
S19-40_02473	araC	Arabinose operon regulatory protein
S19-40_02501	arnB	UDP-4-amino-4-deoxy-L-arabinose--oxoglutarate aminotransferase
S19-40_02720	mshB	thiol_BshB1: bacillithiol biosynthesis deacetylase BshB1
S19-40_02770	ypdA	Bthiol_YpdA: putative bacillithiol system oxidoreductase, YpdA family
S19-40_03197	araQ	L-arabinose transport system permease protein AraQ
S19-40_03210	araQ	L-arabinose transport system permease protein AraQ
S19-40_03228	arnC	Undecaprenyl-phosphate 4-deoxy-4-formamido-L-arabinose transferase
S19-40_03323	yfiT	DinB superfamily protein
S19-40_03344	arnC	Undecaprenyl-phosphate 4-deoxy-4-formamido-L-arabinose transferase
S19-40_03497	arnC	Undecaprenyl-phosphate 4-deoxy-4-formamido-L-arabinose transferase

S19-40_03506	arnB	UDP-4-amino-4-deoxy-L-arabinose--oxoglutarate aminotransferase
S19-40_03591	BshB2	thiol_BshB2: bacillithiol biosynthesis deacetylase BshB2
S19-40_03695	mshD	Mycothiol acetyltransferase
S19-40_03700	rocD	Ornithine aminotransferase
S19-40_03723	arnT, pmrK	4-amino-4-deoxy-L-arabinose transferase
S19-40_03723	-	Dolichyl-phosphate-mannose-protein mannosyltransferase
S19-40_03744	-	Acetyltransferase
S19-40_03746	wecD	dTDP-fucosamine acetyltransferase
S19-40_03758	maa	Maltose O-acetyltransferase
S19-40_03774	rsmG	Ribosomal RNA small subunit methyltransferase G
S19-40_03791	-	phosphotransferase system, EIIB
S19-40_03848	ytmI	putative N-acetyltransferase YtmI
S19-40_03859	-	Glycosyl transferase family, a/b domain
S19-40_03911	cysN	Sulfate adenylyltransferase subunit 1
S19-40_03918	rlmG	Ribosomal RNA large subunit methyltransferase G
S19-40_03927	-	Putative TrmH family tRNA/rRNA methyltransferase
S19-40_03930	cysE	Serine acetyltransferase
S19-40_03933	ispD	2-C-methyl-D-erythritol 4-phosphate cytidylyltransferase
S19-40_03948	-	ilvE_I: branched-chain amino acid aminotransferase
S19-40_03976	glmU	glmU: UDP-N-acetylglucosamine diphosphorylase/glucosamine-1-phosphate N-acetyltransferase
S19-40_03983	rsmA	Ribosomal RNA small subunit methyltransferase A
S19-40_03989	rsmI	Ribosomal RNA small subunit methyltransferase I
S19-40_03991	yfiC	tRNA1(Val) (adenine(37)-N6)-methyltransferase
S19-40_03998	glyA	Serine hydroxymethyltransferase

Locus tag ID	Gene	Function
		lactone hydrolase
S19-40_01709	ahlD, aiiA, attM, blcC	N-acyl homoserine lactone hydrolase
S19-40_02014	-	Dienelactone hydrolase family protein
S19-40_02855	ahlD, aiiA, attM, blcC	N-acyl homoserine lactone hydrolase
S19-40_03601	-	Dienelactone hydrolase family protein
		β-*lactamases*
S19-40_00019	penP	Beta-lactamase
S19-40_00225	-	Beta-lactamase
S19-40_00240	-	Metallo-beta-lactamase superfamily protein
S19-40_00467	-	Metallo-beta-lactamase superfamily protein
S19-40_00991	-	Beta-lactamase
S19-40_01661	-	Beta-lactamase superfamily domain protein
S19-40_01709	-	Metallo-beta-lactamase superfamily protein
S19-40_02214	ybxI	putative beta-lactamase YbxI
S19-40_02259	-	Beta-lactamase
S19-40_02532	-	Beta-lactamase superfamily domain protein
S19-40_02855	-	Metallo-beta-lactamase superfamily protein
S19-40_02861	-	Beta-lactamase superfamily domain protein
S19-40_02961	-	Metallo-beta-lactamase superfamily protein
S19-40_03257	-	Metallo-beta-lactamase superfamily protein
S19-40_03550	bla2, blm, ccrA, blaB	metallo-beta-lactamase class B
S19-40_03707	-	Metallo-beta-lactamase superfamily protein
S19-40_03742	bla2, blm, ccrA, blaB	metallo-beta-lactamase class B
		deaminases
S19-40_00468	adeC	Adenine deaminase
S19-40_00611	guaD	Guanine deaminase
S19-40_00930	nagB	Glucosamine-6-phosphate deaminase 1
S19-40_01533	hemC	Porphobilinogen deaminase
S19-40_01675	mtaD	5-methylthioadenosine/S-adenosylhomocysteine deaminase
S19-40_02187	nagB	Glucosamine-6-phosphate deaminase 1
S19-40_02802	tadA	tRNA-specific adenosine deaminase
S19-40_03012	cdd	Cytidine deaminase

S19-40_03042	tadA	tRNA-specific adenosine deaminase
S19-40_03150	yerA	Putative adenine deaminase YerA
S19-40_03978	yabJ	2-iminobutanoate/2-iminopropanoate deaminase
S19-40_04015	tadA	tRNA-specific adenosine deaminase
		deacetylases
S19-40_00248	pdaA	Peptidoglycan-N-acetylmuramic acid deacetylase PdaA
S19-40_00383	argE	Acetylornithine deacetylase
S19-40_00501	ykuR	N-acetyldiaminopimelate deacetylase
S19-40_00931	nagA	N-acetylglucosamine-6-phosphate deacetylase
S19-40_01649	-	N-acetyldiaminopimelate deacetylase
S19-40_01692	-	Histone deacetylase domain protein
S19-40_02104	cah	Cephalosporin-C deacetylase
S19-40_02121	-	N-acetyldiaminopimelate deacetylase
S19-40_02333	pdaC	Peptidoglycan-N-acetylmuramic acid deacetylase PdaC
S19-40_02535	lysK	N-acetyl-lysine deacetylase
S19-40_02547	-	N-acetyldiaminopimelate deacetylase
S19-40_02585	pgdA	Peptidoglycan-N-acetylglucosamine deacetylase
S19-40_02586	cobB	NAD-dependent protein deacetylase
S19-40_02720	bshB1	N-acetyl-alpha-D-glucosaminyl L-malate deacetylase 1
S19-40_02857	argE	acetylornithine deacetylase
S19-40_03287	pdaA	Peptidoglycan-N-acetylmuramic acid deacetylase PdaA
S19-40_03411	icaB	Poly-beta-1,6-N-acetyl-D-glucosamine N-deacetylase
S19-40_03591	bshB2	putative N-acetyl-alpha-D-glucosaminyl L-malate deacetylase 2
S19-40_03620	argE	Acetylornithine deacetylase
S19-40_03852	-	N-acetyldiaminopimelate deacetylase
S19-40_03867	pdaA	Peptidoglycan-N-acetylmuramic acid deacetylase PdaA
		other deacetylases
S19-40_02720	-	GlcNAc-PI de-N-acetylase
S19-40_03287	-	spore_pdaA: delta-lactam-biosynthetic de-N-acetylase
S19-40_03591	-	GlcNAc-PI de-N-acetylase
S19-40_02720	-	GlcNAc-PI de-N-acetylase
S19-40_03287	-	spore_pdaA: delta-lactam-biosynthetic de-N-acetylase
S19-40_03591	-	GlcNAc-PI de-N-acetylase

S19-40_03824	mmsA, iolA, ALDH6A1	malonate-semialdehyde dehydrogenase (acetylating) / methylmalonate-semialdehyde dehydrogenase
		other (de)acylases
S19-40_00208	faBOT	Malonyl CoA-acyl carrier protein transacylase
S19-40_00210	pksC	Polyketide biosynthesis malonyl CoA-acyl carrier protein transacylase PksC
S19-40_00328	faBOT	Malonyl CoA-acyl carrier protein transacylase
S19-40_01475	dtd	D-aminoacyl-tRNA deacylase
S19-40_02338	ybaK	Cys-tRNA(Pro)/Cys-tRNA(Cys) deacylase YbaK
S19-40_02881	DBT, bkdB	2-oxoisovalerate dehydrogenase E2 component (dihydrolipoyl transacylase)
S19-40_03846	-	Penicillin acylase

Table s7. *Bacillus subtilis* PTA-271 encoding genes for PKS and other acetyltransferases.

Locus tag ID	Gene	Function
		Polyketide related genes
S19-40_00196	pksS	Polyketide biosynthesis cytochrome P450 PksS
S19-40_00197	pksR	Polyketide synthase PksR
S19-40_00198	pksN	Polyketide synthase PksN
S19-40_00199	pksM	Polyketide synthase PksM
S19-40_00200	pksL	Polyketide synthase PksL
S19-40_00201	pksJ	Polyketide synthase PksJ
S19-40_00202	pksI	Putative polyketide biosynthesis enoyl-CoA isomerase PksI
S19-40_00203	pksH	putative polyketide biosynthesis enoyl-CoA hydratase PksH
S19-40_00204	pksG	Polyketide biosynthesis 3-hydroxy-3-methylglutaryl-ACP synthase PksG
S19-40_00205	pksF	Polyketide biosynthesis malonyl-ACP decarboxylase PksF
S19-40_00206	acpK	Polyketide biosynthesis acyl-carrier-protein AcpK
S19-40_00207	pksE	Polyketide biosynthesis protein PksE
S19-40_00208	pksD	Polyketide biosynthesis acyltransferase PksD
S19-40_00210	pksC	Polyketide biosynthesis malonyl CoA-acyl carrier protein transacylase PksC
S19-40_00211	pksB	putative polyketide biosynthesis zinc-dependent hydrolase Pks
S19-40_01385	pksS	Polyketide biosynthesis cytochrome P450 PksS
		Acyl transferase related genes
S19-40_00207	pfaD	Acyl transferase domain protein
S19-40_00208	faBOT	Malonyl CoA-acyl carrier protein transacylase
S19-40_00210	faBOT	Acyl transferase domain protein
S19-40_00210	pksC	Polyketide biosynthesis malonyl CoA-acyl carrier protein transacylase PksC
S19-40_00328	faBOT	Malonyl CoA-acyl carrier protein transacylase
S19-40_00328	faBOT	Malonyl CoA-acyl carrier protein transacylase
S19-40_02881	DBT, bkdB	2-oxoisovalerate dehydrogenase E2 component (dihydrolipoyl transacylase)
S19-40_03846	-	Penicillin acylase
		Keto related genes
S19-40_00120	tkt	Transketolase
S19-40_00205	fabF	beta-ketoacyl-acyl-carrier-protein synthase II
S19-40_00220	-	8-amino-7-oxononanoate synthase/2-amino-3-ketobutyrate coenzyme A ligase

S19-40_00407	apbA	Ketopantoate reductase PanE/ApbA
S19-40_00460	dxs	Transketolase, pyrimidine binding domain
S19-40_00476	apbA_panE: 2-dehydropantoate 2-reductase	Ketopantoate reductase PanE/ApbA
S19-40_00565	mtnX	2-hydroxy-3-keto-5-methylthiopentenyl-1-phosphate phospha
S19-40_00566	mtnW	2,3-diketo-5-methylthiopentyl-1-phosphate enolase
S19-40_00966	ghrB	glyoxylate/hydroxypyruvate/2-ketogluconate reductase
S19-40_01097	-	Aldo/keto reductase family protein
S19-40_01158	fadA	3-ketoacyl-CoA thiolase
S19-40_01396	-	Aldo/keto reductase family protein
S19-40_01493	csbX	Alpha-ketoglutarate permease
S19-40_01547	ilvC	Ketol-acid reductoisomerase (NADP(+))
S19-40_01623	-	Aldo/keto reductase family protein
S19-40_01653	camP	2,5-diketocamphane 1,2-monooxygenase
S19-40_01995	ydaE	putative D-lyxose ketol-isomerase
S19-40_02000	-	Aldo/keto reductase family protein
S19-40_02005	pcaR_pcaU	beta-ketoadipate pathway transcriptional regulators, PcaR/PcaU/PobR family
S19-40_02073	ulaD	3-keto-L-gulonate-6-phosphate decarboxylase UlaD
S19-40_02145	-	Aldo/keto reductase family protein
S19-40_02175	xylA	alpha-ketoglutaric semialdehyde dehydrogenase
S19-40_02310	dlgD	2,3-diketo-L-gulonate reductase
S19-40_02418	fabF	fabF: beta-ketoacyl-acyl-carrier-protein synthase II
S19-40_02521	fadA	3-ketoacyl-CoA thiolase
S19-40_02597	-	Aldo/keto reductase family protein
S19-40_02838	-	Aldo/keto reductase family protein
S19-40_02882	-	Transketolase, pyrimidine binding domain
S19-40_02895	fadA	3-ketoacyl-CoA thiolase
S19-40_03297	dxs	Transketolase, pyrimidine binding domain
S19-40_03393	scoA	putative succinyl-CoA:3-ketoacid coenzyme A transferase subunit A
S19-40_03394	scoB	putative succinyl-CoA:3-ketoacid coenzyme A transferase subunit B

		putative succinyl-CoA:3-ketoacid coenzyme
S19-40_03621	scoB	A transferase subunit B
S19-40_03674	kdgT	2-keto-3-deoxygluconate permease
S19-40_03678	kduI	4-deoxy-L-threo-5-hexosulose-uronate ketol-isomerase
S19-40_03822	-	Aldo/keto reductase family protein
S19-40_03832	iolI	2-keto-myo-inositol isomerase
		Dehydratase related genes
S19-40_00109	leuC	3-isopropylmalate dehydratase large subunit
S19-40_00332	sdhA	L-serine dehydratase, alpha chain
S19-40_00333	sdhB	L-serine dehydratase, beta chain
S19-40_00564	mtnB	Methylthioribulose-1-phosphate dehydratase
S19-40_00785	fabZ	3-hydroxyacyl-[acyl-carrier-protein] dehydratase FabZ
S19-40_00942	hisB	Imidazoleglycerol-phosphate dehydratase
S19-40_01000	pglF	UDP-N-acetyl-alpha-D-glucosamine C6 dehydratase
S19-40_01470	tcdA	tRNA threonylcarbamoyladenosine dehydratase
S19-40_01507	-	Prephenate dehydratase
S19-40_01531	hemB	Delta-aminolevulinic acid dehydratase
S19-40_01543	leuD1	3-isopropylmalate dehydratase small subunit 1
S19-40_01544	leuC	3-isopropylmalate dehydratase large subunit
S19-40_01736	-	NAD dependent epimerase/dehydratase family protein
S19-40_01805	-	NAD dependent epimerase/dehydratase
S19-40_02013	fabZ	3-hydroxyacyl-[acyl-carrier-protein] dehydratase FabZ
S19-40_02171	garD	Galactarate dehydratase (L-threo-forming)
S19-40_02173	gudD	Glucarate dehydratase
S19-40_02176	-	putative 5-dehydro-4-deoxyglucarate dehydratase
S19-40_02303	uxaA	Altronate dehydratase
S19-40_02308	uxuA	Mannonate dehydratase
S19-40_02782	aroD	3-dehydroquinate dehydratase
S19-40_02853	dsdA	D-serine dehydratase
S19-40_02891	prpD	2-methylcitrate dehydratase
S19-40_02926	yqhS	3-dehydroquinate dehydratase
S19-40_03226	rfbG	CDP-glucose 4,6-dehydratase
S19-40_03334	-	NAD dependent epimerase/dehydratase family protein

S19-40_03405	-	GDP-mannose 4,6 dehydratase
S19-40_03419	nnrD	ADP-dependent (S)-NAD(P)H-hydrate dehydratase
S19-40_03512	rfbB	dTDP-glucose 4,6-dehydratase
S19-40_03631	pseB	UDP-N-acetylglucosamine 4,6-dehydratase (inverting)
S19-40_03641	ilvA	L-threonine dehydratase biosynthetic IlvA
S19-40_03651	ilvD	Dihydroxy-acid dehydratase
S19-40_03828	iolE	Inosose dehydratase
S19-40_03831	iolE	Inosose dehydratase
		Enoyl reductase related genes
S19-40_00232	-	Enoyl-(Acyl carrier protein) reductase
S19-40_00327	-	Enoyl-(Acyl carrier protein) reductase
S19-40_00514	fadH	putative 2,4-dienoyl-CoA reductase
S19-40_00548	-	Enoyl-(Acyl carrier protein) reductase
S19-40_01324	-	Enoyl-(Acyl carrier protein) reductase
S19-40_01390	-	putative enoyl-[acyl-carrier-protein] reductase II
S19-40_01662	-	Enoyl-(Acyl carrier protein) reductase
S19-40_01996	-	Enoyl-(Acyl carrier protein) reductase
S19-40_02024	-	Enoyl-(Acyl carrier protein) reductase
S19-40_02139	-	Enoyl-(Acyl carrier protein) reductase
S19-40_02346	-	Enoyl-(Acyl carrier protein) reductase
S19-40_02378	fabI	Enoyl-[acyl-carrier-protein] reductase [NADH] FabI
S19-40_02513	-	Enoyl-(Acyl carrier protein) reductase
S19-40_02516	-	Enoyl-(Acyl carrier protein) reductase
S19-40_02605	-	Enoyl-(Acyl carrier protein) reductase
S19-40_02899	fadH	2,4-dienoyl-CoA reductase (NADPH2)
S19-40_03349	fabL	Enoyl-[acyl-carrier-protein] reductase [NADPH] FabL
S19-40_03372	-	Enoyl-(Acyl carrier protein) reductase
S19-40_03395	-	Enoyl-(Acyl carrier protein) reductase
S19-40_03523	-	Enoyl-(Acyl carrier protein) reductase
S19-40_03527	-	Enoyl-(Acyl carrier protein) reductase
S19-40_03679	-	Enoyl-(Acyl carrier protein) reductase
S19-40_03816	-	Enoyl-(Acyl carrier protein) reductase
		Other acetyltransferase related genes

S19-40_00053	ydaF	Putative ribosomal N-acetyltransferase YdaF
S19-40_00166	speG	Spermidine N(1)-acetyltransferase
S19-40_00220	kbl, GCAT	glycine C-acetyltransferase
S19-40_00408	ylbP	putative N-acetyltransferase YlbP
		Dihydrolipoyllysine-residue acetyltransferase
S19-40_00459	pdhC	component of pyruvate dehydrogenase complex
S19-40_00502	dapH	2,3,4,5-tetrahydropyridine-2,6-dicarboxylate N-acetyltransfera
S19-40_00527	-	Acetyltransferase (GNAT) family protein
S19-40_00621	-	Acetyltransferase (GNAT) domain protein
S19-40_00725	argA	amino-acid N-acetyltransferase
S19-40_00765	ywnH	Putative phosphinothricin acetyltransferase YwnH
S19-40_00936	dapH	2,3,4,5-tetrahydropyridine-2,6-dicarboxylate N-acetyltransfera
S19-40_00960	nat	Arylamine N-acetyltransferase
S19-40_01010	epsM	Putative acetyltransferase EpsM
S19-40_01045	yvbK	putative N-acetyltransferase YvbK
S19-40_01228	paiA	Spermidine/spermine N(1)-acetyltransferase
S19-40_01347	-	Acetyltransferase (GNAT) family protein
S19-40_01371	bltD	Spermine/spermidine acetyltransferase
S19-40_01402	mdpB3	acetyltransferase/esterase
S19-40_01427	oatA	O-acetyltransferase OatA
S19-40_01551	ysnE	putative N-acetyltransferase YsnE
S19-40_01659	ytmI	putative N-acetyltransferase YtmI
S19-40_01771	cysE	Serine acetyltransferase
S19-40_01853	ypeA	Acetyltransferase YpeA
S19-40_01870	yycN	putative N-acetyltransferase YycN
S19-40_01898	-	GNAT acetyltransferase
S19-40_01930	ydaF	Putative ribosomal N-acetyltransferase YdaF
S19-40_01994	ydaF	Putative ribosomal N-acetyltransferase YdaF
S19-40_02207	slyA	rimI: ribosomal-protein-alanine acetyltransferase
S19-40_02340	-	Acetyltransferase (GNAT) domain protein
S19-40_02357	ydaF	Putative ribosomal N-acetyltransferase YdaF
S19-40_02365	yjcF	putative N-acetyltransferase YjcF
S19-40_02403	yjbC	Putative acetyltransferase YjbC

S19-40_02431	argA	Amino-acid acetyltransferase
S19-40_02432	argJ	ArgJ: glutamate N-acetyltransferase/amino-acid acetyltransfer
S19-40_02456	-	Acetyltransferase (GNAT) domain protein
S19-40_02457	-	Acetyltransferase (GNAT) domain protein
S19-40_02521	yhfS	Putative acetyl-CoA C-acetyltransferase YhfS
S19-40_02525	wecD	dTDP-fucosamine acetyltransferase
S19-40_02601	phnO	Aminoalkylphosphonate N-acetyltransferase
S19-40_02798	-	rimI: ribosomal-protein-alanine acetyltransferase
S19-40_02843	mshD	Mycothiol acetyltransferase
S19-40_02845	-	ectoine_EctA: diaminobutyrate acetyltransferase
		Dihydrolipoyllysine-residue acetyltransferase
S19-40_02881	pdhC	component of pyruvate dehydrogenase complex
S19-40_02887	pta	Phosphate acetyltransferase
S19-40_02895	mmgA	Acetyl-CoA acetyltransferase
S19-40_03092	rimI	Ribosomal-protein-alanine acetyltransferase
S19-40_03191	-	Acetyltransferase (GNAT) family protein
S19-40_03241	-	Acetyltransferase (GNAT) family protein
		Dihydrolipoyllysine-residue acetyltransferase
S19-40_03298	pdhC	component of pyruvate dehydrogenase complex
S19-40_03441	patA	Peptidoglycan O-acetyltransferase
S19-40_03507	wecD	dTDP-fucosamine acetyltransferase
S19-40_03529	pta	Phosphate acetyltransferase
S19-40_03548	rimL	rimI: ribosomal-protein-alanine acetyltransferase
S19-40_03619	yodP	N-acetyltransferase YodP
S19-40_03625	rimL	rimI: ribosomal-protein-alanine acetyltransferase
S19-40_03695	yycN	putative N-acetyltransferase YycN
S19-40_03740	yjcF	putative N-acetyltransferase YjcF
S19-40_03744	-	Acetyltransferase
S19-40_03746	wecD	dTDP-fucosamine acetyltransferase
S19-40_03758	maa	Maltose O-acetyltransferase
S19-40_03848	ytmI	putative N-acetyltransferase YtmI
S19-40_03930	cysE	Serine acetyltransferase
S19-40_03976	glmU	glmU: UDP-N-acetylglucosamine

Table s8. Anti-SMASH 5.1.0 prediction of gene clusters responsible for secondary metabolite production in *Bacillus subtilis* PTA-271.

Secondary metabolite	Enzyme	Gene clusters	Compound	Similarity
Betalactone-NRPS	NRPS	1	Fengycin	100%
NRPS	NRPS	2	Bacillibactin	100%
			Surfactin	78%
Other	NRPS	1	Bacilysin	100%
T3PKS	PKS	1	-	0%
TransATPKS-NRPS-PKSlike	PKS/NRPS	1	Bacillaene	100%
tRNA-dependent cyclodipeptide synthases	-	1	-	0%
Terpene	-	2	-	0%
Sactipeptide	RIPP	2	Subtilosin A	100%
			Sporulation killing factor	100%